

VARIATION OF TROPOSPHERIC ENERGY AND ITS FLUXES DURING SEVERE  
CYCLONE AFFECTING BANGLADESH COAST IN THE LAST DECADE

M. Phil Thesis

JAHANARA BEGUM

EXAM ROLL. 9414010F

Session : 1993-94-95



BANGLADESH UNIVERSITY OF ENGINEERING & TECHNOLOGY

DEPARTMENT OF PHYSICS

MARCH 2000



BANGLADESH UNIVERSITY OF ENGINEERING & TECHNOLOGY  
DEPARTMENT OF PHYSICS



Certification of Thesis Work

A thesis  
On

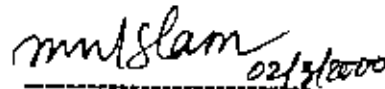
VARIATION OF TROPOSPHERIC ENERGY AND ITS FLUXES DURING SEVERE CYCLONE  
AFFECTING BANGLADESH COAST IN THE LAST DECADE

By  
Jahanara Begum  
Exam Roll. 9414010F

has been accepted as satisfactory in partial fulfillment of the requirements for the degree of  
*Master of Philosophy* in Physics and certify that the student demonstrated a satisfactory  
knowledge of the field covered by thesis in an oral examination held on 2<sup>nd</sup> March, 2000.

*Board of Examiners*

Chairman  
and Supervisor

  
02/3/2000

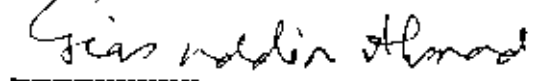
Dr. Md. Nazrul Islam  
Assistant Professor  
Department of Physics  
BUET, Dhaka

Member



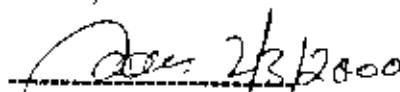
Prof. Dr. Md. Abu Hashan Bhuiyan  
Head  
Department of Physics  
BUET, Dhaka

Member



Prof. Dr. Gias uddin Ahmad  
Department of Physics  
BUET, Dhaka

Member  
(External)

  
02/3/2000

Prof. Dr. Md. Abdul Mannan Chowdhury  
Department of Physics  
Jahangirnagar University  
Savar, Dhaka.

## CERTIFICATE

This is to certify that the thesis on "Variation of Tropospheric energy and its fluxes during severe Cyclone affecting Bangladesh Coast in the last decade" has been performed by me and neither this thesis nor any part thereof has been submitted elsewhere for the award of any other degree or diploma.

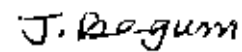
Supervisor



(Dr. Md. Nazrul Islam)

Countersigned by Supervisor

Student



(Jahanara Begum)

Signature of Candidate

## Acknowledgements

I feel extremely delighted to express my indebtedness and deepest sense of gratitude to my respected teacher and supervisor Dr. Md. Nazrul Islam, Assistant professor, Department of Physics, BUET, Dhaka, for his constant encouragement and affectionate guidance throughout the progress of the research work. The work would not have been possible without his indispensable help at various stages of the work.

I gratefully express my thanks to Prof. Dr. Md. Abu Hashan Bhuiyan, Head, Department of Physics, BUET for his constant encouragement and sympathetic suggestions during this research work and also for providing Computer and other facilities available at the Department.

I am extremely grateful to my favourite teachers Prof. Dr. Gias uddin Ahmad, Prof. Dr. M. Ali Asgar, Prof. Dr. Tafazzal Hossain, Prof. Dr. Mominul Huq and other teachers of the Department of Physics, BUET for their valuable suggestions and encouragement during my research work

I also express my gratitude to Dr. C. S. Karim, Director, NPED, BAEC, Dhaka for giving me the opportunity to successfully complete the work.

I am grateful to Mrs. Aijumand Habib, Deputy Director, BMD, Dhaka, Mrs. Fahima Khanam and Md. Faruq-Uz-Zaman Chowdhury, Department of Physics, BUET for their kind help during this research work.

Special thanks are due to Mrs. Ayesha Khatun, Assistant Meteorologist, BMD, Dhaka for her kind help and various suggestions.

Thanks are due to my friend Md. Abu Saklayen, Assistant Professor, Dept. of Physics, SUST, Sylhet, who shared my problems during the whole period of the work.

All thanks are due to Almighty Allah, the only controller and sustainer of the whole universe on Whose command all helps were made available to me for successful completion of the work.

JAHANARA BEGUM

## Abstract

The present study have been made with a view to find out the changes of various atmospheric energy components and their fluxes during "cyclone period" as compared to that of "before occurrence" and "after landfall" for seven cyclones that occurred in the Bay of Bengal in the last decade. Three of them were pre-monsoon cyclone and four of them were post-monsoon cyclone.

It was found that sensible heat decreased with the increase of height. For most of the cyclones sensible heat was large during the "cyclone period" compared to that of other phases. On the other hand, potential energy increased with the increase of height and for most of the cyclones it was large in magnitude during "cyclone period". It was observed that latent heat for most of the cyclones increased to initiate the cyclone. Latent heat was also increased at "after landfall" and was maximum at the middle troposphere (500-250 mb). At the lower level, almost no variation was observed for latent heat at different phases of the cyclone. Kinetic energy was nearly zero from lower to middle troposphere and was increased from middle to upper troposphere for all three phases. It was large at 300-150 mb level. For most of the cyclones kinetic energy was maximum at the initiation of "cyclone period" and at "after landfall".

It was found that zonal flux was westward(westerly) up to about 700 mb level. Beyond this level it was eastward(easterly). For most of the cyclones the magnitude of zonal flux was found large just before starting "cyclone period" and was maximum at 250-150 mb level. "Before occurrence" and during "cyclone period" meridional flux varied between northward and southward. However, at "after landfall" for most of the cyclones it was southward. Its magnitude was large during "cyclone period".

From the energy budget it was found that sensible heat, potential energy, kinetic energy as well as total energy were large for pre-monsoon cyclones as compared to post-monsoon cyclones. It was also found that zonal and meridional fluxes were high in magnitude for pre-monsoon cyclones than that of post-monsoon cyclones.

	Page
<b>CHAPTER 1: INTRODUCTION</b>	<b>1-12</b>
1.1 Introduction	1
1.2 Definition of cyclone	1
1.3 Tropical cyclone	2
1.4 Life cycle of tropical cyclone	3
1.5 Causes of formation of cyclone	5
1.6 How cyclone is formed	6
1.6.1 Synoptic scale features favourable for cyclone formation	6
1.7 Tropical cyclone formation and development	7
1.8 Movement	8
1.9 Dissipation	8
1.10 A clear picture about cyclone	9
1.11 Eye of cyclone	10
1.12 Eye formation	10
1.13 Geographical and seasonal distributions	12
 <b>CHAPTER 2: REVIEW OF THE RELEVANT WORK</b>	 <b>13-17</b>
 <b>CHAPTER 3: MATERIALS AND METHODOLOGY</b>	 <b>18-22</b>
 <b>CHAPTER 4: RESULTS AND DISCUSSION</b>	 <b>23-188</b>
4.1 Variation of energy with time	23
4.1.1 Energy components	23
4.1.1 (a) Latent heat content	23
4.1.1 (b) Kinetic energy	31
4.1.2 Energy fluxes	38
4.1.2 (a): Zonal flux of dry static energy	38
4.1.2 (b): Zonal flux of moist static energy	46
4.1.2 (c): Meridional flux of dry static energy	46
4.1.2 (d): Meridional flux of moist static energy	58
4.2 Atmospheric energy at different isobaric levels	65
4.2.1 Cyclone 1	65
4.2.1 (a). Energy components	65

4.2.1 (b) Energy fluxes	71
4.2.2 Cyclone 2	79
4.2.2 (a): Energy components	79
4.2.2 (b): Energy fluxes	85
4.2.3 Cyclone 3	92
4.2.3 (a): Energy components	92
4.2.3 (b): Energy fluxes	96
4.2.4 Cyclone 4	106
4.2.4 (a): Energy components	106
4.2.4 (b): Energy fluxes	112
4.2.5 Cyclone 5	119
4.2.5 (a): Energy components	119
4.2.5 (b): Energy fluxes	123
4.2.6 Cyclone 6	131
4.2.6 (a): Energy components	131
4.2.6 (b): Energy fluxes	137
4.2.7 Cyclone 7	146
4.2.7 (a): Energy components	146
4.2.7 (b): Energy fluxes	152
4.3 Energy and variables at different cyclonic phases	159
4.3.1 Cyclone 1	159
4.3.1 (a): Energy components at different phases	159
4.3.1 (b): Variables at different phases	160
4.3.2 Cyclone 2	163
4.3.2 (a): Energy components at different phases	163
4.3.2 (b): Variables at different phases	166
4.3.3 Cyclone 3	167
4.3.3 (a): Energy components at different phases	167
4.3.3 (b): Variables at different phases	170
4.3.4 Cyclone 4	171
4.3.4 (a): Energy components at different phases	171
4.3.4 (b): Variables at different phases	174
4.3.5 Cyclone 5	175
4.3.5 (a): Energy components at different phases	175
4.3.5 (b): Variables at different phases	176
4.3.6 Cyclone 6	179
4.3.6 (a): Energy components at different phases	180

4.3.6 (b) Variables at different phases	183
4.3.7 Cyclone 7	184
4.3.7 (a). Energy components at different phases	184
4.3.7 (b): variables at different phases	185
<b>CHAPTER 5: ENERGY BUDGET</b>	<b>189-202</b>
<b>CHAPTER 6: CONCLUSIONS</b>	<b>203</b>
<b>REFERENCES</b>	<b>204-205</b>





# CHAPTR-1

## INTRODUCTION

# CHAPTER-1

## INTRODUCTION



### 1.1 Introduction

One of the greatest problem Bangladesh faces is the frequency of natural calamities. Among such calamities perhaps the most devastating are cyclones which visit us once every year or at least every few years. Because of the special geographical location, Bangladesh is devastated by natural disasters like tropical cyclones, nor'westers, tornado, floods etc. Out of these, tropical cyclones are regarded as the most deadly among all natural disasters. They bring catastrophic ravages to life and property as well as to environment. Among all the areas in the world affected by tropical cyclones, the countries along the rim of the Bay of Bengal suffer most and Bangladesh is the worst sufferer. Among the tropical cyclone forming areas in the world, the Bay of Bengal is one of the most favourable one. Cyclones forming in the Bay of Bengal move initially towards west or northwest; at times they recurve forwards north and then to the northeast. As a result, the countries bordering the Bay of Bengal become very much affected. In order to minimise the future loss of life and property, proper cyclone disaster management action is an absolute necessity. This, in turn, requires a better assessment of risks associated with a cyclone. Therefore, an effective prediction of tropical cyclone is very much essential especially in respect of its energy and the direction of movement.

### 1.2 Definition of Cyclone:

Cyclone is an atmospheric circulation in which the winds are rotating in the same direction as the earth. It is a natural phenomena and is an intense vortex in atmosphere. It is an area of low pressure where strong winds blow spirally inward from all sides. Inward spirals move in anti-clockwise direction in the Northern hemisphere and in clockwise direction in the Southern hemisphere. Wind does not reach the center but stops at a distance defining the limit of connection. No cloud form in this central region and no precipitation takes place. Cyclones in the tropical regions (Eq.,  $\sim 25^{\circ}$  N or S) are called tropical cyclones and the cyclones outside the tropical region are called extra-tropical cyclones. Cyclone has typical lifetimes on the

order of a few days, or almost a couple of weeks. The horizontal dimension is from a few hundred to a few thousand kilometers.

### 1.3 Tropical Cyclone:

Tropical cyclones are intense vortical storms which develop over the tropical oceans in regions of very warm surface water. Mathematically, a tropical cyclone can be assumed to be a cylindrical vortex such that,

the vorticity[1],

$$\xi = \vec{\nabla} \times \vec{V}$$

where  $V$  is the velocity and has a finite value.

Experience has shown that once a tropical cyclone has formed it is a very persistent phenomenon as long as it remains over the waters of the cyclone regions. This indicates a fundamental difference between tropical and extratropical cyclones, namely, that of their sources of energy. Most extratropical cyclones remain for only a short time at the maximum energy level, degenerating almost as rapidly as they formed. This leads one to conclude that extra tropical cyclones derive their energy from a source that soon becomes exhausted. The persistence of the tropical cyclones on a constant energy level for a period of several days indicates that once the cyclonic circulation is induced it in some way maintains its own source of energy. This energy must be easily utilized once the process is started. The rapid decay when a cyclone moves out of the cyclone belts also gives important clues concerning the nature of the energy source.

Tropical cyclones are known by different names in different parts of the world. In the Atlantic and eastern pacific they are called "Hurricanes". In the western pacific they are known as "Typhoons" and in the Philippines they are called as "Bagious" and 'willy-nilly" in Australia. In the north Indian ocean they are called "Tropical cyclones". The tropical cyclones are classified by the wind speed, estimated or observed with the system, as indicated below:

Weather System	Wind Speed	
	(Knots)	(Kmh)
Low Pressure	<17	<31
Depression	17-27	31-49
Deep Depression	28-33	50-61
Cyclonic Storm	34-47	62-88
Severe Cyclonic Storm	48-63	89-117
Sever Cyclonic Storm with a core of hurricane winds/super typhoon.	≥64	≥118

#### 1.4 Life cycle of Tropical Cyclone:

The life span of Tropical cyclones with a core of hurricane wind average is about five to six days from the time they form until the time of landfall. The entire life period of tropical cyclones is divided into four stages. They are (i) Formative (ii) Immature (iii) Mature and (iv) Decaying stage.

##### Formative stage:

Tropical storms form only in or near pre-existing disturbance of weather systems. In this stage, the pattern is not well defined and cloud bands are poorly organized. No eye of visible and the wind speed range is 30-50 mph. Surface pressure drops to about 1000 mb. In this stage one or more of the following developments take place:

- (a) Unusual falls of pressure in and around the center of depending easterly wave.
- (b) Asymmetric strengthening of wind and appearance of gale force in one sector but not of hurricane force.
- (c) On ITCZ large elliptical or circular wind circulation develops. Satellite pictures show isolation of marked cloud mass from other nearby cloud areas.

##### Immature stage:

All the formative eyclones can not reach the hurricane stage. If intensification takes place, the pressure rapidly drops below 1000 mb. In this stage the wind increases to hurricane force, usually at a distance of about 50 km from the cyclone center and pressure fall increases. When the wind speed reaches the hurricane force, a tight band form around the center. The cloud and rain pattern changes form

disorganized squalls to narrow organized bands spiralling inward. The eye is usually visible but ragged and irregular in shape.

#### **Mature stage:**

The mature stage occupies the longest part of the cycle and on the average most often lasts several days. During the mature stage the central wind speed need not increase and pressure need not fall. But the circulation expands and in moving storms, cyclone winds may extend several hundreds of kilometers from the center to the right of the direction of motion (in northern hemisphere). A well-formed inner ring of maximum winds encircles the "eye", where pressure stops falling, wind is light, rainfall ceases and clouds disappear. Even in this stage, the hurricane may undergo wide fluctuations in its intensity; pressure in the center may increase or decrease by as much as 60 mb in a day. At this stage, heating from convective clouds furnishes the largest amount of energy for cyclone maintenance. Wind speed range is between 80-200 m/h. The surface pressure is less than 1000 mb. The structure of a mature cyclone is shown in Fig 1.1.

#### **Decaying stage:**

The tropical storms begin to lose their intensity when they move out of the environment of warm moist tropical air, or move over land or move under an unfavourable large scale flow aloft, winds normally decrease to 80 km/h or less within 80 km from the east, and the weather becomes more gusty and showery. Sometimes they may recurve towards northeast when they come under the influence of an upper air westerly trough due to which they may travel to the regions where ocean temperatures are cooler. Their final dissipation over oceans seems to occur when they move over colder water, or approach within 5° or so of the equator. When the storm enters the land, it rapidly weakens as the central pressure is filled up at a rate of about 2 mb/hr. This weakens the radial pressure gradient, and the radius of maximum wind expands outward. The factors that are responsible to weaken the system after entry over the land are: (a) dramatic reduction in evaporation, (b) due to cooler surface temperatures as the land is cooler than ocean and (c) surface friction.

### 1.5 Causes of Formation of Cyclone:

The earth receives all its energy from the sun. The sun controls the global weather but the phenomena like cyclones are localized phenomena and local peculiarities are responsible for them.

Solar radiation does not fall with equal intensity over all parts of the world. It is maximum at the earth's equator and minimum at the poles. Again different surfaces on the earth have got different capacities for emission or absorption of radiation. Thus the different areas on the earth are heated unequally. This differential heating gives rise to low and high atmospheric pressure areas on the earth. Heat expands the air and it moves upwards making it lighter giving rise to low pressure region. Similarly, cooling makes air heavy giving rise to high pressure area. Usually low pressure areas are associated with bad weather and high pressure areas indicates good weather. Though solar energy ultimately controls the terrestrial weather, certain environmental conditions must be required for the development of cyclones. They are (1) warm ocean temperature (2) absence of strong vertical wind shear and (3) presence of a low pressure region. A tropical storm does not form if the sea temperature is less than 26-27°C. It is thought that the intertropical convergence zone (ITCZ) has got to do something with their formation. The ITCZ (10°N-10°S) is the region where winds from the two hemisphere passes close to the equator. A cyclone derives its spinning motion from the rotational motion of the earth called the Coriolis force. This force is virtually zero at the equator. Hence cyclones do not usually form at the equator, they are formed slightly north or south of the equator to get the necessary spin. It is because of the Coriolis force that winds in a cyclone are anticlockwise in the northern hemisphere and clockwise in the southern hemisphere.

When a low pressure is formed air from all directions converges towards this area. This air becomes very moist by rapid evaporation. This phenomenon is called the "Low level convergence". The coriolis effect turns the incoming air so that it spirals inwards and upwards at an increasing rate, causing heavy rain and thunderstorms. In the low pressure region itself, air again moves upwards and diverges. This is called high level divergence. The latent heat released by the condensation of water vapour warms the air and keeps it unstable. It is also thought that cyclone get energy from this latent heat.

Several theories like wave theory, instability theory etc have been suggested for the development of cyclone but none have been found entirely satisfactory. Some

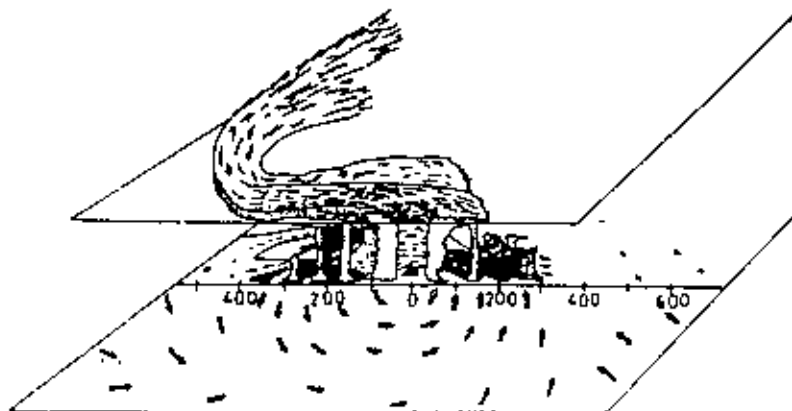


Fig. 1.1 Schematic three-dimensional view of cyclone  
 [Source: Mausam, Vol.48, No. 2, April 1997, P 243]

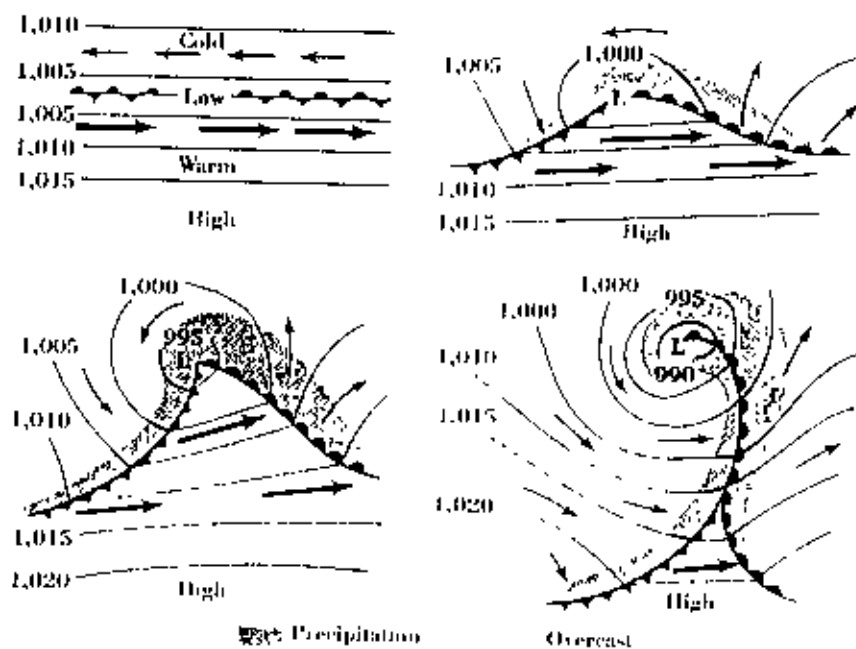


Fig. 1.2 Early stages in the life cycle of cyclones. [Source: Introduction to Meteorology, 3<sup>rd</sup> Edition, By Sverre Pettersen, P 213]

triggering mechanism (upper long waves) in the upper atmosphere could be also responsible for the formation of cyclones.

### 1.6 How Cyclone is Formed:

The main stages in the formation of cyclone are shown in Fig 1.2. In the initial stage (upper left), a warm and a cold air mass are present side by side, separated by a quasi-stationary front. In the next stage (upper right), a wave has formed on the front, and a center of low pressure is developing at the apex of the wave. This is the nascent cyclone, and the process is commonly called cyclogenesis. The young and developing cyclone is shown in the lower-left diagram. During the further development, the cold front overtakes the warm front and the system is said to occlude; the resulting front (warm and cold) is called an occlusion. The vertical structures of well-defined occlusions are shown in Fig 1.3. As the occlusion process continues, the warm air is lifted to higher levels and becomes replaced by colder (denser) air. As a result the center of gravity of the system as a whole is lowered; enormous amounts of potential energy are freed, and this accounts for the bulk of the kinetic energy of the wind system that surrounds the center.

#### 1.6.1 Synoptic scale features favourable for cyclone formation:

- (i) Tropical cyclones form from pre-existing disturbances containing abundant deep convection.
- (ii) The pre-existing disturbance should acquire warm core through the troposphere.
- (iii) Prior to the formation, the lower tropospheric vorticity increases over a horizontal area of 1000-2000 km.
- (iv) The vertical wind shear of the horizontal wind (U-component) should be low in the environment on a large scale.
- (v) Formation often occurs in conjunction with an interaction between the incipient disturbance and an upper tropospheric trough.
- (vi) Existence of low level wind surges that propagate inward to the center of the incipient disturbance.
- (vii) Appearance of curved banding features in the deep convection of the incipient disturbance is an indication of the cyclone development.



Though the above conditions are, in general, required for the formation of tropical cyclone, all cloud clusters do not develop into cyclones. The developing systems differ from the non-developing ones in the following respects:

- (a) The warm area at 300 mb and the low-level height anomaly are much more pronounced in the developing system.
- (b) Existence of low level wind maximum.
- (c) The developing system has an upper level anticyclone while the non-developing does not have it.
- (d) Low level easterlies to the north of the system should persist.
- (e) Warmer atmosphere over a large horizontal scale about  $8^\circ$  radius in all directions.
- (f) Large positive zonal shear poleward and negative zonal shear equatorward and southerly shear to the west and northerly shear to the east. The scale of this shear pattern is over a  $10^\circ$  latitude.

### 1.7 Tropical Cyclone Formation and Development:

Palment [2] listed the following prerequisites for the development of an intense tropical cyclone:

1. Sufficiently large sea or ocean areas with the temperature of the sea surface so high (above  $26^\circ\text{C}$  to  $27^\circ\text{C}$ ) that an air mass lifted from the lowest layers of the atmosphere and expanded adiabatically with condensation remains considerably warmer than the surrounding undisturbed atmosphere at least up to a level of about 12 km.
2. The value of the Coriolis parameter larger than a certain minimum value, thus excluding a belt of the width of about  $5^\circ$  to  $8^\circ$  latitude on both sides of the equator.
3. Weak vertical wind shear in the basic current, this limiting formation to latitudes far equatorwards of the subtropical jet stream.

Riehl [3] listed these additional requirements:

4. A pre-existing low-level disturbance (areas of bad weather and relatively low pressure).
5. Upper-tropospheric outflow above the surface disturbance.

A fully developed tropical cyclone is a warm-cored energy-exporting system, which usually remains intense for many days over the ocean. Essential to this is an extremely large surface pressure gradient near the core of the cyclone, sometimes

exceeding 3mb/km. Antheims and Johnson [4] pointed out, "As the air flows toward lower pressure, sensible heating serves to raise the equivalent potential temperature and is a necessary element in the maintenance of convection surrounding the eye". Ultimately, the latent heat release occurring in the air with the higher equivalent potential temperature maintains the warm core, baroclinicity and the high efficiency factors, thus making the release of latent heat in this region more effective in the direct generation of available potential energy. Although the sensible heat generation is small, the role of sensible heating in maintaining the core of high equivalent potential temperature is an essential process in the energetics of hurricanes.

A fully developed hurricane often excess 100 km in diameter, and on occasion may range up to 1500 km. The surface winds spiral cyclonically inward, becoming nearly circular around the central eye of the storm. The pressure pattern is that of a closed cyclonic vortex with central pressure very low, on the order of 90 Omb or less. Typical cloud patterns display spiraling bands of cumulus and towering cumulonimbus seperated by bands of relatively clear sky. The central eye is essentially cloudless.

### 1.8 Movement:

Cyclones (including tropical cyclones) move toward falling pressures, that is toward upper-tropospheric divergence[5]. In a climatological sense, this means in the general direction of the upper tropospheric current in the vicinity of the cyclone. Miller [6] provided statistical confirmation, finding that hurricanes on an average moved with the mean flow in the 6-12.5 km layer in the ring of 200-450 km radius centered on the individual storm. For our purposes at this stage it suffices to point out that mean resultant 200 mb winds tend to parallel climatological tropical cyclone tracks.

### 1.9 Dissipation:

Hurricanes dissipate when the supply of sensible heat to the core is cut off, destroying the gradient of equivalent potential temperature at the surface [7, 8]. This heat can be efficiently provided only by a uniformly warm ocean surface. The circulation weakens rapidly when it moves over land, or when a relatively cold or dry air mass penetrates the core.

### 1.10 A Clear Picture about Cyclone:

A clear demonstration of a cyclone can be obtained by knowing a composite picture from the ocean surface to the upper troposphere.

#### (a) Pressure:

Tropical cyclones are relatively small, intense low pressure areas having a more or less circular shape. Within 200 km of the cyclone center, the pressure field and its isobars are very nearly circular and symmetric around the eye. The central pressure of cyclones, however, may be 5% or even 10% below average sea level pressure. Sea level pressure in the eye below 950 mb of a mature hurricane. The fall of pressure from the periphery to the center of the storm commonly varies between 20 and 70 mb.

#### (b) Wind fields:

According to the wind distribution, two types of cyclone storms have been recognized. In one type, the concentration of the maximum winds in the region of the wall cloud is very pronounced, and may extend only 35-45 km from the center. In another type, hurricane force wind may extend about 100 km from the center.

The extremely high winds of the cyclone reach their maximum intensity near the center, owing to the increasing pressure gradient. As the wind spirals toward the center it suffers increased deflection and finally travels in a circular path, never quite reaching the center. Thus the central region remains relatively calm. To the right of the direction of motion of the center, the direction of vortex motion and steering current coincide. On the left-side they are opposite to each other. Thus speeds are almost invariably higher to the right than to the left of the direction of motion in moving cyclones.

From the 28 years study of pacific typhoon records [9] has feel to the formula for maximum winds [10]

$$V_m = 3.35(1010 - P_c)^{0.644} \text{ m/sec}$$

where  $P_c$  is the central pressure of the cyclone.

Maximum wind speed exists just outside the eye at heights from 1 to 3 km above the surface. The region of maximum wind is concentrated on the right front

quadrant of a tropical cyclone, measured in the direction of drift. Wind speeds in this region reach values as great as 375 km/hr.

**(c) Cloud pattern:**

Cloud photographs obtained from weather satellite have revealed that a cyclone seedling initially appears as a cluster of rain clouds. A mature cyclone has a well organized cloud pattern. It is possible to deduce the wind speeds from the size and degree of organization of this cloud. The clouds, especially at the outer edges, form long streets that spiral inward. The most intense part is situated off center to the right of the direction of motion, which is towards north-northwest. Usually a central dot denoting the eye is visible.

**(d) Precipitation:**

When tropical cyclones become stationary for protracted periods, 500 mm or more of rainfall may accumulate in one place. Maximum precipitation is concentrated in a narrow band surrounding the central core; amounts decrease rapidly toward the center, which is normally rain free. From radar observations it appears that the precipitation is concentrated in lines resembling squall lines of the extratropical cyclones.

### 1.11 Eye of Cyclone:

When the tropical cyclone intensifies the innermost spiral band tends to reduce its crossing angle and become a circle. At the end of the band an eyewall forms approximately in the form of an arc of a circle. Gradually this may separate from the band into a distinct ring or part of a ring with an echofree (or nearly echofree) area inside, namely the eye [11,12]

The eye is defined as the following [13]: A point in a dense, cold overcast centered within the curvature of a colder band that curves at least halfway around the point with a diameter of curvature  $1.1/2^0$  (one half) latitude or less.

### 1.12 Eye Formation:

In most of the mature hurricanes, eye formation takes place where the weather is absent and subsidence is observed. Any theory provided to explain the formation of the eye in a hurricane must be able to explain the phenomenon of why the maximum

upward motion occurs at some distance from the center of the storm rather than at the center and the reason for the occurrence of the subsidence with the eye. Though a number of theories are formulated, no single theory is able to explain both the phenomena.

Different theories and observation lead to the following conceptual model of eye formation. As a tropical storm intensifies, the air rises in vigorous thunderstorms and tends to spread out horizontally near the tropopause. As air spreads out aloft, a positive perturbation pressure at high levels is produced, which accelerates downward motion next to the convection. With the inducement of subsidence air warms up by compression and warm "eye" is generated.

Weatherford [14] investigated 101 cyclones over the Pacific during the period 1980-84 and his findings about the "eye" of the storms are summarized below:

- (i) Basically three shapes of "eye" walls are observed. They are (a) circular (b) concentric and (c) elliptical as shown in Fig 1.4.
- (ii) The size of the "eye" varied from 7 to 220 km in diameter for the typhoons and the averaged value is 42 km. The measurement of the diameter may be classified into 4 groups as: (a) small eyes (0-28 km) (b) medium eyes (28-55 km) (c) large eyes (>55 km) and (d) cyclones exhibiting no eye. Medium "eyes" are the most common. It is also noticed that the intensity of the cyclone does not determine the size of the eye.
- (iii) The eye contracts while the cyclone intensifies and expands at the time of filling up of the system. There is a period of time, common to the most intense cyclones in which the eye reaches a minimum size and remains locked even though the central pressure continues to fall.
- (iv) The initial eye often elliptical and become more circular with intensity. Large changes in the elliptical size are typical. Elliptical eyes generally appeared in the early stages or late filling stages of the cyclone. Elliptical eyes are rarely found in intense stages.
- (v) The eye in a cyclone normally develops when the pressure falls to 980 mb. If the eye develops at an early stage (985 mb), the cyclone deepens rapidly and the eye generally is small.
- (vi) As the cyclone intensifies, the eye becomes smaller and circular and once it obtains its maximum intensity. It usually exhibits the smallest eye and reaches

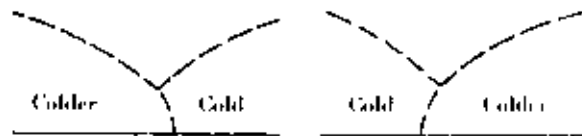


Fig. 1.3 Schematic sections through occlusions. [Source: Introduction to Meteorology, 3<sup>rd</sup> Edition, By Sverre Petterssen, P 213]

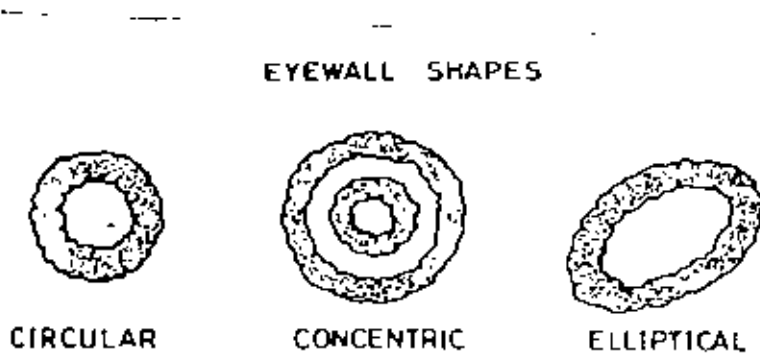


Fig. 1.4 Schematic depiction of three types of eye-walls observed: circular, concentric and elliptical. [Source: Mausam, Vol.48, No. 2, April 1997, P247]

a minimum value. Further intensification may occur, but the eye does not contract. If at this stage, the pressure falls lower than 945 mb, concentric eyes form, though it is a rare phenomena.

- (vii) During the filling stage, the eye wall generally expands until it is so diffuse that it can no longer be recognized as an eye. The faster the filling rate the quicker the eye disappears.
- (viii) The temperature inside the eye is indirectly an indication of the force of vertical motions in the eye wall convection, which in turn induces subsidence warming in the center. The stronger the eye wall convection, the warmer one would expect the eye temperature to be. The eye temperature not only increases with lower central pressure but also with the shape and structure of the eye. The temperature inside the concentric eye is cooler for the same intensity than either a circular or an elliptical eye.

### 1.13 Geographical and seasonal distributions:

Each year about 80 tropical cyclones occur over the earth. Of these one half to two-thirds become hurricanes. About two thirds of all cyclones form in the northern hemisphere (NH). Tropical cyclones do not form in the south Atlantic and eastern south pacific. They do not form within 4-5° of the equator and only a few form poleward of 22°N. About 65% of the cyclones form in the zone between 10° and 20° from the equator. The formation of tropical cyclones in the eastern and western hemisphere is in the ratio of 2:1. The frequency of formation is maximum during the summer to early fall with peak occurring during January to March in the southern hemisphere (SH) and July to September in the northern hemisphere, with the exception of the north Indian ocean.

The long time average of tropical cyclones in the north Indian ocean is about 5.6 per year, which is the least in the world and is about 7% of the global total. Out of these 6 tropical cyclones, 2-3 intensify to the severe cyclonic storm stage.

The frequency of tropical cyclones in the Bay of Bengal is more than that in the Arabian Sea. About 35% of the initial disturbances reach tropical cyclone strength, which 45% of these cyclones reach the severe tropical cyclone stage. The seasonal variation has a bimodal distribution with the primary peak in November and a secondary peak in May. During the monsoon season, these disturbances form in the north Bay and generally move westwards.

# CHAPTER-2

## REVIEW OF THE RELEVANT WORK



## CHAPTER-2

### REVIEW OF THE RELEVANT WORK

Raghavan *et al.* [15] studied the structural feature of a cyclone formed in the Bay of Bengal. The cyclone was formed on 7th November and crossed the coast through the northern edge of Sriharikota at about 03 UTC on 14th November 1989. In their study they found that the cyclone was a small horizontal extent and had small core region. The pressure gradient in the core probably exceeded 1 mb/km. After the landfall the system continued to be a cyclone exhibiting and had eye over land. The eye size remained the same and eyewall thickness showed a sharp increase indicative.

Sikka [16] made a study on forecasting the movement of tropical cyclones in the Indian seas by nondivergent barotropic model. In his study he obtained reasonably good forecasts on the movement of tropical storm by the barotropic model. In fact such forecasts when used judiciously along with other aids would improve the operational capability of the forecasts.

Natarajan and Ramamurthy [17] estimates the central pressure of cyclonic storms in the Indian seas. They also obtain the relationship between the minimum central pressure ( $P_0$ ) and the maximum surface wind speed ( $V_m$ ) when cyclonic storms are in the open seas. This provided a linear regression equation  $V_m = 13.4\sqrt{P_n - P_0}$  which was found to be better than Fletcher's [18] formula for calculation of minimum central pressure for the case of cyclonic storms over the Indian seas for away from the coast.

Ghosh and Roy [19] developed a cyclonic storm wave model to compute maximum significant wave heights in deep waters in the Bay of Bengal and Arabian Sea with the help of surface wind field simulated by a cyclonic storm model [20]. By this model one can find maximum significant wave heights and can be computed objectively within 90 percent accuracy if pressure and radius of maximum pressure gradient are known. Speed of the cyclonic storm can be computed by using the wave model.

Tripathi and Saxena [21] studied "Vertical structure of a Bay of Bengal cyclonic storm". Most of the existing knowledge on the structure of hurricanes is derived from data collected by U.S. research aircraft in the Atlantic and the Pacific. The vertical structure of

the storm is characterized by a warm core with temperature anomalies exceeding  $8^{\circ}\text{C}$  centered around the 250 mb level. There was evidence of a cold area at 125mb and 100mb levels where the negative anomalies of temperature were lower than  $8^{\circ}\text{C}$  and less occurred in the core. The broad features of the vertical structure of the storm were, however, quite well brought out in the study.

Mandal *et al.* [22] studied some aspects of a Bay of Bengal cyclone occurred on 29 January-4 February, 1987. In their study they showed that

- (a) Equatorial burst band surge from the southern hemisphere into pre-existing low pressure area increased cyclonic shear which led to enhance convection.
- (b) New convective cloud mass growth observed in the direction of the movement and before recurving or changing its direction of movement, the speed of movement slow or it remained stationary for same time.
- (c) The changes in the shape of cloud pattern are highly correlated with the change in the direction of movement and gave good signals for its movements.
- (d) Deformation of cloud pattern towards its end suggested its increased interaction with the westerlies and dry-cold air penetration into the cloud were leading to its rapid decay. Low sea surface temperature also might be one of the causes for its rapid weakening right over the sea.

Das *et al.* [23] made a study on the cyclones and depressions over Indian seas and Indian sub-continent during 1987. In this study they mainly showed that the structural features, life time, locatin, formation, landfall, rainfall distribution, pressure gradient, damage caused during the five cyclones and depressions of this year.

The same study was made by Gupta *et al.* [24] for the year 1989.

A new convection parameterization scheme proposed by Emanuel (1991) is used by Rao [25] to simulate the evolution of tropical cyclone. The numerical model used for this study is a 19 level axis-symmetric primitive equation, hydrostatic model in a  $z$  co-ordinate system. The vertical domain ranges from 0 to 18 km and the horizontal domain ranges up to 3114 km with a resolution of 20 km in the central 400 km radius and with increasing radial distance thereafter.

The evolution of an initially balanced vortex with an initial strength of 9m/sec is studied. It is shown that Emanuel's convection scheme is successful in simulating the development of the initial vortex into a mature, intense cyclonic storm. At the mature stage, a minimum surface pressure of 930 mb is attained with the associated low level maximum tangential wind speed of 70 m/sec. The simulated circulation features at the mature stage show the formation of an intense cyclone.

Two different sensitivity experiments were performed. A set of experiments with the variation of sea surface temperature (SST) from 300.5° to 302°K in steps of 0.5°K have shown that the intensity of model cyclone increases with the increase of SST. Another set of experiments with variation of latitude has shown that the cyclonic storm is more intense at lower latitudes.

Kelkar [26] showed the impact made by the satellite data in the intensity estimation and track prediction of tropical cyclones and also reviews the universally applied Dvorak algorithm for performing tropical cyclone intensity analysis.

Extensive use of Dvorak's intensity estimation scheme has revealed many of its limitations and elements of subjectivity in the analysis of tropical cyclones over the Arabian sea and the Bay of Bengal, which like cyclones in other ocean basins, also exhibit wide structural variability as seen in the satellite imagery.

Satellite-based cyclone tracking techniques include:

- (i) use of satellite-derived mean wind flow
- (ii) animation of sequence of satellite images and extrapolation of the apparent motion of the cloud system and
- (iii) monitoring changes in the upper level moisture patterns in the water vapour absorption channel imagery.

Satellite-based techniques on tropical cyclone intensity estimation and track prediction had led to very significant improvement in disaster warning and consequent saving of life and property.

Prasad [27] has analysed a review of some past and recent developments in cyclone track prediction problem by dynamical models. The early attempts aimed at predicting tropical cyclone motion by using simple barotropic models based on vertically integrated

vorticity tendency equation. Barotropic models are still used operationally in some centers due to their simplicity. However, current emphasis is on advanced primitive equation models incorporating physical processes, like cumulus convection, which are necessary to account for a major component of the cyclone movement. An important aspect of cyclone prediction by dynamical models is prescription of a correctly analysed synthetic vortex in the initial fields for running a forecast model. Several approaches developed by various groups for generating synthetic vortex are discussed. Examples of some cases of track prediction by limited area model in IMD and by global models are illustrated.

Mohanty and Gupta [28] studied deterministic methods for prediction of tropical cyclone tracks. Their study presents a state of art review of different objective techniques available for tropical cyclone track prediction. A brief description of current theories of tropical cyclone motion is given. Deterministic models with statistical and dynamical methods have been discussed. Recent advances in the understanding of cyclone structure and motion aspects have led to improve prediction of tropical cyclones. High resolution Limited Area Models (LAM) as well as Global Circulation Models(GCM) are now being used extensively by most of the leading operational numerical weather prediction (NWP) centers in the world. The major achievements towards improvement of such models have come from improved horizontal resolution of the models, inclusion of physical processes, use of synthetic and other non-conventional data in the data assimilation schemes and nudging method for initial matching of analysed cyclone centers with corresponding observations.

A brief description of further improvement in deterministic approach for prediction of tropical cyclone tracks is outlined.

Gupta and mohanty [29] analysed a severe cyclonic storm with a core of hurricane winds of 4-11 May 1990, which crossed the Indian east coast was one of the most intense cyclones over the Bay of Bengal region of the north Indian ocean. They observed that the storm exhibited certain interesting structural characteristics. The most striking feature observed was the formation of secondary convective rings wrapped around the primary eye wall. They found that the double eyewall structure of the storm has undergone a repetitive cycle characterised by the contraction of the outer eyewall and the weakening of the inner

eyewall during the life of the cyclone. These interesting characteristics are observed for the first in the north aspects of double eye wall features, such as, the possible role of double eyewall structure on the recurvature or turning of the storm and the effect of land obstacle in the development of a secondary eyewall are discussed.

Fahima Khanam [1] studied track prediction of tropical cyclones formed in the Bay of Bengal with the help of numerical model. The governing equation of the model is the barotropic vorticity equation in x-y-t space. The model area covers 0 to 30N latitude and 70 to 100E longitude. The horizontal x, y space is equally divided into 25×25 grid points. Computed extrapolated values of stream functions are converted into geo-potential and contours are drawn and then compared with the corresponding actual one. Track of cyclone is predicted by following the path of the center which determines the location of the cyclone at different times.

A large discussion have been made above. The researcher is very much interested to take up the present study with respect to the evaluation of atmospheric energy at different stages of cyclone viz., before cyclone, cyclone period and after landfall. Then it is interested to make an energy budget of the selected cyclones. It is also interested to show variation of different components of energy with time and pressure and their fluxes. The variation of different kind of energy components and their fluxes are very helpful to understand the comprehensive movement of cyclones in its different stages, specially at the landfall region.

# CHAPTER-3

## MATERIALS AND METHODOLOGY

## CHAPTER-3

### MATERIALS AND METHODOLOGY

In the present study we have selected seven cyclones occurred over Bay of Bengal in the last decade. Out of these seven cyclones three of them were April-May (pre-monsoon) cyclone and four of them were November-December (post-monsoon) cyclone.

We have collected the rawinsonde (RS) data from Bangladesh Meteorological Department (BMD) at different isobaric levels (1000 mb-100 mb) for Dhaka and Chittagong stations. Data were taken at "cyclone period" and for five days of "before occurrence" and for five days of "after landfall". Throughout the data the variables were temperature (T), dew-point temperature ( $T_d$ ), geopotential height (Z) in meter and wind speed  $V$ (m/s) and wind direction  $\alpha$ (in degree).

Tropospheric energies and their fluxes are calculated to make an energy budget and to show the direction of movement of the selected cyclones shown in Table 1.

Table 1 Date of different phases of the analyzed cyclones.

	Date		
	Before occurrence	Cyclone period	After landfall
Cyclone 1	01.05.90-04.05.90	05.05.90-09.05.90	10.05.90-13.05.90
Cyclone 2	11.12.90-15.12.90	16.12.90-18.12.90	19.12.90-23.12.90
Cyclone 3	20.04.91-24.04.91	25.04.91-30.04.91	01.05.91-05.05.91
Cyclone 4	24.04.94-28.04.94	29.04.94-03.05.94	04.05.94-08.05.94
cyclone 5	16.11.95-20.11.95	21.11.95-25.11.95	26.11.95-30.11.95
Cyclone 6	01.11.96-04.11.96	5.11.96-7.11.96	08.11.96-12.11.96
Cyclone 7	23.11.96-27.11.96	28.11.96-3.12.96	04.12.96-08.12.96

For each pressure level (1000 mb-100 mb), atmosphere energy components and their fluxes are calculated at the study period for each cyclone, using the following equations:

The sensible heat,  $SH = c_p T$

$$= 0.24(t+273) \times 10^3 \text{ cal/kg} \quad (1)$$

where  $c_p$  = specific heat at constant pressure

$$= 0.24 \times 10^3 \text{ cal/kg/}^\circ\text{C}$$

and  $t$  is in  $^\circ\text{C}$ .

The gravitational potential energy

$$\begin{aligned} PE &= gZ \\ &= 9.81 \times Z \text{ joule/kg.} \\ &= 2.34352 \times Z \text{ Cal/kg} \end{aligned} \quad (2)$$

Where  $Z$  is the geopotential in meter and  $g = 9.81 \text{ m sec}^{-2}$ .

If  $L$  is the latent heat of condensation and  $q$  is specific humidity then released heat in the atmosphere per unit mass by condensation is

$$LH = Lq \quad (3)$$

The specific humidity  $q$  can be determined as follows:

$$q = \frac{0.62197 e}{P - 0.37803 e} \quad (4)$$

where  $e$  is the actual vapor pressure and  $P$  is the atmospheric pressure.

The actual vapor pressure can be calculated by using Clausius-Clapeyron equation

$$\ln\left(\frac{e}{6.11}\right) = 18L\left(\frac{1}{273} - \frac{1}{T_d}\right) / 8.3144 \quad (5)$$

Where  $T_d$  is the dew point temperature in  $^\circ\text{K}$  and  $L$  is the latent heat.

Now latent heat is a function of temperature and is given by

$$LH = \{597.3 - 0.566(T-273)\} \times 10^3 \text{ cal/kg} \quad (6)$$



Where,  $T$  is the temperature of the parcel in  $^{\circ}\text{K}$ .

An air parcel acquired kinetic energy when it is in motion. Where a air parcel of unit mass moves with a speed of  $V$  cm/sec then

$$\text{Kinetic energy, } KE = V^2/2 \quad (7)$$

In the Meteorological observation wind speed is measured in knots. If  $V$  is the magnitude of wind vector, it can be converted into  $\text{cm sec}^{-1}$  as follows:

$$\begin{aligned} V_{\text{knots}} &= \frac{1 \times 6080.21 \times 12 \times 2.54 \times V}{60 \times 60} \text{ cm sec}^{-1} \\ &= 51.47911V \text{ cm sec}^{-1} \\ &= 0.5147911V \text{ m sec}^{-1} \end{aligned} \quad (8)$$

$$\begin{aligned} \text{Then } KE &= (51.47911)^2 V^2/2 \text{ erg/gm} \\ &= 0.1325049 V^2 \text{ Joule/kg} \\ &= 0.0316543 V^2 \text{ cal/kg} \end{aligned} \quad (9)$$

The zonal flux(ZF) of dry static energy(DSE) and moist static energy(MSE) and meridional flux(MF) of dry static energy(DSE) and moist static energy(MSE) are calculated by using the following equations:

$$ZFDSE = (C_p T + gz) u \quad (10)$$

$$MFDSE = (C_p T + gz + Lq) u \quad (11)$$

$$ZFMSE = (C_p T + gz) v \quad (12)$$

$$MFMSE = (C_p T + gz + Lq) v \quad (13)$$

where  $u$  and  $v$  are the zonal and meridional wind components respectively.

Wind components (zonal and meridional) are obtained as follows :

$$u = -V \sin \alpha$$

$$v = -V \cos \alpha$$

where  $V$  is the magnitude of the wind vector and  $\alpha$  is its direction. Since  $V$  is in knots,  $u$  and  $v$  are expressed in m/sec by the following equations

$$u = -(0.5147911)V \sin \alpha \text{ m sec}^{-1} \quad (14)$$

$$v = -(0.5147911)V \cos \alpha \text{ m sec}^{-1} \quad (15)$$

The variation of latent heat content and kinetic energy with time were obtained to see the changes of energy with time. The variation of these energy fluxes with time were also obtained to see the direction of movement with time of the cyclone. Next we have observed the variation of sensible heat, potential energy, latent heat content and kinetic energy with pressure at the three phases of cyclone such as before occurrence, cyclone period and after landfall to show the vertical profiles of these energies. We have also calculated the variation of zonal flux of dry static energy and moist static energy and meridional flux of dry static energy and moist static energy to show the vertical profiles of these fluxes and the direction of movement of the analyzed cyclones.

Then we have calculated the maximum, minimum and average of the energies mentioned above and total energy by arithmetic addition. Next we have made an energy budget to show a comparison of the seven observed cyclones. We have also calculated the maximum, minimum and average of the above mentioned fluxes and have made a comparison. Next we have also calculated the maximum, minimum and average of the above mentioned energies for Chittagong and Dhaka station and showed it graphically to make a comparison between these two stations. Finally, at surface level (1000 mb), the sensible heat, potential energy, latent heat content, kinetic energy and total energy at different phases of cyclone i.e., phase 1 (before occurrence), phase 2 (cyclone period) and phase 3 (after landfall) are calculated. The variation of temperature, wind speed and wind direction with time at these three phases are also observed.

The track of the analyzed cyclones is shown in Fig. 3.

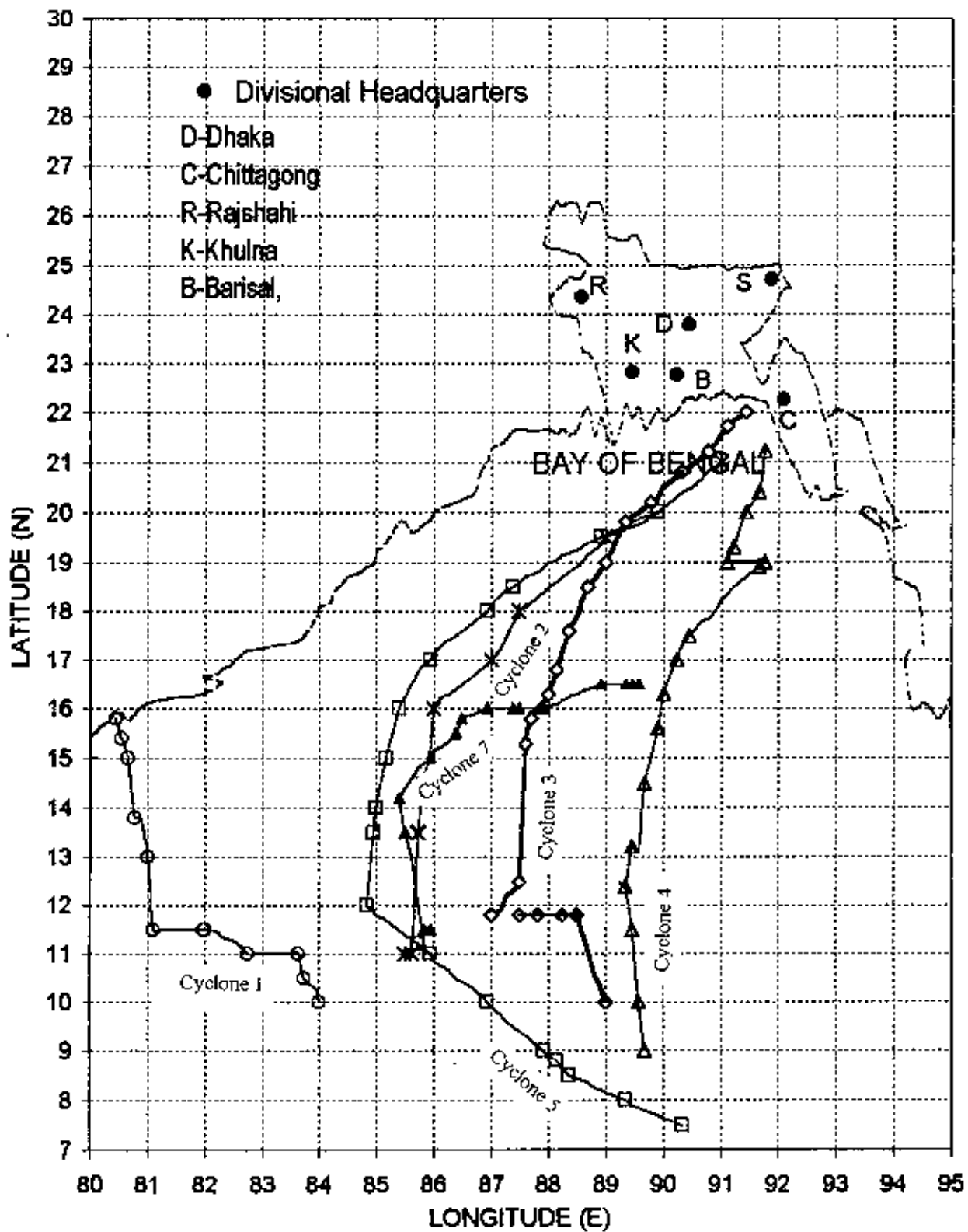


Fig. 3 Tracks of the analyzed cyclones.

# CHAPTER-4

## RESULTS AND DISCUSSION

## Chapter 4

### Results and discussion

#### 4.1 Variation of energy with time

##### 4.1.1 Energy Components

##### 4.1.1.(a): Latent Heat Content (LHC):

##### Cyclone 1

Fig. 4.1 (i-vii) shows the variation of Latent heat content (LHC) with time for seven cyclones occurred from 1990-1996. From Fig. 4.1(i) for cyclone 1 it is observed that at 1000 mb latent heat content was near about the same from 1st May to 8 May. It slightly increased on 9 May and maintained a constant value till 13 May. At 850 mb it decreased on 2 May and remain constant on 3 May. It again increased from 4 May and attained a constant value for 5-6 May. It again increased for one day and after 7 of May it decreased again up to 10 May. From 11 of May it further increased up to 13 May. At 700 mb, 400 mb, 300 mb and 250 mb LHC increased for 2 May and then decreased and remained constant up to 4 May. At 500 mb it decreased up to 4 May. After 4 May it again increased for two days i.e. from 5-6 May. On 7 May it further decreased for all levels (700, 400, 300, 250) but on 8 May it again increased. After 8 May it increased with fluctuation up to 13 May. From the above figure (Fig. 4.1(i)) it is observed that latent heat increased at the time of landfall (10-13 May). This was because during landfall more cloud formed and released Latent heat. Latent heat content was also large at cyclone period (5-9 May 1990).

##### Cyclone 2

It is found that LHC was almost constant at 1000 mb-700 mb from 11-16 December for cyclone 2 [Fig. 4.1(ii)]. It then increased from 16-18 December i.e., during cyclone period. Beyond 18th December it decreased on 19th December and then attained a constant value up to 23 December i.e. after landfall. At levels 500-250 mb, LHC increased at first on 12 December and then it decreased on 13 December. It increased on 14 December and they maintained a constant value up to 16th of December. From 16-18 December (i.e., during cyclone period) LHC increased for all levels. But for levels 300 and 250 mb it was very significant. It reached its highest value on 18th December (i.e., at

the end of cyclone). After 18th December it decreased and attained a constant value and continued up to 23rd of December. But at 22 December it slightly increased.

### Cyclone 3

The variation of Latent heat content (LHC) with time is shown in Fig. 4.1(iii) for cyclone 3. It is found that on 20-23 April, LHC fluctuated for every day. Beyond 23rd April it remained constant on 29th April, and then slightly decreased on 30 April (i.e., at the end of cyclone period). After landfall it slightly increased and remained constant value up to 5 May (at the end of landfall). At 850 mb-700 mb it fluctuated every time. At 500 mb every time LHC increased or decreased up to 29th April. From 29 April to 1 May it was almost same and then abruptly decreased on 2 May and then fluctuated. At 400 mb it is seen that LHC fluctuated up to 26th April. Beyond 26 April (cyclone period) it increased gradually and then remained constant up to 1 May (at the end of cyclone). During landfall (2 May) it decreased suddenly and then fluctuated. At 300 mb LHC was maximum on 25 April (i.e. when cyclone is just formed) and 1st May (during landfall). It is seen that LHC was maximum for all levels (except 1000 mb and 850 mb) on 25 April (i.e., at the starting of cyclone) and also two peaks are found on 1 May for levels 300 mb and 250 mb. It is also observed that LHC was maximum at levels 500 mb-250 mb i.e. at the middle troposphere. This was because middle troposphere is the cloud forming zone.

### Cyclone 4

Fig. 4.1(iv) shows the variation of latent heat content (LHC) with time for cyclone 4. It is found that LHC was almost same for levels 1000 mb-700 mb on 24 April. On 25 April it increased a little bit at 1000 mb and 700 mb but it decreased at 850 mb up to 29 April. Beyond 28 April LHC was almost constant up to 8 May at levels 1000 mb-700 mb. At levels 500 mb-250mb, LHC was fluctuated for first three days (24-26 April). After 26 April it increased rapidly but on 29 April it decreased sharply. Beyond 30 April it again increased up to 2 May and then again decreased up to 5 May. After 5 May it increased and then decreased up to 8 May. From the figure [Fig. 4.1(iv)] it is seen that at levels (500 mb-250 mb) LHC was fluctuated i.e. at time to time it increased and decreased. This was

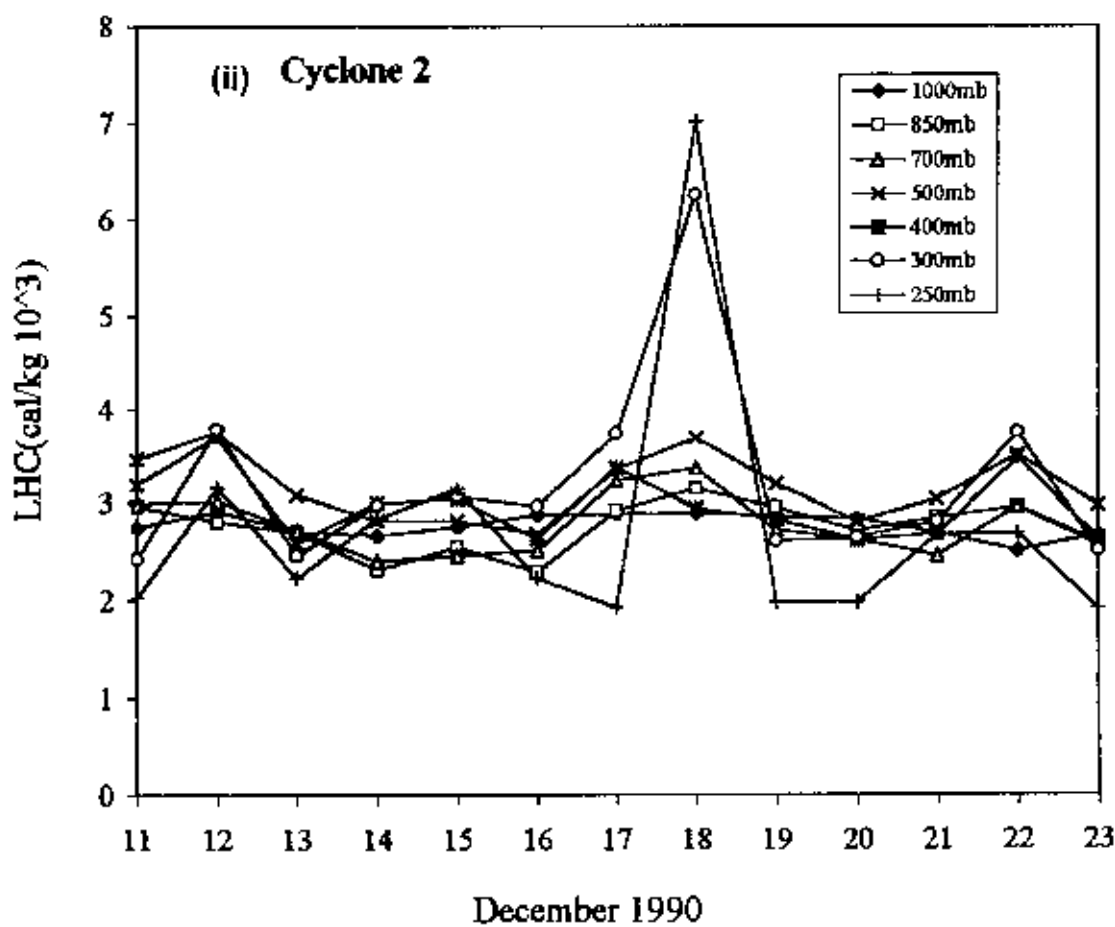
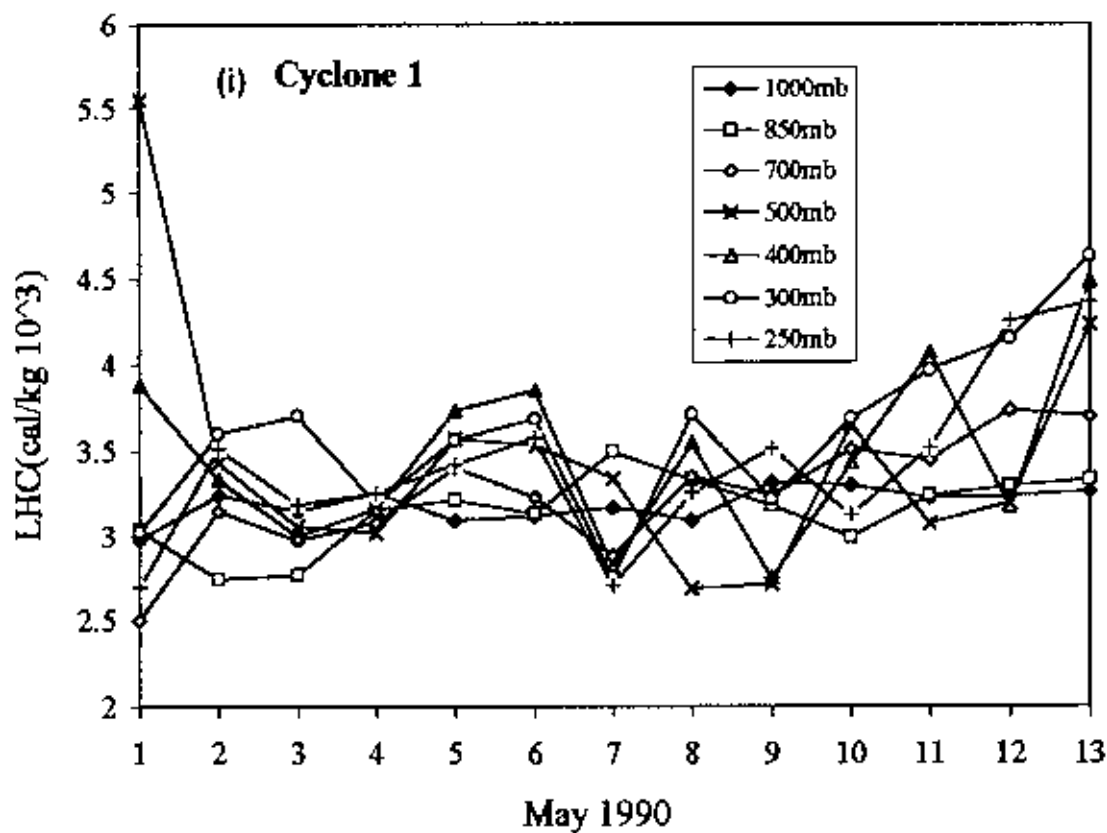
because 500 mb-250 mb is the cloud forming zone and when cloud is formed it increased and when rainfall occurs it decreased.

### Cyclone 5

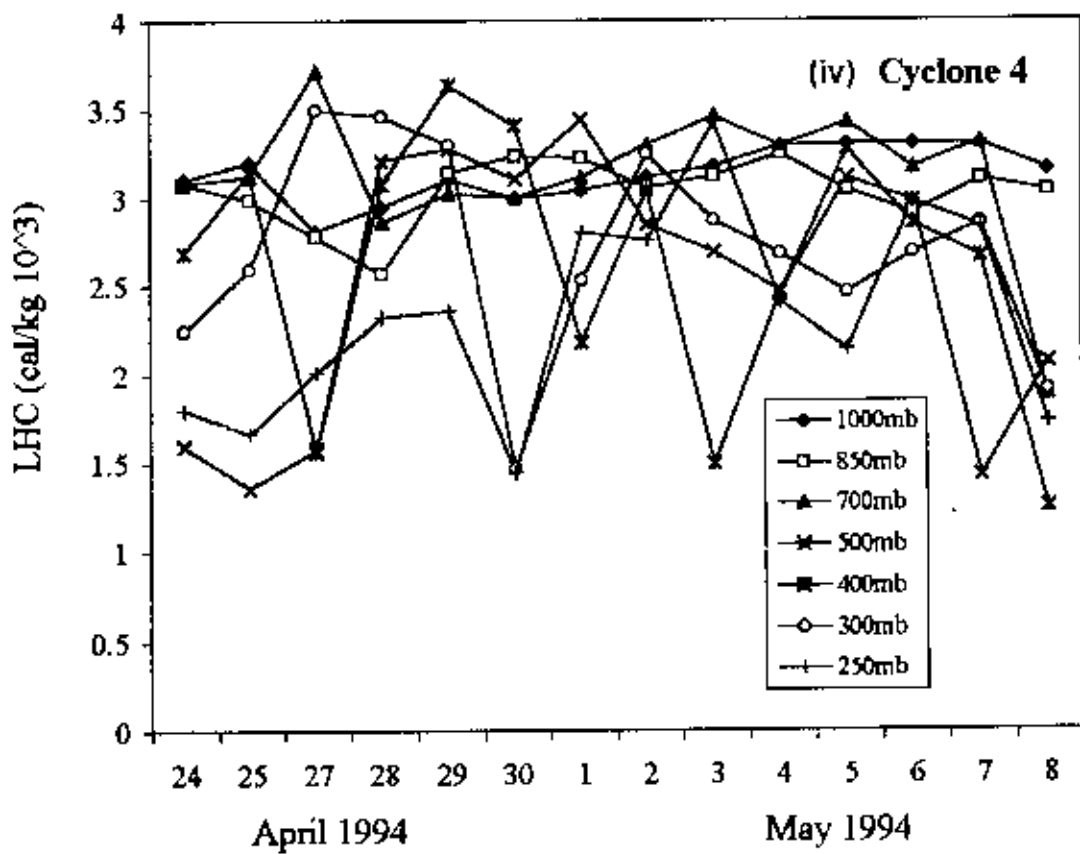
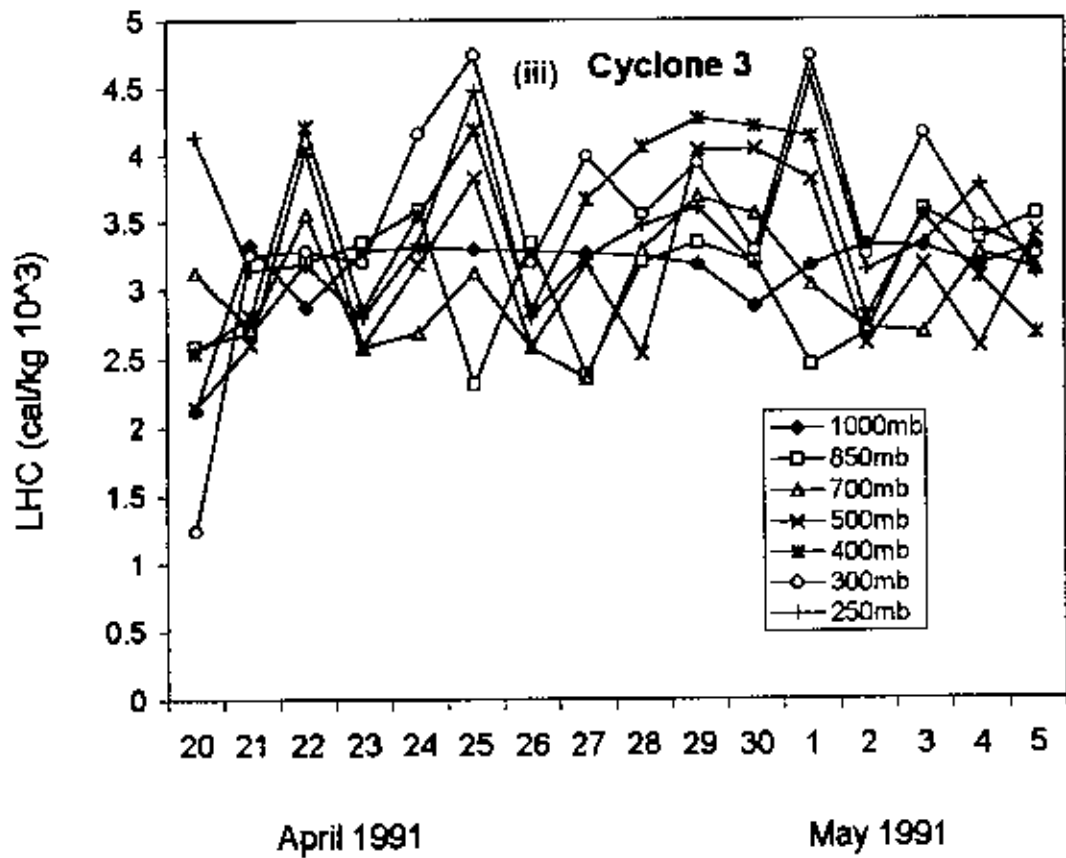
For cyclone 5 the variation of latent heat content with time is shown in Fig. 4.1(v). It is seen that LHC was linearly decreased from 16-22 November at 1000 mb and then it increased from 22-25 November (cyclone period) and then decreased and maintained the same value at the end of landfall. i.e. up to 30 November. From 16-22 November, it is seen that for all the levels (except 1000 mb) LHC was more or less same with time except 18, 19, 21 and 22. On 18th November at 400 mb it increased abruptly and on 19 November it decreased rapidly. On 21-28 at 700 mb and 400 mb it sharply increased and attained maximum value on 21 November (at the starting of cyclone) and then decreased on 22 November. But it is seen that on 22-25 November (cyclone period) LHC was gradually increased for all the levels and decreased on 26 November. Beyond 26 November there was no variation of LHC with time i.e., after landfall (27-30 November) it was almost same for all the days. From this figure it is seen that LHC gradually increased during cyclone period and was maximum at the starting of cyclone (21 November) at 700 mb. So we can conclude that for cyclone more cloud is formed at cyclone period and heavy rainfall occurs.

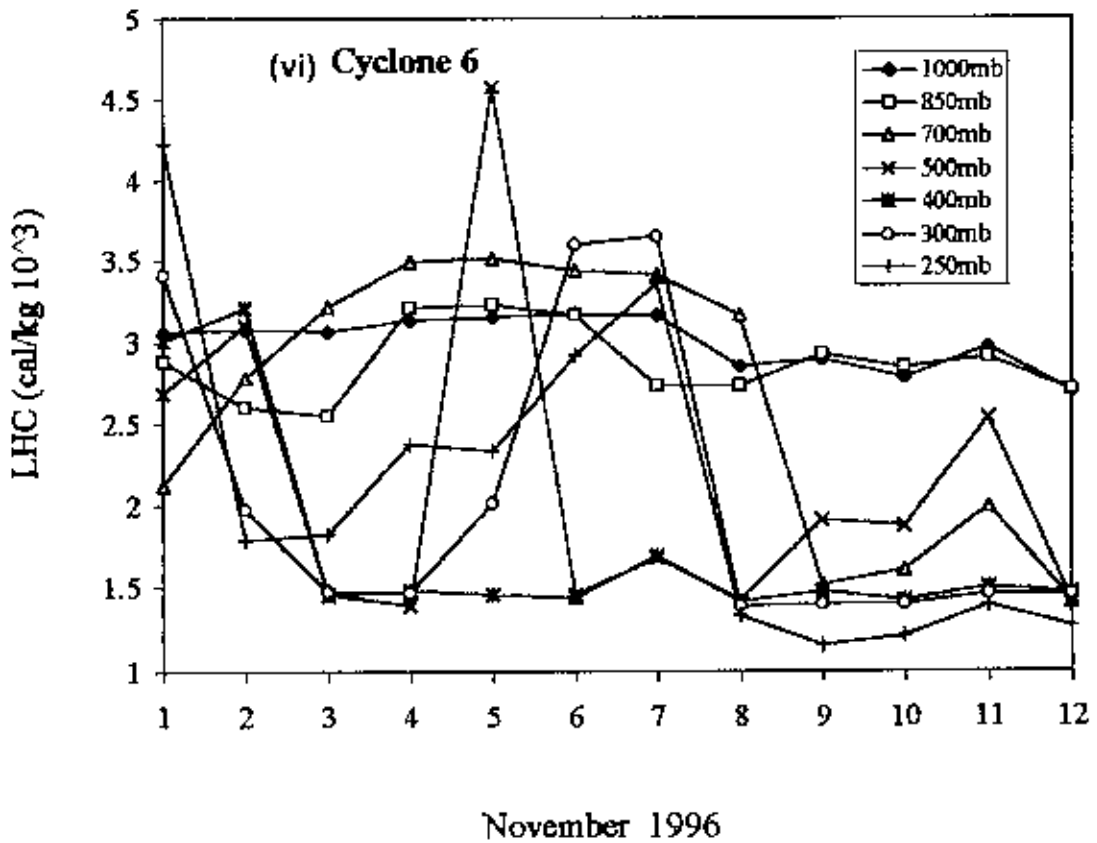
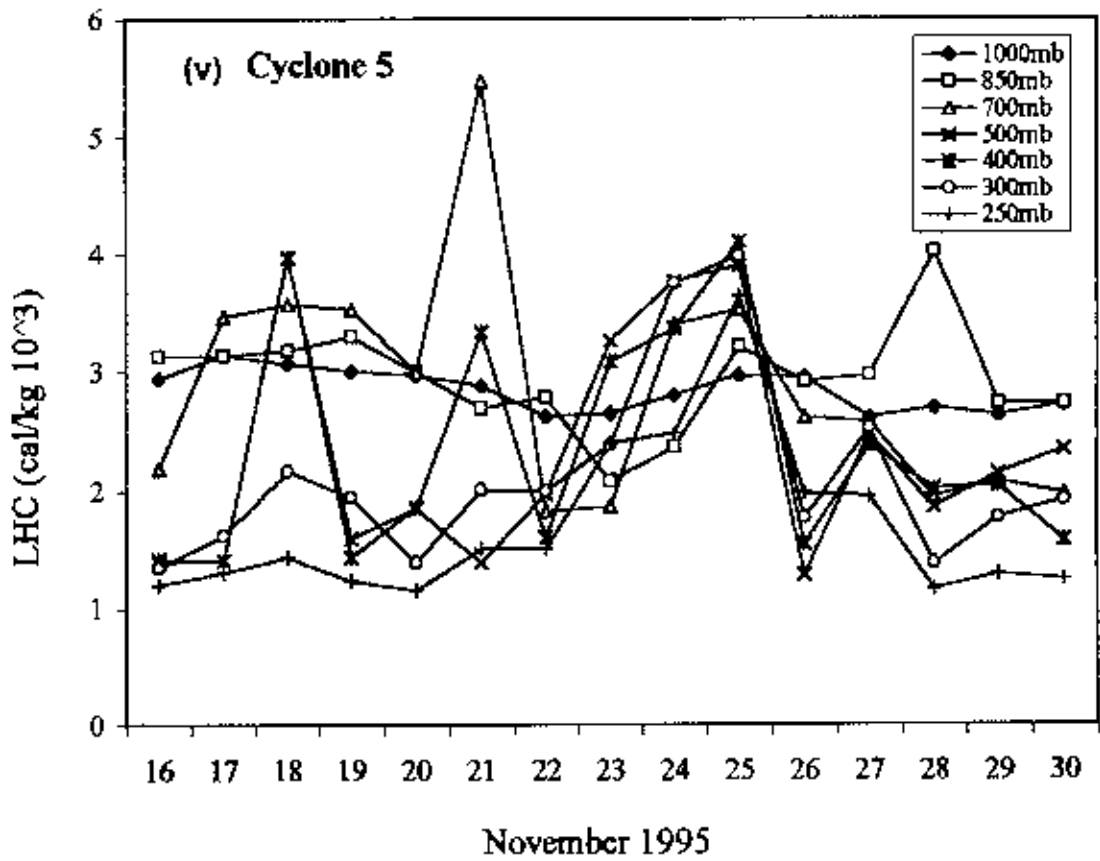
### Cyclone 6

Fig. 4.1(vi) shows the variation of Latent heat content with time for cyclone 6. From this figure it is observed that latent heat content was same on 1-7 November 1996 at level 1000mb. It slightly decreased on 8 November and continued with small fluctuation up to 12 November. At level 850mb it decreased on 1-3 November, then it increased on 4 November and remain constant up to 6 November. After 6 November it decreased slightly on 7 November and then increased slightly up to 9 November. Beyond 9 November LHC was almost same for all the days i.e. 9-12 November. At level 700 mb it increased gradually with time on 1-4 November (before cyclone) and then remain constant for 4-7









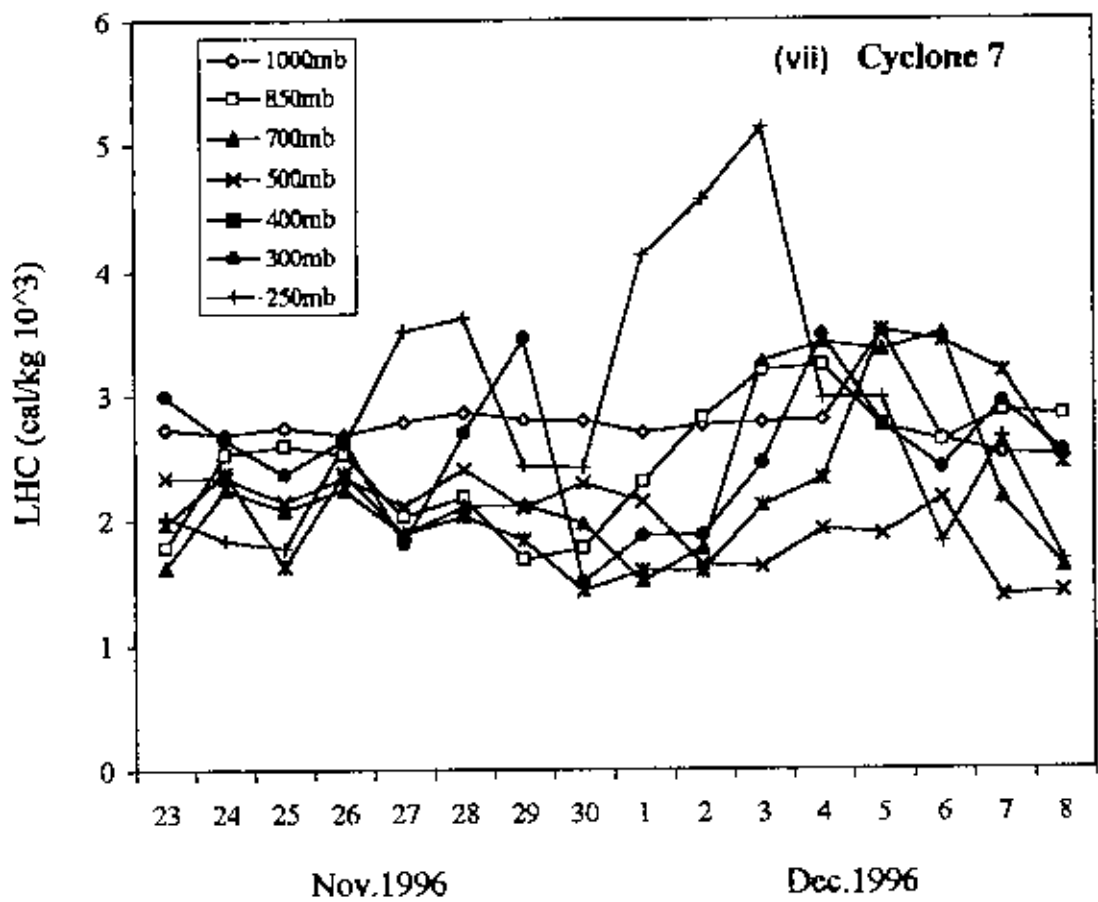


Fig. 4 (i-vii). Latent heat content variation with time for cyclone 1-cyclone 7.

November (cyclone period) and then decreased sharply on 9 November. Beyond 9 November it increased slightly up to 11 November.

At 500 mb it increased from 1-2 November. But on 3 November it decreased largely and then remained constant up to 4 November. On 5 November it increased suddenly and attained maximum value. After 6 November it increased gradually with fluctuation up to 11 November and then decreased. At 400 mb LHC increased for first two days and then abruptly decreased on 3rd November. After 3rd November it was almost constant at the end of landfall i.e. up to 12 November except 7 November. On 7 November it slightly increased. At 300 mb LHC gradually decreased with time up to 4 November (before cyclone). After 4 November it increased gradually up to 7 November (cyclone period) and then decreased largely on 8 November. After 8 November it was almost same for all the time (i.e., after landfall). At 250 mb it is seen that LHC decreased for first two days. But from 3-7 November (cyclone period) it increased gradually at time to time. On 8 November it decreased abruptly and then increased up to 11 November and then decreased.

From the above figure [Fig. 4.1(vi)] it is seen that LHC was same during cyclone period (5-7 November) for levels 1000 mb-700 mb. But at 700 mb it increased gradually before cyclone (1-4 November). For level 250 mb LHC increased gradually during cyclone period. On 5 November (at the beginning of cyclone) it was maximum at 500 mb. After landfall it was more or less constant with time for all the levels (except 700 mb and 500 mb).

### Cyclone 7

Fig. 4.1(vii) shows that at 1000 mb LHC was almost constant for all the days (except 5 November) i.e. there was no variation with time. At 850 mb it increased for first two days (23-24 November 1996), then remained constant up to 26 November and then decreased up to 29 November. But from 29 November to 4 December LHC increased gradually with time and then decreased on 5 December. Beyond 5 December it was almost same. At 700 mb it was almost constant from 23 November to 1 December 1996. From 2 December it increased with time up to 6 December. After 6 December it decreased till 8

December. From 500 mb-300 mb LHC changed with a small fluctuation from 23 November to 30 November. After 30 November it increased gradually up to 6 December and then decreased. At 250mb it decreased from 23-25, November then it increased from 26-28 November and then decreased up to 30 November. After 30 November it increased gradually with time and attained the maximum value on 3 December ( i.e., at the end of cyclone) and then decreased till 8 December.

From the above figure [Fig. 4.1(i-vii)] it is seen that at 1000 mb there was no change of LHC with time. At levels 500-300 mb, LHC increased from 30 November to 6 December (i.e., from cyclone period to landfall) i.e. at that time cloud is formed. It is also seen that at 250 mb it was maximum at 3 December (at the end of cyclone).

#### 4.1.1.(b): Kinetic energy (KE):

##### Cyclone 1

Fig. 4.2 (i-vii) shows the kinetic energy (KE) variation with time at different isobaric levels from 1000-100mb. From Fig. 4.2(I) for cyclone 1, it is observed that at levels 1000-400 mb KE was very low (0-0.1) and it was almost same for all the days i.e., there was no variation of KE with time at lower troposphere. At levels 300-100 mb KE increased and fluctuated randomly. For all the levels (except 1000-700 mb) KE increased on 8 May (at the end of cyclone). It is seen that at 150 mb upper troposphere) KE was maximum on 5 May i.e. at the starting of cyclone. It is also seen that after 10 May it decreased for all the levels and close to zero on 13 May.

##### Cyclone 2

Fig. 4.2(ii) shows the variation of KE with time for cyclone 2. It is observed that from Fig 4.2(ii) at levels 1000-700 mb, KE was nearly zero for all the time i.e. at these levels KE was not change with time. At levels 500-400 mb it was very low and remained constant at every time. At levels 300-100 mb it increased and fluctuated due to change of wind velocity. It is also seen that for 250 mb there were two peaks on 18 December (at the end of cyclone) and 22 December (after landfall) because of maximum wind speed.

### Cyclone 3

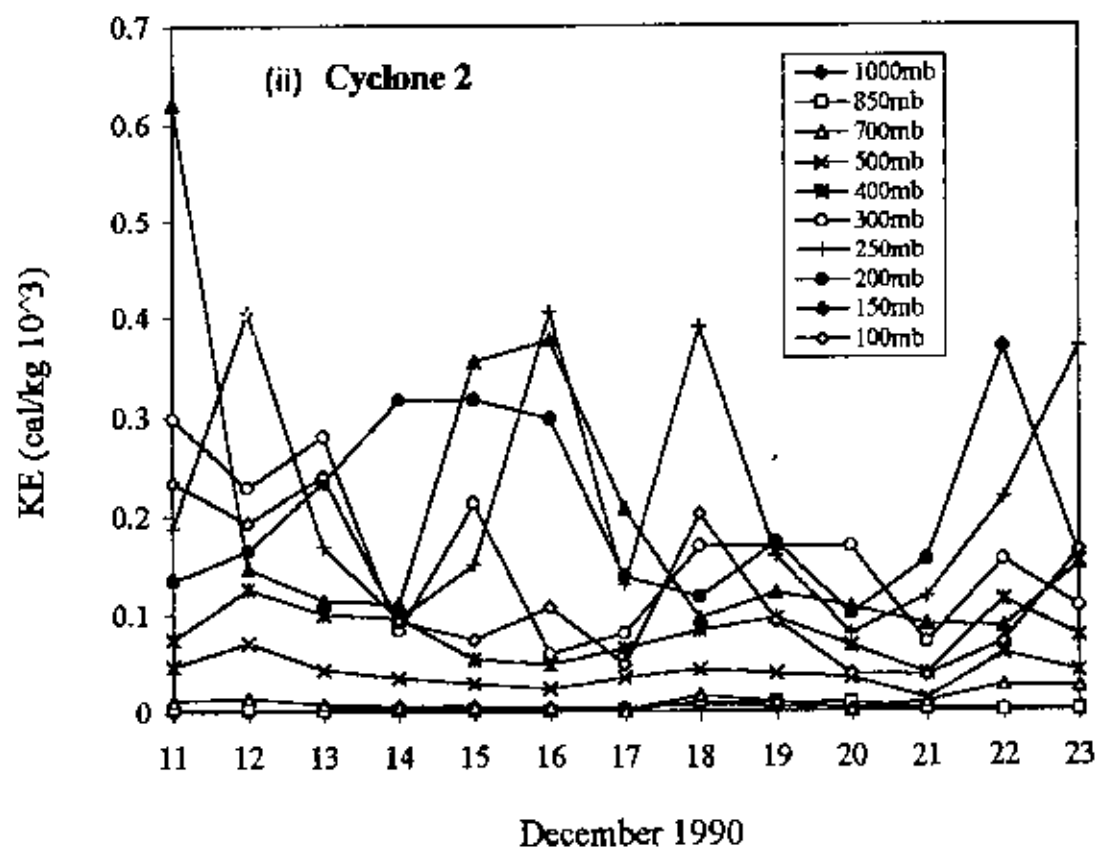
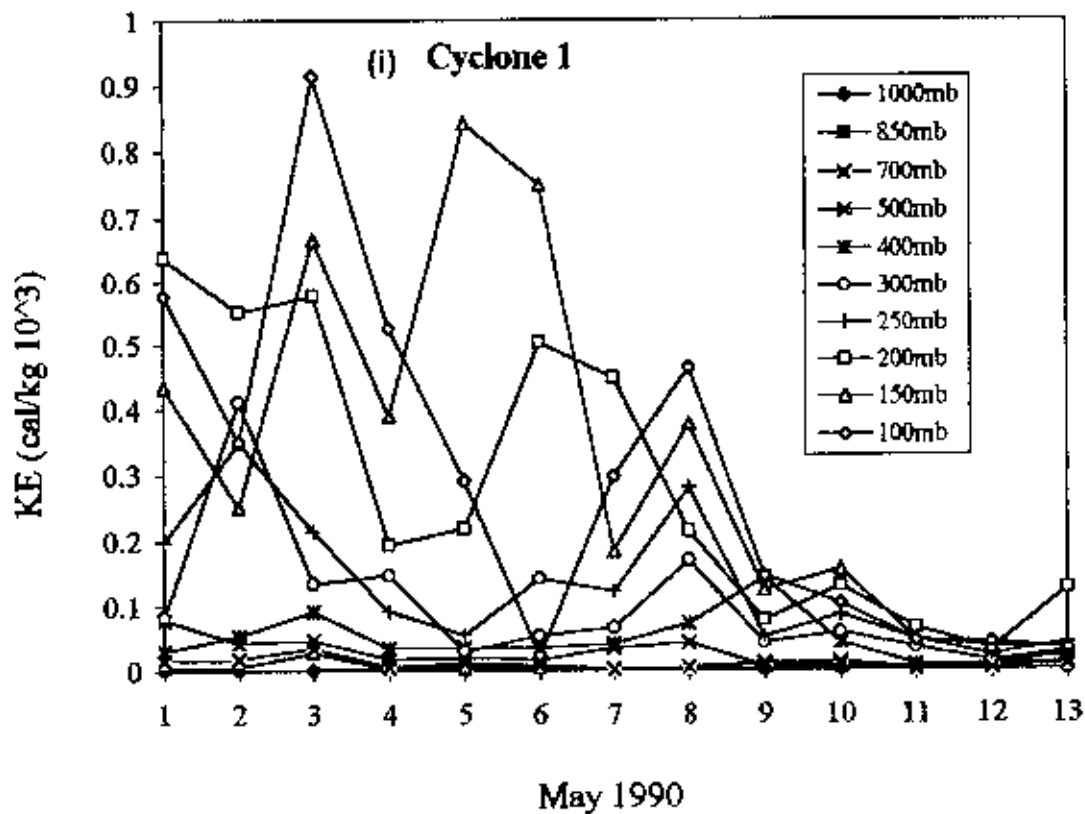
Fig. 4.2(iii) shows the variation of KE with time at different isobaric levels from 1000-100 mb for cyclone 3. It is seen that KE was very low and near about zero for all the time at levels 1000-400 mb. From 250-100 mb it increased with fluctuation at time to time. At 150 mb it is observed that KE gradually increased from 23 April 1991 and was maximum at 25 April (at the starting of cyclone) and then decreased. At the end of landfall (5 May) it decreased to nearly zero for all the levels.

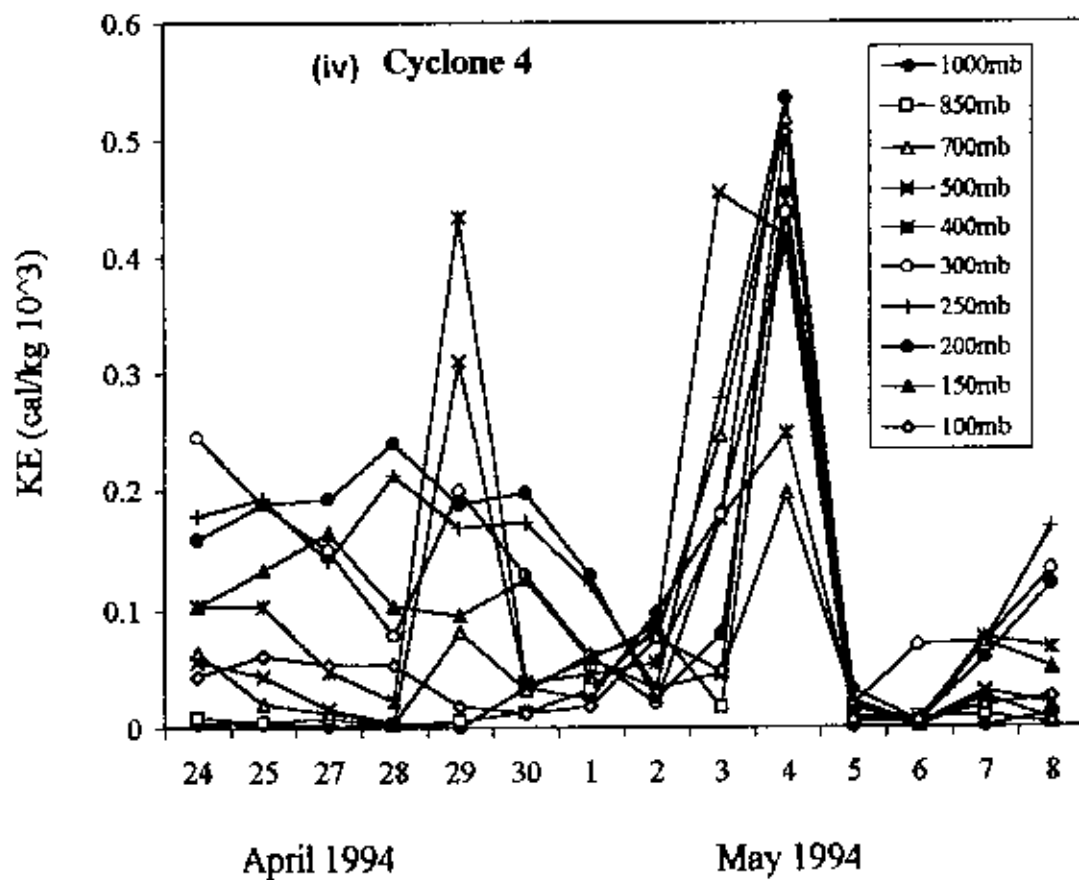
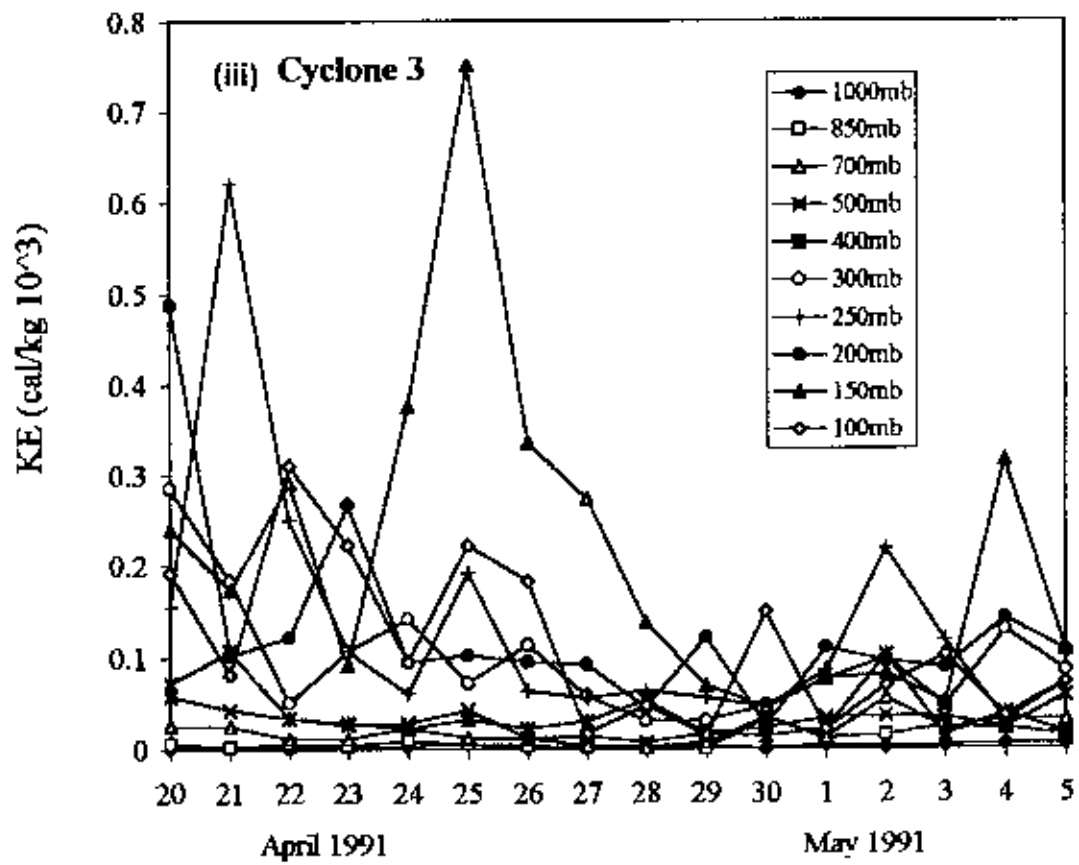
### Cyclone 4

The variation of kinetic Energy (KE) with time is shown in figure 4.2(iv) for cyclone 4. At 1000-850 mb, KE was zero from 24-29 April 1994 and then increased. At 700-100mb KE increased and decreased i.e. fluctuated from 24 April - 2 May. On 29 April (when cyclone is started) KE attained maximum value at 500-400 mb and showed a sharp peak. After 2 May, KE increased for all the levels and was maximum at 4 May (i.e., at the time of landfall) and then decreased. At the time of landfall (4 May) KE was maximum for all the levels due to high wind speed and showed a sharp peak.

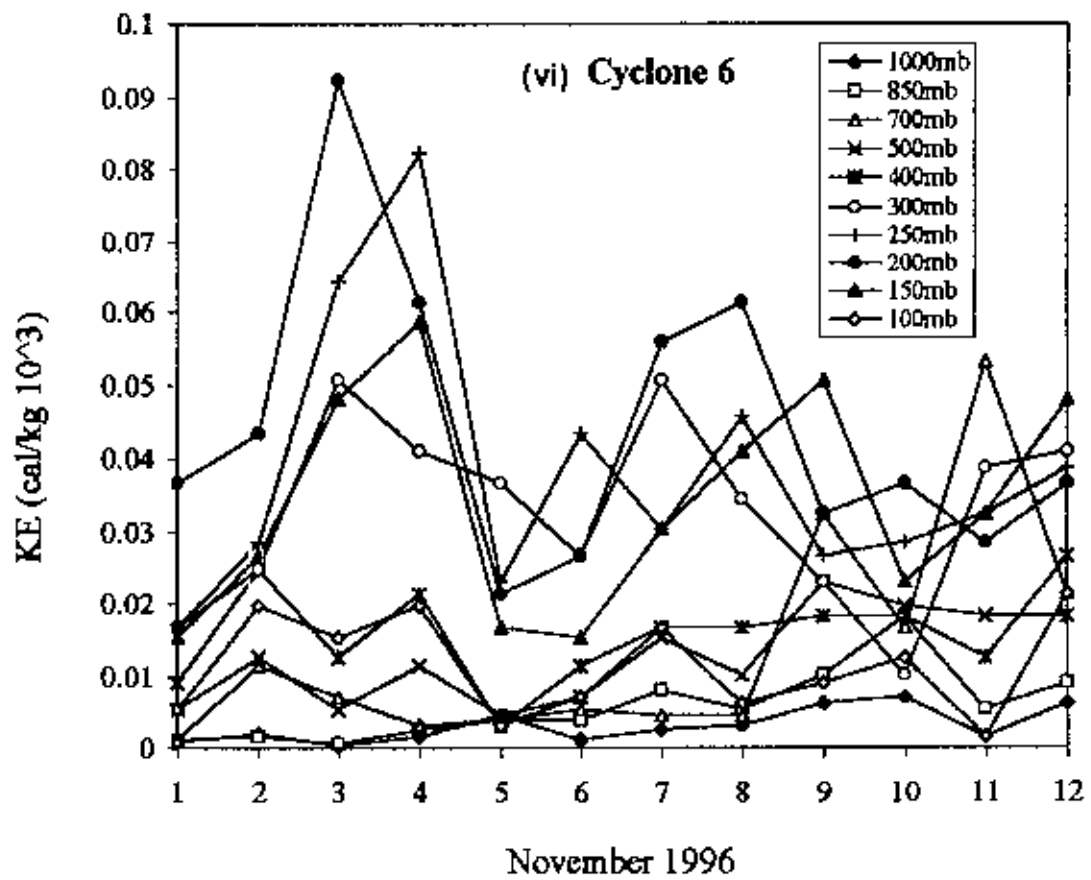
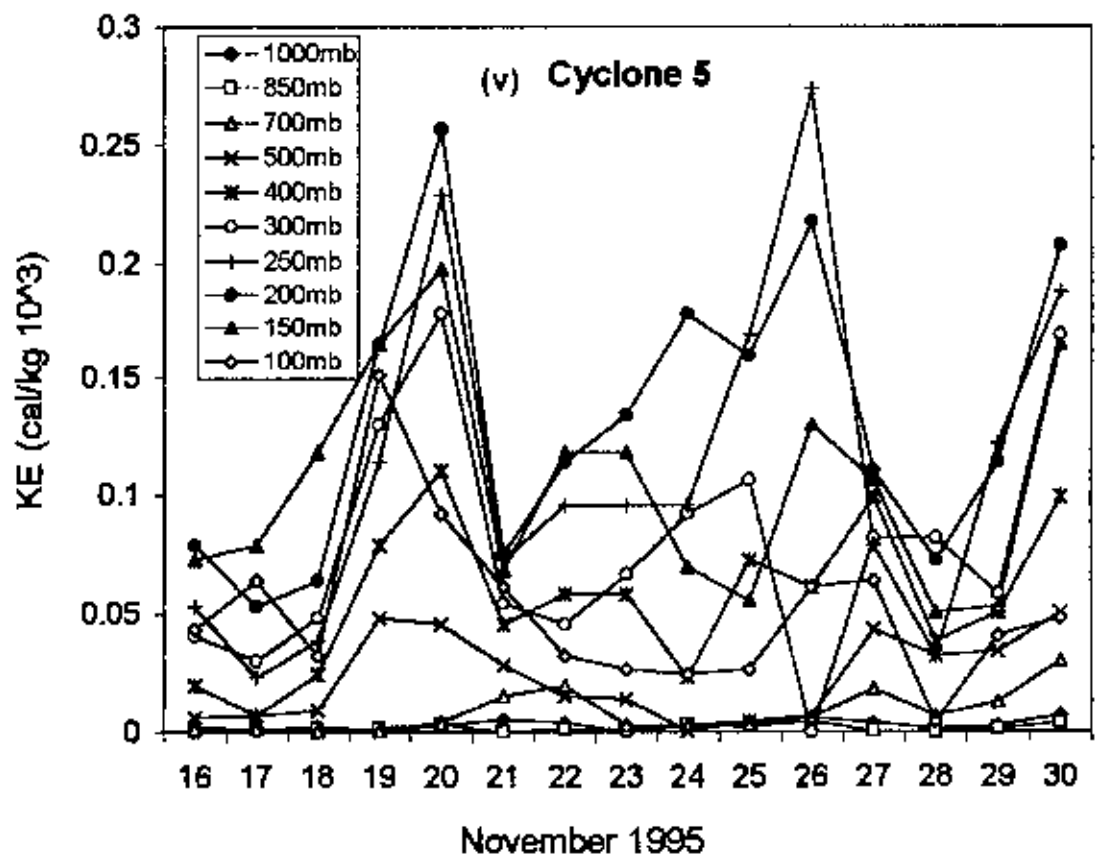
### Cyclone 5

Fig. 4.2(v) shows the variation of KE with time at different isobaric levels for cyclone 5. It is observed that KE was nearly zero for all the time at levels 1000-700mb i.e. in the lower troposphere. For first two days KE was about same at levels 500-100mb. It significantly increased from 18-21 November and it attained its highest value at 20 November (just before cyclone). It is observed that for all the levels KE decreased at 21 November, then it again increased gradually and it reached its highest value at 26 November (during landfall). Beyond 26 November it again decreased. Two maximum peaks are observed in this study: one was 20 November i.e., just before cyclone and the other was 26 November i.e., during landfall.









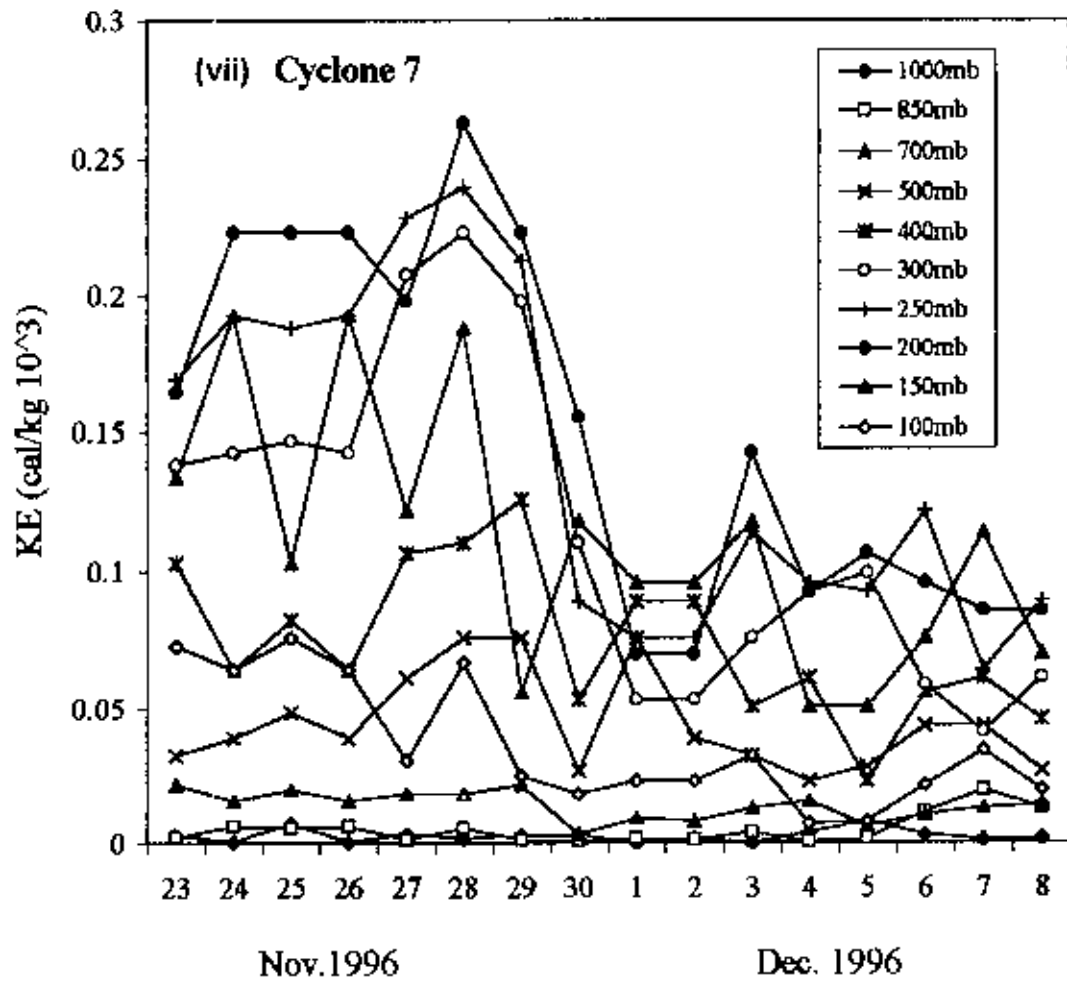


Fig. 4.2(i-vii). Kinetic energy variation with time for cyclone 1-cyclone 7.

### Cyclone 6

The variation of KE with time is shown in figure 4.2(vi) for cyclone 6. It is seen that at levels 1000 mb and 850 mb, KE was nearly zero for first three days. Beyond 3 November it increased gradually a little bit up to 12 November. At 200mb, all the time, it increased slightly. At 500-300 mb it fluctuated with time to time i.e., at these levels wind speed changed with time to time. At 250-100 mb KE increased gradually from 1 November and attained maximum at 3 November. Beyond 3 November it decreased (except 250 mb) up to 5 November. After 5 November it increased till 8 November and then decreased. It is seen that during cyclone period (5-7 November) KE increased for all the levels (1000-100 mb) and was maximum at 200 mb i.e., at the upper level of the troposphere.

### Cyclone 7

The variation of KE with time is shown in Fig. 4.2(vii) for cyclone 7. From this Fig. it is observed that KE at lower troposphere (1000-700 mb) was minimum and constant with time. At middle to upper troposphere (500-100 mb) it fluctuated. At levels 300-200 mb it is seen that KE was constant on 24-26 November then it increased and reached its highest value at 28 November (at the starting of cyclone) and then decreased up to 1 December.

After 1 December it was almost same. At 150mb (upper troposphere) it is observed that there was large fluctuation in every time. This was because at the upper troposphere light air was there and every time wind speed changed largely.

From Fig. 4.2(i-vii) it is observed that at lower troposphere (1000-700 mb) KE was very low (near about) and was not change with time. KE increased from middle to upper troposphere and changed with time.

It is seen that KE was maximum at the upper troposphere i.e. 250-100 mb. It is seen that for some cyclone KE was maximum just before cyclone, most of the cyclone it was maximum during cyclone period. For some cyclone it was maximum at the time of landfall.



### 4.1.2 Energy Fluxes

#### 4.1.2.(a): Zonal Flux of Dry static Energy (ZFDSE):

##### Cyclone 1

Fig. 4.3(i-vii) shows the variation of zonal flux of dry static energy (ZFDSE) with time at different isobaric levels. For cyclone 1 [Fig. 4.3(i)] it is observed that at 1000 mb zonal flux of dry static energy was near about zero for first three days i.e. 1-3 May 1990, then it fluctuated from positive (eastward) to negative (westward) and vice-versa. At 850 mb it was positive (eastward) for all the days except on 4-5 May. Only for these two days (4-5 May) it was negative (westward). At levels 700-100mb it was completely positive (eastward) for all the time. At 700-400 mb, ZFDSE was same for all the time. This was because at these levels there was no change of zonal wind component. At 300 mb and 250 mb it is observed that ZFDSE decreased from 2-5 May, but at cyclone period (5-9 May) it increased due to increased zonal wind component and then decreased. At 200-100 mb it is seen that ZFDSE increased and decreased with time. This means that every time zonal wind component changed in the upper troposphere. It is also observed that it was maximum on 3 May at 100 mb and on 5 May (at the starting of cyclone) at 150 mb. This maximum ZFDSE means that at the upper troposphere zonal wind component was maximum at that day. After 9 May (at the time of landfall) it decreased for all the levels and then remained constant (i.e., no change of wind speed).

##### Cyclone 2

Variation of zonal flux of dry static energy with time is shown in Fig. 4.3(ii) for cyclone 2. It is observed that zonal flux of dry static energy (ZFDSE) fluctuated from positive (eastward) to negative (westward) and vice-versa at levels 1000 mb and 850 mb from 11-23 December 1990. At 700mb-400 mb, ZFDSE was near about same for all the time i.e. there was no change of wind speed at these two levels. From level 300-100mb it fluctuated randomly. It is also seen that on 16 December (at the starting of cyclone) and 18 December (at the end of cyclone) its intensity was highest at 250 mb.

### Cyclone 3

Variation of zonal flux of dry static energy with time is shown in Fig. 4.3(iii) for cyclone 3. From this figure it is observed that at level 1000 mb, ZFDSE changed from positive (eastward) to negative (westward) and vice-versa up to 29 April. After 29 April it was zero up to 4 May and then turned into negative (westward) on 5 May. At 850 mb it was positive (eastward) and remained constant with time up to 26 April and then turned into negative (westward) for two days (27-28 May). After 29 May it turned into positive (eastward) and increased slightly. At 700 mb it was positive (eastward) and remained same up to 26 April, then decreased and turned into negative (westward) on 29 April. Beyond 29 April it turned into positive (eastward) and increased gradually up to 5 May. At 500 mb and 400 mb ZFDSE was same up to 28 April and then it became minimum on 29 April. After 29 April it increased gradually up to 5 May. For level 300-100 mb, ZFDSE changed with time with a small fluctuation. Here it is seen that at the upper troposphere (300-100 mb) ZFDSE changed with time due to change of zonal wind component. At 150 mb it significantly increased from 23 April -28 April and was maximum when cyclone is just started (i.e., on 25 April).

### Cyclone 4

From Fig. 4.3(iv) it is observed that at 1000 mb, ZFDSE was nearly zero and changed a little bit from positive to negative and vice-versa. At 850 mb, first it decreased and then turned into negative (westward) up to 2 May. After 2 May it turned into positive (eastward) and increased gradually up to 8 May. At levels 700-100 mb it is observed that ZFDSE was more or less decreased gradually with time and was minimum on 3 May (at the end of cyclone). After 3 May it increased gradually from 3-8 May (i.e. after landfall).

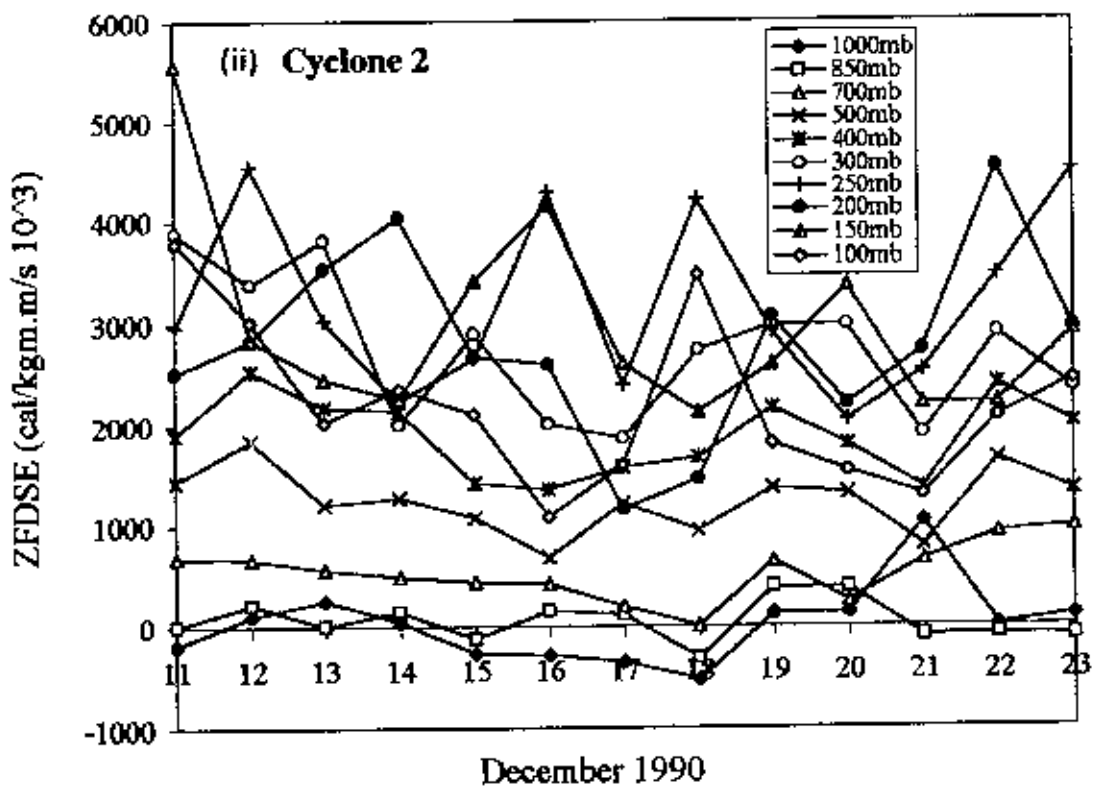
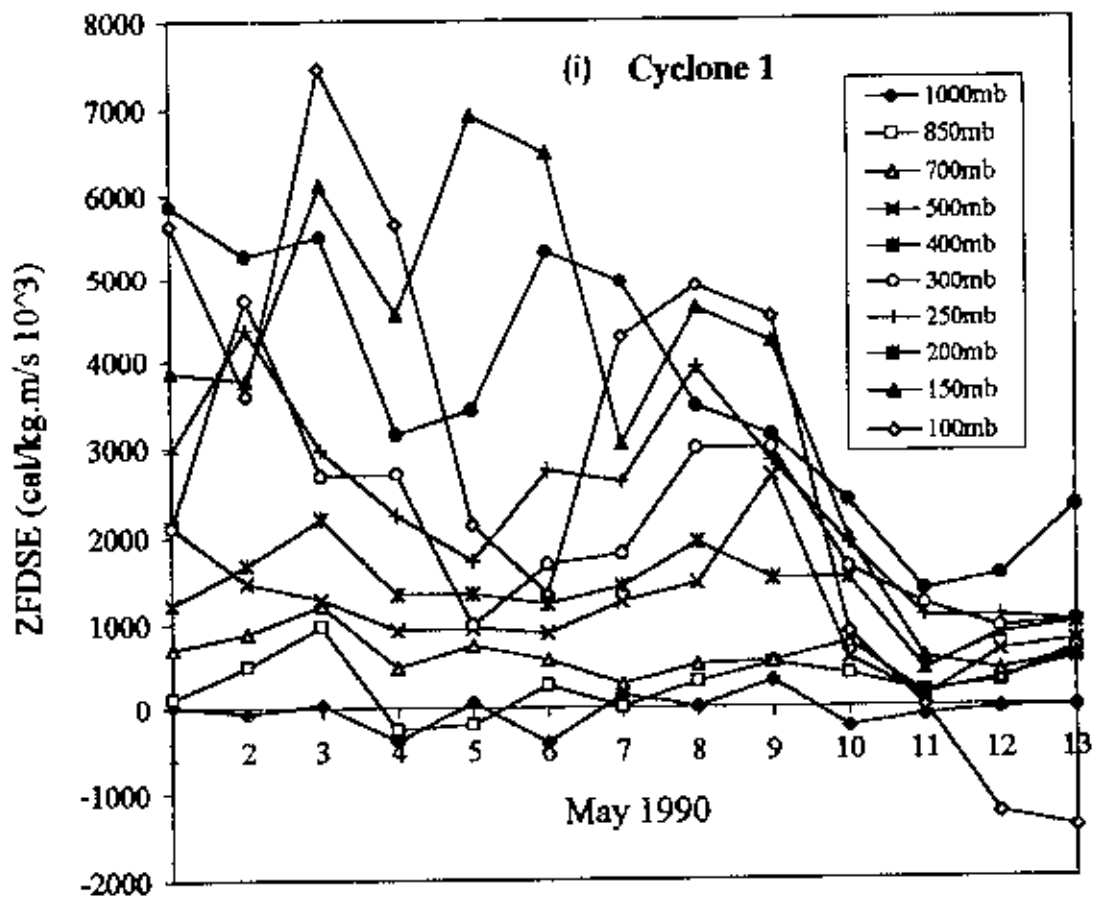
From this figure [Fig. 4.3(iv)] it is observed that at the time of landfall ZFDSE increased. This means that during landfall wind speed increased. At 150 mb it is also observed that on 30 May (cyclone period) ZFDSE was maximum at the upper troposphere (150 mb).

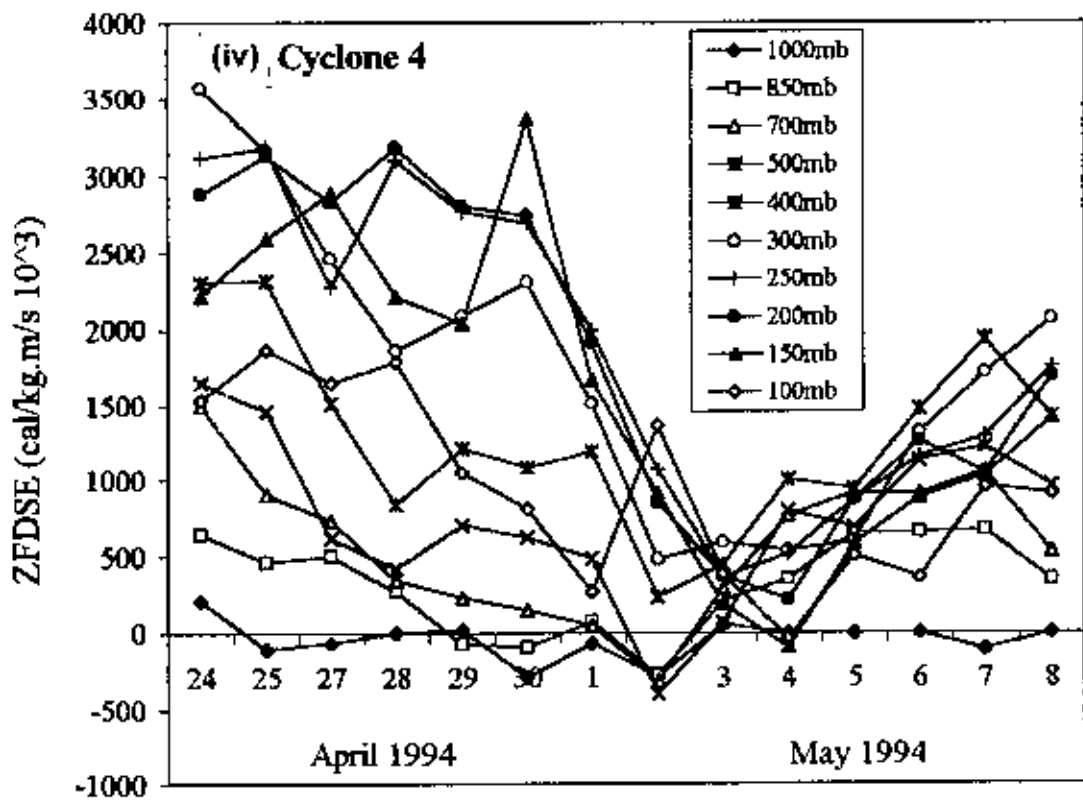
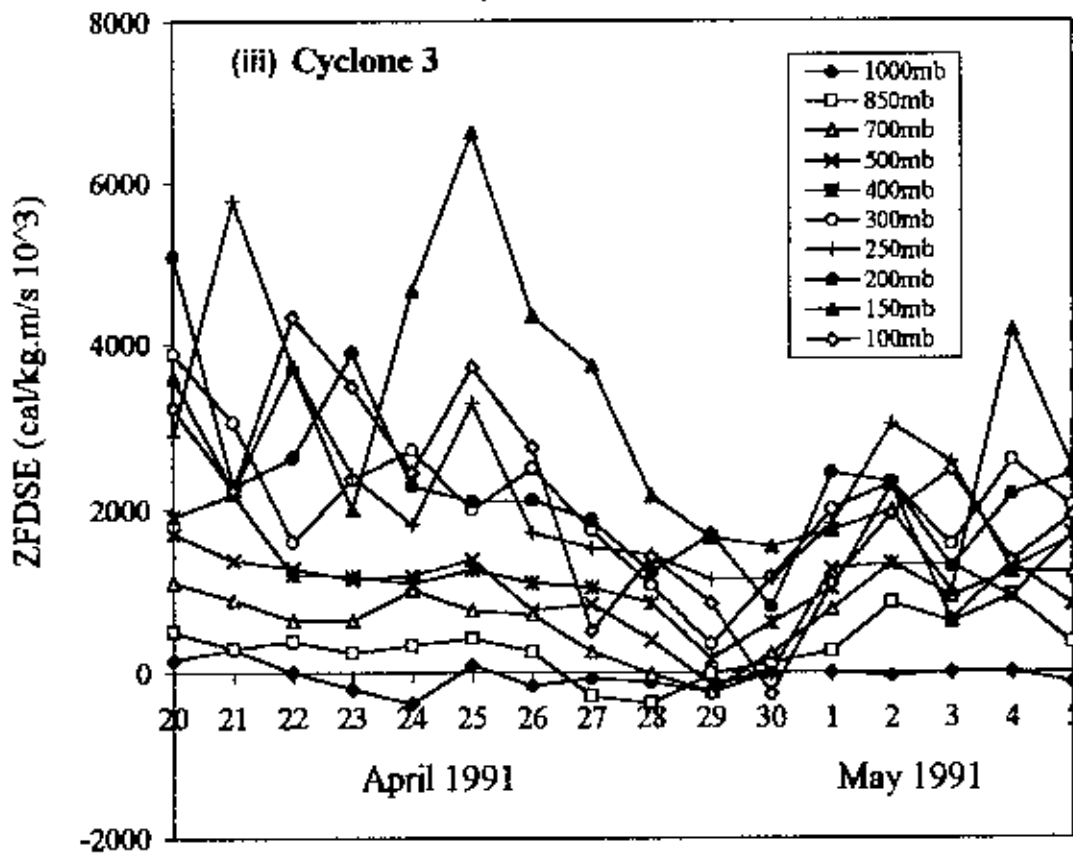
### Cyclone 5

Variation of zonal flux of dry static energy with time is shown in Fig. 4.3(v) for cyclone 5. From Fig. 4.3(v) it is observed that zonal flux of dry static energy was nearly same with time at the lower level of the troposphere (1000 mb and 850 mb) i.e., at these levels wind speed was nearly constant in all time but its direction changed from positive (eastward) to negative (westward) and vice-versa. At 700 mb, it was nearly zero up to 10 November and then increased up to 22 November (Cyclone period). Beyond 22 November, it gradually decreased with time and attained minimum value at 25 November (at the end of cyclone). After 25 November, it increased gradually up to 30 November. At 500-100 mb it is seen that ZFDSE increased from 17 November and attained maximum value on 20 November (just before cyclone). It is also observed that for all the levels ZFDSE was minimum on 25 November (at the end of cyclone) and it increased gradually beyond 25 November i.e., during landfall. From this figure it is observed that during landfall wind speed increased.

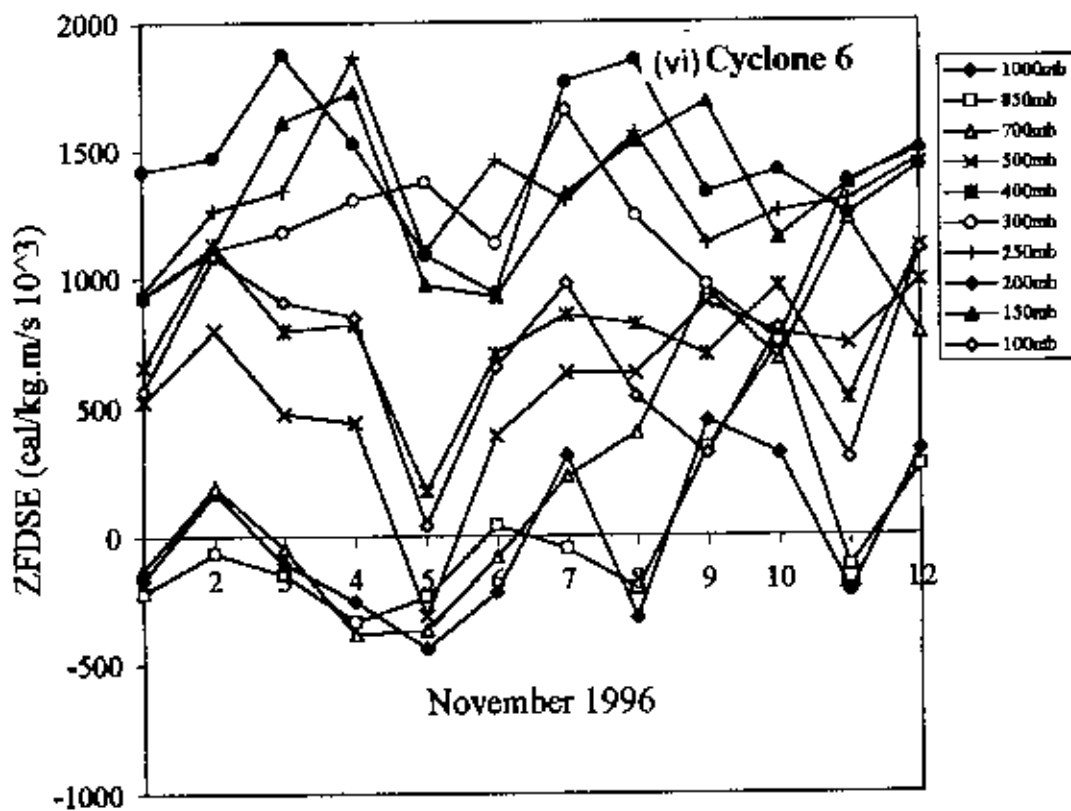
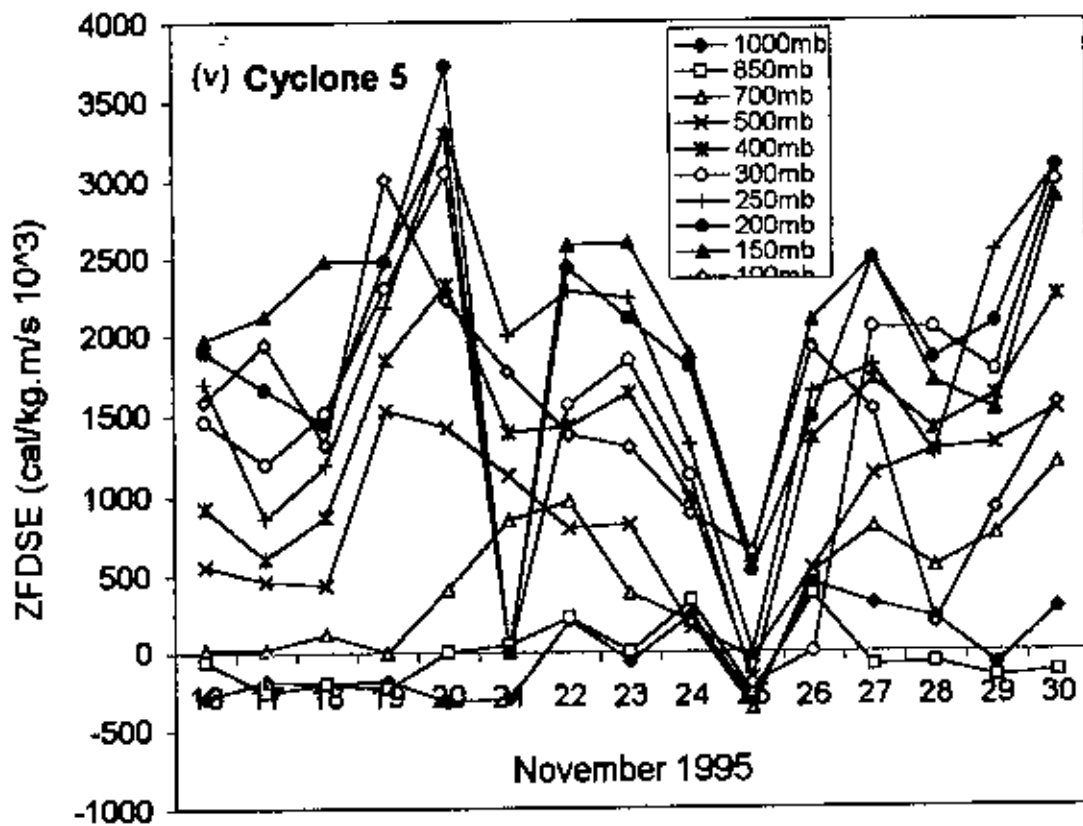
### Cyclone 6

Fig. 4.3(vi) shows the variation of zonal flux of dry static energy with time at different isobaric levels for cyclone 6. Here ZFDSE fluctuated from positive (eastward) to negative (westward) and vice-versa at the lower level of the troposphere (1000-700 mb). But here the fluctuation was large compared to the previous Fig.4.3(i-v). From middle to upper troposphere (4000-100 mb) ZFDSE was completely positive (eastward). It is observed that at 500 mb, ZFDSE decreased at time to time and then turned into negative (westward) on 5 November (when cyclone is started). Here we have seen that wind direction before cyclone was opposite to that at cyclone started. After 5 November it increased gradually with time up to 12 November. At this level (500 mb) ZFDSE increased from cyclone period to landfall. At levels 400 mb and 300 mb it decreased and attained the minimum value on 5 November (when cyclone is just started). After 5 November every time it fluctuated due to change of wind speed. At the upper level of the troposphere (250-100 mb) every time it fluctuated. This was because at the upper level there was very unstable condition and wind speed changed (increased or decreased) and ZFDSE is









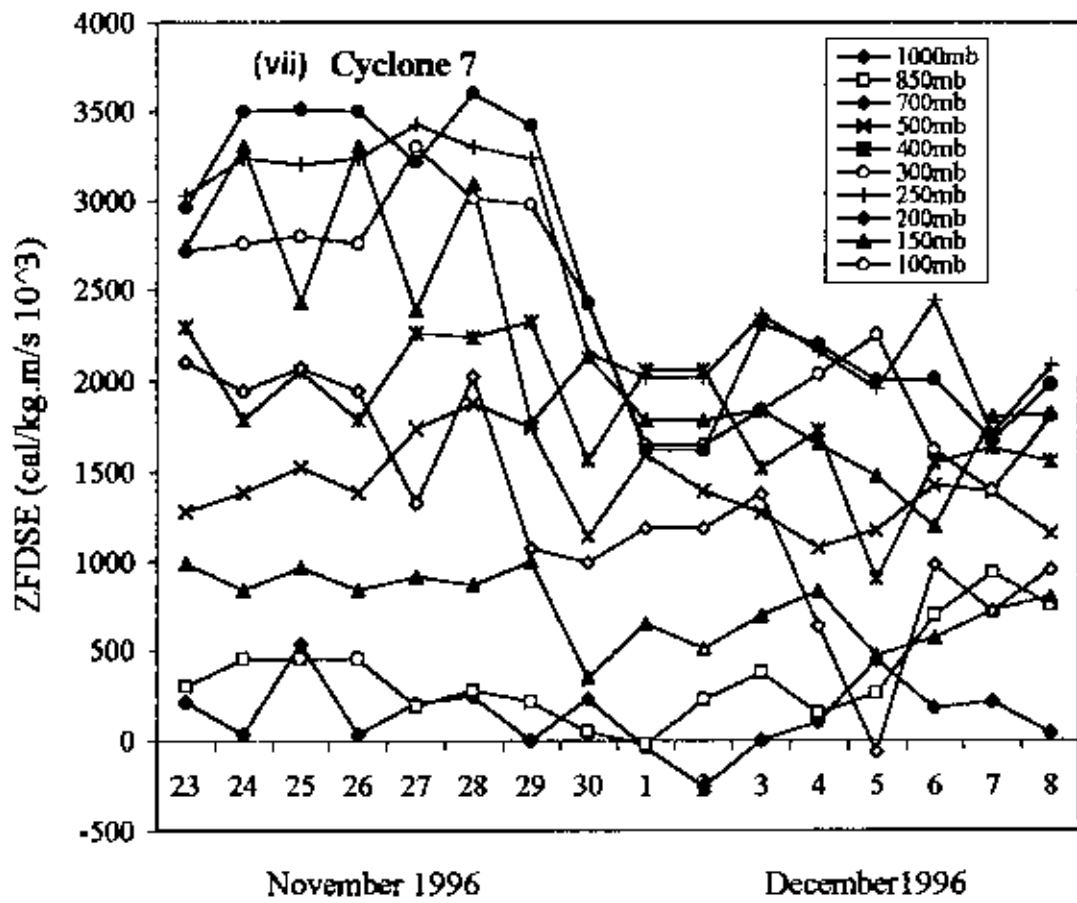


Fig. 4.3(i-vii). Variation of zonal fluxes of dry static energy with time for cyclone 1-cyclone 7.

fluctuated. From this figure it is observed that when cyclone is just started (5 November), ZFDSE was minimum for all the level (level 1000-100 mb).

### Cyclone 7

The Variation of zonal flux of dry static energy with time is shown in Fig. 4.3(vii) for cyclone 7. This figure is slightly different from the previous figures. At the lower level of the troposphere (i.e., 1000-700 mb), every time ZFDSE is fluctuated from positive (eastward) to negative (westward). But here [Fig. 4.3(vii)] it was completely positive for all the levels and all the days (except 2 December). Here for only one day (2 December) ZFDSE was negative (westward), at 1000mb. Here it is observed that from levels 1000-300 mb, there was no significant change of ZFDSE. Every time it was near about constant due to less change of wind speed. But at upper level of the troposphere (250-100 mb), ZFDSE was low from 1-8 December compared to 23-30 November. It is also observed that at 150 mb (upper level of the troposphere) every time it fluctuated largely from 23-30 November. This was due to much change of zonal wind component.

From the above Fig. [Fig. 4.3 (i-vii)] it is concluded that the direction of zonal fluxes of dry static energy changed from positive (eastward) to negative (westward) and vice-versa at the lower level of the troposphere (i.e., 1000-700 mb). But its value changed little bit or near about constant with time. This was because of nearly same zonal wind component at the lower level of the troposphere. From middle to higher level of the troposphere (500-100 mb), every time ZFDSE was positive (eastward). At these levels (500-100 mb), ZFDSE was fluctuated at time to time. It is also observed that at the higher level of the troposphere (250-150 mb) it fluctuated largely. This was due to the large zonal wind component. It is also observed that for some cyclones, ZFDSE was maximum at cyclone period at the higher level of the troposphere and for some cyclones it was maximum just before cyclone (20 November 1995) and minimum just at the end of cyclone (25 November).

#### 4.1.2.(b): Zonal Flux of Moist Static Energy (ZFMSE):

Fig. 4.4(i-vii) shows the variation of zonal flux of moist static energy with time at different isobaric levels from 1000-100 mb for seven cyclones. From these figures [Fig. 4.4(i-vii)] it is observed that the pattern of zonal fluxes of moist static energy (ZFMSE) was similar to the graph pattern of zonal fluxes of dry static energy (ZFDSE) which is discussed earlier in the previous Fig. 4.3(i-vii). Here [in figures 4.4(i-vii)] only the difference in magnitude. This is because moist static energy is simply an addition of latent heat content with dry static energy.

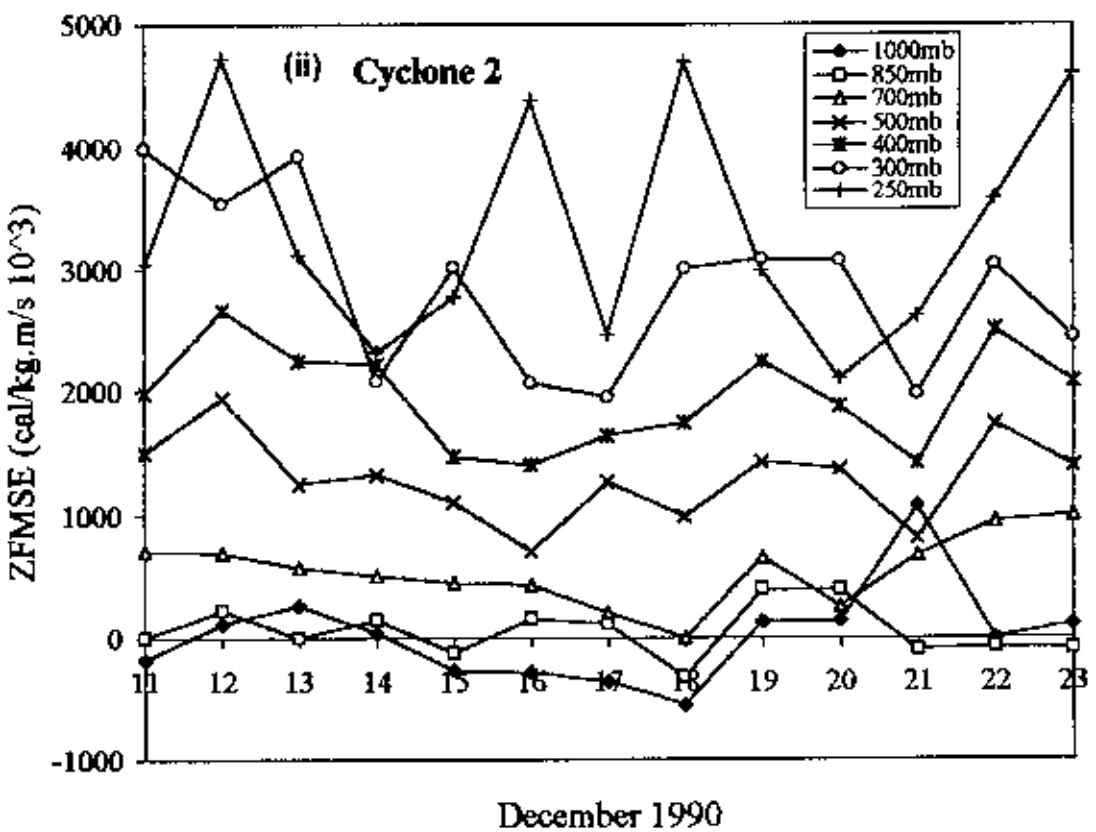
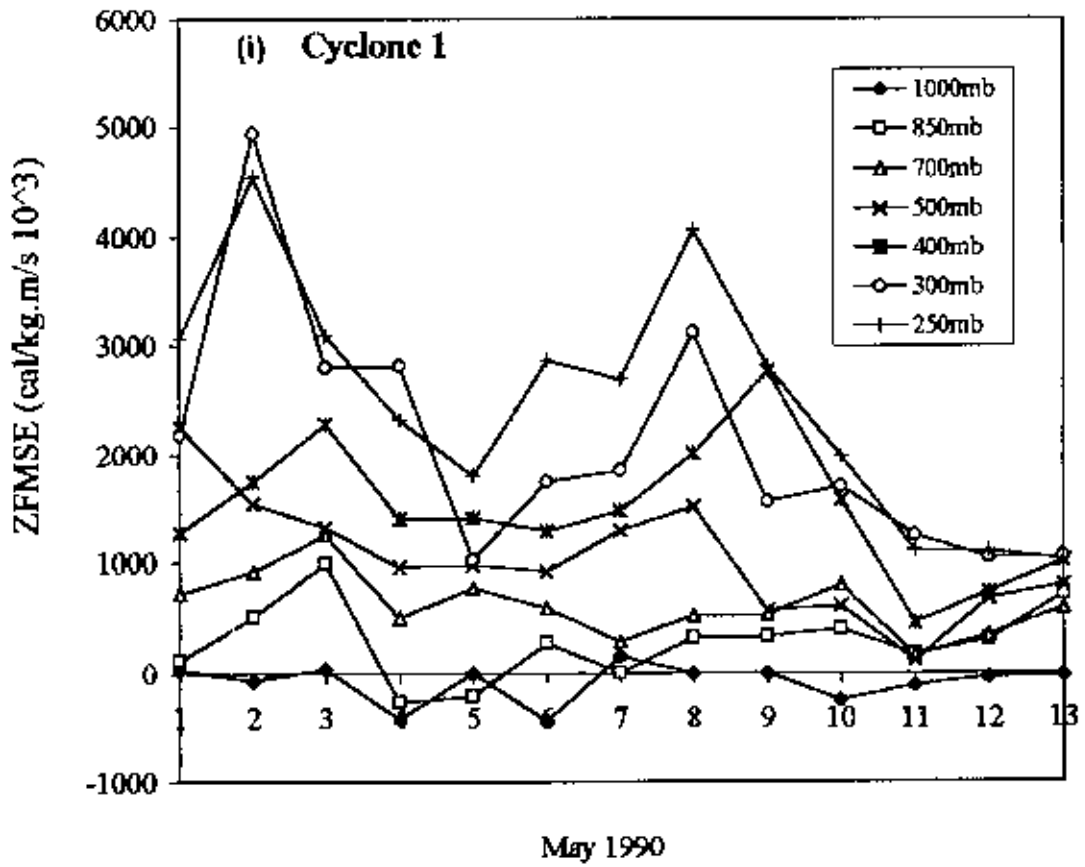
#### 4.1.2.(c): Meridional Flux of Dry Static Energy (MFDSE):

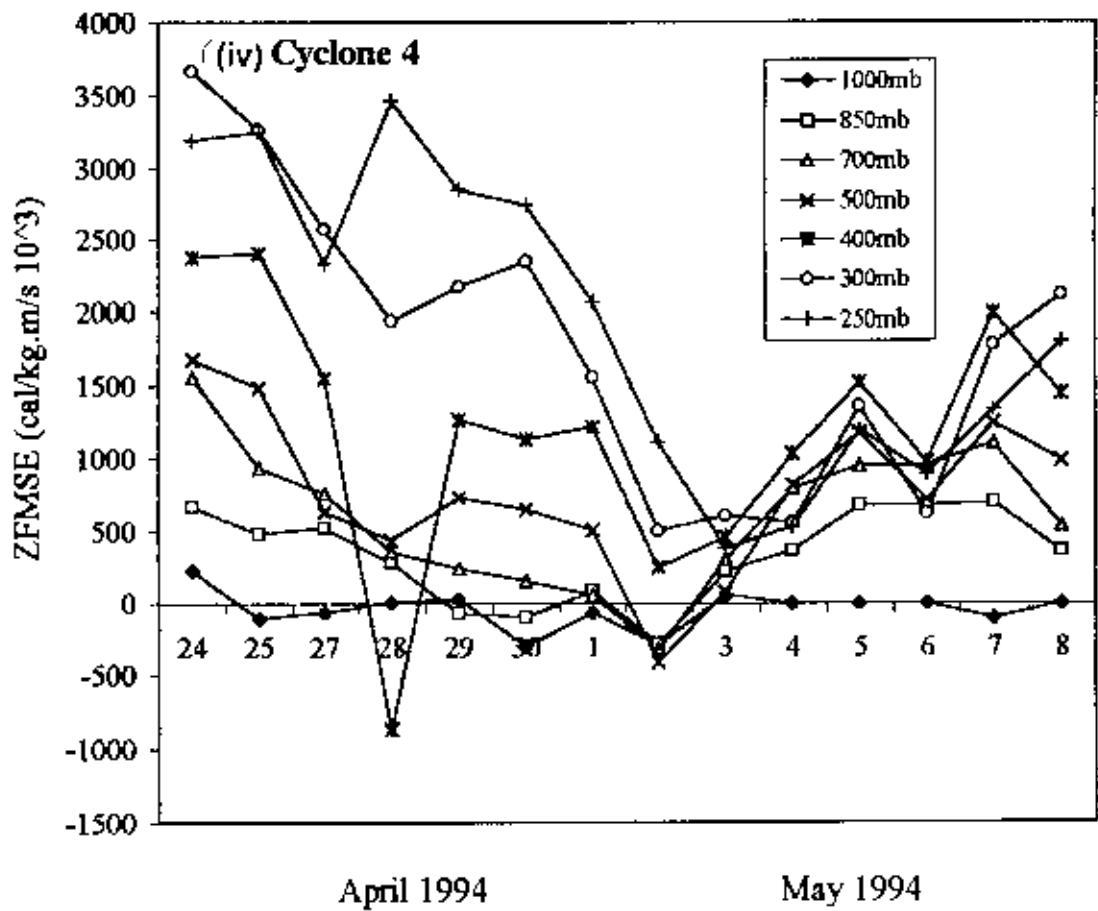
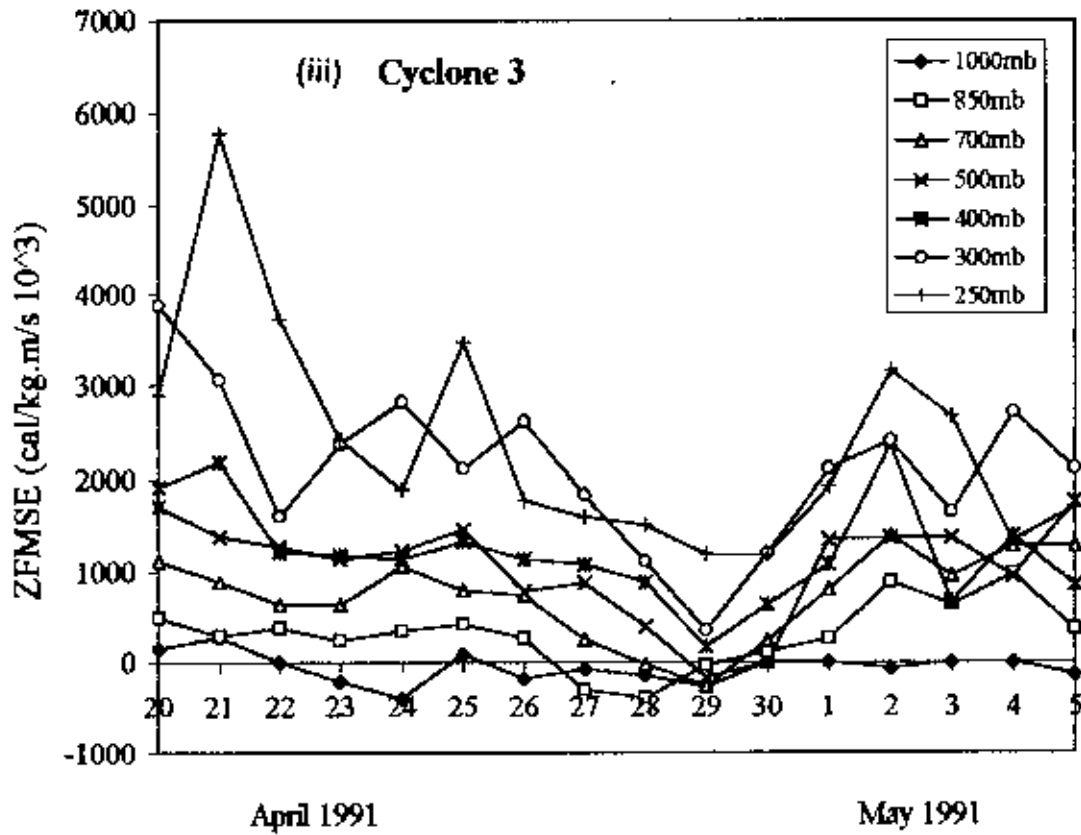
##### Cyclone 1

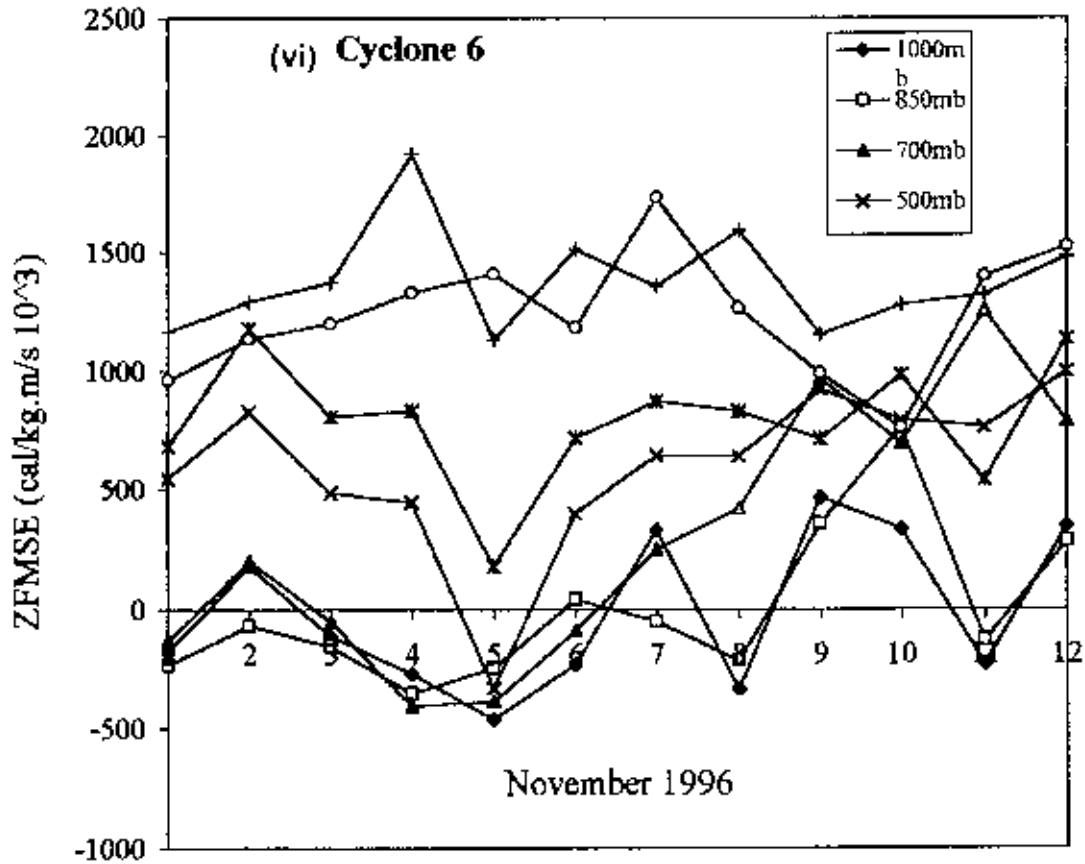
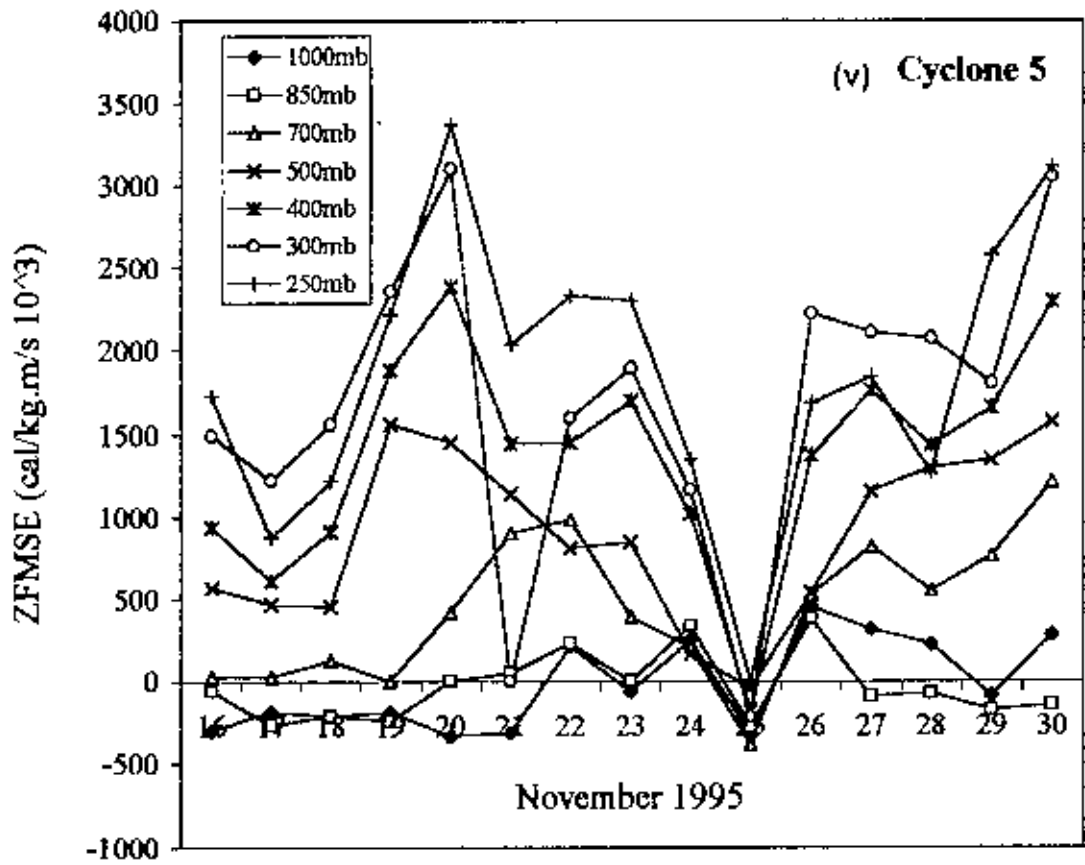
Fig. 4.5(i-vii) represents the variation of meridional flux of dry static energy (MFDSE) with time at different isobaric levels from 1000-100 mb for seven cyclones. For cyclone 1 [Fig. 4.5(i)], it is observed that from 1000-300 mb meridional flux of dry static energy was nearly zero and almost same from 1-9 May 1990 i.e., at that time there was no significant change of meridional wind component. But at 100mb and 700mb it changed its direction from positive (northward) to negative (southward) and vice-versa. It was positive from 250-150 mb from 1-9 May (at the end of cyclone period) and its value fluctuated at time to time due to changes of meridional wind component. At 100 mb, i.e., at the top of the troposphere we saw that every time there was large fluctuation and it was maximum on 5 May (when cyclone is just started). At 100 mb it is also observed that it changed its direction from positive (northward) to negative (southward) and vice-versa. It is also seen that after 9 May (during landfall) meridional flux of dry static energy was negative (southward) for all the levels (except 1000mb) from 9-13 May. Here at cyclone period (5-9 May) and after landfall (9-13 May) wind direction was opposite to each other.

##### Cyclone 2

Fig. 4.5(ii) shows the variation of meridional flux of dry static energy (MFDSE) with time at different levels for cyclone 2. At 1000 mb, MFDSE was completely negative (southward) at every time i.e. from 11-23 December, 1990 and all the time its value did







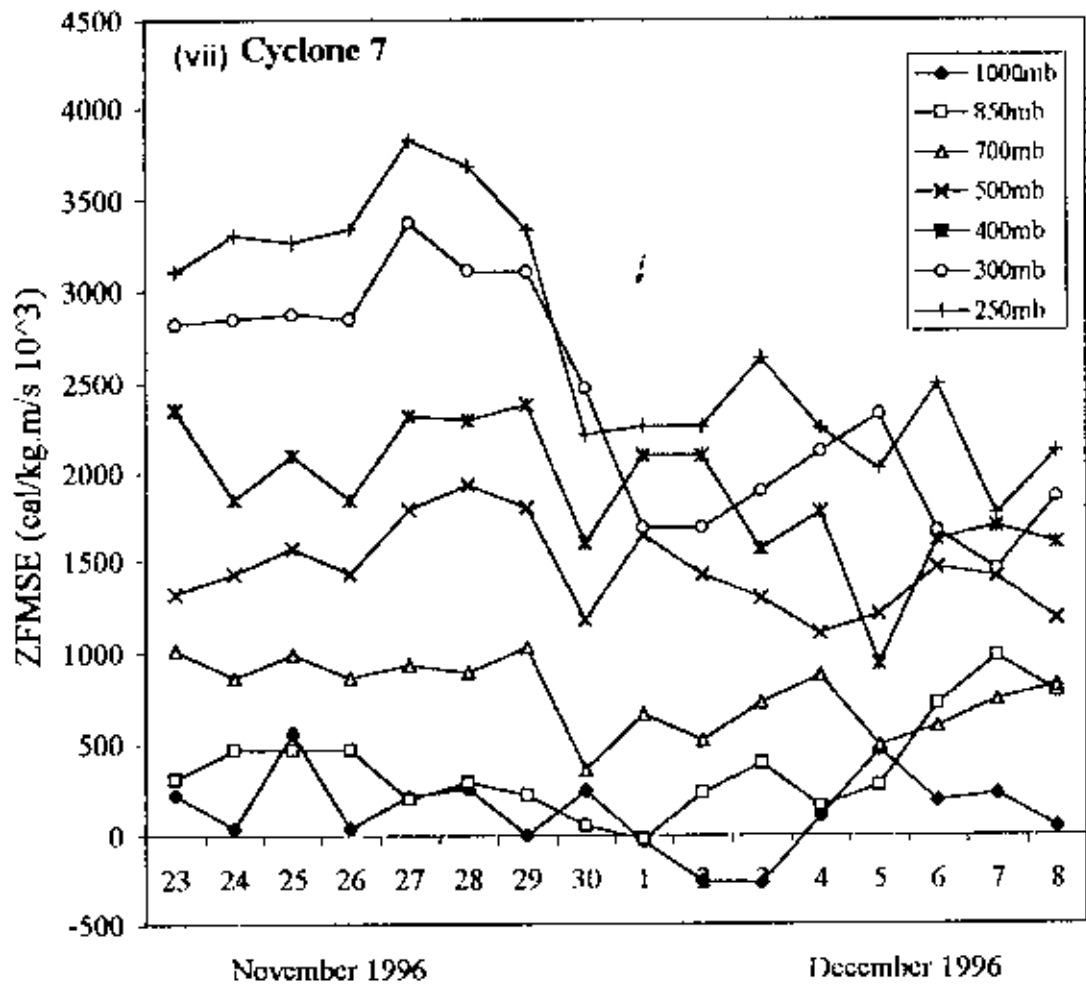


Fig. 4.4(i-vii). Variation of zonal fluxes of moist static energy with time for cyclone 1-cyclone 7.



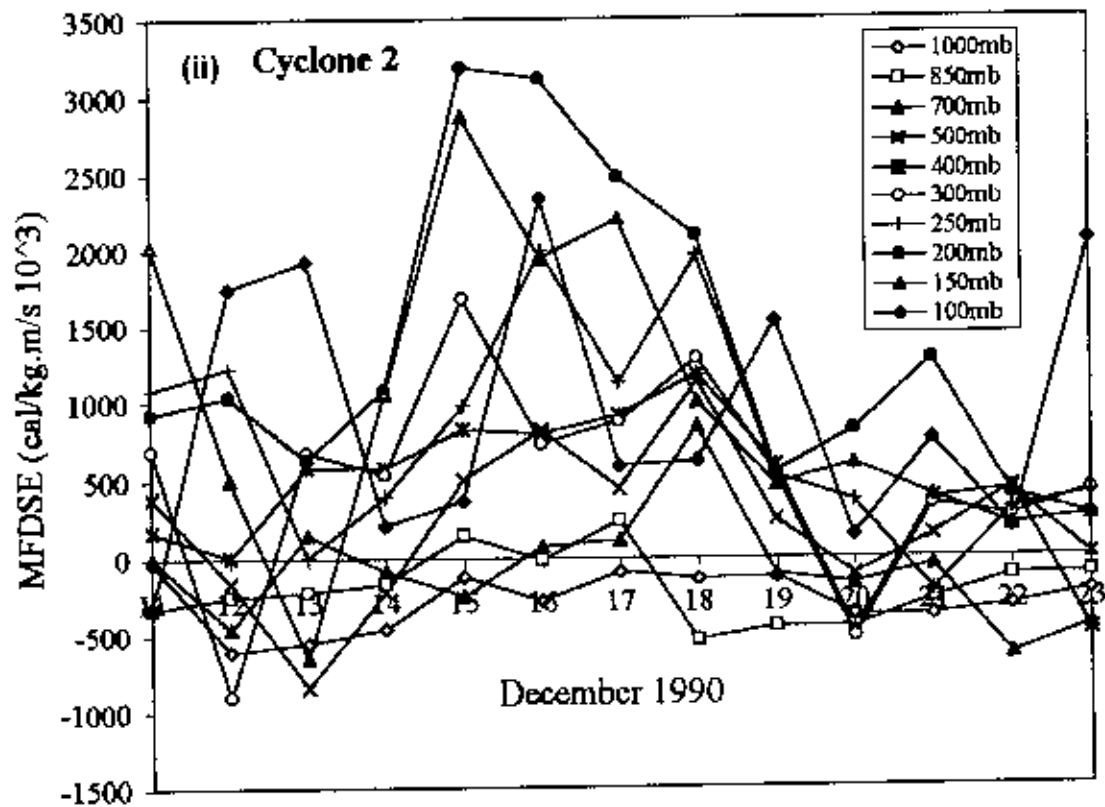
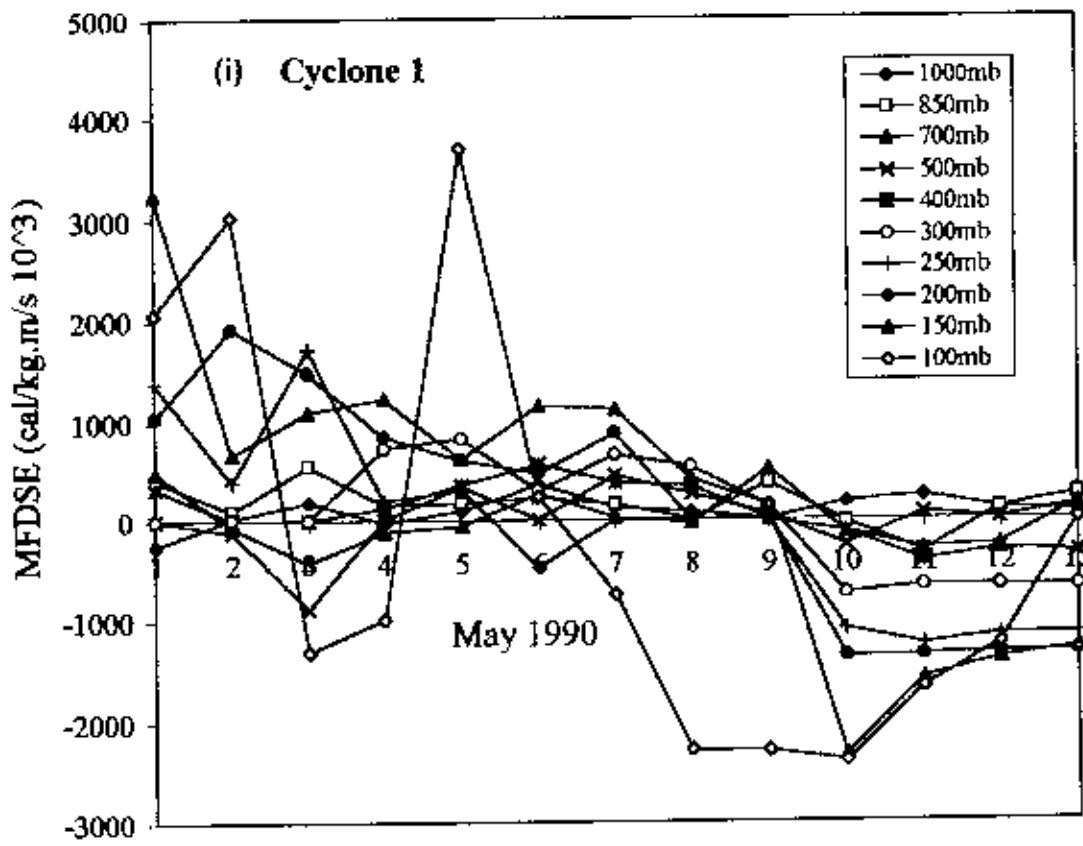
not change much. At 850 mb and 700 mb it is fluctuated at time to time because of change of meridional wind component and changed its direction from positive (northward) to negative (southward) and vice-versa. From middle to upper troposphere (300-100 mb) it is observed that at time to time there was large fluctuation due to large change of meridional wind component at these levels (300-100 mb) and was maximum at the cyclone period (15-18 December).

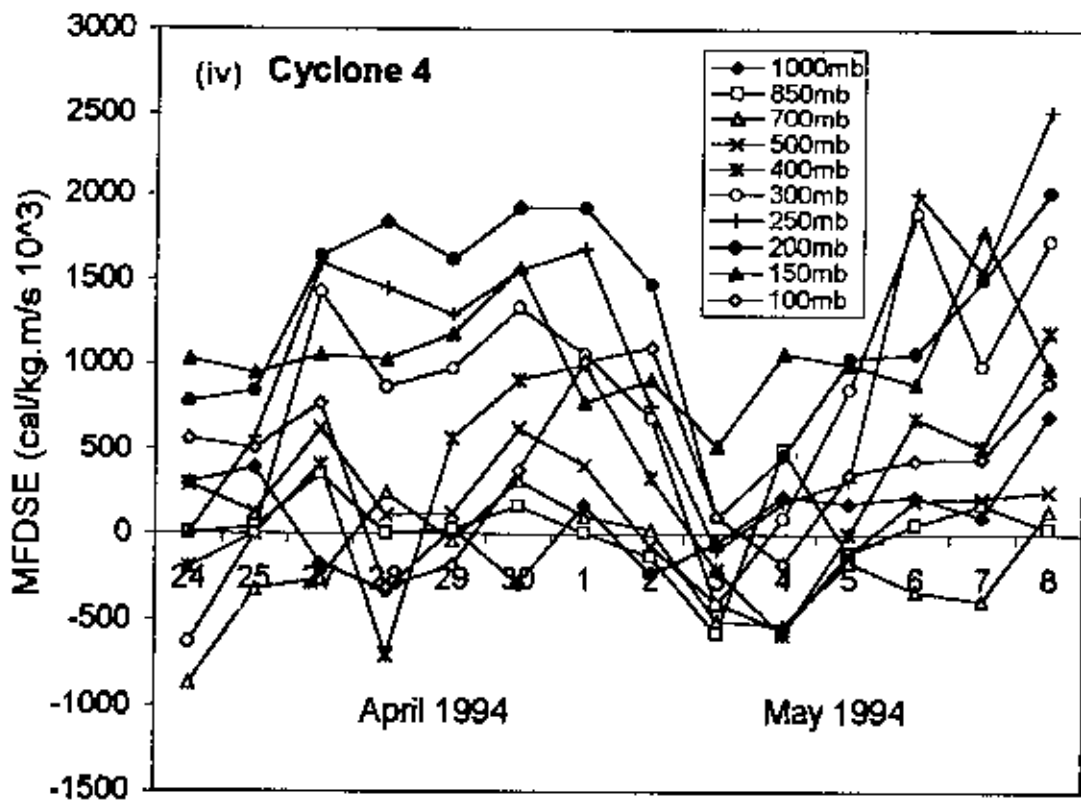
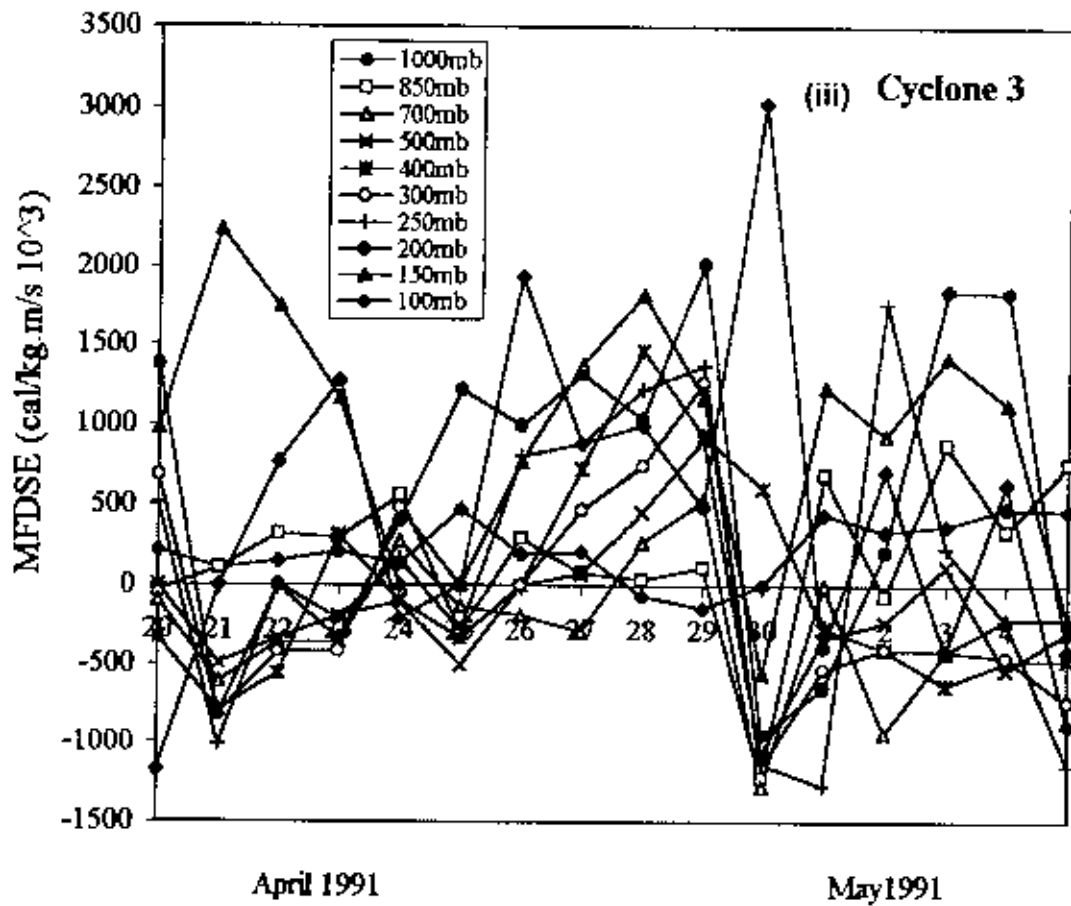
### Cyclone 3

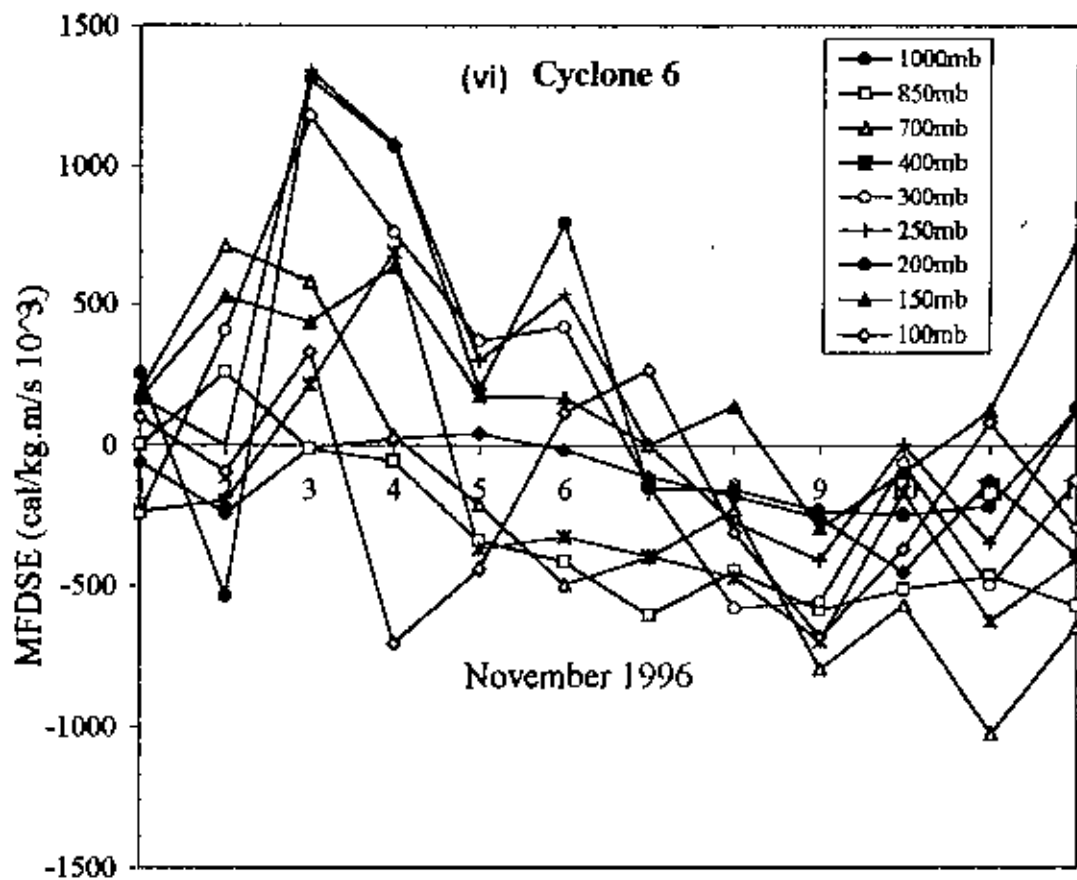
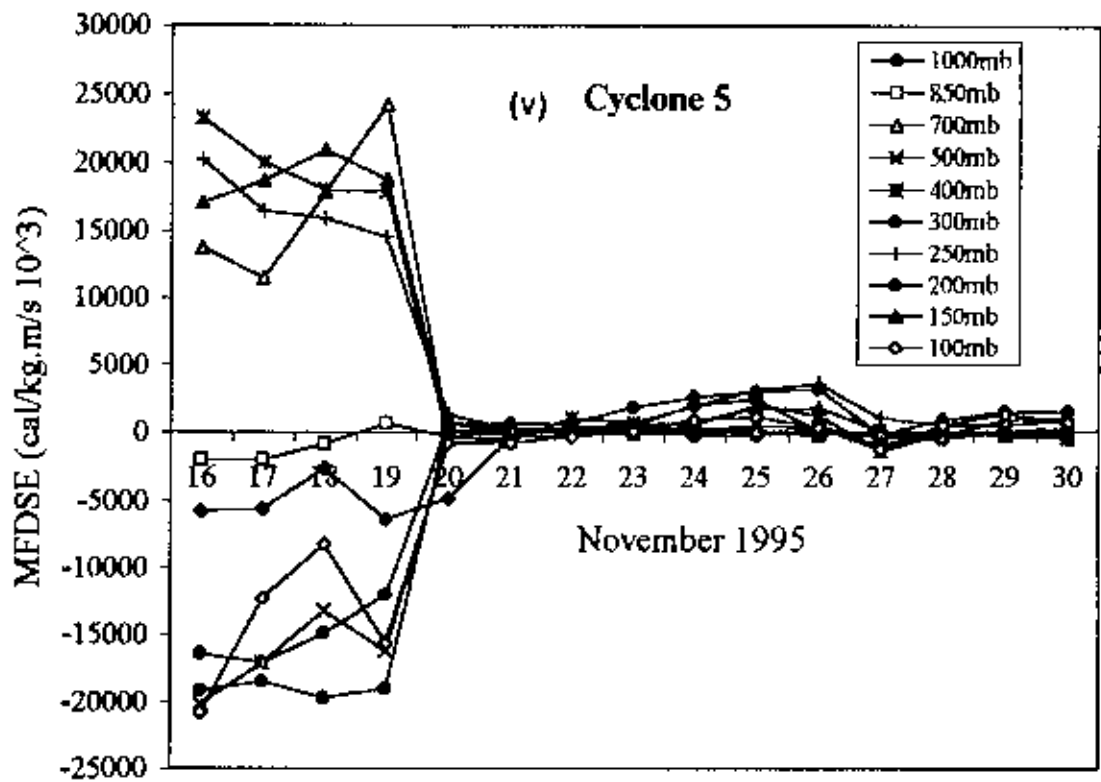
From Fig. 4.5(iii) it is observed that meridional flux of dry static energy changed from positive (northward) to negative (southward) and from negative (southward) to positive (northward) for all levels 1000-100 mb from 20-29 April. But at 30 April (at the end of cyclone) it turned into negative (southward) for all levels except 1000 mb, 400 mb and 100 mb. Beyond 30 May it increased and fluctuated. From this figure.[Fig. 4.5(iii)] it is observed that at 30 April (at the end of cyclone), MFDSE was zero at 1000 mb. It was maximum at the upper level of the troposphere (100 mb) and was maximum in the negative direction (southward) at level 850 mb and 700 mb. At 200 mb (upper level of the troposphere) it is seen that at first MFDSE was negative (southward) from 21-23 April, then it turned into positive (southward) and increased gradually with time and attained maximum value on 29 April (at the last of cyclone).

### Cyclone 4

Fig. 4.5(iv) shows the variation of meridional flux of dry static every (MFDSE) with time at different levels for cyclone 4. From this figure it is seen that at 1000mb (lower level of the troposphere), MFDSE is fluctuated and turned its direction from positive (northward) to negative (southward) and vice-versa from 24 April to 3 May 1994. Beyond 3 May (after landfall) it was always positive (northward) and remained same up to 7 May but it slightly increased on 8 May. At 850 mb and 700 mb it changed its direction from positive to negative and negative to positive from 24 April-8 May. At middle to upper troposphere (500-100 mb) it was positive (northward) from 24 April-2 May. It is also observed that on 3 May (at the end of cyclone) it turned into negative (southward) for all







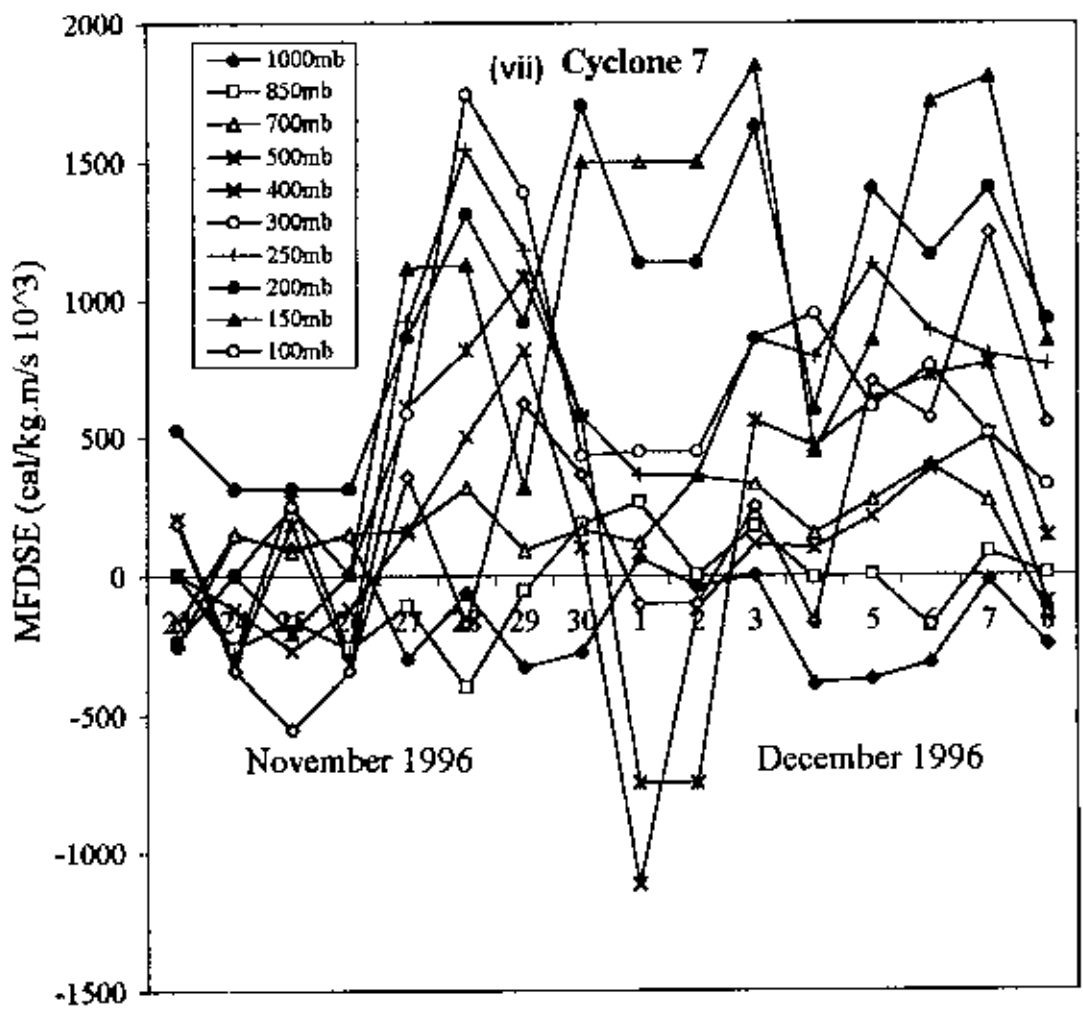


Fig. 4 5(i-vii). Variation of meridional fluxes of dry static energy with time for cyclone 1-cyclone 7

the level except 150 mb and 100 mb i.e., upper level of the troposphere. Beyond 5 May it was completely positive (northward) for all levels (except 700 mb) up to 8 May.

From the above figure [Fig. 4.5(iv)], it is observed that for all the levels (without some exception) the wind direction was negative (southward) at the end of cyclone (3 April) and positive at the end of landfall (6-8 May). It is also observed that MFDSE was maximum for 200 mb at the peak time of cyclone period (30 April-1 May) due to the higher meridional wind component at this level.

#### Cyclone 5

From Fig. 4.5(v), it is observed that MFDSE were positive (northward) at levels 700 mb, 400 mb, 250 mb and 150 mb whereas it was negative (southward) at levels 1000 mb, 850 mb, 500 mb, 400 mb, 200 mb and 100 mb from 16-19 November (before cyclone). It is seen that at cyclone period (21-25 November) its value abruptly reduced and tends to nearly zero and continue at the end of landfall (30 November). This cyclone (cyclone 5) was an exceptional case compared to other six cyclones. This was because for other six cyclones we saw that at cyclone period, MFDSE was maximum and layer to layer it was fluctuated. But for this cyclone (cyclone 5), MFDSE was minimum at cyclone period and was nearly same for all levels. We also observed that there was a common feature that MFDSE was roughly negative (southward) at lower level of the troposphere (1000-700 mb) and positive (northward) from middle to upper level of the troposphere (500-100 mb). But for this cyclone (cyclone 5) wind direction was randomly changed from layer to layer on 16-19 November (before cyclone) and was positive for all the levels at cyclone period and after landfall.

#### Cyclone 6

Fig. 4.5(vi) shows the variation of meridional flux of dry static every (MFDSE) with time at different levels for cyclone 6. From Fig. 4.5(vi) it is seen that at 1000 mb MFDSE was negative (southward) and then turned into zero on 6 November. Beyond 6 November it again turned to negative and then maintained a constant value. At 850 mb it is seen that beyond 3 November, MFDSE increased gradually in the negative (southward)

direction up to 7 November (at the end of cyclone). Then it slightly reduced on 8 November and then maintained a constant value up to 12 November (after landfall) due to no change of meridional wind component. At 700 mb it increased for first two days (1-2 November) in the positive direction and then decreased and attained nearly zero on 4 November (just before cyclone). But when cyclone started (on 5 November) it increased in the negative (southward) direction and then from day to day it increased with fluctuation due to change of meridional wind component. At 400 mb it fluctuated in the positive and negative direction from 1-4 November (before cyclone). But at cyclone period (5-7 November) it turned to negative (southward) and remain constant and then (8-12 November) it fluctuated due to change of wind velocity. For 300-100 mb it was positive (northward) up to 7 November (at the end of cyclone). Beyond 7 November (after landfall) it is seen that for all the levels (1000-100 mb) it was completely negative (southward) and continued with this negative value with fluctuation up to 12 November. Here it is seen that from middle to upper level (300-100 mb) of the troposphere it was positive (northward) for before cyclone period(1-4 November) and during cyclone period (5-7 November). But it was completely negative (southward) for all the levels after landfall.

From Fig. 4.5(vii) it is observed that at 1000 mb MFDSE was negative (southward) and fluctuated from 23 -30 November and then turned into positive (northward) and remained same up to 3 December (at the end of cyclone period). It again turned into negative direction after landfall and continued with negative value up to 8 December. At 850 mb it slightly fluctuated and changed its direction from positive to negative and vice-versa. At 700 mb it is seen that MFDSE was positive (northward) for all the time and remained near about same. It is observed that after 26 November MFDSE increased in the positive direction for all the levels (except 1000 mb and 850 mb) and reached maximum value on 28 November (when cyclone started) and then decreased and fluctuated with positive sign up to 8 December. At 150 mb (upper level of the troposphere) it is seen that MFDSE was highest on 3 December (at the end of cyclone period). This was due to the high wind speed during landfall. It is also observed that MFDSE was maximum in the negative (southward) direction at 500 mb at cyclone period (1 December).

**4.1.2.(d): Meridional Flux of Moist Static Energy (MFMSE):****Cyclone 1**

Fig. 4.6(i-vii) shows the variation of meridional flux of moist static energy (MFMSE) with time at different isobaric levels from 1000-100 mb for seven cyclones. From Fig. 4.6(i) it is seen that at 1000 mb MFMSE was negative on 1 May and then turned into zero on 2nd May. It was negative (southward) on 3 May and then positive (northward) and continued up to 13 May. At 850 mb, it was always positive (northward) except 11 May. At 700 mb, it changed its direction from positive (northward) to negative (southward) and vice-versa. For 400-250 mb it fluctuated in the positive direction up to 9 May (at the end of cyclone). During landfall it changed its direction i.e. from positive to negative and remained same for all the rest of the time (10-13 May). From this figure it is also seen that MFMSE was maximum at 250 mb on 3 May.

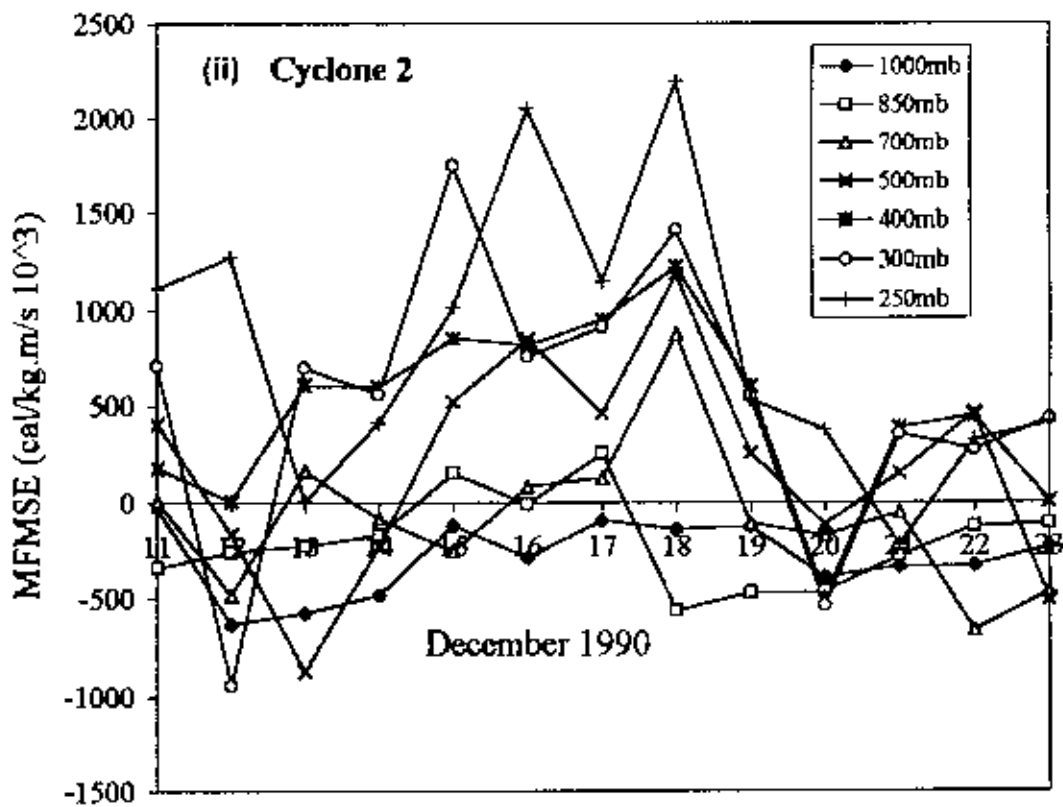
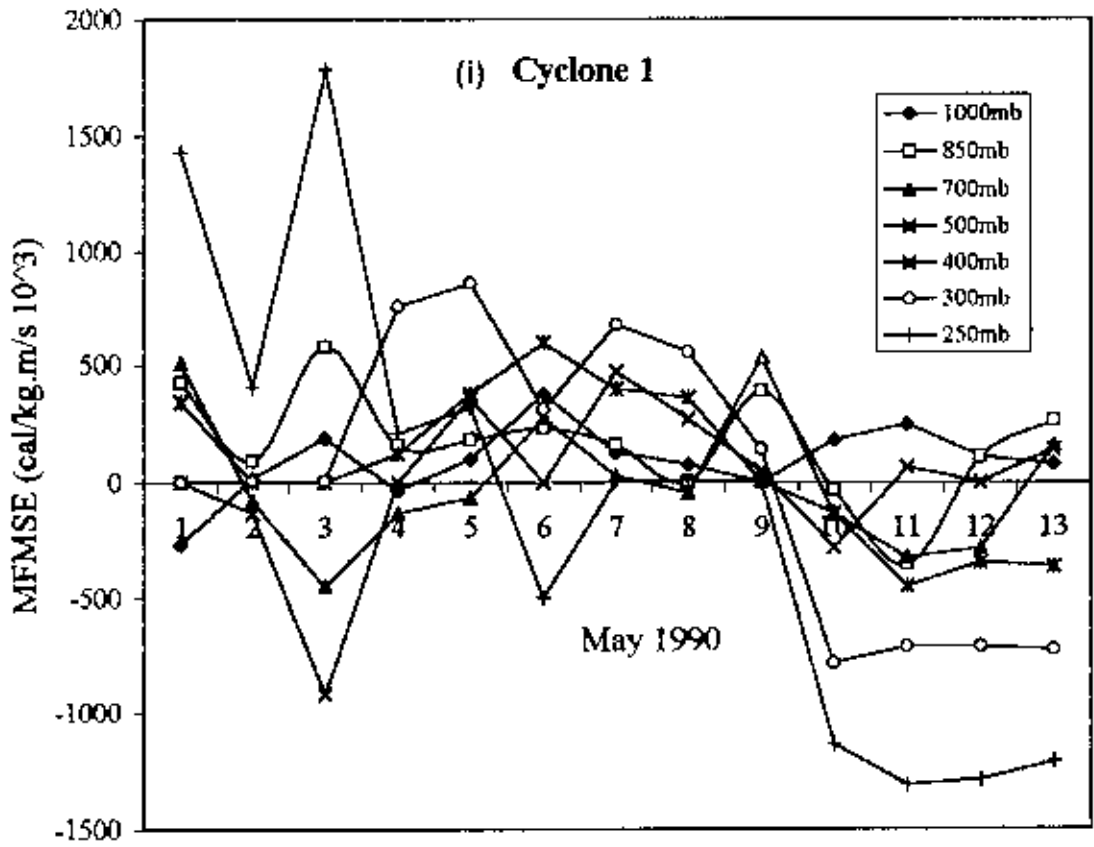
**Cyclone 2**

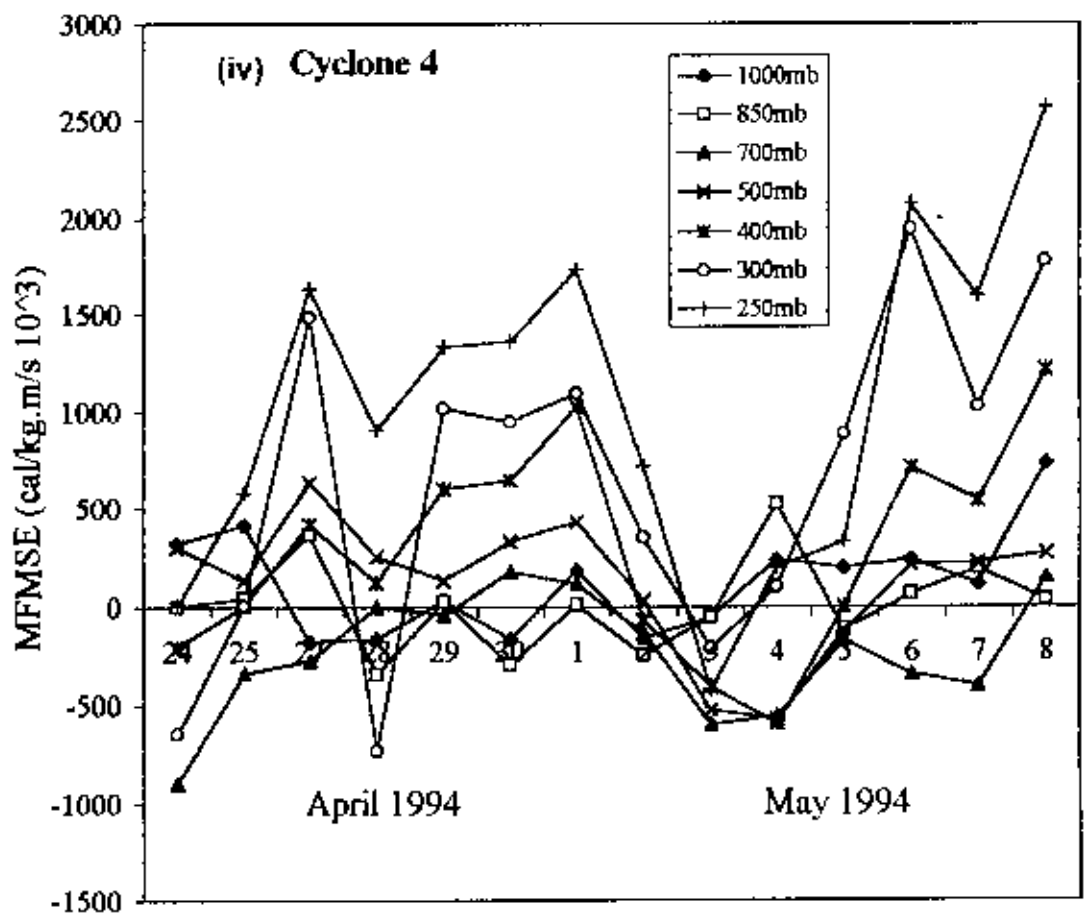
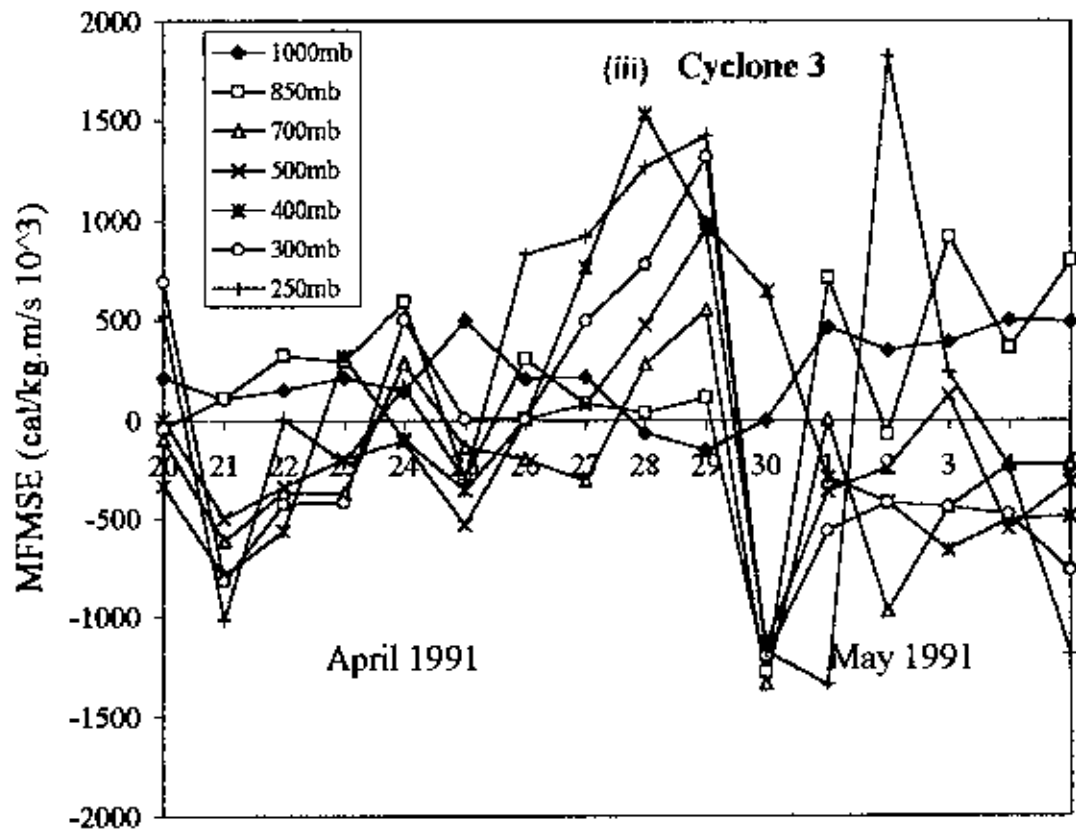
The variation of meridional flux of moist static energy (MFMSE) with time at different isobaric levels is shown in Fig. 4.6(ii) for cyclone 2. From this figure it is observed that MFMSE was always negative (southward) at 1000 mb. At 850 mb at first it was negative (southward) and remain same up to 14 December and then turned from negative to positive and vice-versa. At 700 mb, with day to day it fluctuated and changed its direction due to the change of wind velocity. At 400 mb it increased gradually up to 18 December (at the end of cyclone period) and then decreased. At 300 mb and 250 mb it is seen that day to day variation the fluctuation was large due to large variation of wind component. From this figure [Fig. 4.6(ii)] it is also seen that on 18 December (at the end of cyclone) MFMSE increased for all the levels in the positive direction except 1000 mb and 850 mb and was maximum for 250 mb. This was due to the higher wind component at this level.

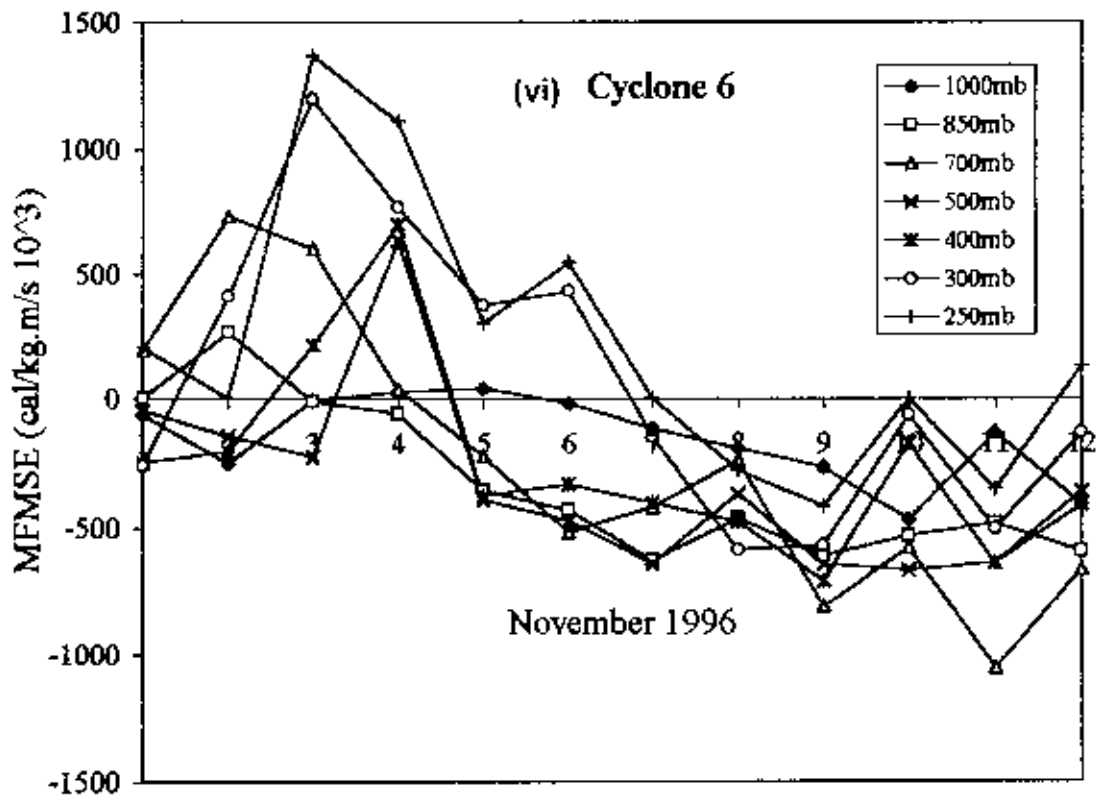
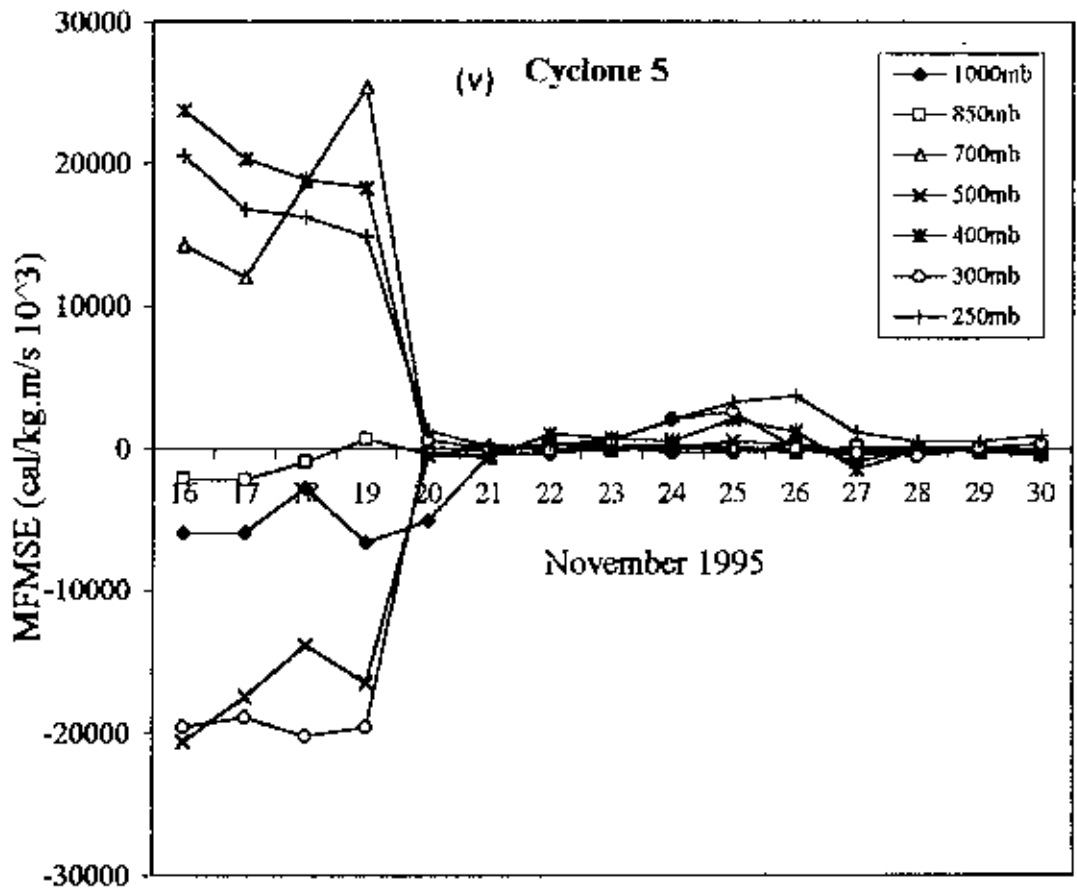
**Cyclone 3**

Fig. 4.6(iii) shows the variation of meridional flux of moist static energy (MFMSE) with time for cyclone 3. From this figure it is observed that the graph pattern was almost









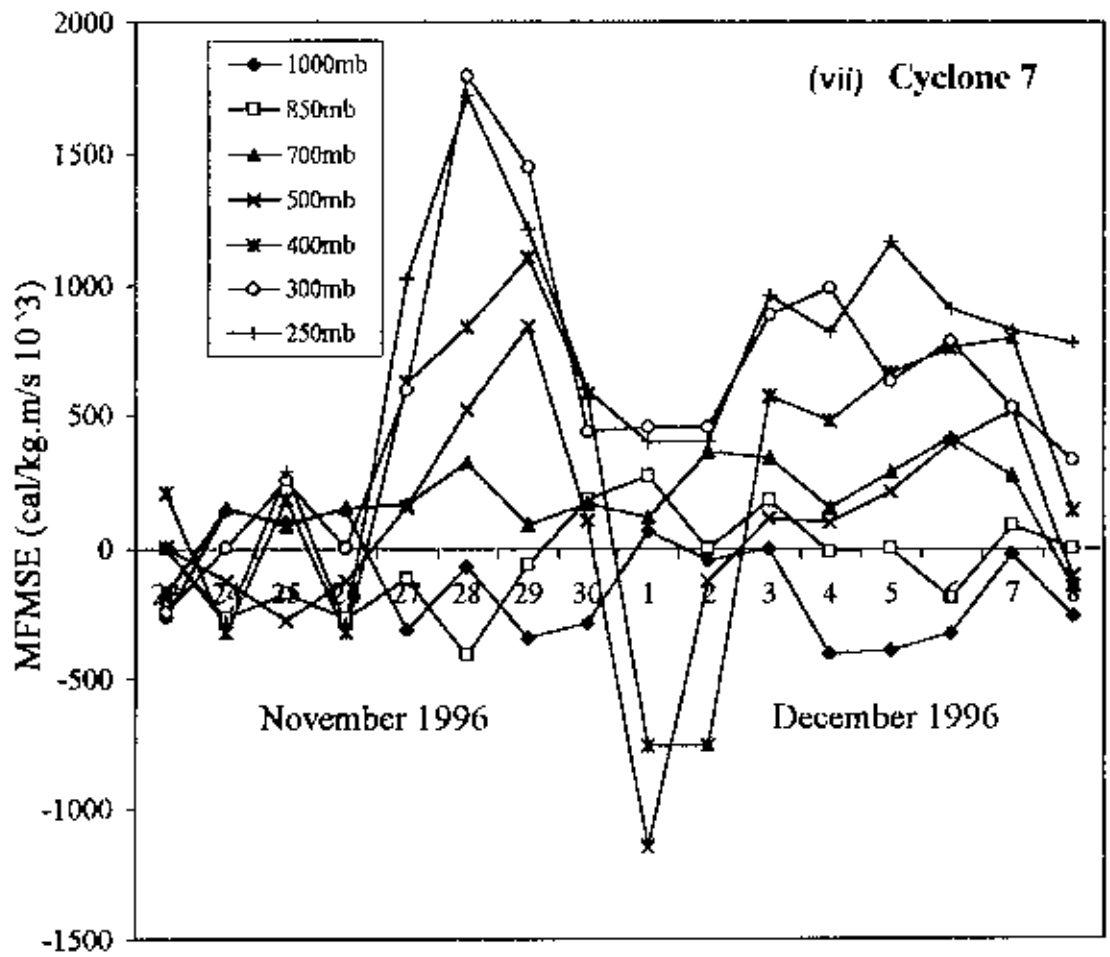


Fig. 4.6(i-vii) Variation of meridional fluxes of moist static energy with time for cyclone 1-cyclone 7.

same as the meridional flux of dry static energy (MFMSE) which is discussed earlier [Fig. 4.5(iii)]. This was because meridional flux of moist static energy is simply an addition of latent heat content with meridional flux of dry static energy. Here only the difference is that in the previous figure [Fig. 4.5(iii)] flux is maximum at the upper level (100 mb) of the troposphere but here flux is maximum at the middle of the troposphere (i.e. ,at 250 mb).

#### Cyclone 4

From Fig. 4.6(iv) it is observed that at 1000 mb, with day to day MFMSE fluctuated slightly and changed its direction from positive (northward) to negative (southward) and vice-versa up to 3 May (at the end of cyclone period). Beyond 3 May it remained same up to 7 May due to no change of wind speed after landfall. At 850 mb, all the time it fluctuated. At 700 mb, most of the time the flux was negative (southward). For 500-250 mb, MFMSE was positive (northward) and increased up to 1 May (at the peak time of cyclone period) MFMSE decreased and negative (southward) for all the levels. Beyond 3 may it again increased (except 700 mb) due to increasing wind speed after landfall.

#### Cyclone 5

Fig. 4.6(v) shows the variation of meridional flux of moist static energy (MFMSE) with time for cyclone 5. From this figure it is observed that the pattern is same as that of meridional flux of dry static energy which is discussed earlier in figure 4.5(v). The only difference was in magnitude.

#### Cyclone 6

From Fig. 4.6(vi) it is observed that at first (before occurrence) for most of the level MFMSE was positive (northward). When cyclone is formed (5 November) for most of the level it turned into negative (southward) and increased in the negative direction. Beyond 7 November (at the end of cyclone) for all the levels MFMSE was negative (southward) and fluctuated.

### Cyclone 7

Fig. 4.6(vii) shows the variation of meridional flux of moist static energy (MFMSE) with time for cyclone 7. From this figure it is observed that at 1000 mb, MFMSE was always negative (except 1 December) and slightly fluctuated. At 850 mb, it fluctuated and changed its direction at different time but at the peak time of cyclone (30 November 1 December) it was positive (northward). At 700 mb MFMSE was always positive (northward). At 500-250 mb, it is seen that from 26 November it increased and attained maximum intensity when cyclone is started i.e., on 28 November. It is also observed that at the peak time of cyclone (1 December) it was maximum in the negative (southward) direction at 500 mb.

## 4.2 Atmospheric Energy at Different Isobaric Levels

### 4.2.1. Cyclone 1

A cyclone named cyclone 1 is formed in the Bay of Bengal from 5 May 1990 to 9 May 1990 is explained in this section. This period is called "cyclone period". To observe its pre-condition, energy is calculated from 1 May 1990 to 4 May 1990 and this period is called "before occurrence". To observe the post condition of the observed cyclone, energy is also calculated from 10 May 1990 to 13 May 1990. This period is called after landfall. The movement of this cyclone is shown in Fig. 3.

#### 4.2.1(a). Energy components:

##### Sensible Heat (SH):

Fig. 5.1.1(a-c) shows the variation of Sensible heat at different isobaric level in different phases (before occurrence, cyclone period and after landfall) of a cyclone occurring from 5.5.90 to 9.5.90. From these fig it is observed that sensible heat decreased with decreasing pressure i.e. with increasing height. This is due to the decrease of temperature with the increase of height. It is also observed that the sensible heat on 9.5.90 was low compared to the other days at 300 mb - 100mb. This is due to the decrease of temperature at the end (9.5.90) of the cyclone period. It is also seen that at the end of the landfall (13.5.94) sensible heat was lowest. This was due to the heavy rainfall.

##### Potential Energy (PE):

Fig. 5.1.2(a-c) shows the variation of potential energy at different isobaric level in different phases of a cyclone occurring from 5.5.90 to 9.5.90. It is seen that potential energy increased linearly with increasing height (pressure decreased).

There is no day to day variation of PE before occurrence. At cyclone period [Fig. 5.1.2(b)] it is seen that at 300mb - 100mb potential energy slightly decreased. This was due to the slightly decrease of geopotential height at these levels.

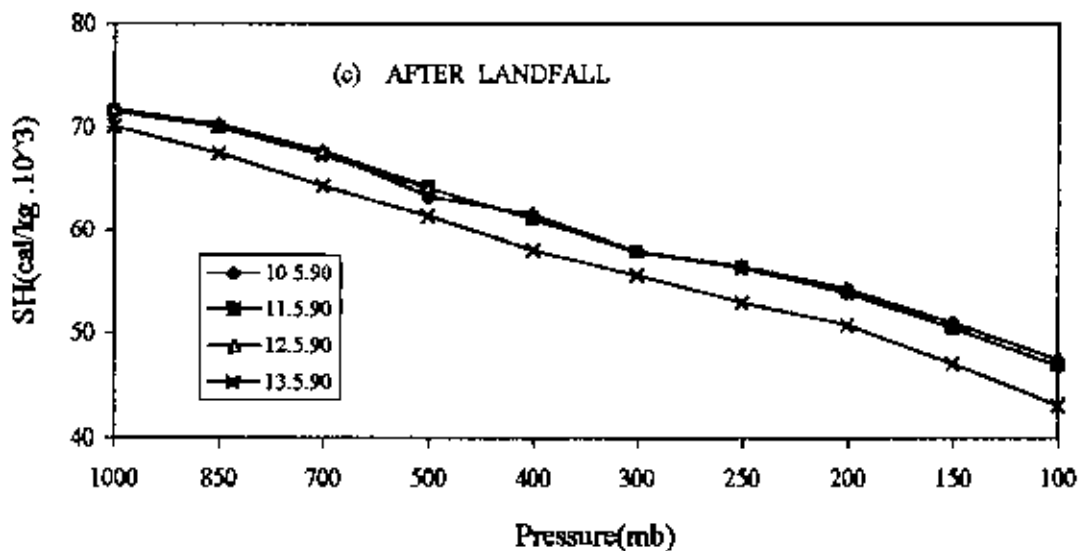
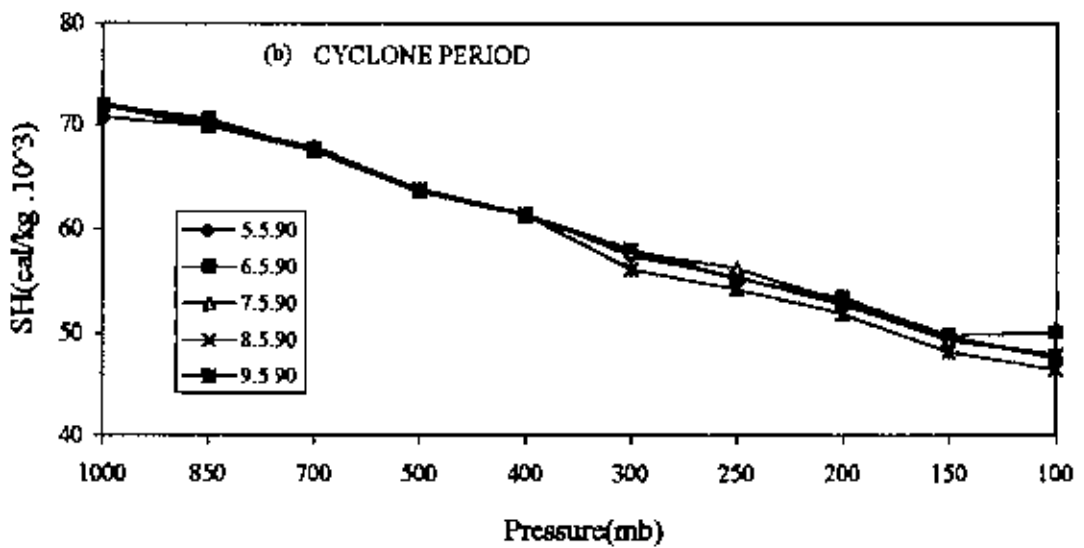
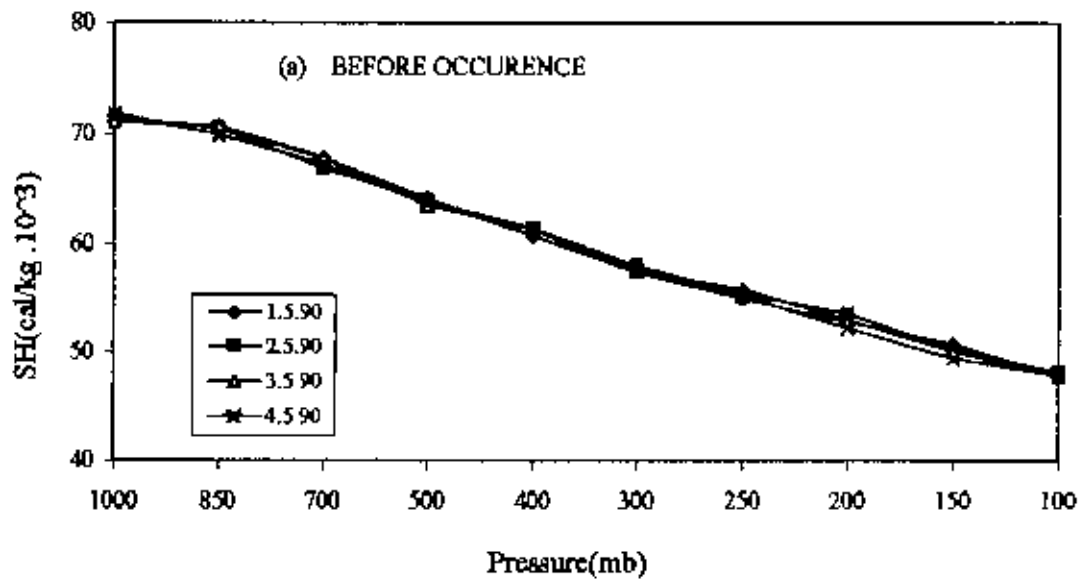


Fig. 5.1.1. (a-c) Sensible heat variation at different isobaric levels



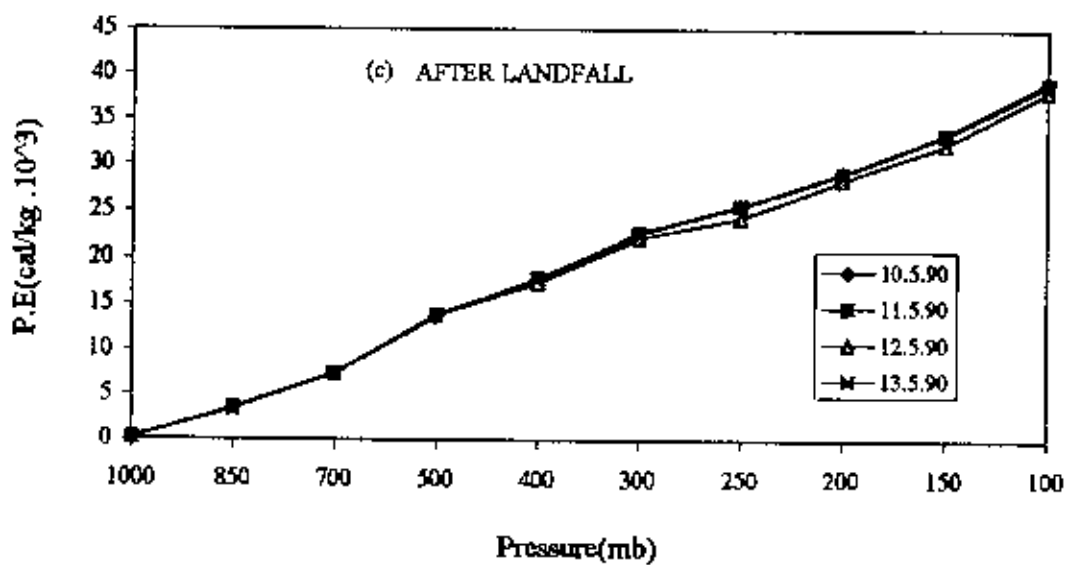
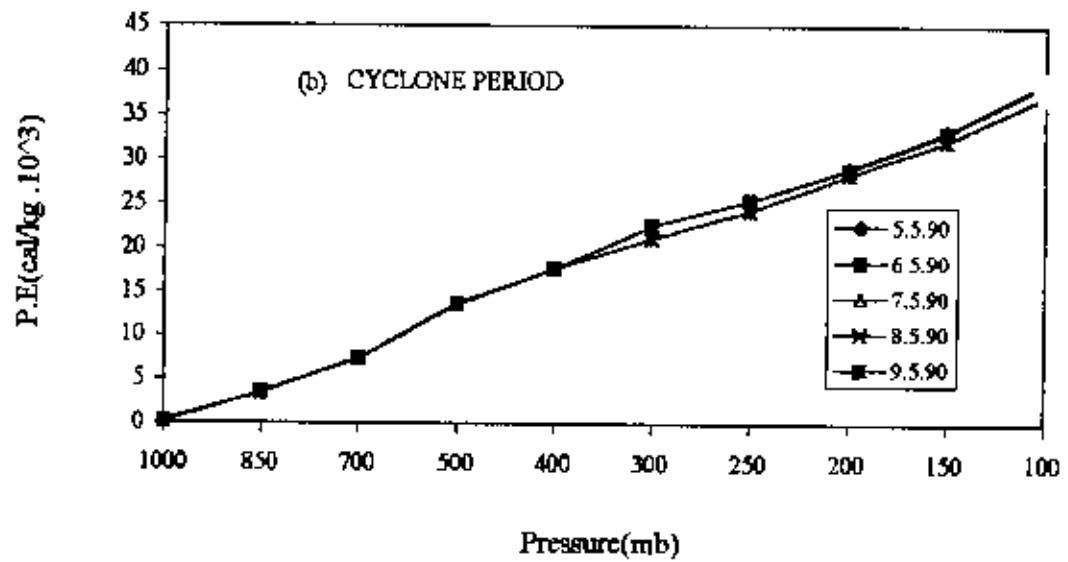
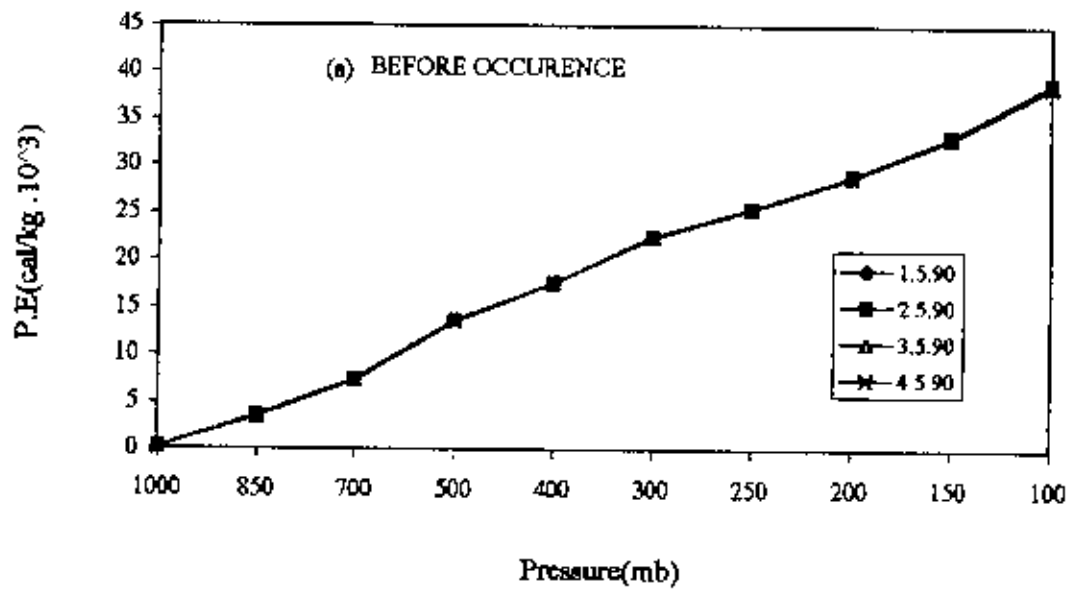


Fig. 5.1.2 (a-c) Variation of potential energy per unit mass at different isobaric levels.

### Latent Heat Content (LHC) :

The variation of Latent heat content at different isobaric level is shown in Fig. 5.1.3(a-c). From Fig. 5.1.3(a) it is seen that before occurrence LHC fluctuated for all the days at all the levels with an exception of 4.5.90. At that day it was almost constant up to 400 mb and then slightly increased. At 400 mb on 1.5.90 the LHC was maximum.

From Fig. 5.1.3(b) it is seen that Latent heat content was almost constant from 1000 mb - 700 mb for all days with an exception of 7.5.90. It is also seen that at the peak time of the cyclone [7.5.90] LHC was unstable and maintained a zigzag Path up to 400 mb and then decreased slightly. Beyond 700 mb for first two days of the cyclone period [5.5.90-6.5.90] LHC increased up to 400 mb and then decreased slightly. After 700 mb for the last two days of cyclone period [8.5.90-9.5.90] LHC decreased up to 500 mb and then increased.

The variation of Latent heat content after landfall [10.5.90 - 13.5.90] is shown in Fig. 5.1.3(c). It is seen that for all the days Latent heat content was constant from 1000 mb to 850 mb with an exception on 10.5.90. At 700 mb it increased for all the days. Beyond 700mb for 13.5.90 it increased linearly up to 300mb and then decreased at 250mb. At the very beginning of land fall [10.5.90] after 700mb it remains near about constant up to 400mb and then fluctuate. After 700mb for 11.5.90 and 12.5.90 it increased and then decreased at 250 mb.

From these figures [Fig. 5.1.3(a-c)] it is observed that Latent heat content increased at middle troposphere (i.e. 700mb - 300mb) due to more moisture. This is the cloud-forming region and in this zone water vapor condensed release latent heat. It was also seen that LHC is maximum after landfall.

### Kinetic Energy (KE):

Fig. 5.1.4(a-c) shows the variation of kinetic energy variation at different isobaric level. From this figure it is seen that KE was near about zero for all the phases (Before occurrence, cyclone period and after landfall) at 1000 mb and then increased linearly up to 200mb and then decreased for 1.5.90, 2.5.90, 7.5.90 and 13.5.90 (at the end of the cyclone). But for other days it increased linearly except for 5.5.90 and 6.5.90 (at the

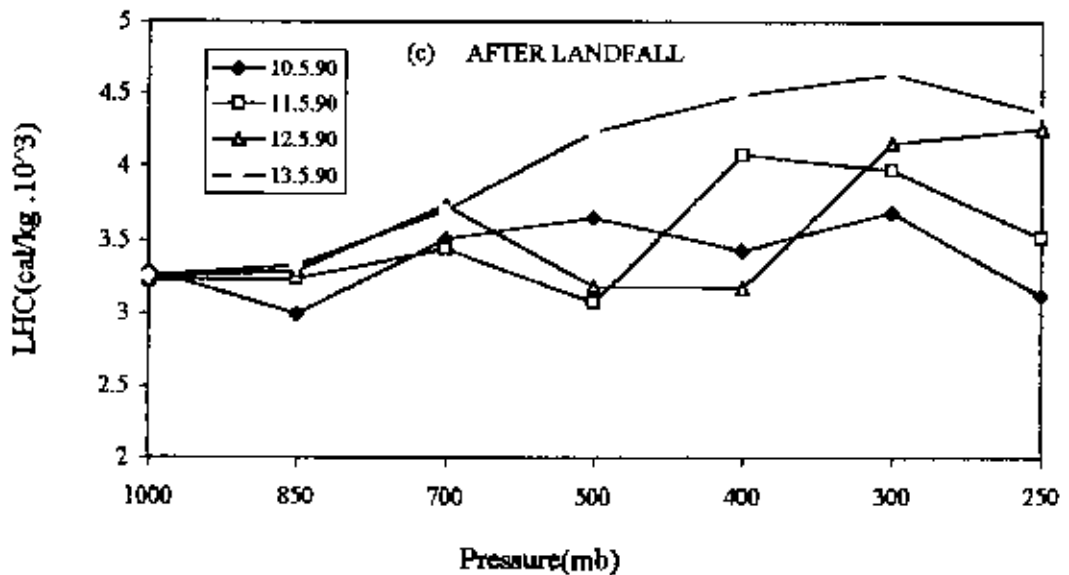
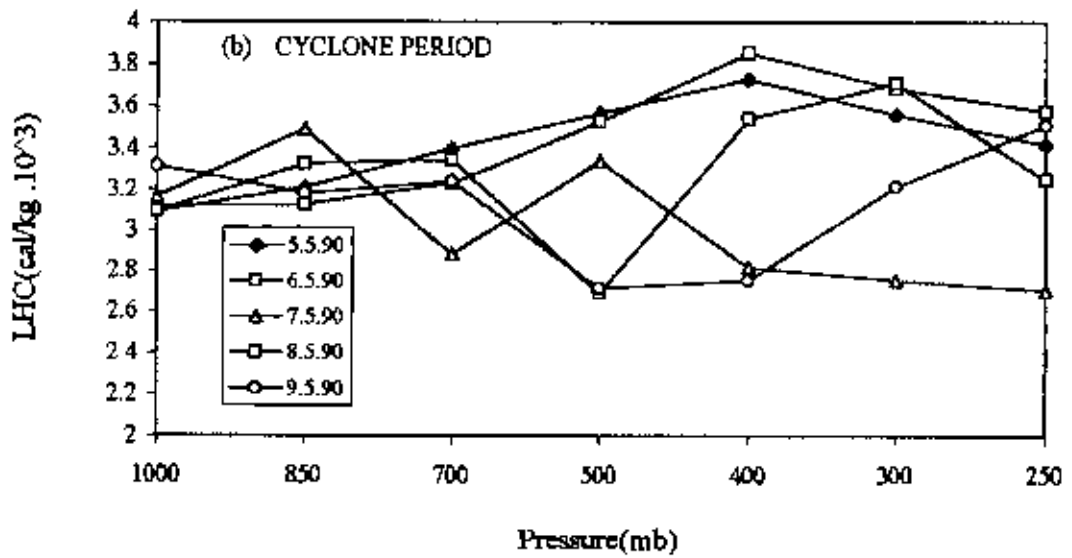
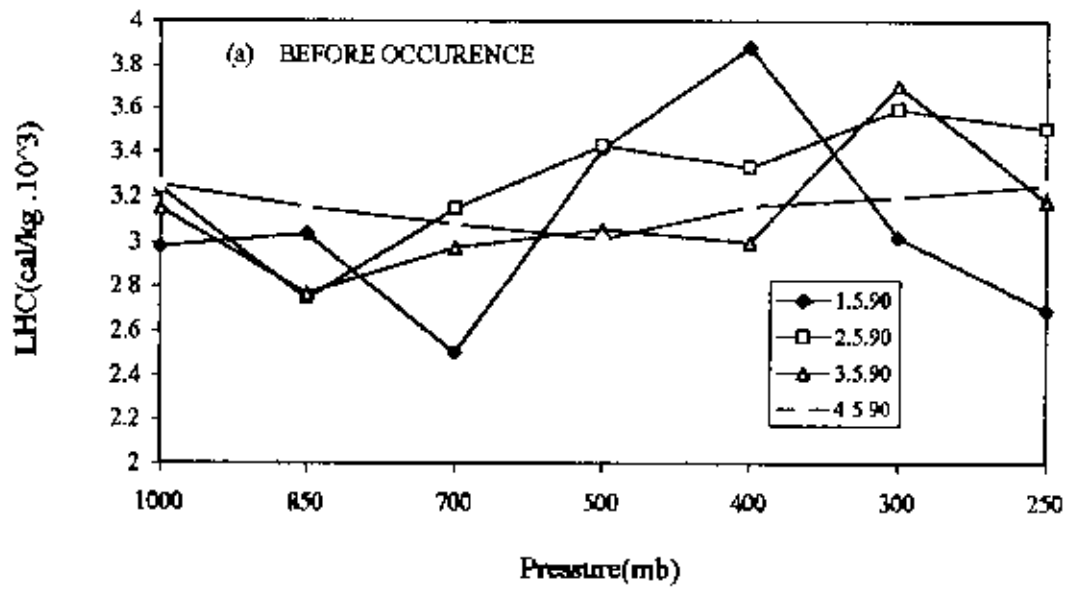


Fig. 5.1.3 (a-c) Latent heat content variation at different isobaric levels.

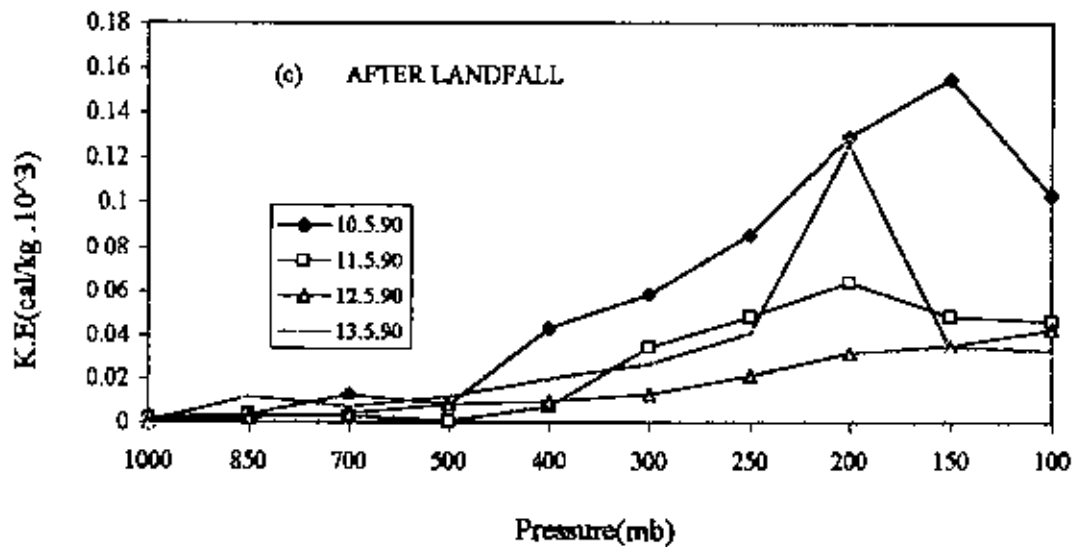
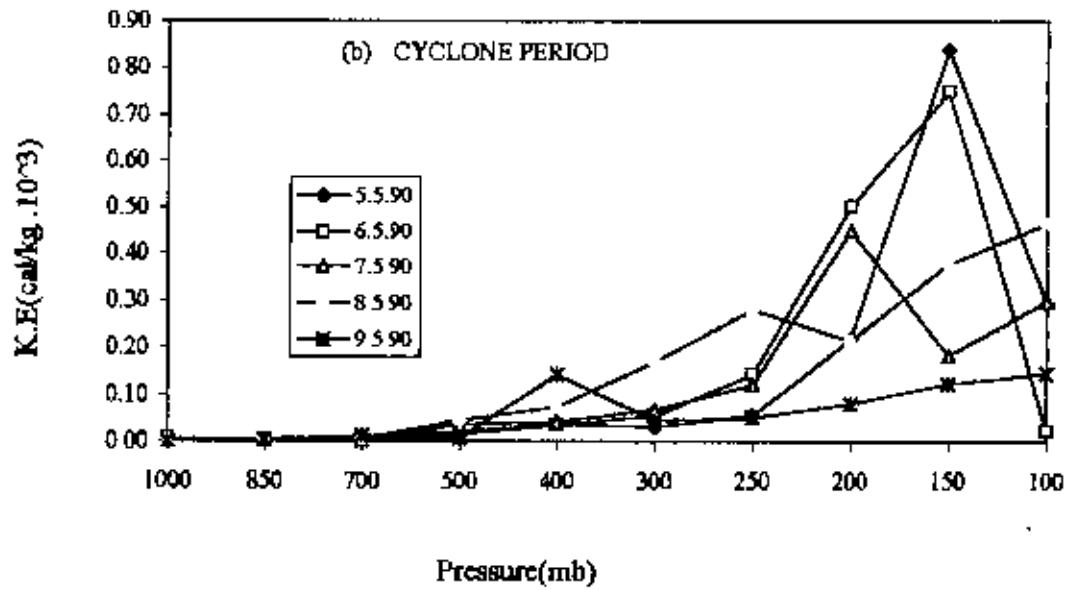
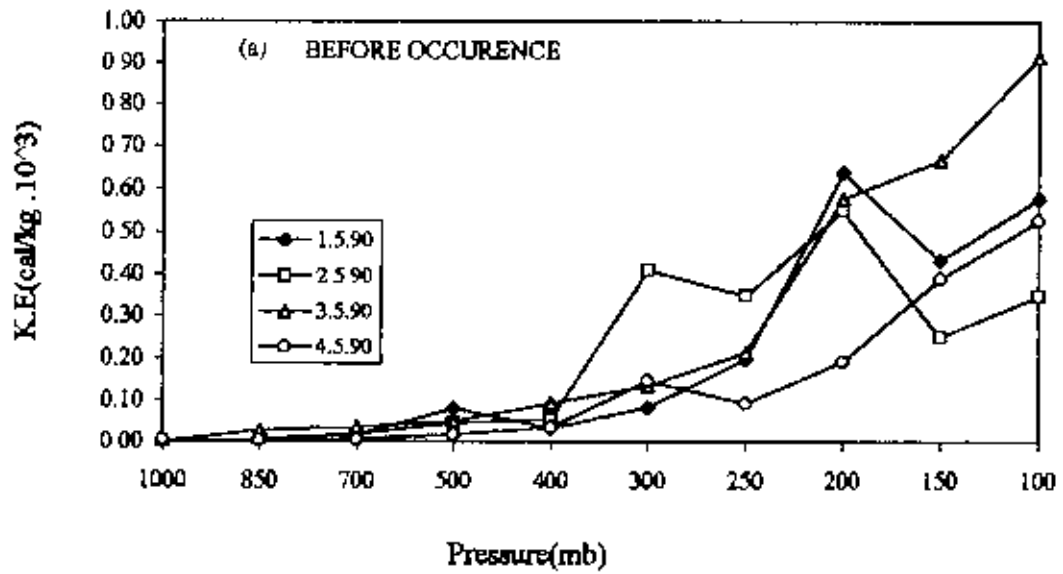


Fig. 5.1.4 (a-c): K.E Variation at different isobaric Levels

cyclone period). It is seen that KE was large at the early cyclone period [Fig. 5.1.4(b)] compared with that at the end of cyclone period. After landfall the amount of KE was smaller than that of cyclone period or before occurrence.

#### 4.2.1(b). Energy fluxes:

##### Zonal Flux of Dry Static Energy (ZFDSE):

Zonal flux of dry static energy (ZFDSE) at different isobaric level is shown in Fig 5.1.5(a-c). Before occurrence (1.5.90-4.5.90) it is seen that ZFDSE was near about zero at 1000mb and then increased as pressure decreased. But at 4th May (just before cyclone period) it was negative (westward) from 1000 mb to 700 mb. After 700mb it turned into positive (Eastward) and then increased linearly with the same sign up to the top of the troposphere.

At cyclone period [Fig. 5.1.5(b)] it is observed that for first two days at 1000 mb and 850 mb ZFDSE was negative (westward) and for all other days it was positive (eastward). It is seen that ZFDSE increased linearly with height and attained maximum value at 150 mb at the very beginning of the cyclone period (5.5.90 and 6.5.90) and then decreased at 100 mb. At 7th May it increased up to 200 mb and then decreased at 150 mb. It increased again at 100 mb. So we can say that at cyclone period ZFDSE was very unstable condition.

After landfall [Fig. 5.1.5(c)] it is seen that at 1000 mb ZFDSE was negative (westward). Beyond 1000 mb it turned to positive (eastward) and increased up to 200 mb and then decreased with the same sign on 10.5.90 (just at the time of landfall). We saw that after landfall for 2nd day (11.5.90) it was almost zero at 100 mb. This is an indication of no wind at that level. It is also seen that on 12.5.90 and 13.5.90 at 100 mb it was negative (westward).

From the above figure [Fig. 5.1.5(a-c)] it is observed that at the lower level of the troposphere (1000 mb) ZFDSE was near about zero and beyond 1000 mb it increased linearly due to the increase of geopotential height. It is also seen that at cyclone period and after landfall at 1000 mb it was negative (westward). After that it was positive (eastward) and at the end of landfall it was again negative (westward).

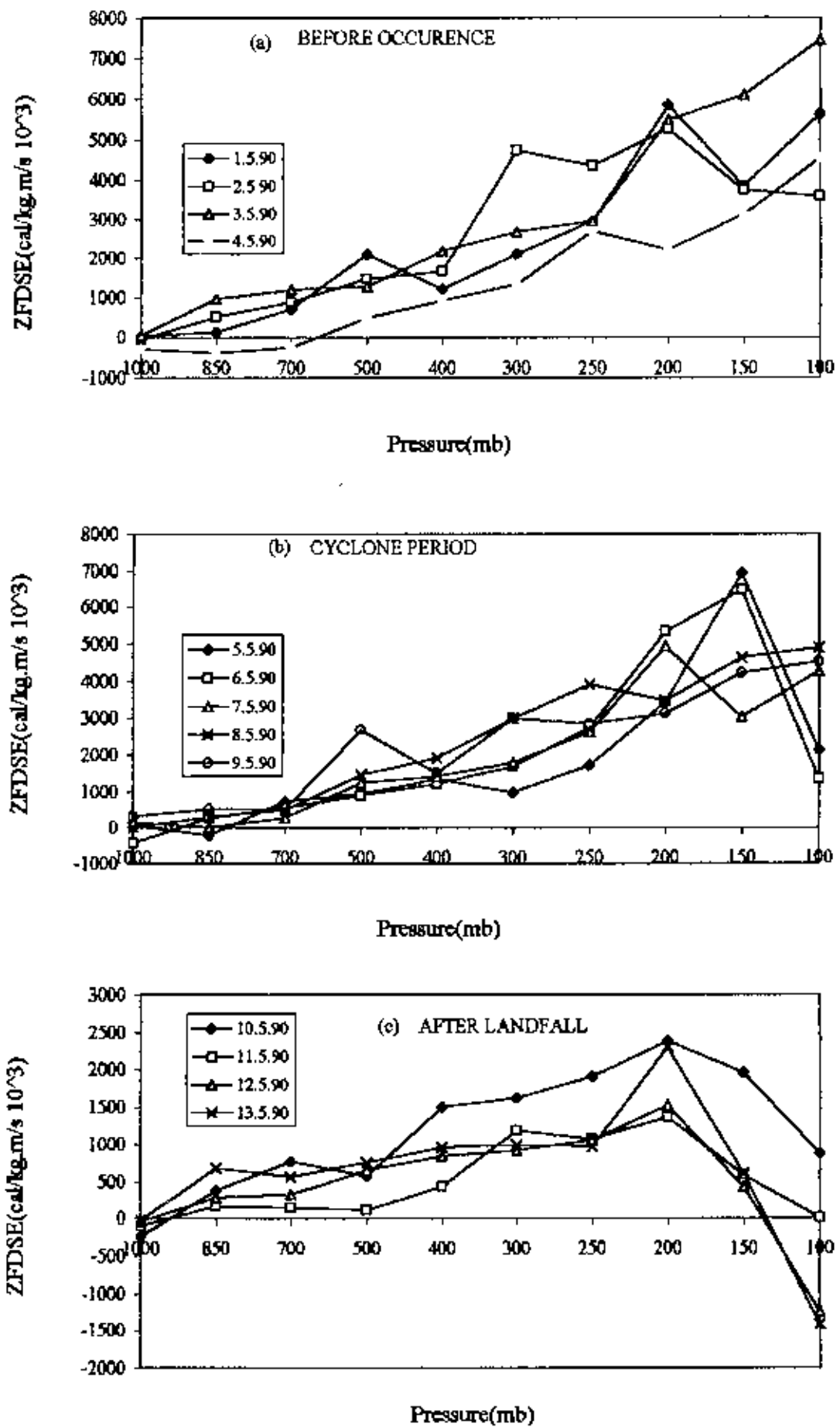


Fig. 5.1.5 (a-c): Variation of zonal fluxes of dry static energy at different isobaric levels

During cyclone period it is observed that at 150mb ZFDSE was maximum and shows two peaks. This was due to the increase of zonal wind component at 150 mb.

#### **Zonal Flux of Moist Static Energy (ZFMSE):**

Zonal flux of moist static energy (ZFMSE) at different phases (before occurrence, cyclone period and after landfall) is shown in Fig. 5.1.6(a-c). From these figure it is seen that ZFMSE was negative (westward) for all the phases at 1000 mb and then increased with increasing height (as pressure decreased). It is also seen that the increasing rate of ZFMSE was the same as that of ZFDSE which was discussed earlier [Fig. 5.1.5(a-c)]. This is because moist static energy is simply an addition of latent heat content with dry static energy. But at cyclone period on 9th May, ZFMSE increased up to 400 mb, then decreased at 300 mb and then increased again at 250 mb. This instability was due to the change of zonal wind component. It is also seen that ZFMSE was maximum at early cyclone period (6th May) at 250 mb (i.e., upper level of the troposphere).

#### **Meridional Flux of Dry Static Energy (MFDSE):**

Fig. 5.1.7(a-c) shows the MFDSE at different isobaric level. Before occurrence it is seen that on first May MFDSE was negative (southward) at 1000 mb and then it turned into positive (northward) and fluctuated at layer to layer maintaining a zigzag path. On 2nd May, it was near about zero up to 400 mb and then increased and fluctuated. On 3rd May, it was positive (northward) at 1000 mb-800 mb. Beyond 850 mb it was negative (southward) at 700 mb - 500 mb due to the change of wind direction. After 500 mb it was zero up to 300 mb and then increased to the positive (northward) direction up to 150 mb and then decreased to the negative (southward) at 100 mb. On 4th May it is seen that MFDSE increased linearly up to 150 mb and then decreased to negative (southward) direction at 100 mb.

At cyclone period [Fig. 5.1.7(b)] layer to layer variation of MFDSE for all the days was symmetric. It was fluctuated and increased from 1000 mb-150 mb. Beyond 150 mb, it is seen that at the very beginning of the cyclone (5th May) it increased abruptly at 100 mb.

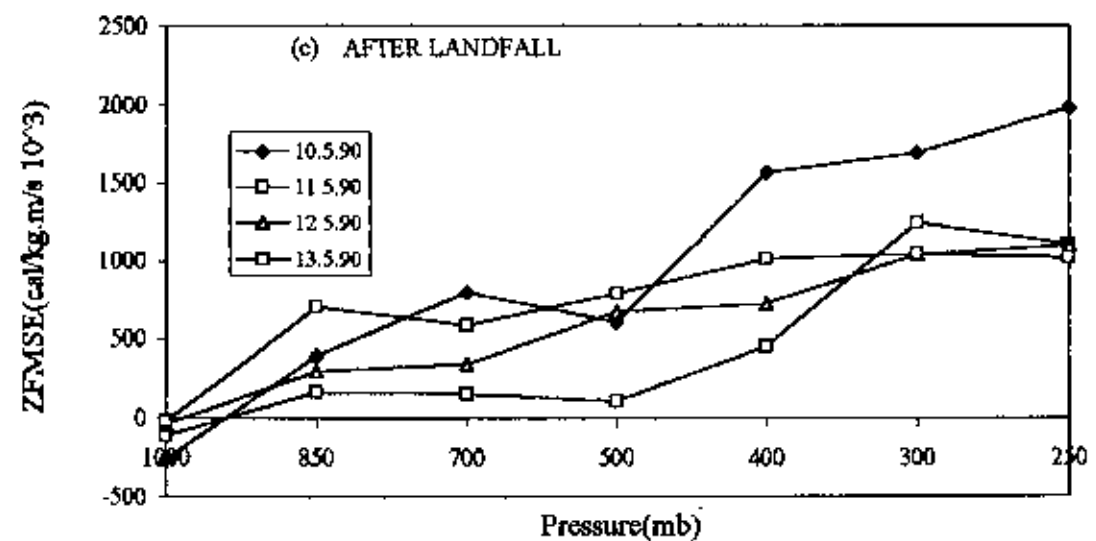
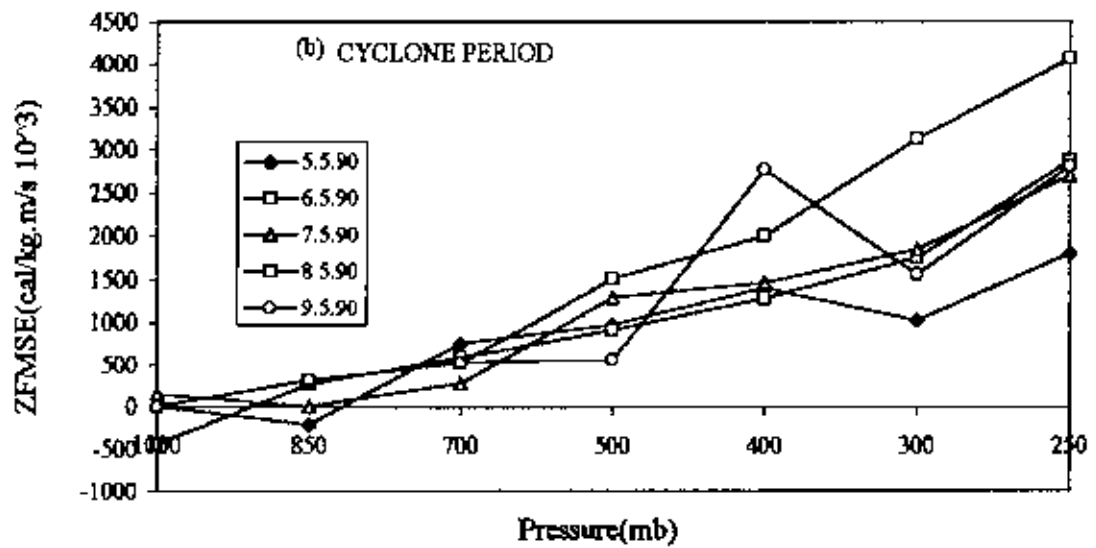
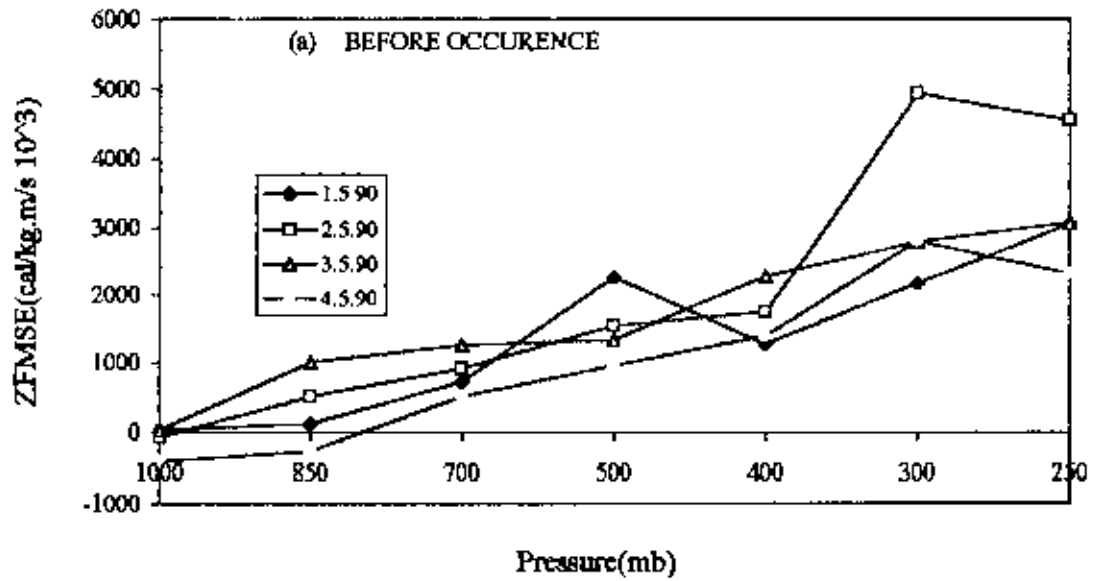


Fig. 5.1.6 (a-c) Variation of zonal fluxes of moist static energy at different isobaric levels.



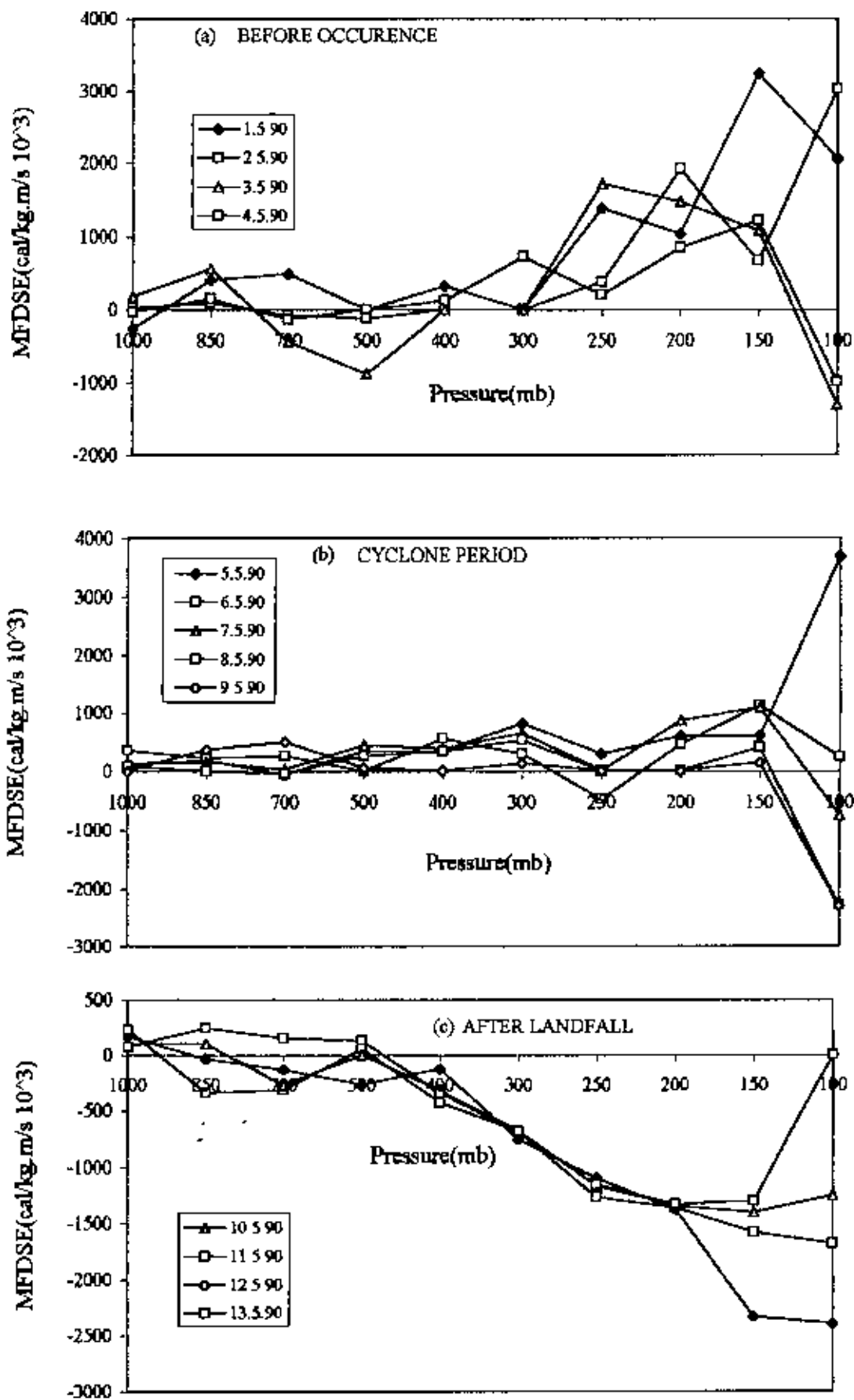


Fig. 5.1.7. (a-c). Variation of meridional fluxes of dry static energy at different isobars levels

But for all other days it decreased at 100 mb. It is also seen that on 7-9 May it decreased to the negative (southward) direction.

After landfall it is observed that at 1000 mb MFDSE was positive (northward) and then turned into negative (southward) for all the days with an exception of 11th May. On 11th May it was positive (northward) up to 500 mb. Beyond 500 mb for all the days it was negative (southward) and increased to the negative direction up to the top of the troposphere. It is also seen that at 11th May it was zero at 100 mb. This was because meridional wind component was zero at that level.

From Fig. [5.1.7(a-c)] it is observed that before occurrence and during cyclone period MFDSE was positive (northward) for all the days and levels with an exception of 3rd May at 100 mb. At 100 mb level it was negative (southward). But after landfall it was in reverse characteristics i.e., it was negative (southward) and changes its direction with an exception of 11th May. At 11th May it is seen that MFDSE was positive up to 500 mb and then turned into negative (southward). It is also seen that MFDSE was maximum at 100 mb during cyclone period. This shows that wind velocity was maximum at the top of the troposphere.

#### **Meridional Flux of Moist Static Energy(MFMSE):**

Meridional flux of moist static energy (MFMSE) at different isobaric levels is shown in Fig. 5.1.8(a-c). Before occurrence it is seen that on 1st May it was negative (southward) at 1000 mb and then it increased and fluctuated with positive direction. On 2nd May, it was near about zero at 1000 mb and then increased slightly at 850 mb. Beyond 850 mb it was again nearly zero up to 300 mb and then increased at 250 mb. At 700 mb and 500 mb it was southward. On 3rd May MFMSE was fluctuated both in positive and negative direction. On 4th May it was nearly zero up to 400 mb. Beyond 400 mb it increased and then decreased.

At cyclone period for all the days MFMSE is fluctuated at layer to layer due to the change of the direction of wind component. But this fluctuation was symmetric for all the days. Here it is also seen that it was increased up to 300 mb and then decreased.

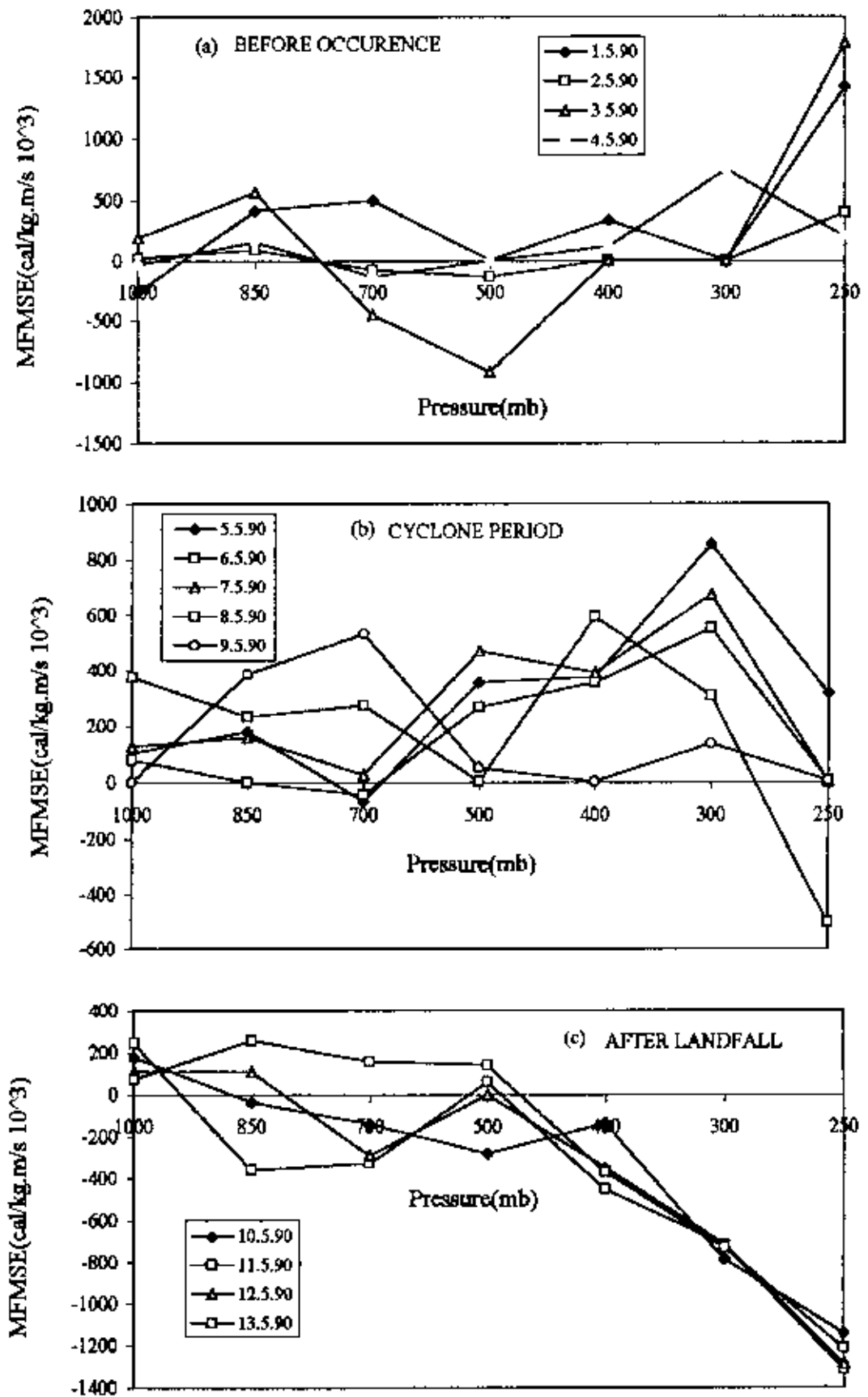


Fig. 5.1.8 (a-c): Variation of meridional fluxes of most static energy at different isobaric le

After landfall [Fig. 5.1.8(c)] it is seen that graph pattern was same with that of Fig. 5.1.7(c) which is discussed earlier. This is because moist static energy is an addition of latent heat content with dry static energy.

From the above figure [Fig. 5.1.8(a-c)] we observed that at cyclone period MFMSE at 100 mb was positive at the beginning of cyclone, then became zero during cyclone due to the absence of wind component. On 8.5.90 it was negative at 250 mb. After landfall it was more or less negative (southward) from 850 mb-500 mb. Beyond 500 mb it was completely negative for all the days and increased up to 250 mb. It is also seen that MFMSE was maximum at upper levels for all the days. This was because maximum cloud is formed at the upper levels and released latent heat so increased moist static energy. Hence it is also saw that the direction of meridional wind component was reversed between cyclone period and after landfall.

#### 4.2.2. Cyclone 2

Cyclone 2 occurred during the period 16-18 December 1990. To observe its “before occurrence” and “after landfall” conditions, data were analyzed from 11 December 1990 to 23 December 1990. The track of this cyclone is shown in Fig. 3.

##### 4.2.2. (a) Energy components:

###### Sensible Heat (SH):

Fig. 5.2.1(a-c) shows the variation of sensible heat (SH) at different isobaric levels. From these figure it is observed that sensible heat decreased with the increase of height i.e. as pressure decreased. It is seen that day to day variation for all the levels was symmetric with some exception. At cyclone period [Fig. 5.2.1(b)] it is observed that at the beginning of cyclone (16.12.90) at 300 mb sensible heat decreased abruptly. This is due to the large decrease of temperature at that level. After landfall [Fig. 5.2.1(c)] it is seen that at 200 mb sensible heat increased more for 21.12.90 compared to the other day. This is because of increasing temperature compared to the other day.

We know sensible heat is the product of specific heat at constant pressure,  $C_p$  with temperature,  $T$  (i.e.,  $C_p T$ ). From the above figure we observed that sensible heat was maximum at 1000 mb i.e., at the lower level of the troposphere and minimum at 100 mb i.e. at the upper level of the troposphere. This is because the earth surface receives solar energy from the sun and becomes heated. The layer of 1000 mb is very close to the earth surface compared to the other layer. And for this reason temperature is maximum at 1000 mb. So sensible heat was maximum at 1000 mb and then decreased linearly as the height increases from the earth surface.

###### Potential Energy (PE):

The variation of Potential energy at different isobaric levels is shown in Fig. 5.2 2(a-c). Here for all phases (before occurrence, cyclone period and after landfall) It is seen that potential energy increased linearly as pressure decreased. This linear increased was due to the increase of geopotential height. Here for all phase day to day variation was symmetric and the values were almost same at all levels. For this reason at all levels, the

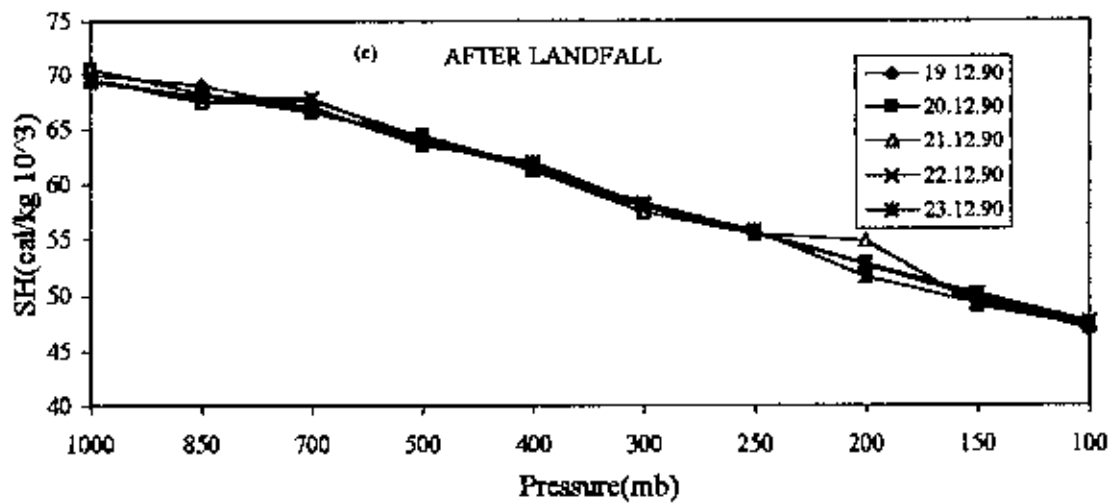
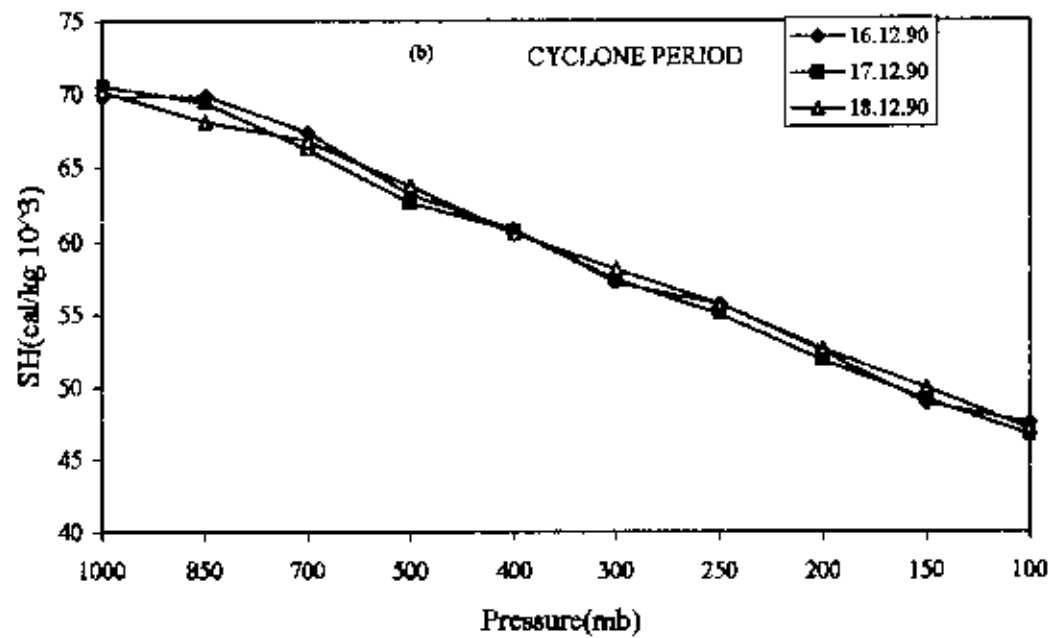
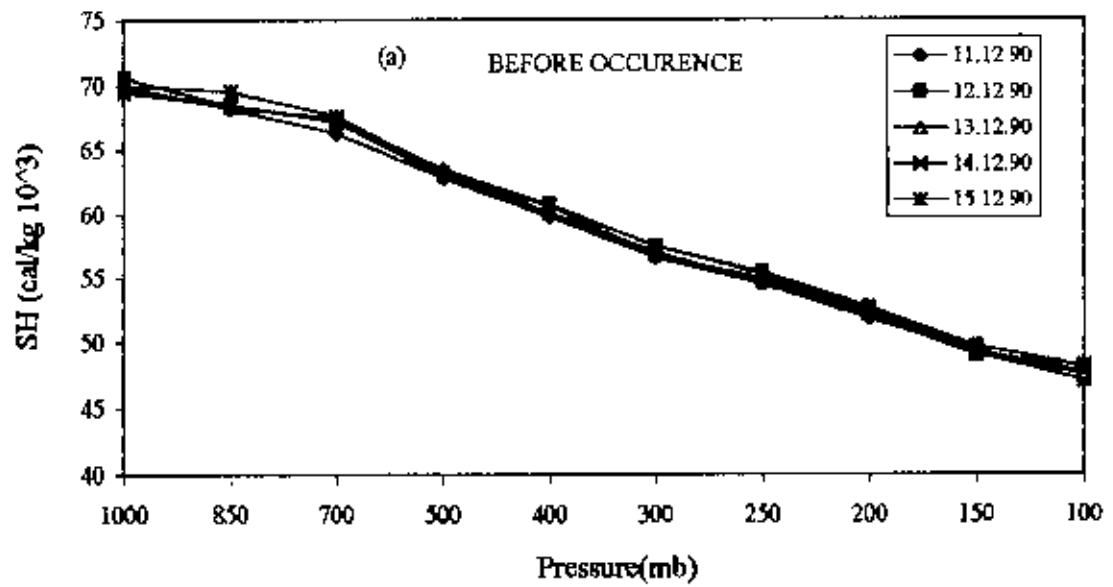


Fig. 5.2.1. (a-c)Sensible heat variation at different isobaric level.

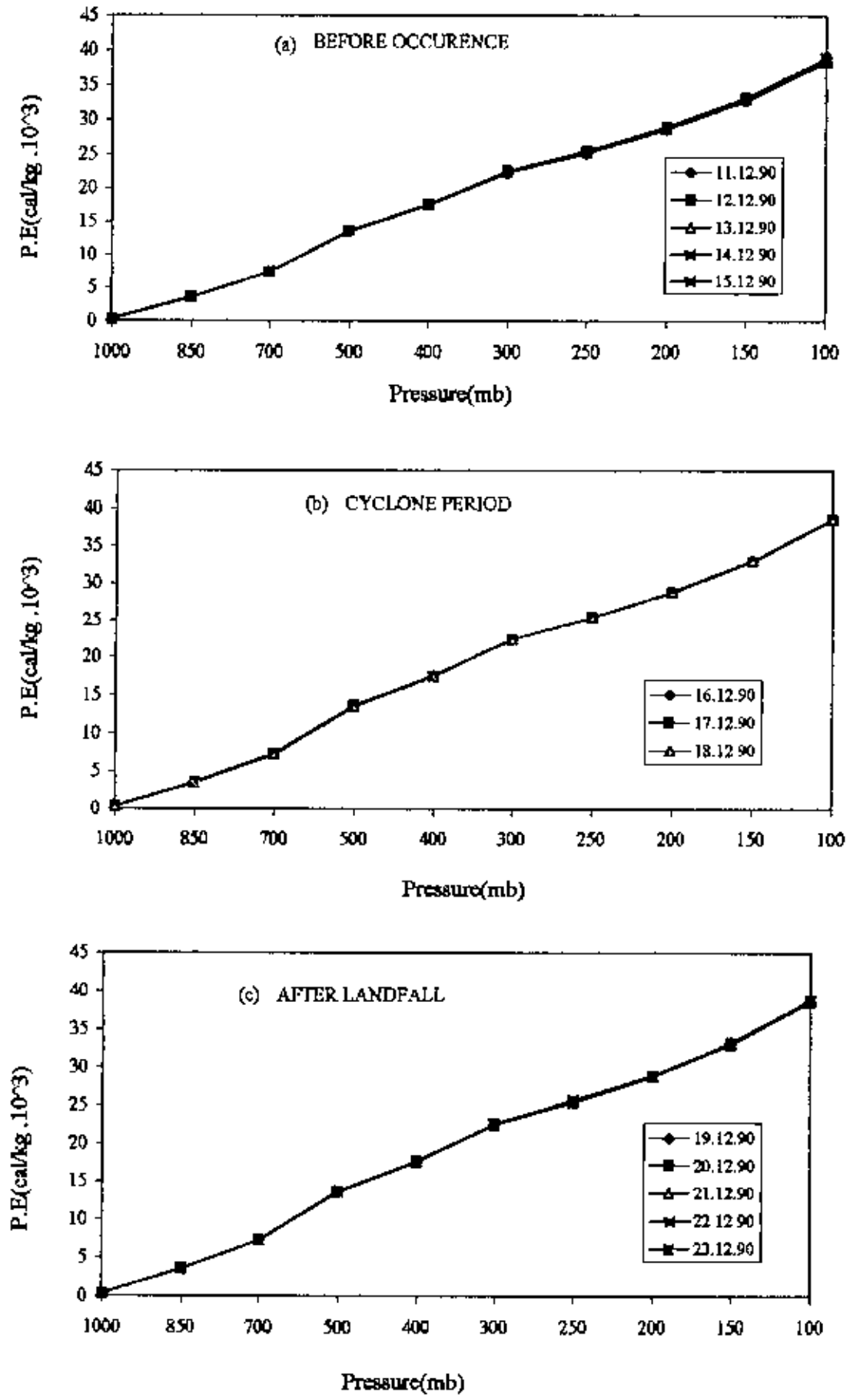


Fig. 5.2.2 (a-c) Potential energy variation at different isobaric levels.

points overlap each other. It is also observed that, before occurrence, at cyclone period and after landfall there was approximately no change of potential energy. But for all phases potential energy increased as pressure decreased. It was about zero at 1000 mb i.e. at lower level of the troposphere and maximum at 100 mb i.e. at upper level of the troposphere.

#### Latent Heat Content (LHC):

Fig. 5.2.3(a-c) shows the variation of latent heat content at different isobaric levels. Before occurrence at 1000 mb-700 mb latent heat content was almost same. Beyond 700 mb it increased slightly at 500 mb and maintained the same value up to 300 mb except 11 and 13 December 1990.. At 250 mb for all the days it decreased except on 15 Dec. 1990.

At cyclone period it increased slightly up to 400mb. From 300 mb to 250 mb LHIC increased abruptly on 18.12.90.. This was due to the more cloud formation. At 250 mb it decreased but for 18.12.90 latent heat content increased. This indicates that more cloud existed at the upper level on 18 Dec. 1990.

From Fig. 5.2.3(c) it is seen that LHC is fluctuated for all the days and levels and it was maximum between 500 mb-300 mb.

From the above figures [Figs. 5.2.3(a-c)] it is observed that latent heat content increased from 700 mb-300 mb for before occurrence and after landfall. It increased because this is the cloud forming region (700 mb-300 mb) and released latent heat. But at cyclone period it was maximum at 300 mb and 250 mb for 18.12.90. This means that at the end of the cyclone period (18.12.90) more cloud is formed and rain occurs.

#### Kinetic Energy (KE):

The variation of kinetic energy at different isobaric levels is shown in Fig. 5.2.4(a-c). It is seen that at 1000 mb-700 mb K.E. was nearly zero. After 700 mb it increased up to 150 mb and then decreased at 100 mb. At cyclone period it is also seen that at the beginning of the cyclone (16.12.90) it increased from 1000 mb to 250 mb and then fluctuated. This means that at cyclone period the weather was very unstable and the wind velocity randomly changed. At cyclone period and after landfall we observed that from



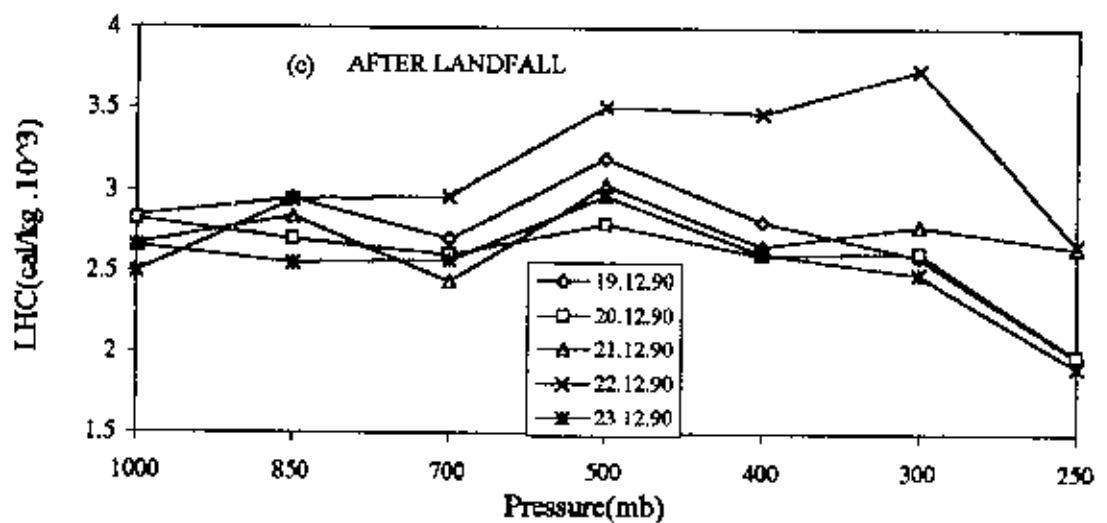
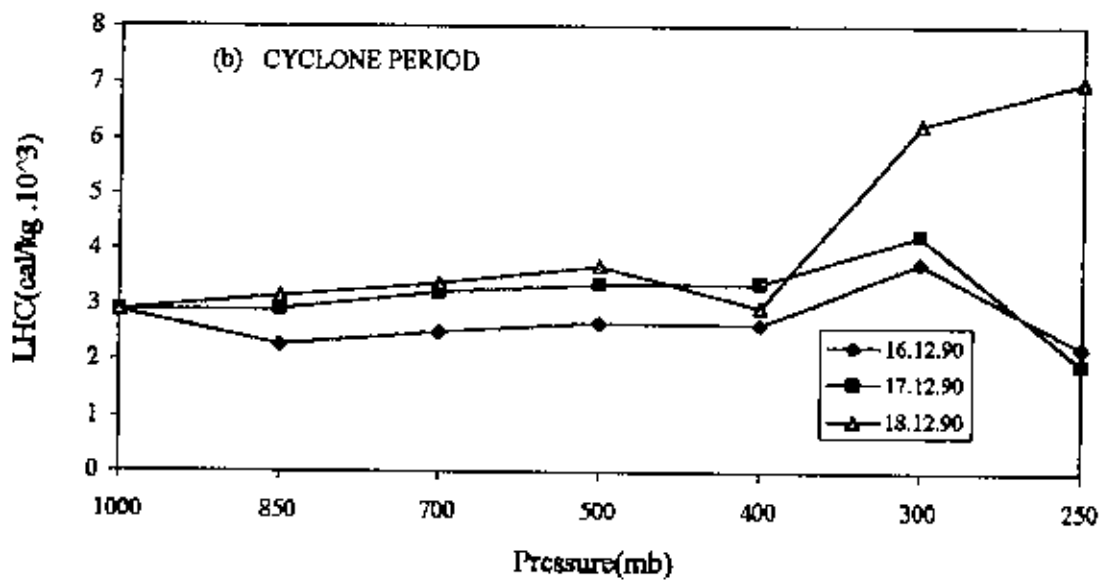
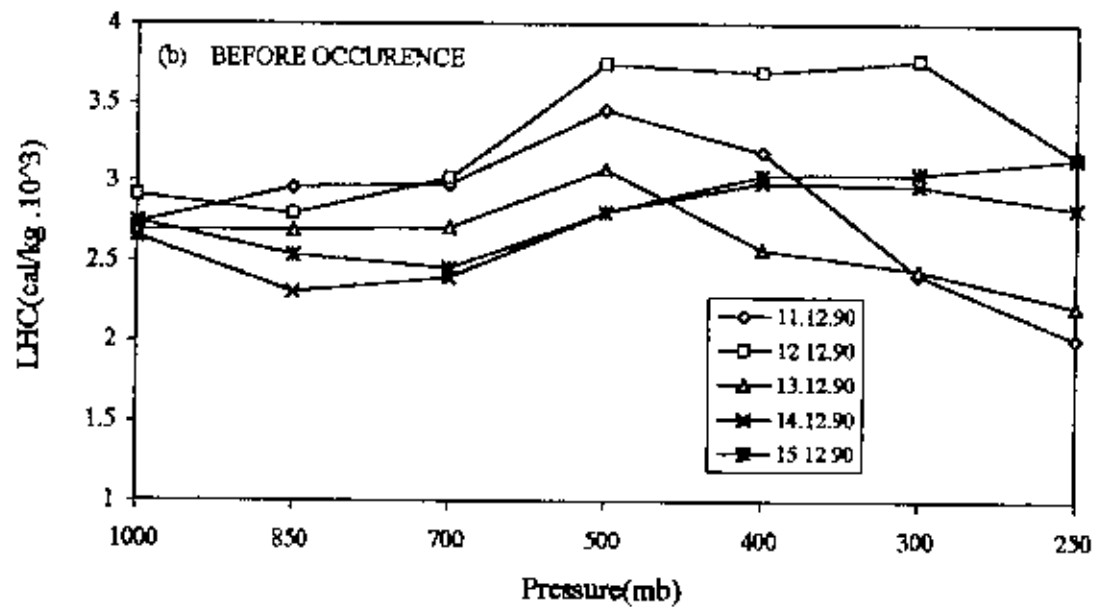


Fig. 5.2.3 (a-c) Latent heat content variation at different isobaric levels.

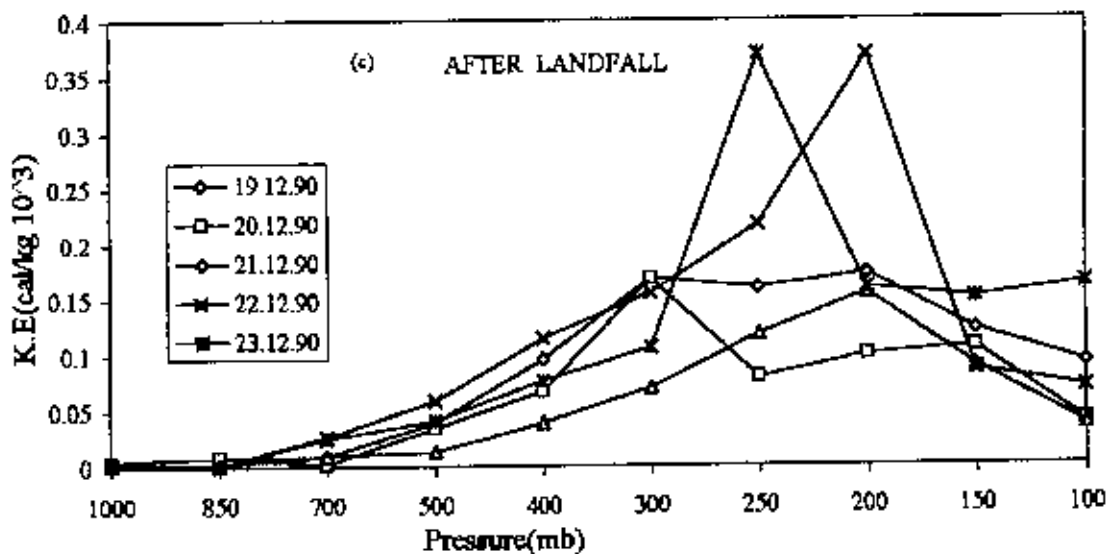
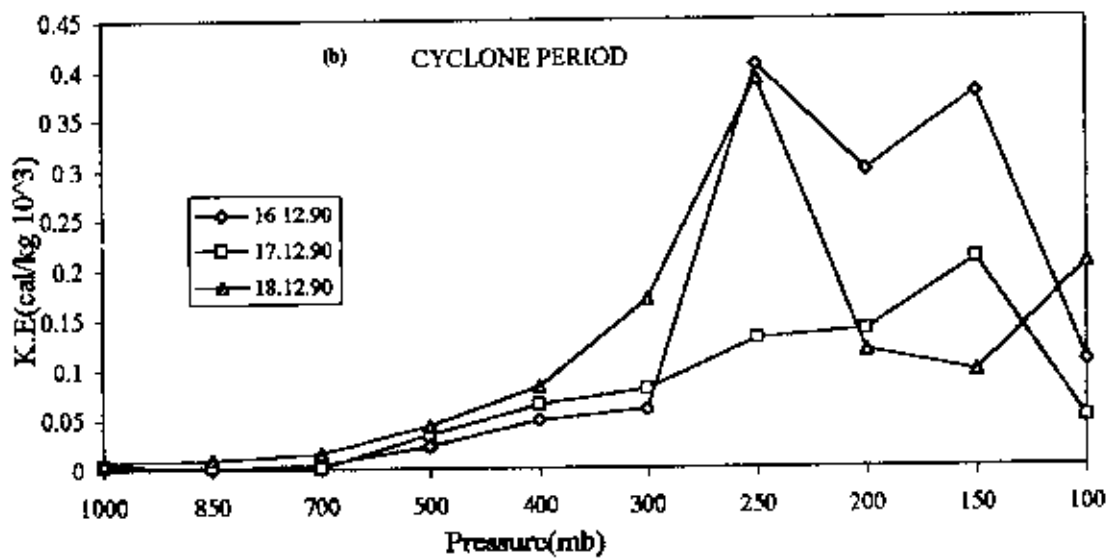
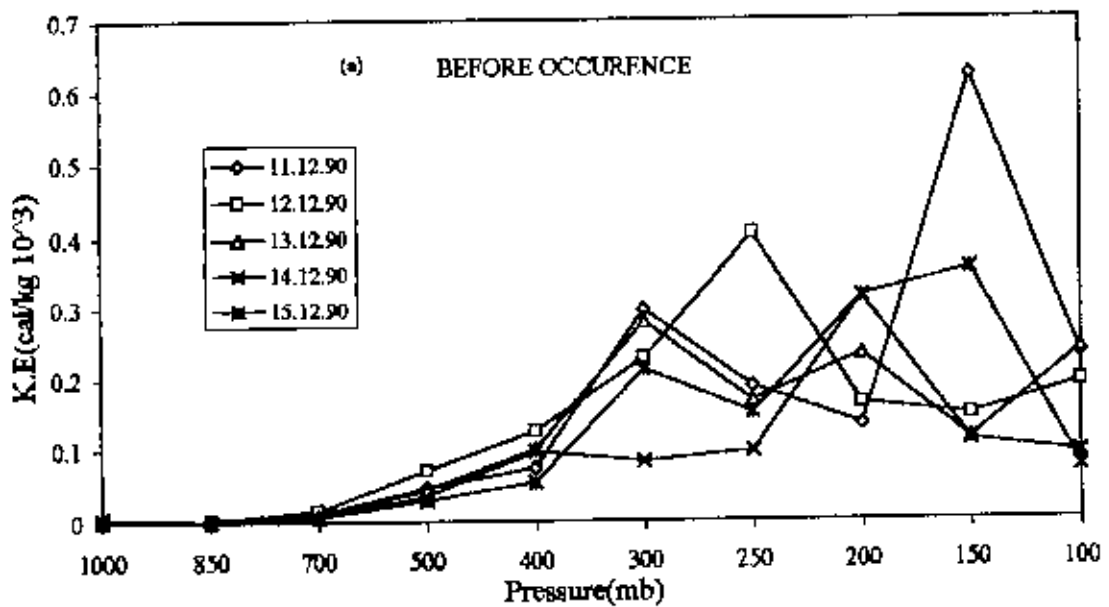


Fig. 5.2.4 (a-c) Kinetic Energy Variation at different isobaric level.

middle to upper level of the troposphere (without 100 mb) KE was maximum. This is due to the increase of wind velocity in these region.

#### 4.2.2. (b) Energy fluxes:

##### Zonal Flux of Dry Static Energy (ZFDSE):

Fig. 5.2.5(a-c) shows the variation of zonal flux of dry static energy (ZFDSE) at different isobaric levels. Here it is observed that for before occurrence, cyclone period ZFDSE was almost zero and negative (westward) at 1000 mb-850 mb. After 850 mb it increased more or less linearly in the positive (eastward) direction. At cyclone period [Fig. 5.2.5(b)]. It is seen that from 300 mb to 100 mb for all the days it increased and decreased from layer to layer. This is due to the randomness of the wind velocity from middle to the upper level of the troposphere.

After landfall ZFDSE increased linearly up to 200 mb except 20.12.90. At this day it was pulsating in nature above 300 mb. Beyond 200 mb it decreased.

From the above figure [Fig. 5.2.5(a-c)] it is observed that ZFDSE was maximum between 250 mb-150 mb. Here it is also seen that at 1000 mb ZFDSE was zero and negative (westward) for before occurrence and at cyclone period. But after landfall at 1000 mb it was completely positive (eastward). Here we observed that near about the surface layer (1000 mb) wind direction was opposite at cyclone period and after landfall.

##### Zonal Flux of Moist Static Energy (ZFMSE):

Fig. 5.2.6(a-c) shows the variation of zonal flux of moist static energy (ZFMSE) at different isobaric levels. Before occurrence [Fig. 5.2.6(a)] it was zero and negative (westward) at 1000 mb and 850 mb. Beyond 850 mb it increased up to 300 mb, then decreased at 250 mb with an exception of 11.12.90. At 11.12.90 it increased for 250 mb.

At cyclone period [Fig. 5.2.6(b)] ZFMSE was negative (westward) at 1000 mb for all the days. At the end of the cyclone period (18.12.90) it was also negative (westward) for 850 mb. Then for all the days it turned into positive (eastward) and increased linearly with the same sign up to 250 mb.

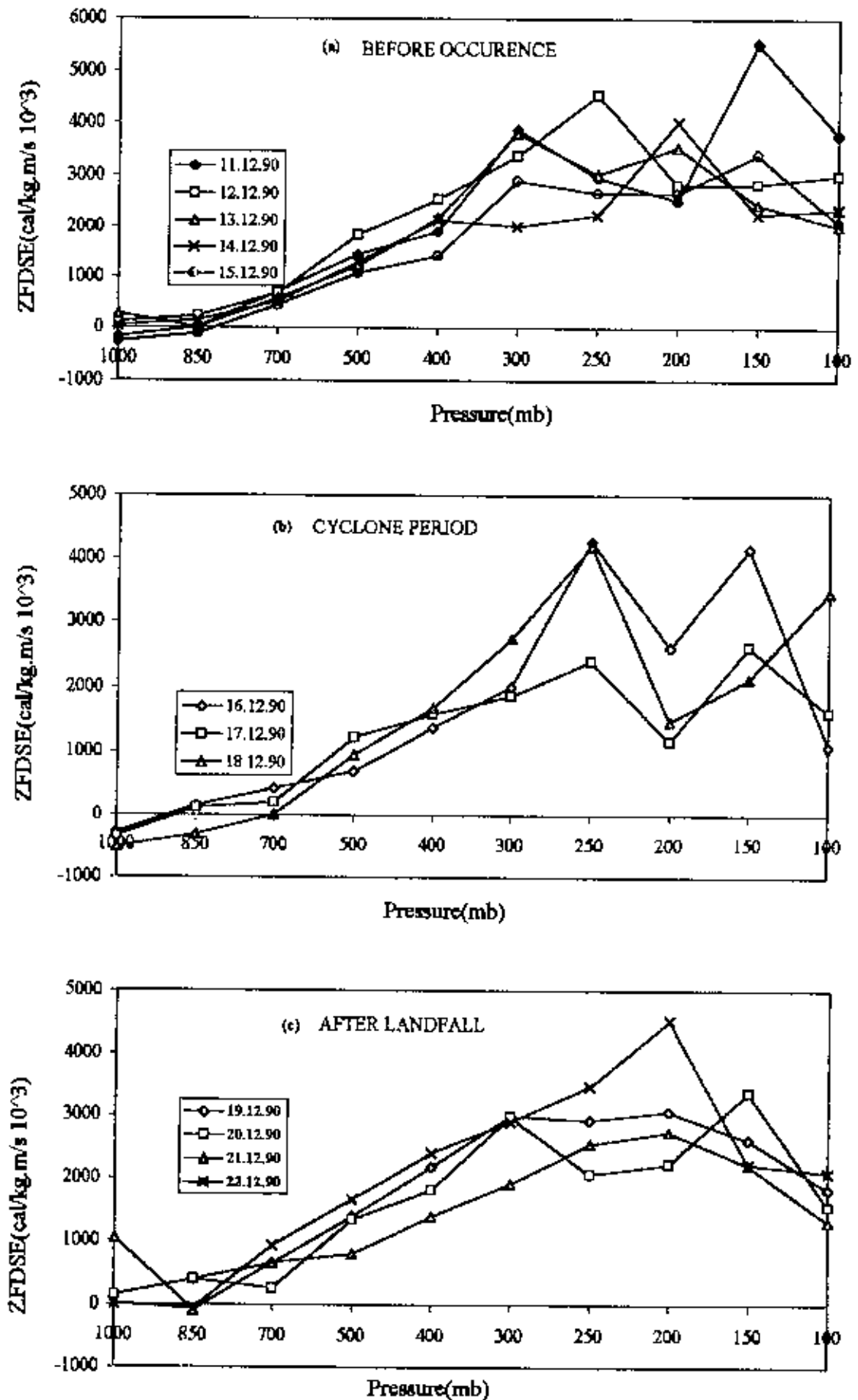


Fig. 5.2.5 (a-c) Variation of zonal fluxes of dry static energy at different isobaric levels.

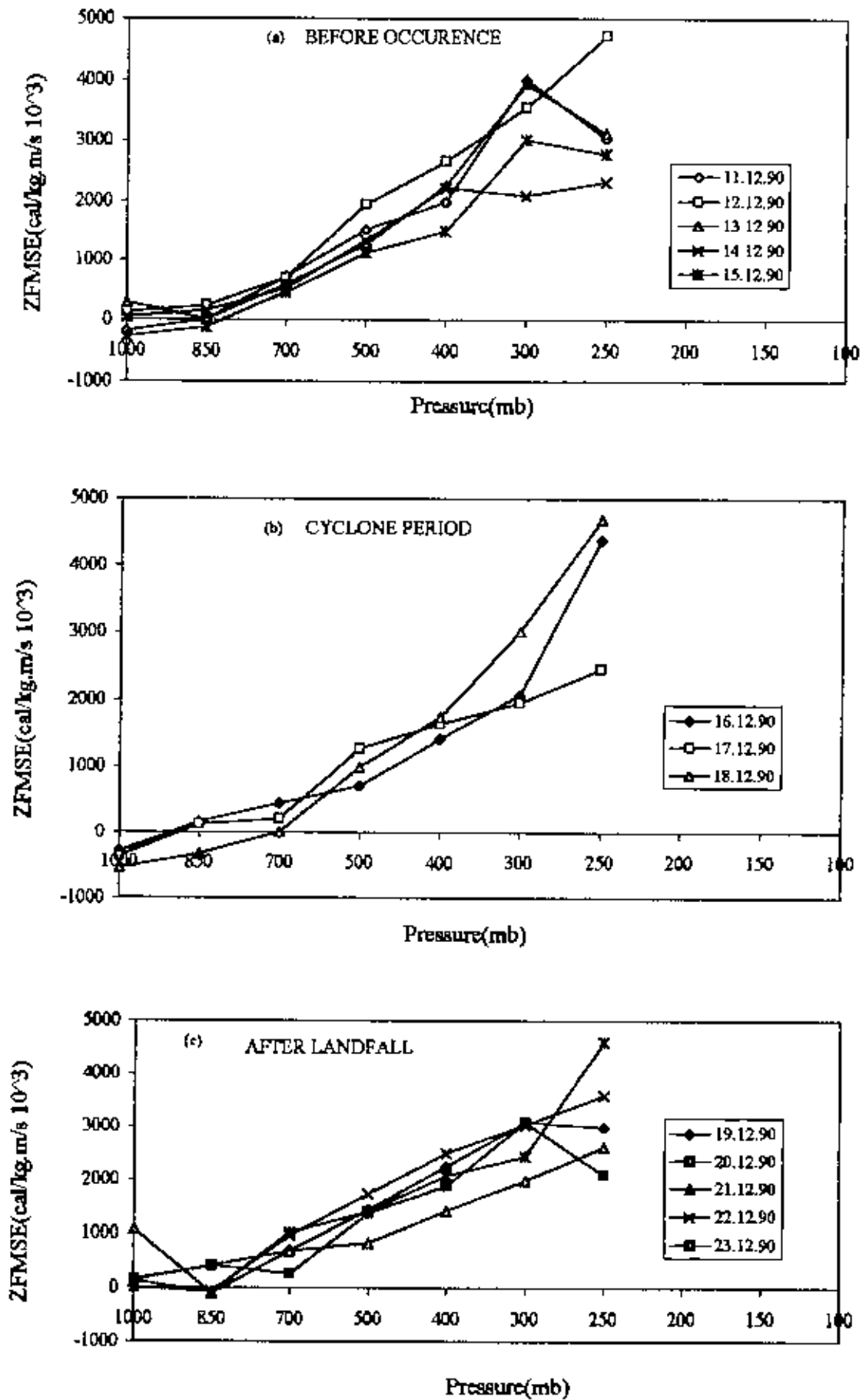


Fig. 5.2.6 (a-c). Variation of zonal fluxes of moist static energy at different isobaric levels.

After landfall [Fig. 5.2.6(c)] it is seen that at 1000 mb-850 mb ZFMSE was nearly zero and positive (eastward). After 850 mb it increased up to 300 mb for all the days. At 250 mb it decreased for 19-20, December but increased for 21-23 December. It is seen that at 1000 mb ZFMSE was zero and negative (westward) for before occurrence and positive (eastward) for after landfall. But at cyclone period (Fig. 5.2.6(b)) at 1000 mb, ZFMSE was completely negative (westward) for all days. Here at the surface level (1000 mb) wind direction was opposite between cyclone period and after landfall. It is also observed that at 250 mb ZFMSE was more or less decreased for before occurrence and after landfall. But at cyclone period it increased at 250 mb for all days. This is due to the more cloud formation at that level at cyclone period. It is seen that at 250 mb for cyclone period ZFMSE was maximum at 18.12.90 because of zonal wind component was maximum at that day.

#### Meridional Flux of Dry Static Energy (MFDSE):

Meridional flux of dry static energy (MFDSE) at different isobaric levels is shown in Fig. 5.2.7(a-c). Before occurrence [Fig. 5.2.7(a)] at 1000 mb-700 mb, MFDSE was zero and negative (southward) for all the days. Beyond 700 mb it was fluctuated up to 100 mb due to the randomness of wind speed and direction.

At cyclone period [Fig. 5.2.7(b)] at 1000 mb MFDSE was negative (southward) for all the days. At 850 mb it increased (except 18.12.90) to the positive (northward) direction at 850 mb. But on 18.12.90 it increased in the negative (southward) direction at 850 mb. Beyond 850 mb it increased in the positive (northward) direction and increased linearly up to 200 mb, then decreased. For other days, beyond 700 mb it increased linearly up to 200 mb and then decreased.

After landfall [Fig. 5.2.7(c)] MFDSE was completely negative (southward) at 1000 mb-700 mb. For 20.12.90 this negative value exists up to 300 mb and then increased to the positive (northward) direction. Beyond 700 mb it was positive (northward) for all the days (except 23.12.90) and exists near about constant up to 150 mb. After 150 mb it increased at 100mb except 20.12.90 and 23.12.90.

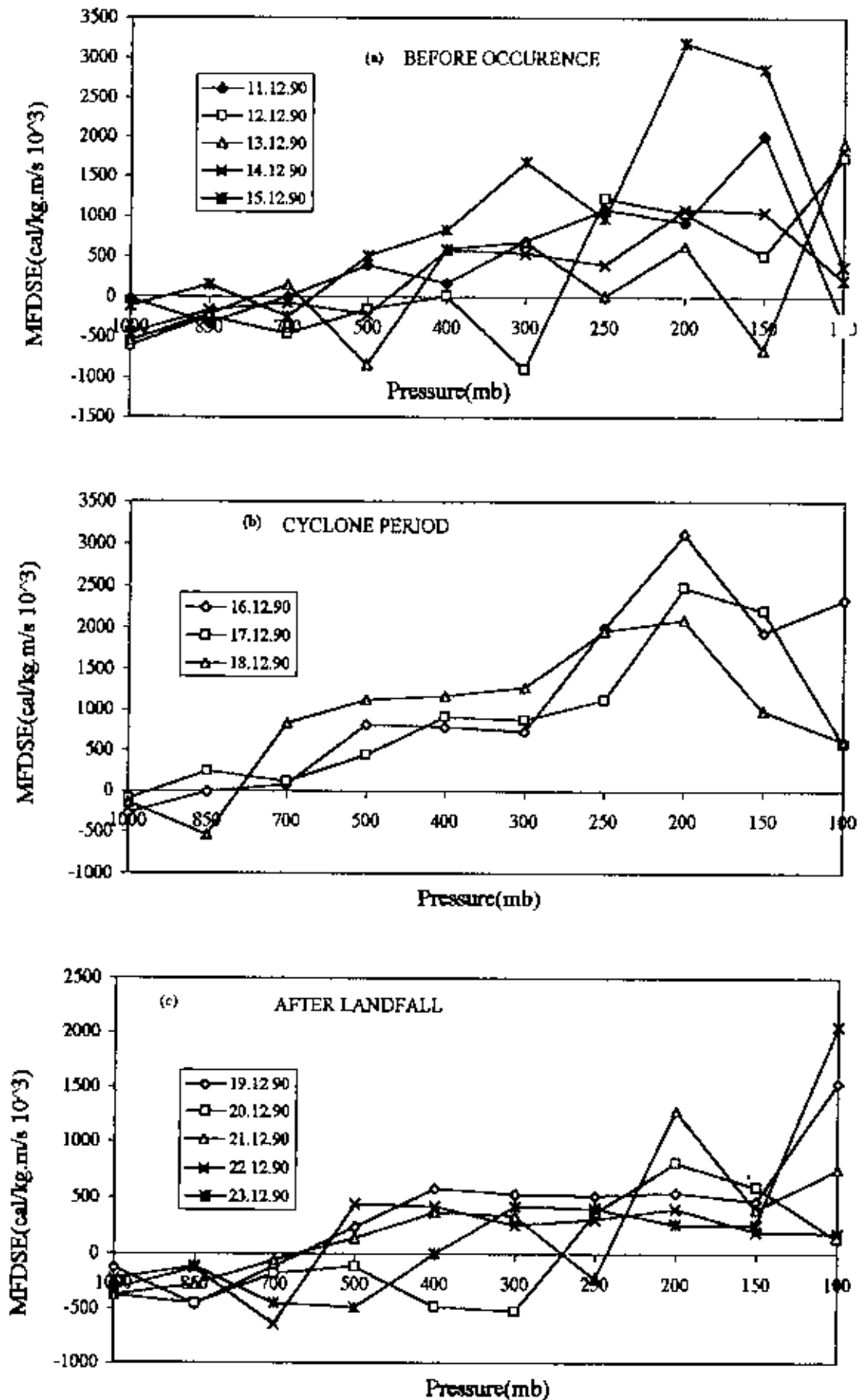


Fig. 5.2.7. (a-c). Variation of meridional Fluxes of dry static energy at different isobaric levels.

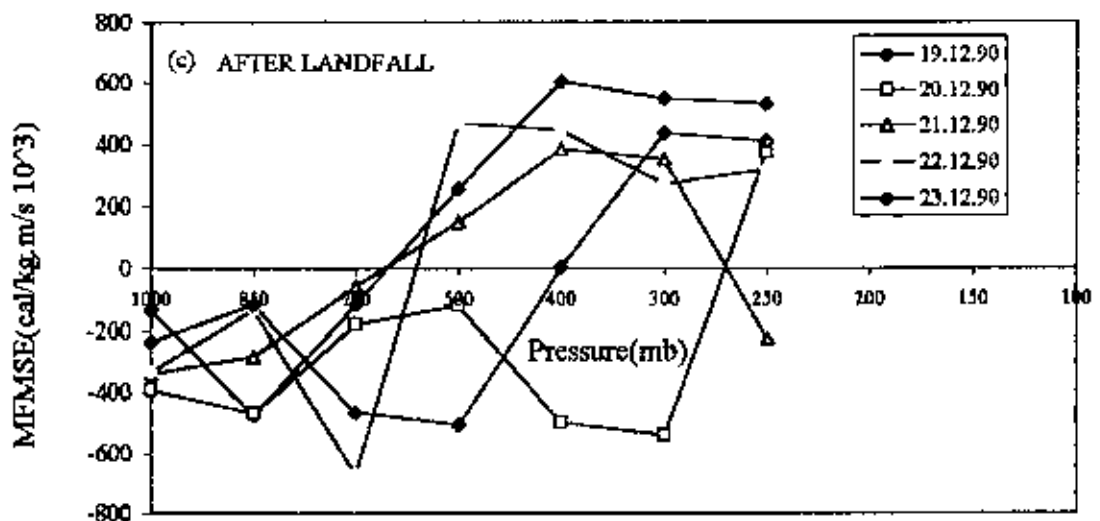
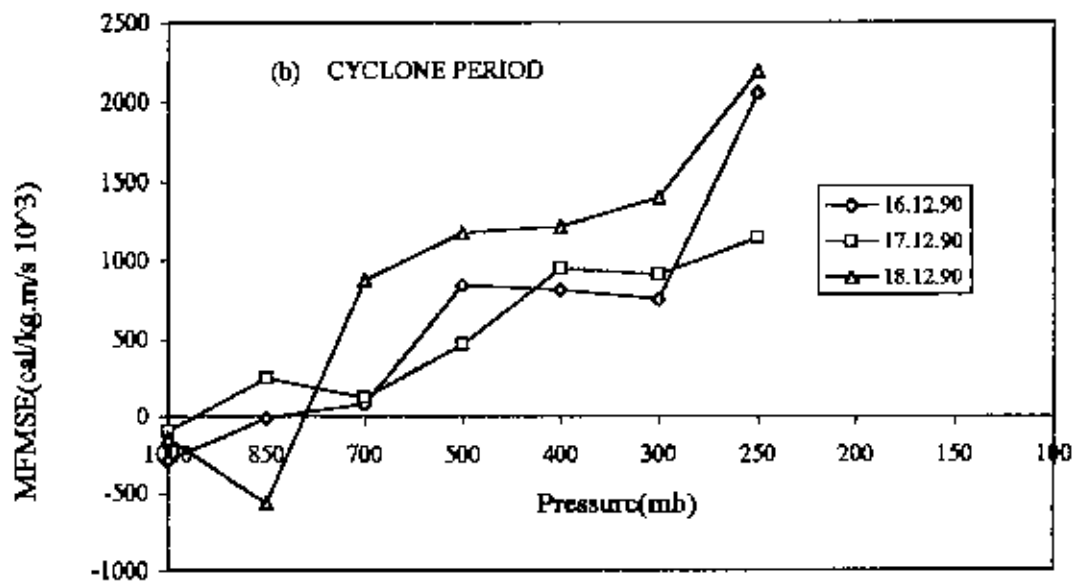
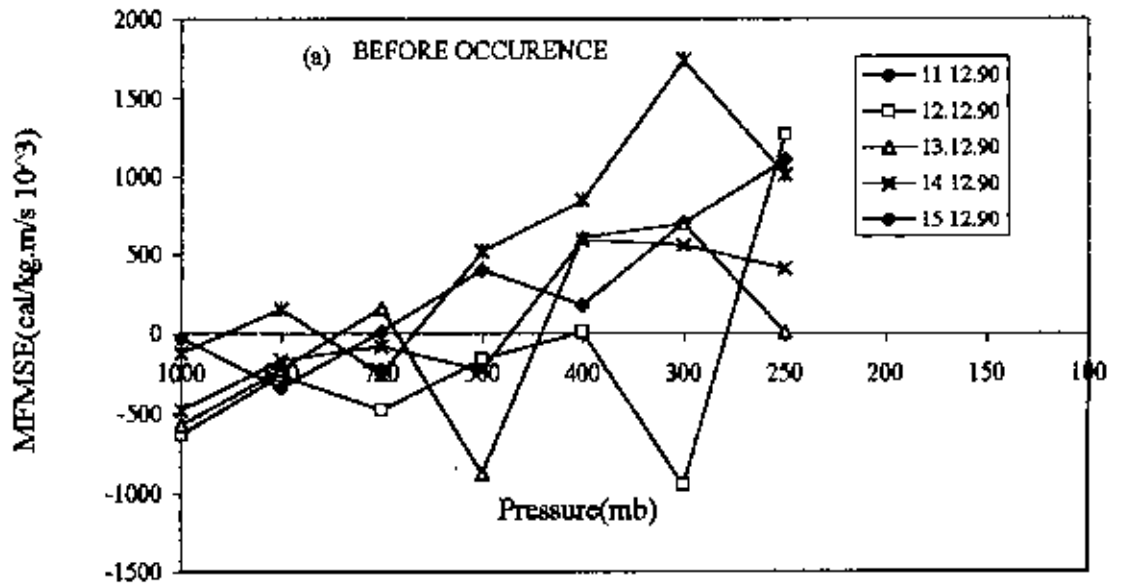


Fig. 5.2.8. (a-c) Variation of meridional fluxes of moist static energy at different isobaric levels



From the above figure [Fig. 5.2.7(a-c)] it is observed that at 1000 mb MFDSE was negative (southward) at cyclone period and this negative value was higher for after landfall. This means that after landfall wind velocity was larger compared to cyclone period. Here we also observed that both for cyclone period and after landfall it was near about same or symmetric at middle troposphere (500-250 mb) and maximum at upper troposphere (200 mb and 100 mb). This higher value was due to the high wind velocity.

#### Meridional Flux of Moist Static Energy (MFMSE):

Fig. 5.2.8(a-c) shows the variation of meridional fluxes of moist static energy (MFMSE) at different isobaric levels. Here we observed that before occurrence and cyclone period the pattern was same as Fig. 5.2.7(a-b) which was discussed earlier. This is because MFMSE is simply an addition of latent content with MFDSE. But after landfall [Fig. 5.2.8(c)] it is seen that MFMSE was negative (southward) for all the days up to 700 mb. Beyond 700 mb it was both in direction (northward and southward). It is fluctuated due to the change of wind velocity.

From the above figures [Figs. 5.2.8(a-c)] it is seen that MFMSE was high at 250 mb. This was because in this region more cloud is formed and release latent heat. It is also observed that at 250 mb it was maximum at 18.12.90. This was due to the higher wind speed at that day i.e. at the end of the cyclone (18.12.90).

### 4.2.3 cyclone 3

Cyclone 3 formed during the period 25-30 April 1991. To observe its 'before occurrence' and 'after landfall' conditions, data were analyzed from 20 April to 5 May 1991. The track of this cyclone is shown in Fig. 3.

#### 4.2.3 (a): energy components

##### Sensible heat (SH):

Fig 5.3.1(a-c) shows the variation of sensible heat (SH) with pressure at different phases of cyclone occurring from 25-30 April 1991. From these figures it is observed that at day to day there was almost no change of SH i.e., the day to day variation of SH was very little. But it is observed that SH decreased with decreasing pressure i.e., increasing height. It is also observed that SH was maximum at 1000 mb. This was due to the maximum temperature at the earth surface. The magnitude of SH at different phases was almost same.

##### Potential energy (PE):

The variation of Potential energy (PE) at different isobaric levels at different phases of cyclone is shown in figure 5.3.2(a-c). From this figures it is observed that PE at each phase coincide for different days. There was no change of PE at day to day. But PE linearly increased with decreasing pressure and was maximum at the top of the troposphere. Potential energy was maximum at the upper level of the troposphere because geopotential height is higher at the top of the troposphere. The pattern of PE at different phases was very similar.

##### Latent heat content (LHC):

The variation of latent heat content (LHC) at different isobaric levels is shown in figure 5.3.3 (a-c). From these figures it is observed that LHC changed at day to day and layer to layer. Before occurrence [Fig. 5.3.3(a)] it is seen that from 1000 mb-700 mb at first LHC increased and then decreased. Between 700 mb-300 mb, LHC gradually increased. Beyond 300 mb it is slightly decreased for all the days except 20<sup>th</sup> April. On 20<sup>th</sup> April LHC fluctuated and from 300 mb to 250 mb it increased abruptly.

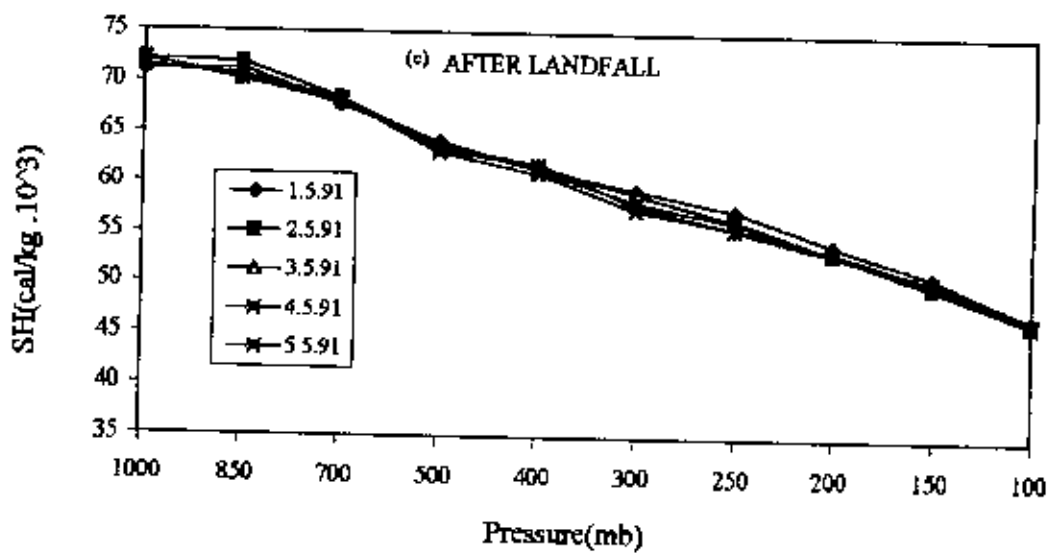
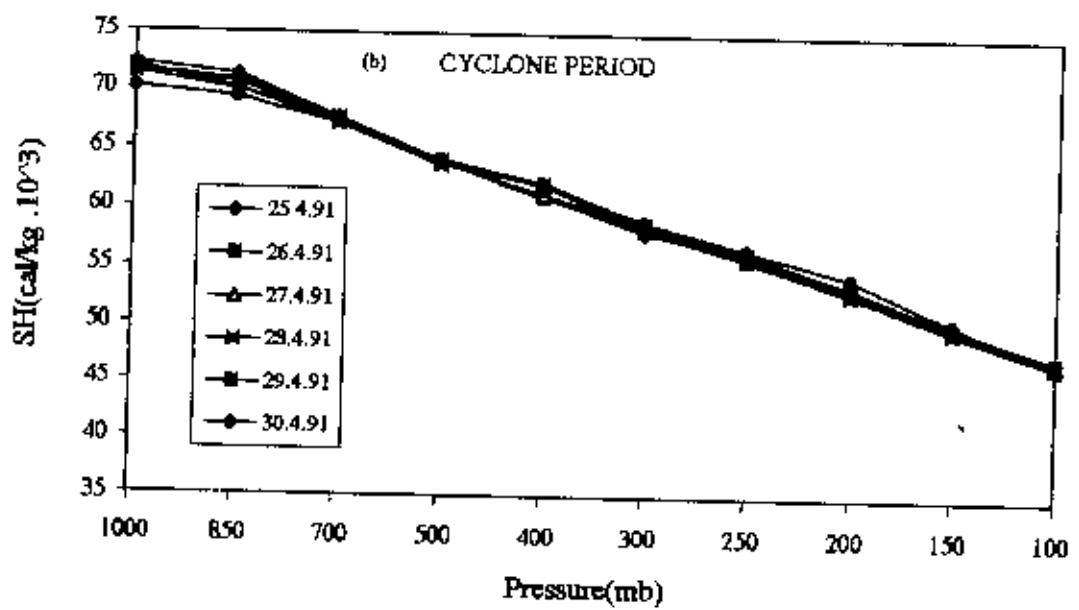
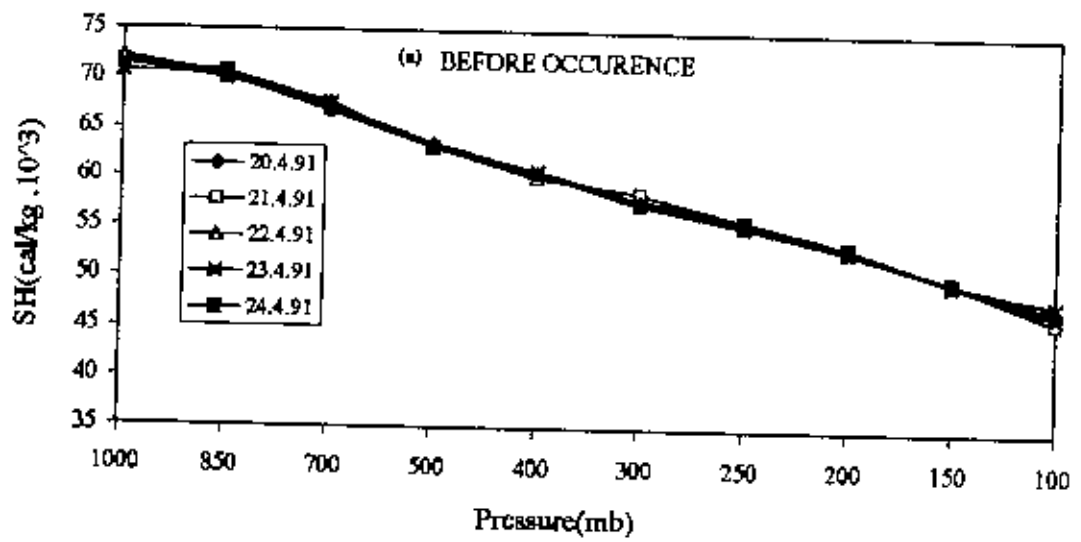


Fig. 5.3.1 (a-c): Sensible heat variation at different isobaric levels

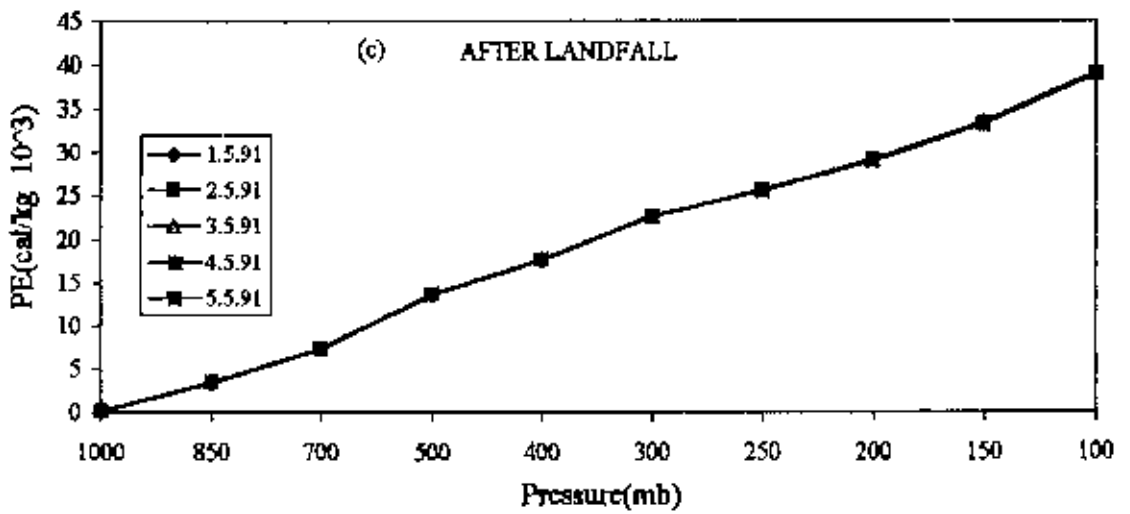
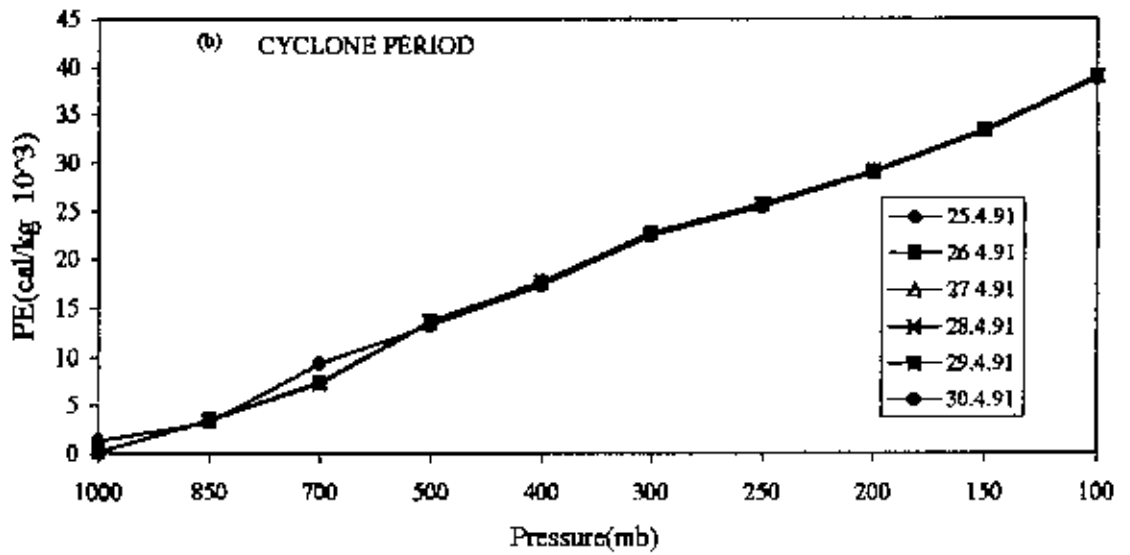
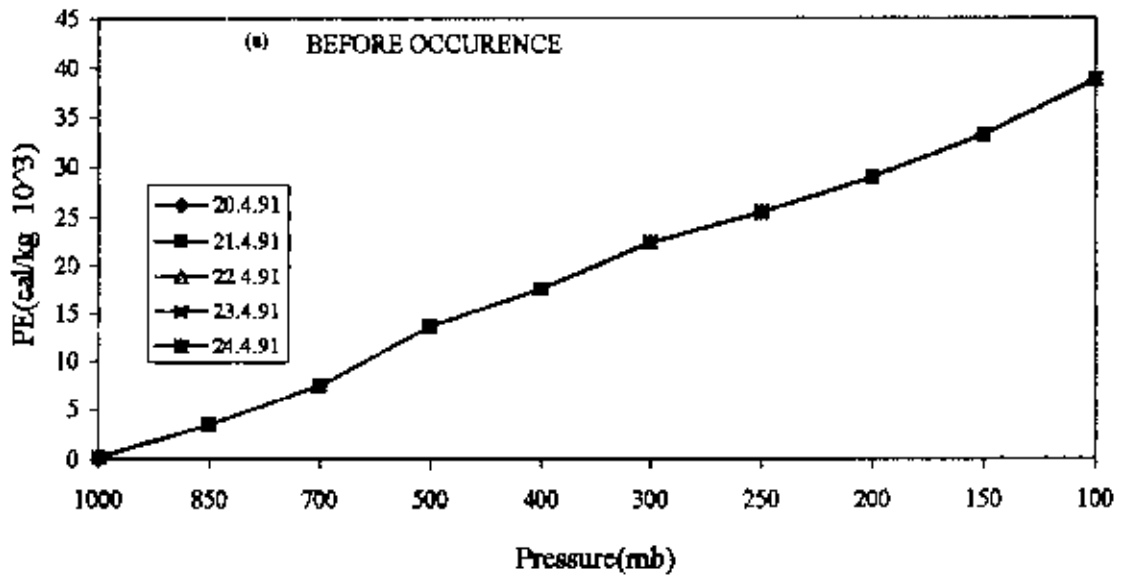


Fig. 5.3.2(a-c). Potential energy variation at different isobaric levels.

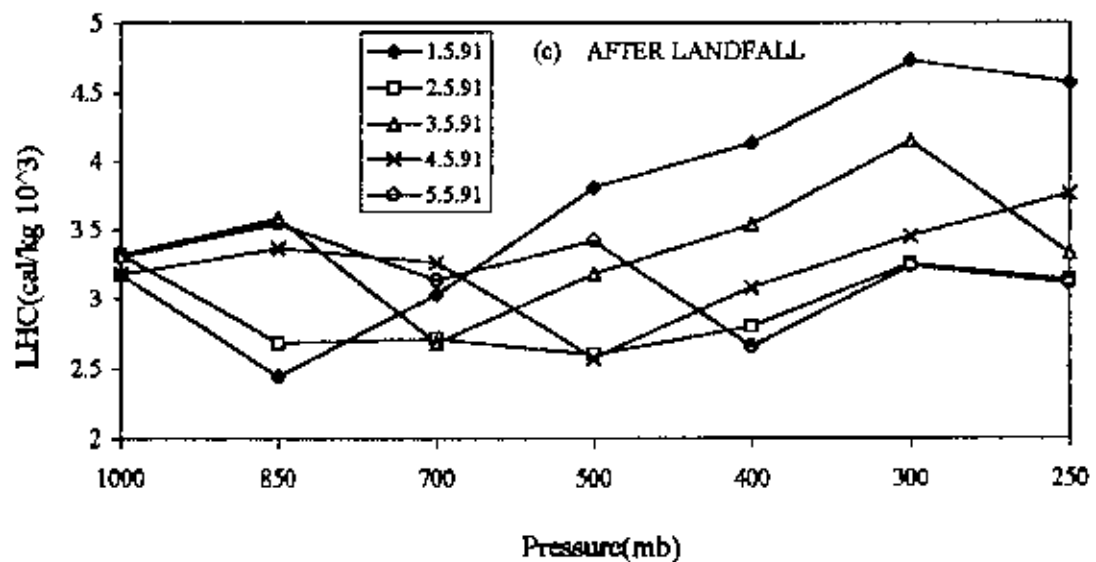
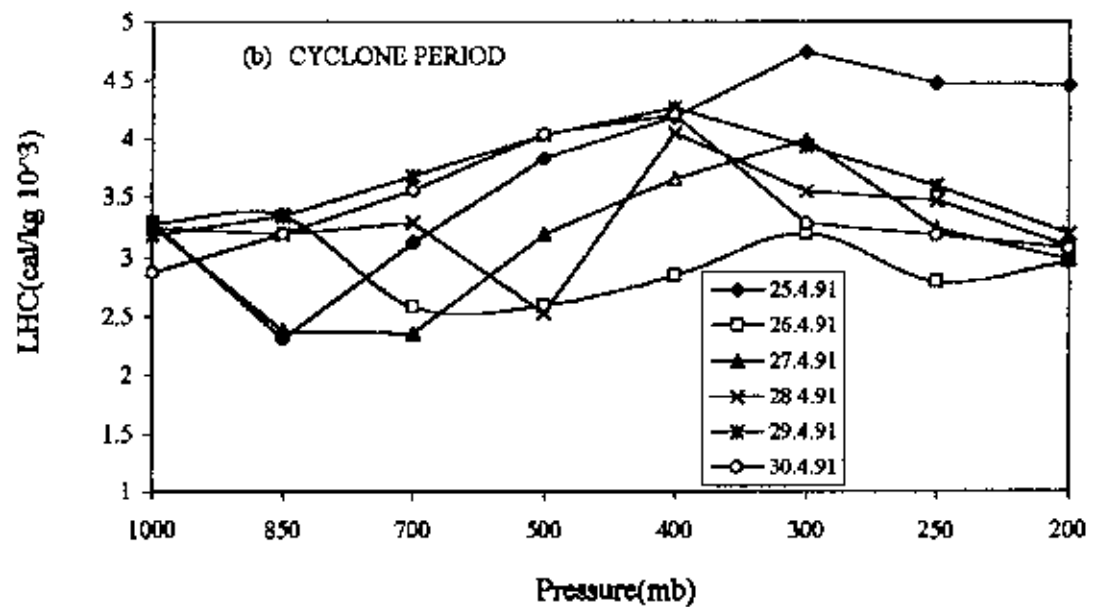
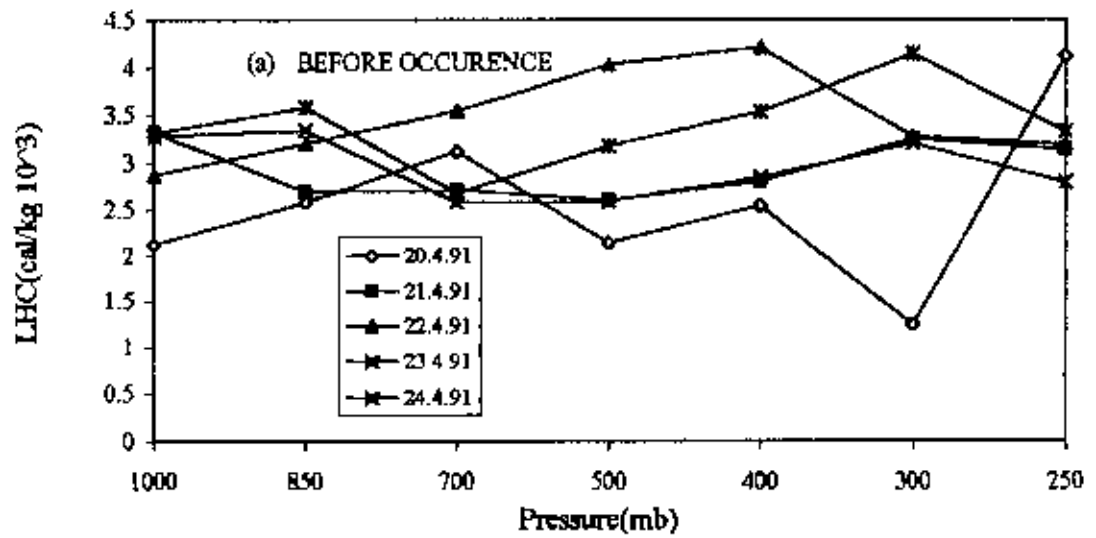


Fig. 5.3.3. (a-c): Latent heat content variation at different isobaric levels.

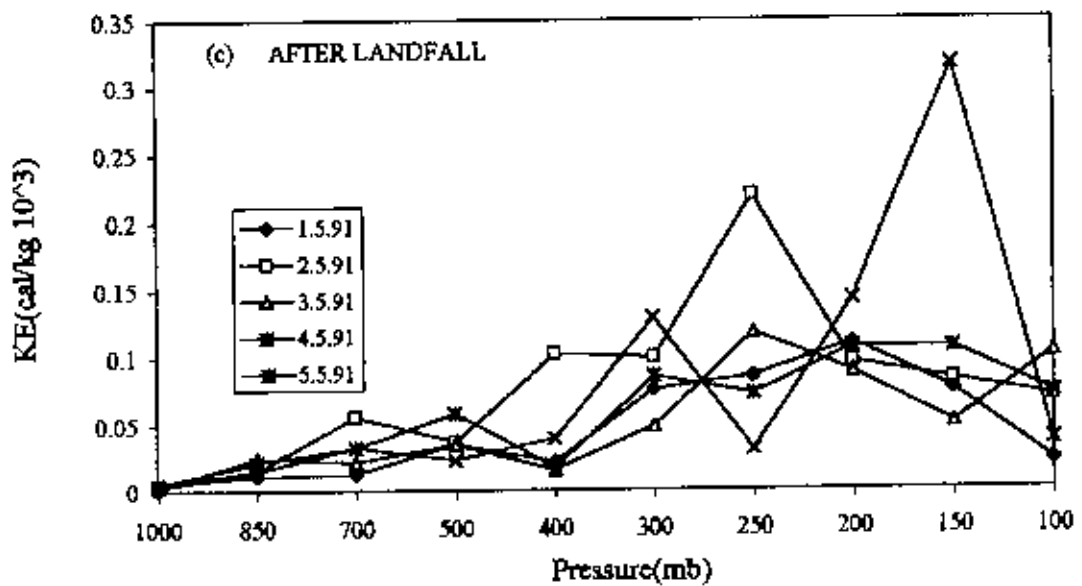
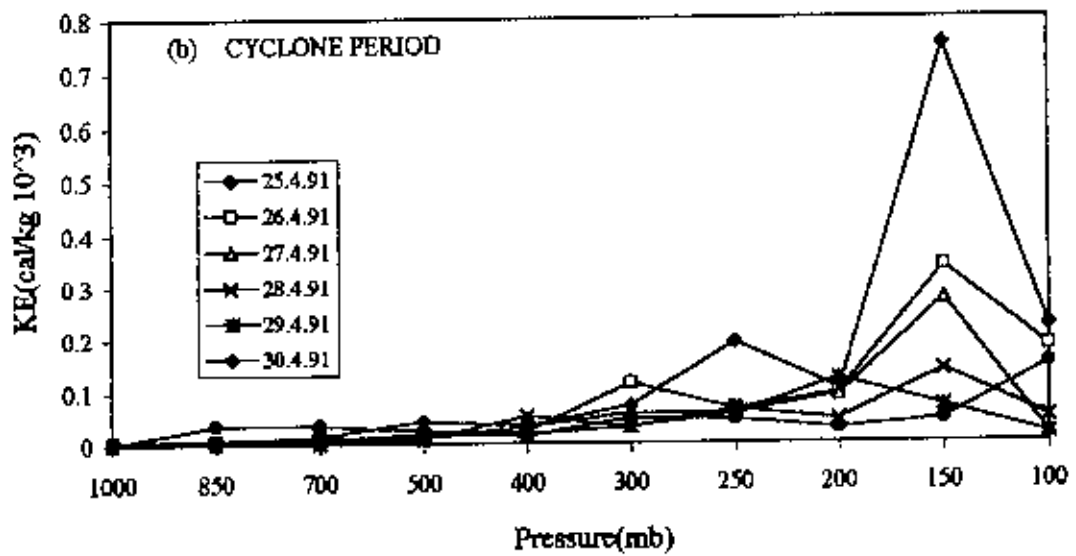
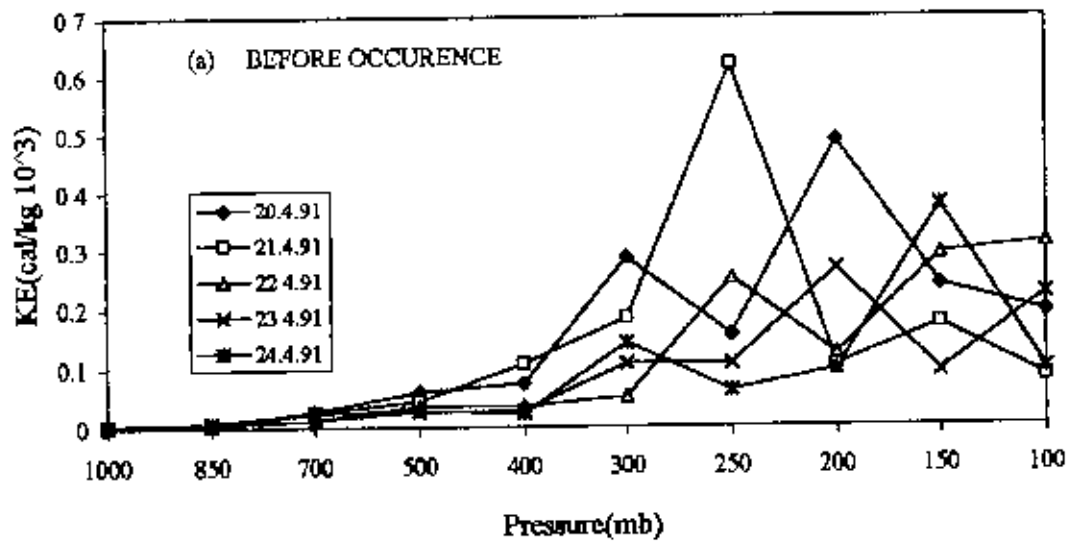


Fig. 5.3.4 (a-c): Kinetic energy variation at different isobaric levels.

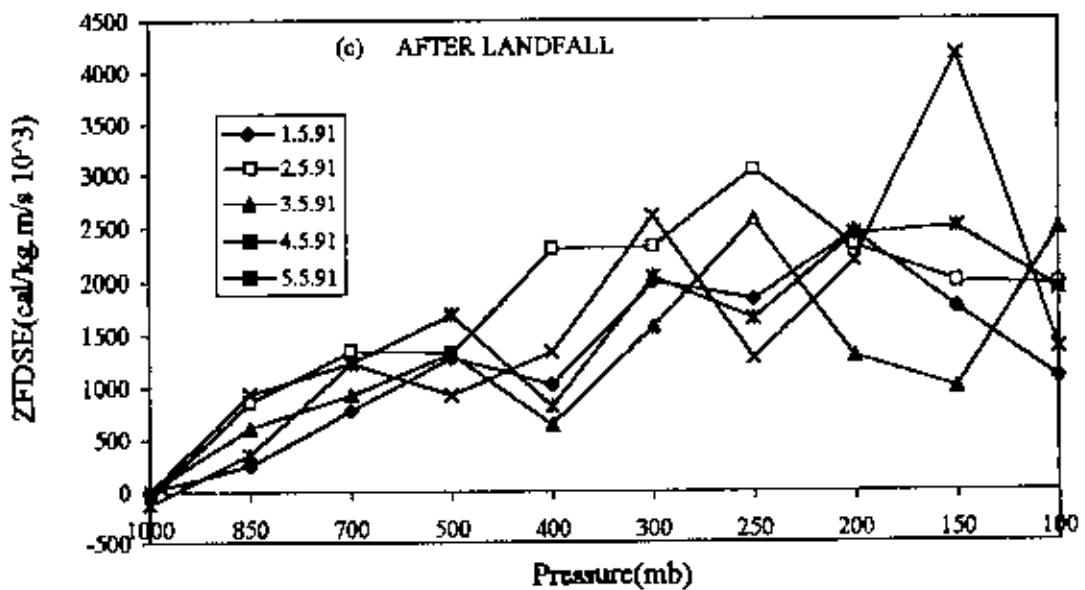
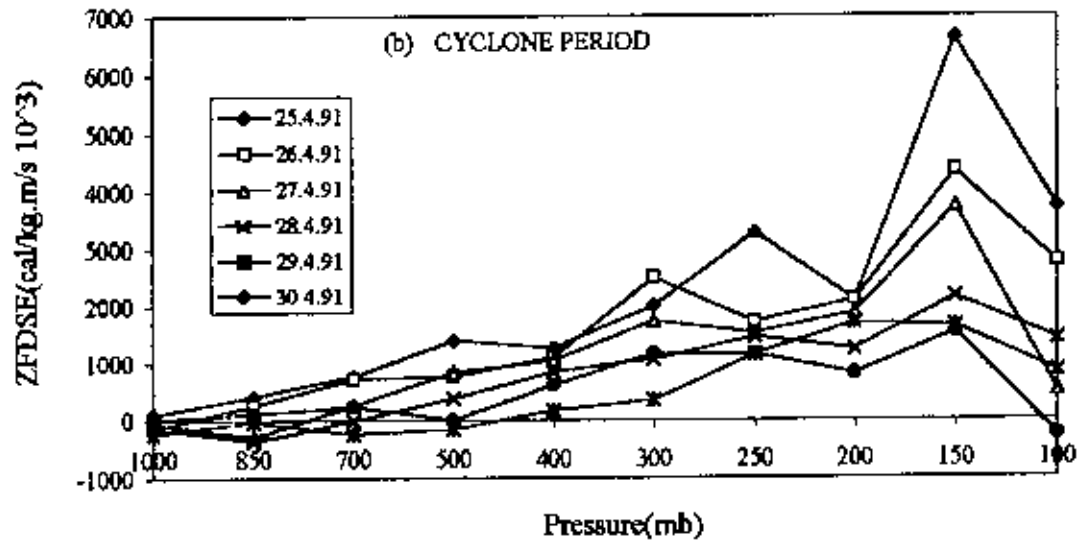
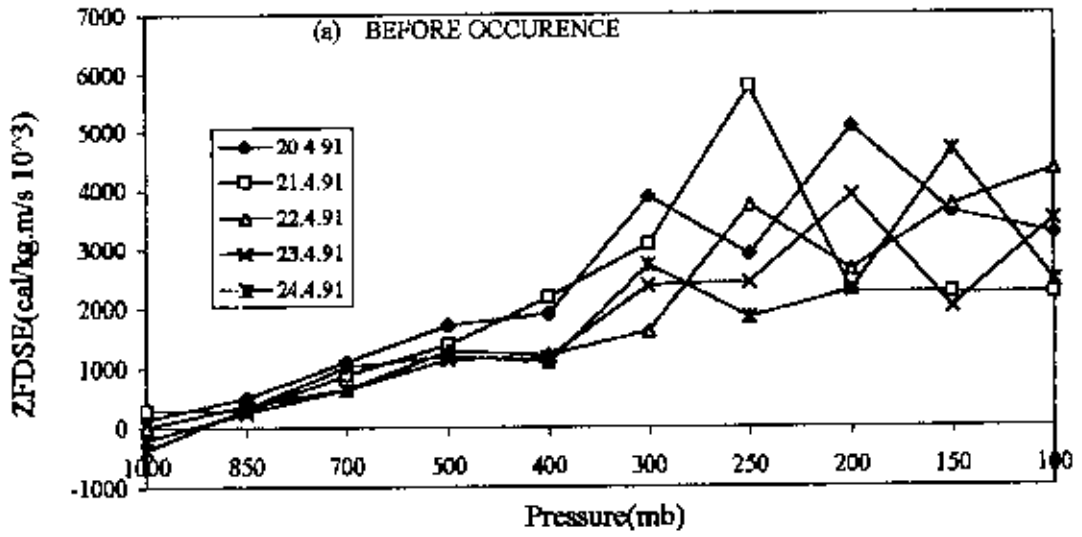


Fig. 5.3.5: (a-c). Variation of zonal fluxes of dry static energy at different isobaric levels.

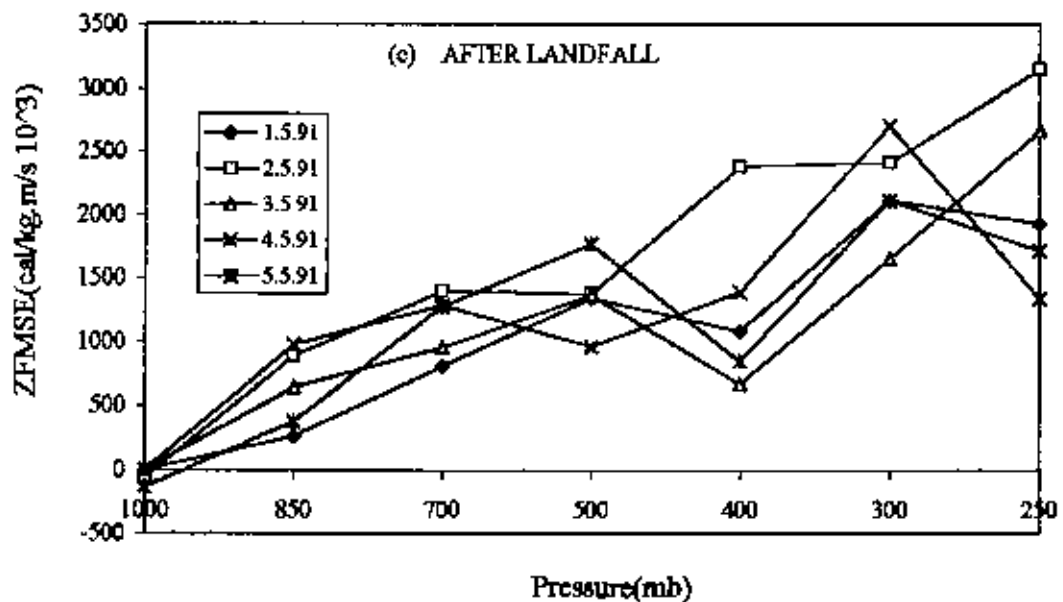
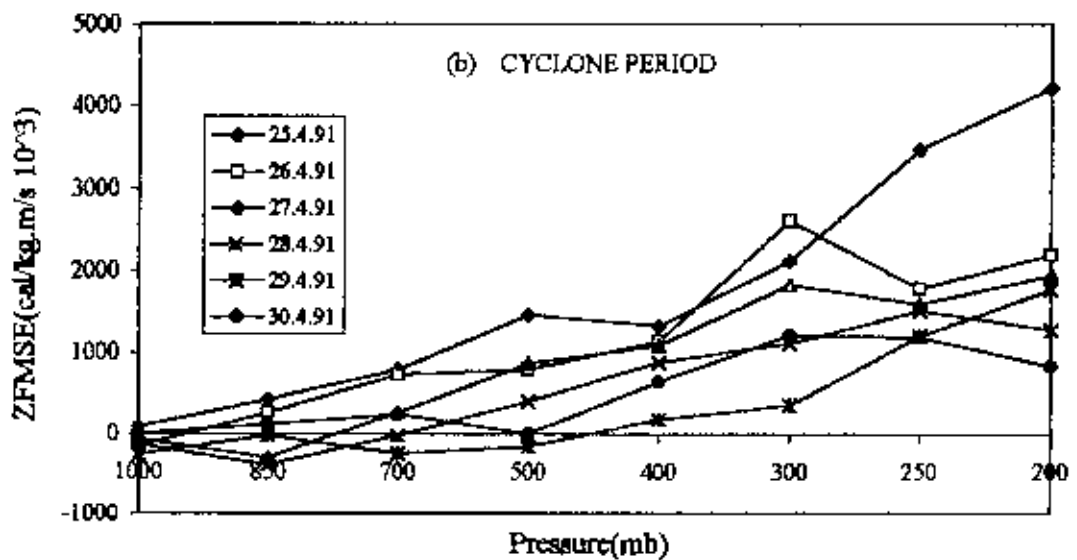
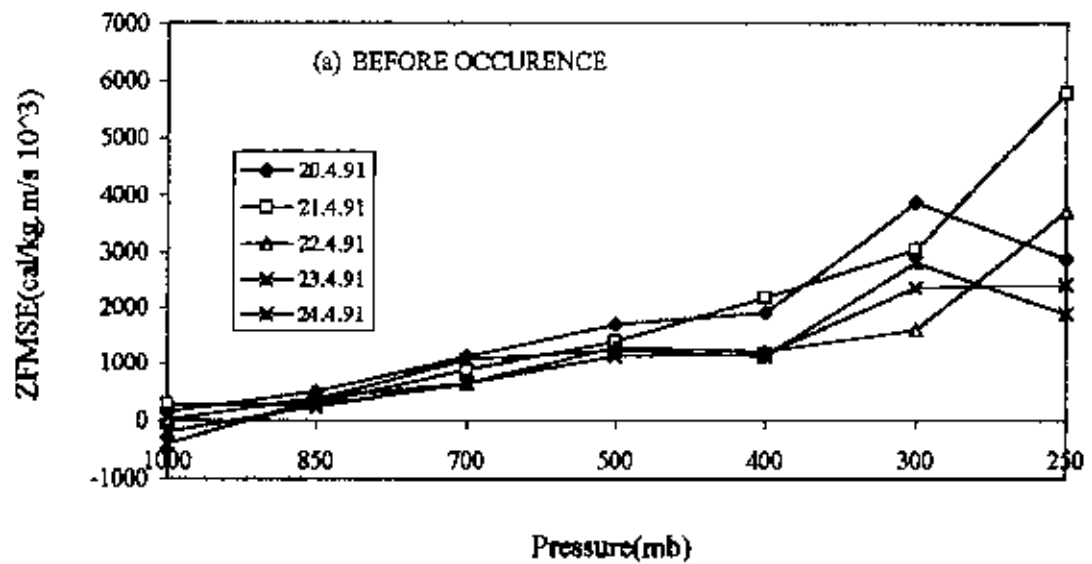


Fig. 5.3.6 (a-c). Variation of zonal fluxes of moist static energy at different isobaric levels.



At cyclone period [Fig. 5.3.6(b)], ZFMSE increased linearly up to 300 mb and then it was nearly constant in magnitude. But at the initiation of cyclone period (25<sup>th</sup> April) it increased gradually up to 200 mb and attained maximum value at 200 mb.

After landfall [Fig. 5.3.6(c)], it is seen that at 1000 mb, ZFMSE was either zero or slightly negative (westward) and then gradually increased up to 500 mb. Beyond 500 mb it increased with fluctuation.

From the above figures [Fig. 5.3.6(a-c)], it is observed that, ZFMSE linearly increased at cyclone period. But after landfall ZFMSE increased gradually up to 500 mb and then increased with fluctuation. This fluctuation was due to the change of wind velocity during landfall.

#### **Meridional flux of dry static energy (MFDSE):**

Fig 5.3.7(a-c) shows the variation of meridional flux of dry static energy (MFDSE) from 20 April-5 May for isobaric levels 1000 mb-100 mb. Before occurrence [Fig.5.3.7(a)], it is observed that at 1000 mb MFDSE was positive (northward) with a small value for all the days. At 850 mb, it slightly increased and then decreased in the negative (southward) direction. At 500 mb, it is observed that MFDSE was completely negative (southward) for all the days. Beyond 500 mb, MFDSE increased gradually in the positive (northward) direction up to 200 mb and then decreased at 150 mb. At 100 mb it turned into negative (southward) direction and attained maximum value. Beyond 500 mb, on 21-22 April, it was negative (southward) and maintained a constant value with the same sign up to 200 mb. At 150 mb it turned into positive and increased abruptly and showed a sharp peak at this level (150 mb). On 23<sup>rd</sup> April, it was nearly constant from 300-200 mb with negative sign. Beyond 200 mb it turned into positive (northward) and increased up to 100 mb. On 24 April i.e., at the initiation of cyclone period it fluctuated due to the change of wind speed beyond 500 mb.

At cyclone period [Fig. 5.3.7(b)], it is seen that at 1000 mb, MFDSE was positive for 25-27 April. It was negative for 28-29 April and was zero for 30 April. At the initiation of cyclone (25 April), it was positive (northward) at 1000 mb, then it turned into negative southward and maintained a constant value with the same direction up to 250 mb. At 200 mb it turned into northward and increased. At 150-100 mb it decreased

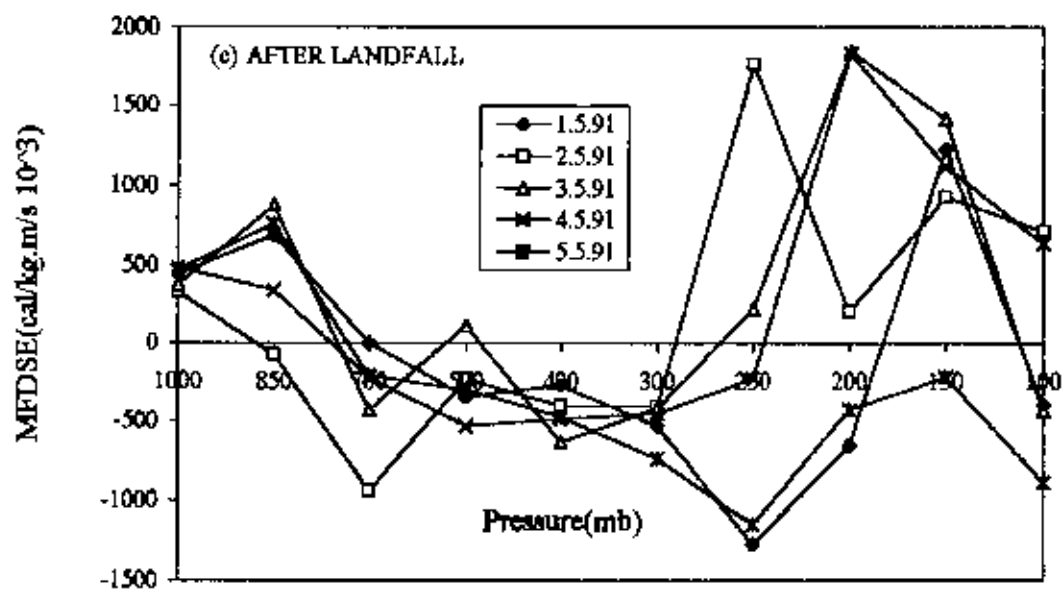
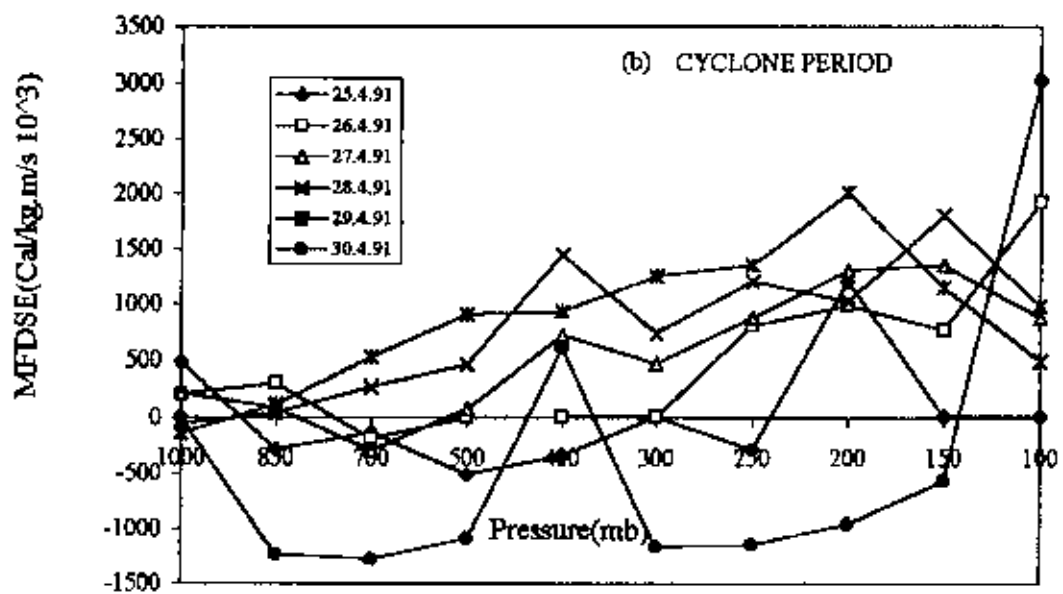
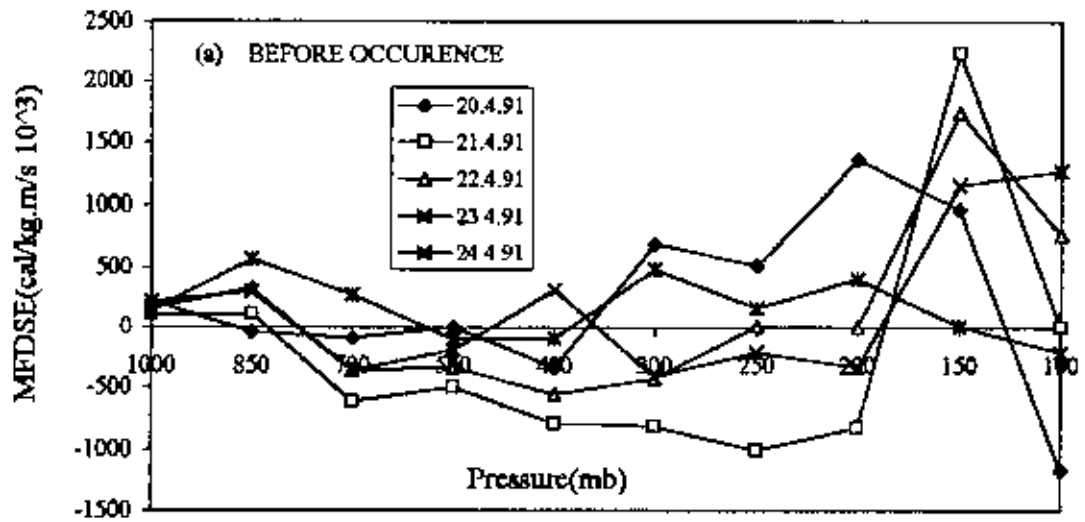


Fig. 5.3.7 (a-c). Variation of meridional fluxes of dry static energy at different isobaric level:

abruptly and goes to zero due to the absence of wind speed. On 26<sup>th</sup> April, it was zero up to 300 mb and then increased gradually. On 27<sup>th</sup> April it was nearly zero up to 500 mb and then gradually increased. On 28<sup>th</sup> April, it gradually increased with a small fluctuation. On 29<sup>th</sup> April it increased linearly up to 200 mb and then decreased. At the end of cyclone (30 April), it is observed that MFDSE was negative (southward) for all isobaric levels except 400 and 100 mb and maintained almost a constant value. At 100 mb it turned into positive (northward) and attained the maximum value at cyclone period.

Meridional flux of dry static energy after landfall is shown in Fig 5.3.7(c). On 1<sup>st</sup> May, at first it was positive (northward) and increased. At 700 mb it was zero due to absence of wind speed. Beyond 700 mb it turned into negative (southward) and gradually increased with the same sign up to 250 mb. Beyond 250 mb it changed its direction and became positive (northward) at 150 mb and show a peak. At 2<sup>nd</sup> May, at first it was positive (northward), and then turned into negative (southward) and increased at 700 mb. From 500-300 mb it was nearly constant with the same sign. Beyond 300 mb it turned into positive (northward) and increased abruptly at 250 mb. This was because wind speed suddenly increased during landfall at this level. Beyond 250 mb it decreased with fluctuation. On 3<sup>rd</sup> May it fluctuated in both positive and negative direction. This fluctuation was due to the change of wind speed and direction during landfall. On 4<sup>th</sup> May, at first it was positive (northward) and then turned into negative (southward) and maintained a constant value with the same sign from 700-250 mb. Beyond 250 mb it turned into positive (northward) and increased abruptly at 200 mb and then decreased.

From the above figures [Fig. 5.3.7(a-c)] it is observed that, for before occurrence and after landfall meridional fluxes of dry static energy was positive (northward) for all the days at 1000 mb but after landfall the value was slightly greater than before occurrence. This was due to the high wind speed during landfall. But at cyclone period, it was either zero or positive (northward) or negative (southward) at 1000 mb. Before occurrence and after landfall peaks are found at 150 mb but at cyclone period such peaks are not observed. At cyclone period it is observed that MFDSE gradually increased for most of the days. From this figures it is also observed that MFDSE is decreased for all the days at the top of the troposphere i.e., at 100 mb (without 26 and 30 April). At cyclone period it is also observed that at the end of the cyclone (30<sup>th</sup> April), MFDSE was negative

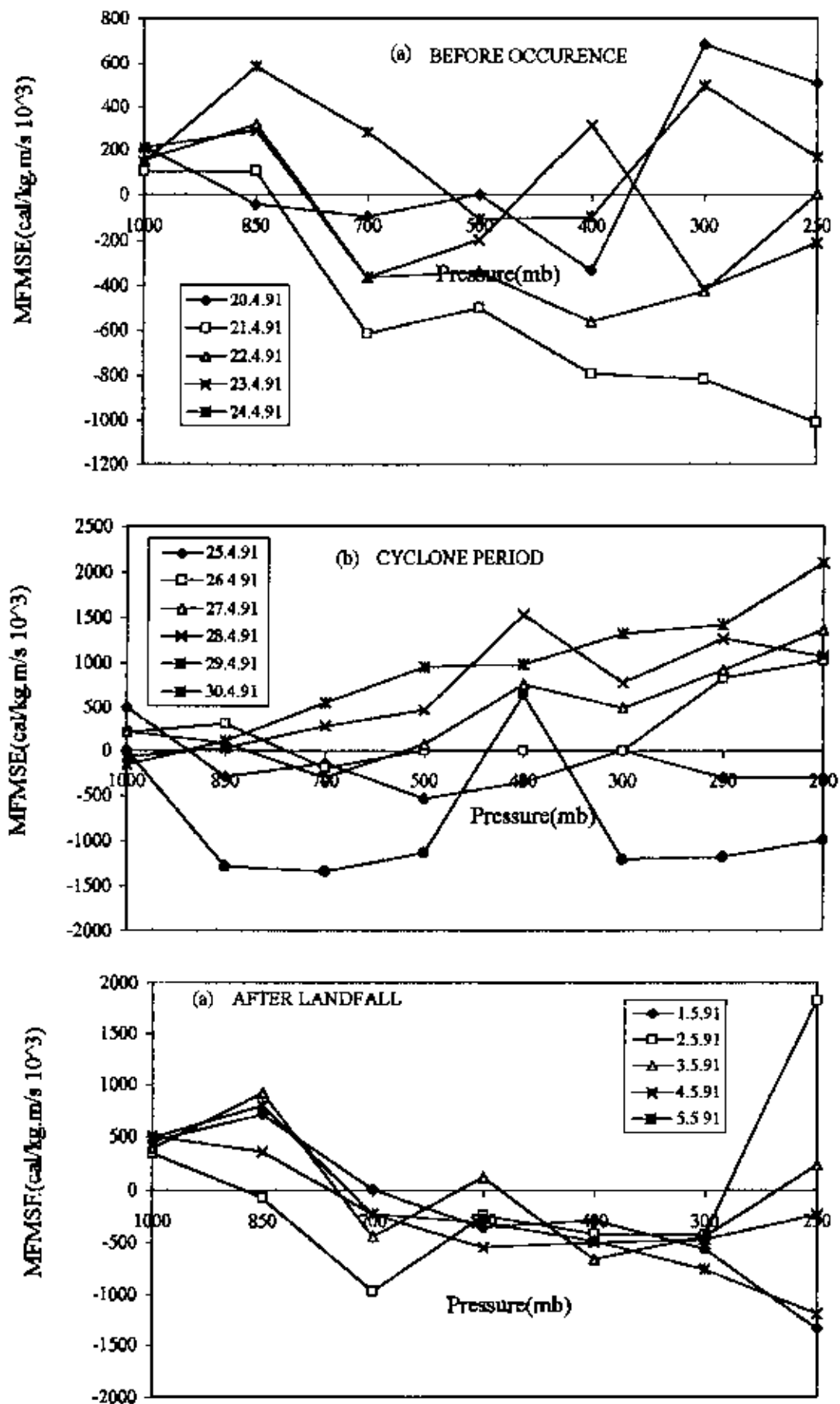


Fig. 5.3.8 Variation of meridional fluxes of moist static energy at different isobaric level

(southward) for all the levels and was nearly constant. It turned into positive (northward) at 100 mb and attained the highest value. This was because wind speed was high at the end of cyclone period.

#### **Meridional flux of moist static energy (MFMSE):**

Figure 5.3.8(a-c) represents the variation of meridional fluxes of moist static energy (MFMSE) at different isobaric levels, at different phases of the analyzed cyclone. Before occurrence, it is observed that on 20<sup>th</sup> April, at first it was positive (northward) and then turned into negative (southward), and continued with the same sign up to 400 mb. Beyond 400 mb it turned into positive (northward) due to change of wind direction. Beyond 850 mb it turned into negative (southward) for all the days. For 21-22 April, it was nearly constant from 700-300 mb due to negligible change of wind speed. For 23-24 April, it was fluctuated.

At cyclone period [Fig. 5.3.8(b)], it is observed that the graph pattern was similar to that of meridional flux of dry static energy which is discussed earlier [Fig. 5.3.7(b)]. Here the only difference was in magnitude. Another change is observed on 30<sup>th</sup> April. On 30<sup>th</sup> April, at the upper level of the troposphere MFMSE was constant in the negative (southward) direction due to no change of wind speed at these levels.

After landfall [Fig. 5.3.8(c)], it is observed that at 1000 mb, MFMSE was positive (northward) for all the days. At 850 mb it slightly increased. Beyond 850 mb it decreased for all the days and turned into negative (southward). From 700-300 mb it was constant with the same sign due to no change of wind speed. But for 1<sup>st</sup> and 2<sup>nd</sup> May i.e., during landfall it is fluctuated due to change of wind speed and direction and attained the maximum value at 100 mb.

From the above figures [Fig. 5.3.8(a-c)], it is seen that at cyclonic period MFMSE was positive (northward) for most of the days and increased gradually from lower to the upper level of the troposphere. But during landfall, we observed the reverse characteristics i.e., from 700-300 mb, MFMSE was completely negative (southward). It is also observed that during landfall (2<sup>nd</sup> May) MFMSE changed its direction (i.e., from positive to negative) and increased abruptly at 250 mb

#### 4.2.4. Cyclone 4

A cyclone formed in the Bay of Bengal from 29 April 1994 to 3 May 1994, is explained in this section. This period is called "cyclone period". To observe its pre-condition, energy is calculated from 24 April 1994 to 28 April 1994 and this period is called "before occurrence". To observe the post-condition of the observed cyclone, energy is also calculated from 4 May 1994 to 8 May 1994. This period is called "after landfall". The track of this cyclone is shown in Fig. 3.

##### 4.2.4.(a) Energy components

###### Sensible heat (SH):

Fig 5.4.1(a-c) shows the variation of sensible heat (SH) at different isobaric levels for before occurrence, cyclone period and after landfall. From these figures it is seen that at day to day there was no change of SH. But at layer to layer SH heat changes and the changes were symmetric for all the days. It is also observed that SH decreased linearly as pressure decreased. This was because temperature was maximum at the earth surface.

###### Potential energy (PE):

The variation of potential energy (PE) at different isobaric levels is shown in Fig 5.4.2(a-c). It is observed that at day to day there was no significant change of potential energy. But at layer to layer PE changed. From this figures [Fig. 5.4.2(a-c)], it is found that at 1000 mb, PE was nearly zero for all the phases i.e., before occurrence, cyclone period and after landfall. Beyond 1000 mb, it increased linearly as pressure decreased and attained maximum value at 100 mb i.e., at the top of the troposphere. Potential energy was maximum at 100 mb because geopotential height was highest at this level.

###### Latent heat content (LHC):

Fig. 5.4.3 (a-c) shows the variation of latent heat content (LHC) at different isobaric levels from 1000 mb-100 mb at different phases of cyclone i.e., before occurrence, cyclone period and after landfall. At before occurrence [Fig. 5.4.3(a)], it is seen that from 1000-700 mb, LHC was almost same for all the days (except 27<sup>th</sup> April). Beyond 700 mb it is fluctuated due to the formation of cloud. It is also seen that at the



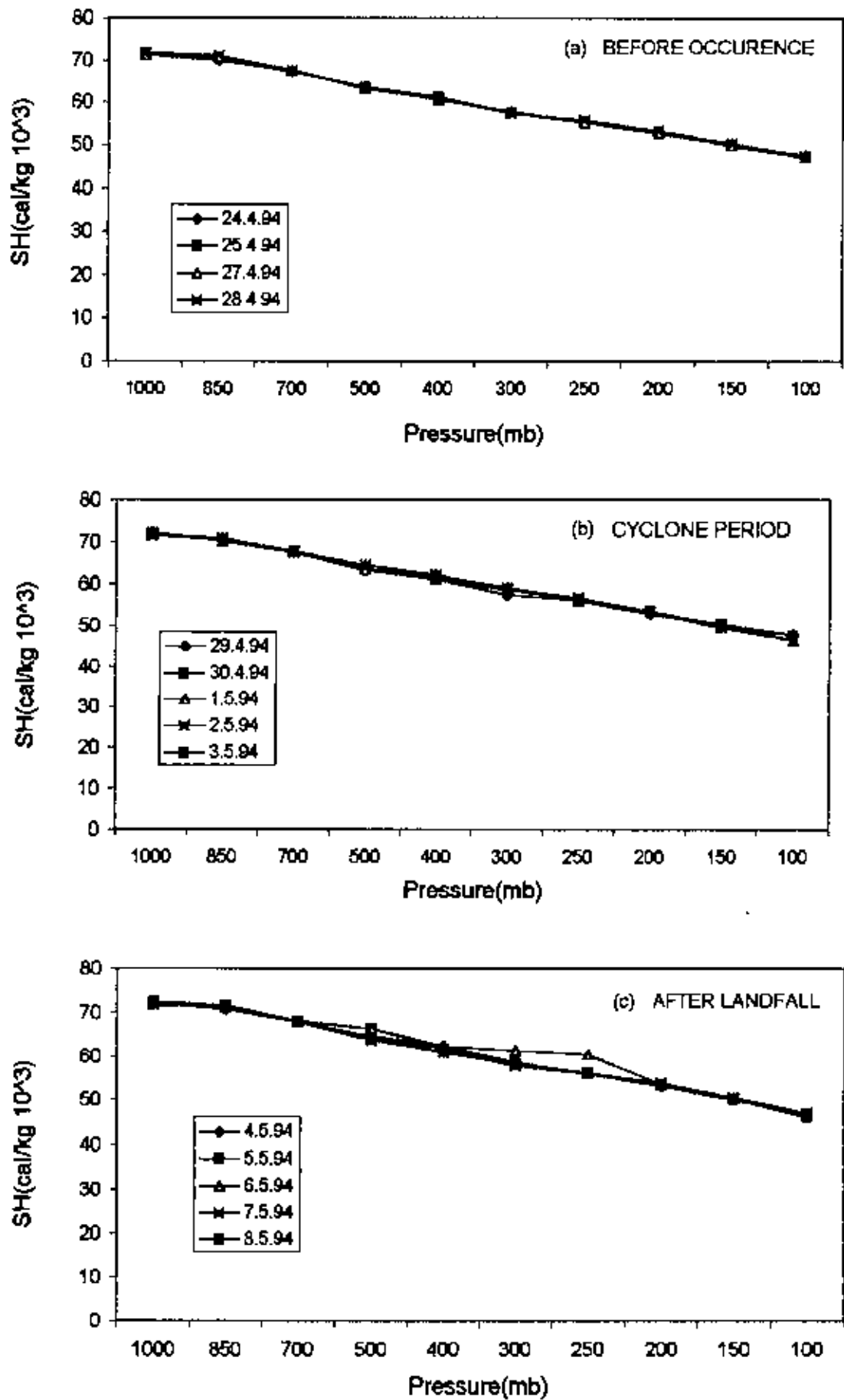


Fig. 5.4.1. (a-c). Sensible heat variation at different isobaric levels.

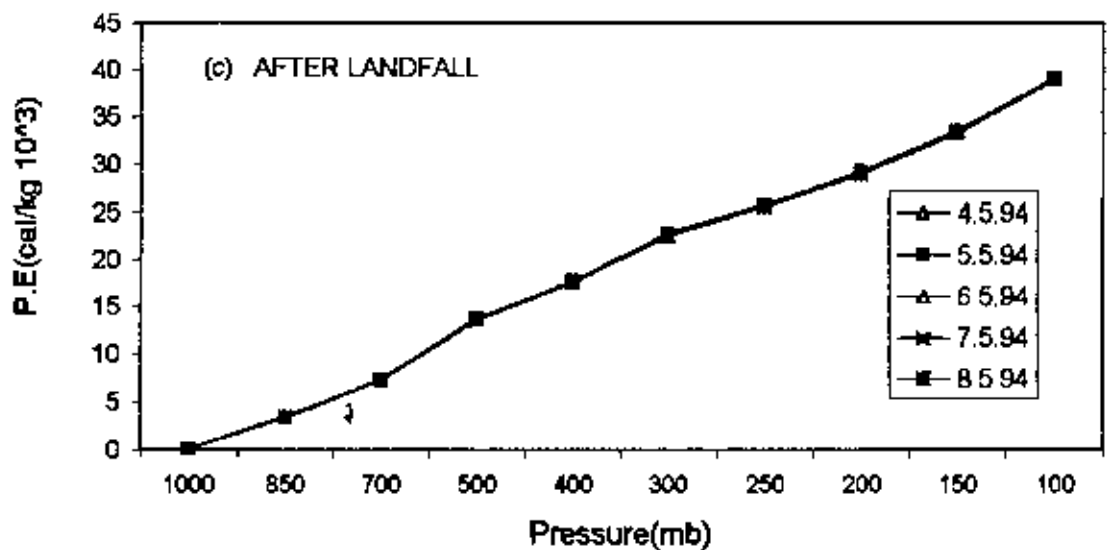
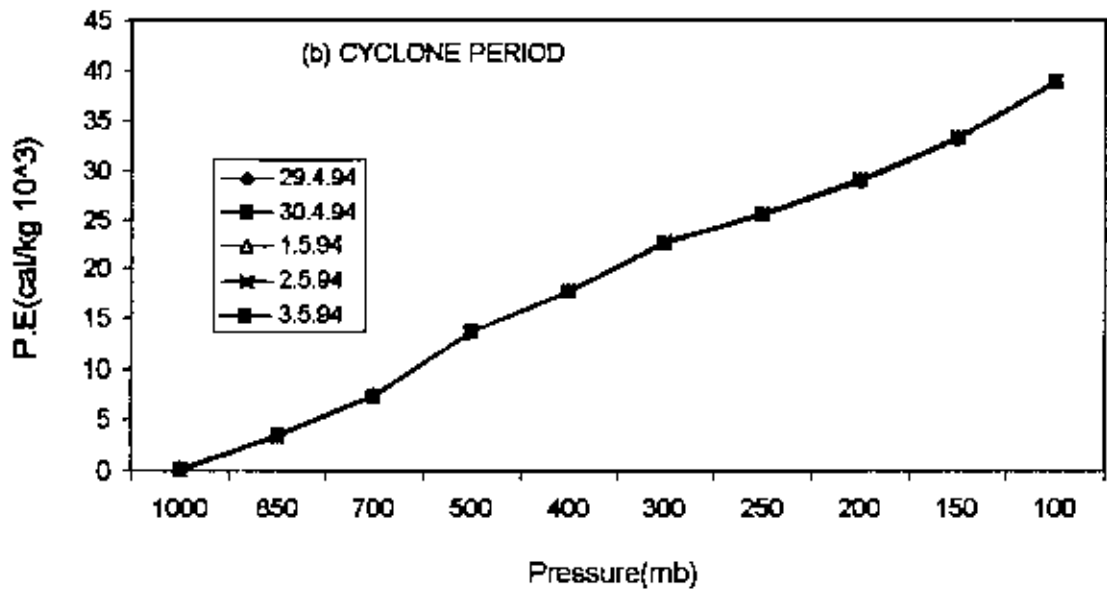
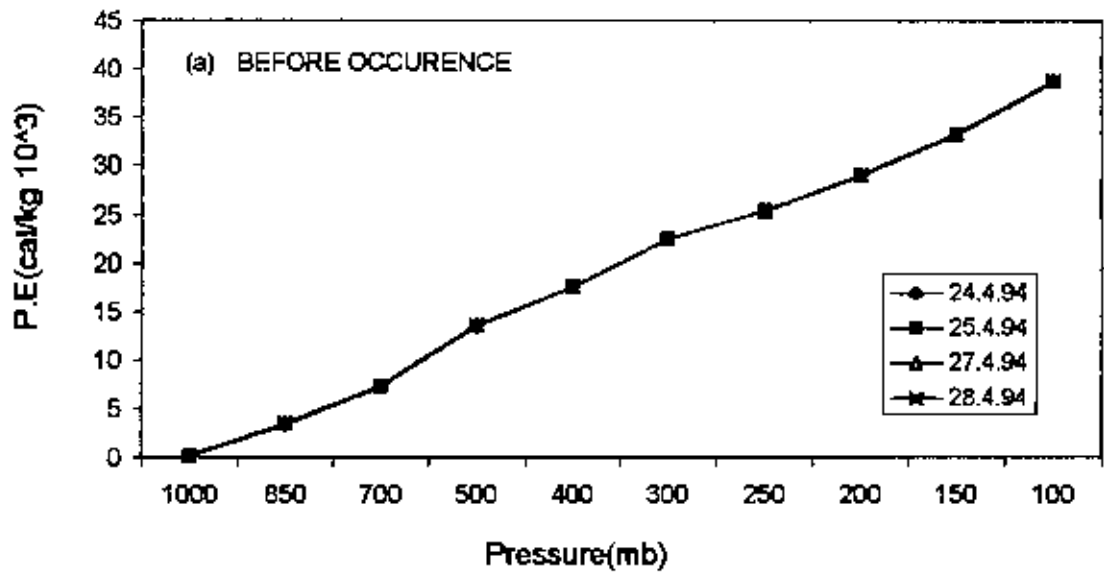


Fig. 5.4.2 (a-c). Potential energy variation at different isobaric levels.



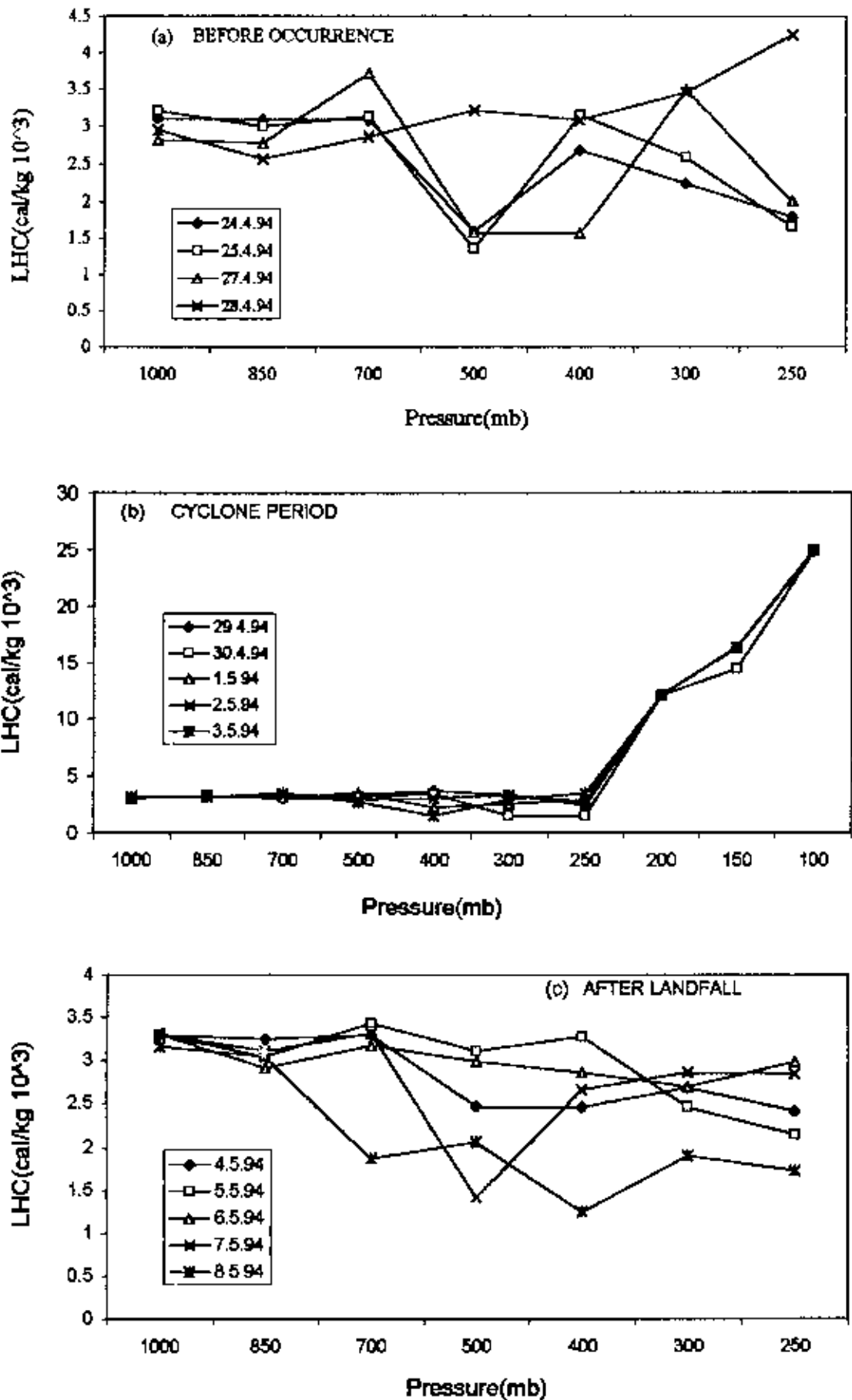


Fig. 5.4.3 (a-c). Latent heat content variation at different isobaric levels.

initiation of cyclone i.e., on 28<sup>th</sup> April, LHC increased linearly from 850-250 mb. This was because more cloud is formed just before the formation of cyclone.

At cyclone period [Fig. 5.4.3(b)], it is observed that LHC was constant for all the days and maintained their constant value up to 250 mb. Beyond 250 mb it increased abruptly and was maximum at 100 mb. It is also seen that, no cloud is formed from lower to middle troposphere i.e., from 1000-250 mb and more cloud is formed from middle to upper troposphere i.e., from 250-100 mb.

After landfall [Fig. 5.4.3(c)], it is observed that LHC was almost same at layer to layer for all the days (except 8<sup>th</sup> May). On 8<sup>th</sup> May i.e., at the end of landfall, LHC fluctuated from layer to layer. This was because cloud is formed and rainfall occurs at the end of landfall.

#### **Kinetic energy (KE):**

Fig. 5.4.4(a-c) shows the variation of kinetic energy (KE) at different isobaric levels. From the above figure it is seen that, for before occurrence [Fig. 5.4.4(a)], KE was nearly zero for all the days from 1000-850 mb. Beyond 850 mb, KE linearly increased up to 300 mb. At 300-200 mb, KE was almost same and then decreased.

At cyclone period [Fig. 5.4.4(b)], KE was nearly zero for all the days from 1000-500 mb. Beyond 500 mb, KE linearly increased up to 200 mb and then decreased. It is also seen that at the end of cyclone (3<sup>rd</sup> May), KE was nearly zero for all the levels.

After landfall [Fig. 5.4.4(c)], KE was nearly zero for all the days from 1000-850 mb. Beyond 850 mb, KE gradually increased for all the days up to 400 mb (except 8<sup>th</sup> May) and then almost constant up to 200 mb. Beyond 200 mb, KE decreased for all the days. At the end of landfall i.e., on 8<sup>th</sup> May, it is seen that KE linearly increased from layer to layer and attained maximum value at 250 mb. After 250 mb, KE decreased linearly and a sharp peak was found at 250 mb.

From the above figure [Fig. 5.4.4(a-c)], it is observed that KE was nearly zero at the lower troposphere. KE gradually increased at the middle troposphere and then decreased from upper to the top of the troposphere. At before occurrence, it is seen that KE gradually increased up to 300 mb and after landfall it increased up to 400 mb. But at

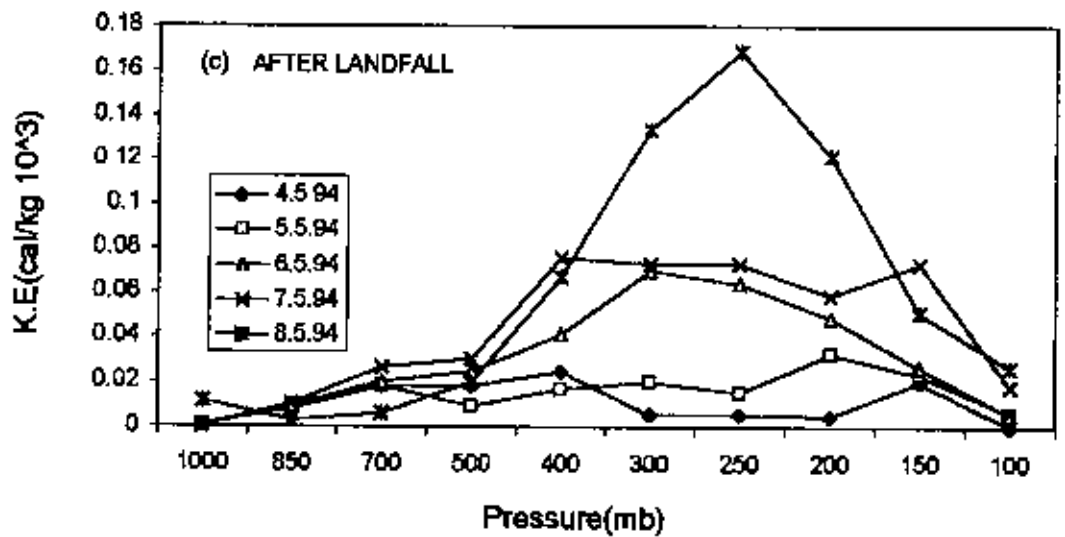
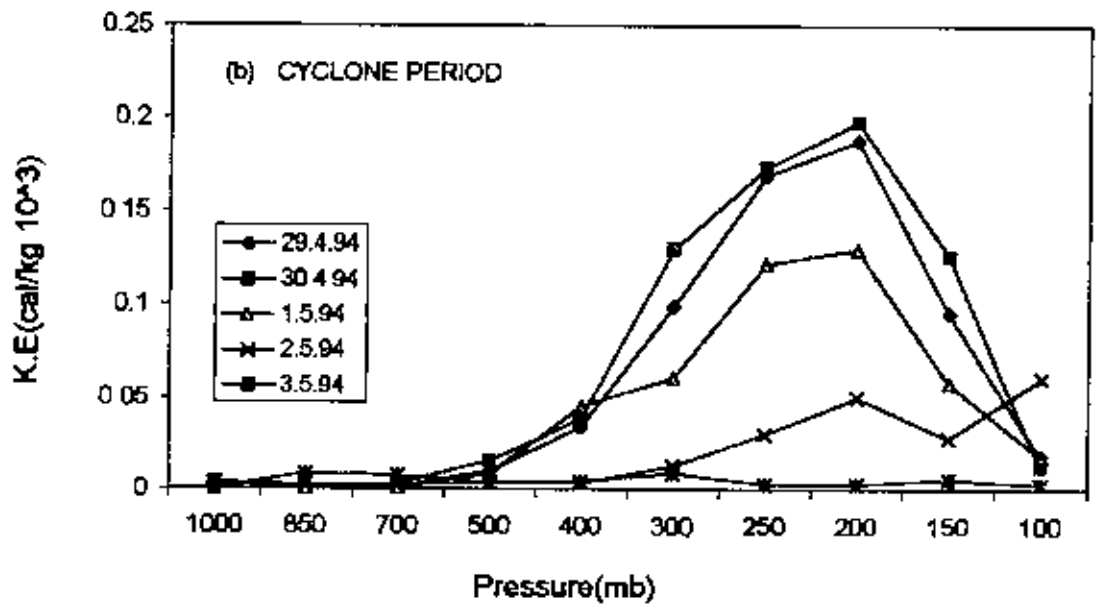
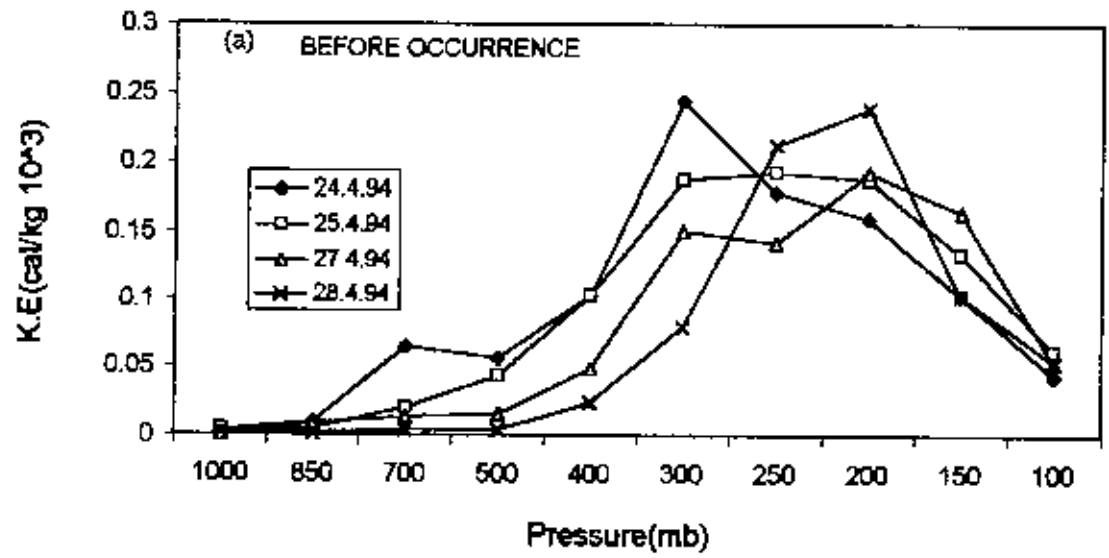


Fig. 5.4.4 (a-c). Kinetic energy variation at different isobaric levels.

cyclonic period, KE gradually increased up to 200 mb and three peaks were observed at this level.

#### 4.2.4 (b): Energy fluxes

##### Zonal flux of dry static energy (ZFDSE):

Fig. 5.4.5(a-c) shows the variation of zonal fluxes of dry static energy (ZFDSE) at different isobaric levels. Before occurrence it is found that ZFDSE was positive (eastward) on 24<sup>th</sup> of April whereas it was negative (westward) on 25-28<sup>th</sup> of April at 1000 mb. Beyond 1000 mb it turned into positive (eastward) and linearly increased up to 300 mb for all the days. Beyond 300 mb ZFDSE decreased.

At cyclone period [Fig. 5.4.5(b)], it is seen that ZFDSE was negative (westward) for all the days (except 3<sup>rd</sup> May) from 1000-850 mb. Beyond 850 mb, on 29 April to 1<sup>st</sup> May, it turned into positive (eastward) and increased linearly up to 250 mb and then remain constant up to 150 mb and then decreased at 100 mb. On 2<sup>nd</sup> May it was negative (westward) from 1000-500 mb. Above 500 mb it turned into positive and gradually increased up to 250 mb and then remain constant. At the end of cyclone i.e., on 3<sup>rd</sup> May, it was completely positive (eastward) with a lower value and at layer to layer there was no change of zonal flux of dry static energy. This means that at the end of cyclone the weather remained calm.

After landfall [Fig. 5.4.5(c)], it is seen that at 1000 mb ZFDSE was nearly zero and negative (westward). After 1000 mb, it turned into positive (eastward) for all the days and increased linearly with the same sign up to 400 mb. Beyond 400 mb, ZFDSE decreased gradually up to 100 mb.

From the above figure [Fig. 5.4.5(a-c)], it is observed that, for before occurrence and after landfall ZFDSE was very low at 1000 mb, but at cyclone period this low value exist up to 700 mb. For all the three phases there was a common feature that at first it increased linearly. For before occurrence it increased up to 300 mb and for after landfall it increased up to 400 mb and then decreased gradually for both phases (i.e., before occurrence and after landfall). But at cyclone period, zonal fluxes of dry static energy reached their highest value and remain constant up to 150 mb and then decreased at 100 mb.

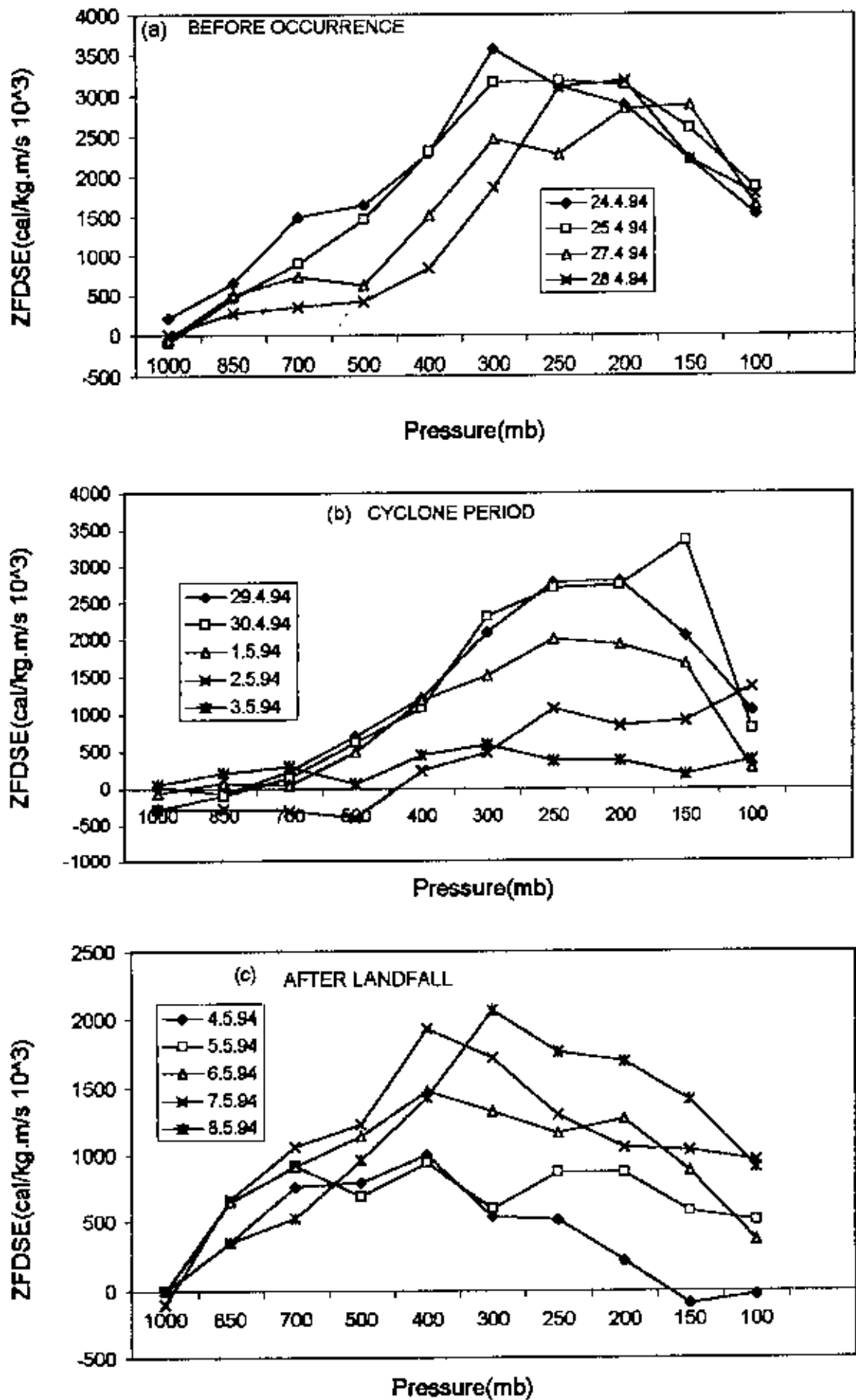


Fig. 5.4.5 (a-c). Variation of zonal fluxes of dry static energy at different isobar

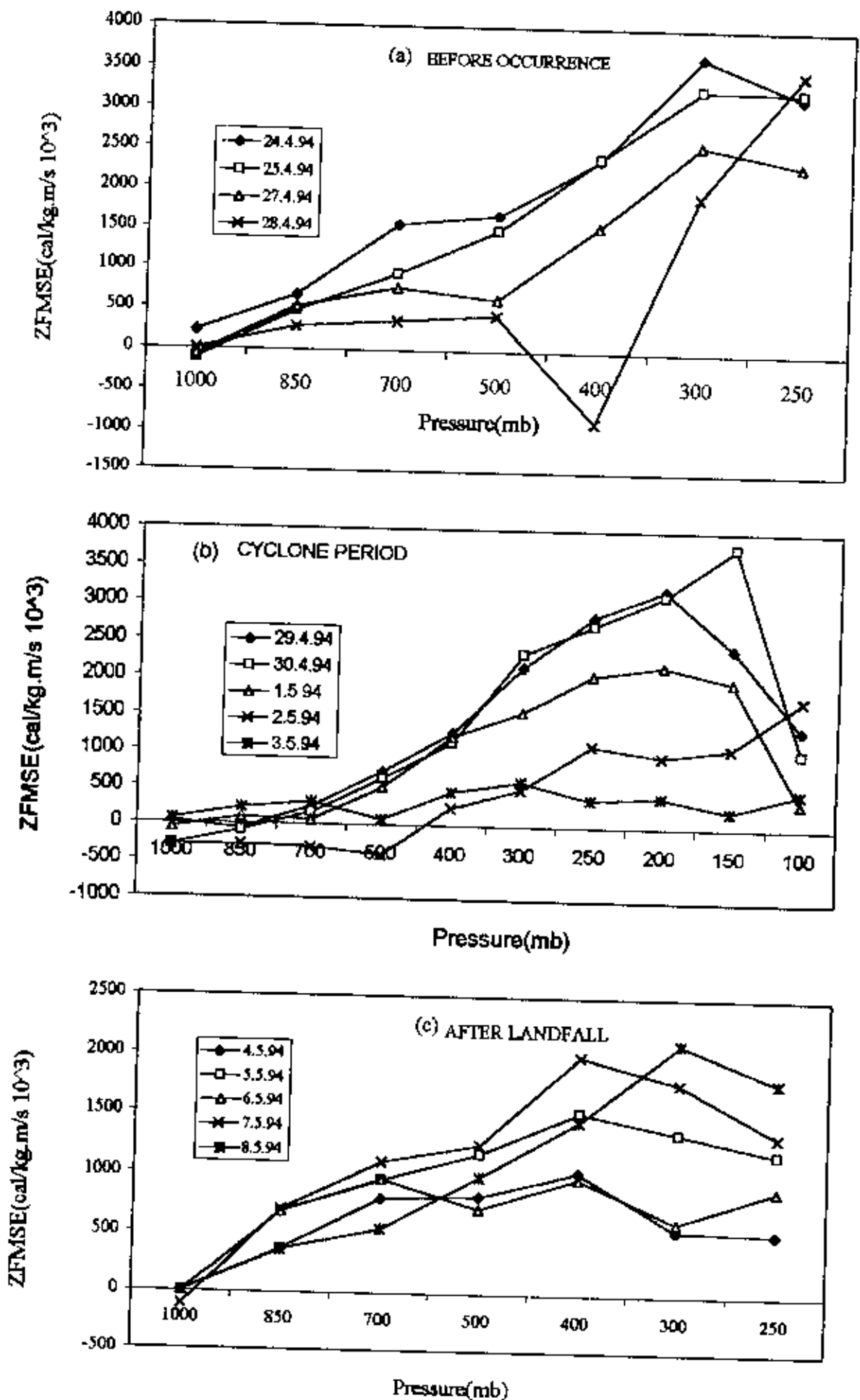


Fig. 5.4.6 (a-c). Variation of zonal fluxes of moist static energy at different isobaric levels.

### Zonal flux of moist static energy (ZFMSE):

Fig. 5.4.6(a-c) shows the variation of zonal flux of moist static energy at different isobaric levels at different phases of the studied cyclone. From the above figure it is observed that the graph pattern gave the same variation as that of zonal flux of dry static energy which is discussed earlier [Fig. 5.4.5(a-c)]. There was only difference in magnitude. This was because zonal flux of moist static energy is simply an addition of latent heat content with zonal fluxes of dry static energy.

### Meridional flux of dry static energy (MFDSE):

Meridional flux of dry static energy (MFDSE) at different isobaric levels is shown in Fig 5.4.7(a-c). It is observed that, before occurrence [Fig. 5.4.7(a)], MFDSE was positive (northward) on 24-25 of April and it was negative (southward) on 27-28 of April at 1000 mb. It is also seen that MFDSE fluctuated for all the days from positive (northward) to negative (southward) and vice-versa at 1000-400 mb. Beyond 400 mb it turned into positive (except 24 April) and gradually increased and attained the highest value at 200 mb on 27-28 April and at 150 mb on 24-25 April. At 100 mb for all the days it decreased.

At cyclone period [Fig. 5.4.7(b)], it showed that, at 1000 mb MFDSE was negative (southward) for all the days except 1<sup>st</sup> May. But at 850 mb it was negative (southward) for all the days except 30<sup>th</sup> April. Beyond 850 mb it turned into positive (northward) for all the days (except at the end of cyclone i.e., on 3<sup>rd</sup> May) and from layer to layer it increased linearly due to the linear increase of meridional wind component. It attained the highest value at 200 mb. Beyond 200 mb it decreased. It is also observed that at the end of cyclone, for most of the levels (1000-250 mb) flux direction was opposite (southward) compared to the other cyclone days.

After landfall [Fig. 5.4.7(c)], it is found that, at 1000 mb MFDSE was positive (northward) for all the days. Beyond 850 mb it turned into negative (southward) at 700 mb for all the days except 8<sup>th</sup> May i.e., at the end of landfall. Beyond 700 mb it is observed that MFDSE increased linearly up to 250 mb on 6-8<sup>th</sup> May and then decreased. But at the initiation of landfall i.e., on 4-5 May, it is found that MFDSE was negative

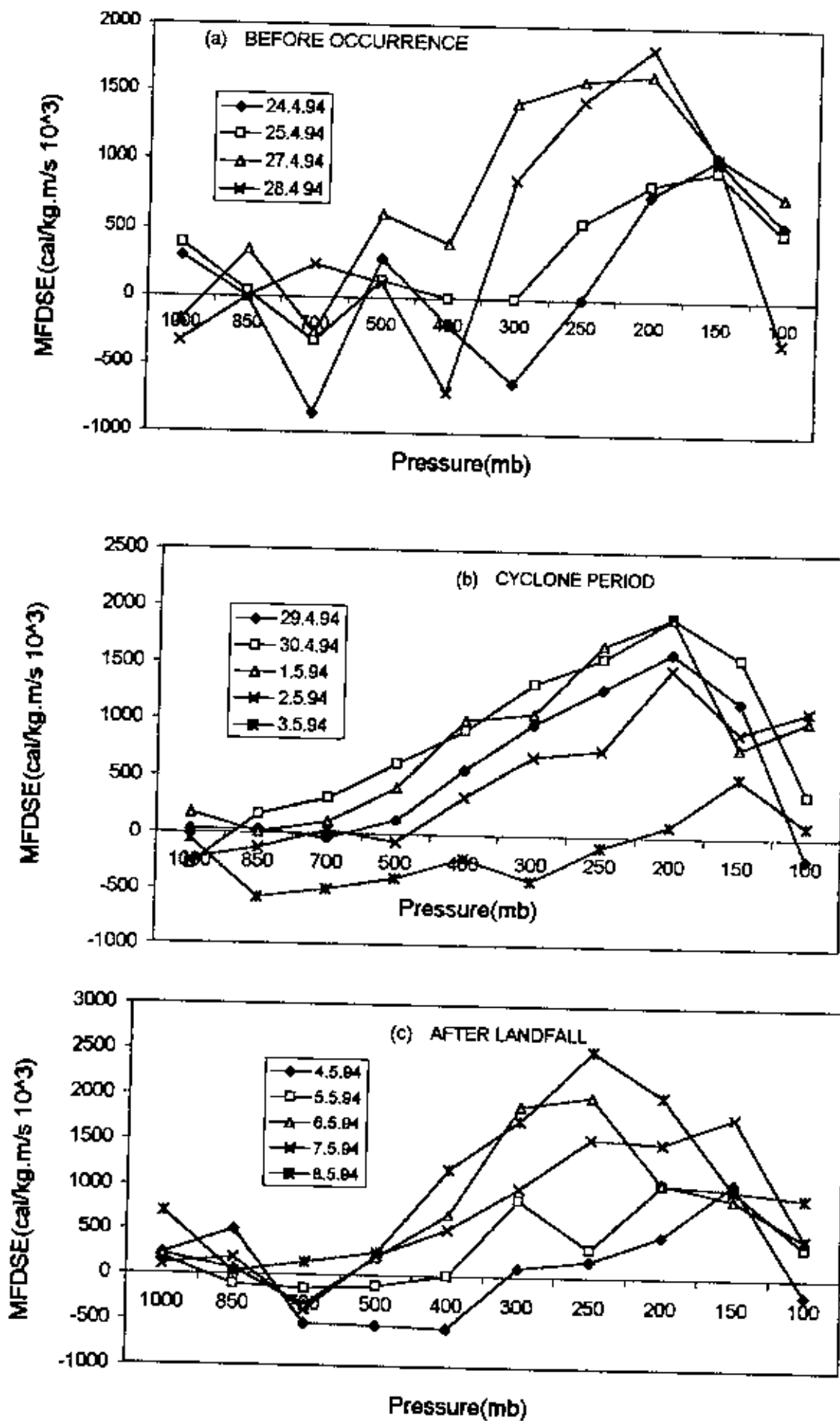


Fig. 5.4.7 (a-c). Variation of meridional fluxes of dry static energy at different isobaric levels.



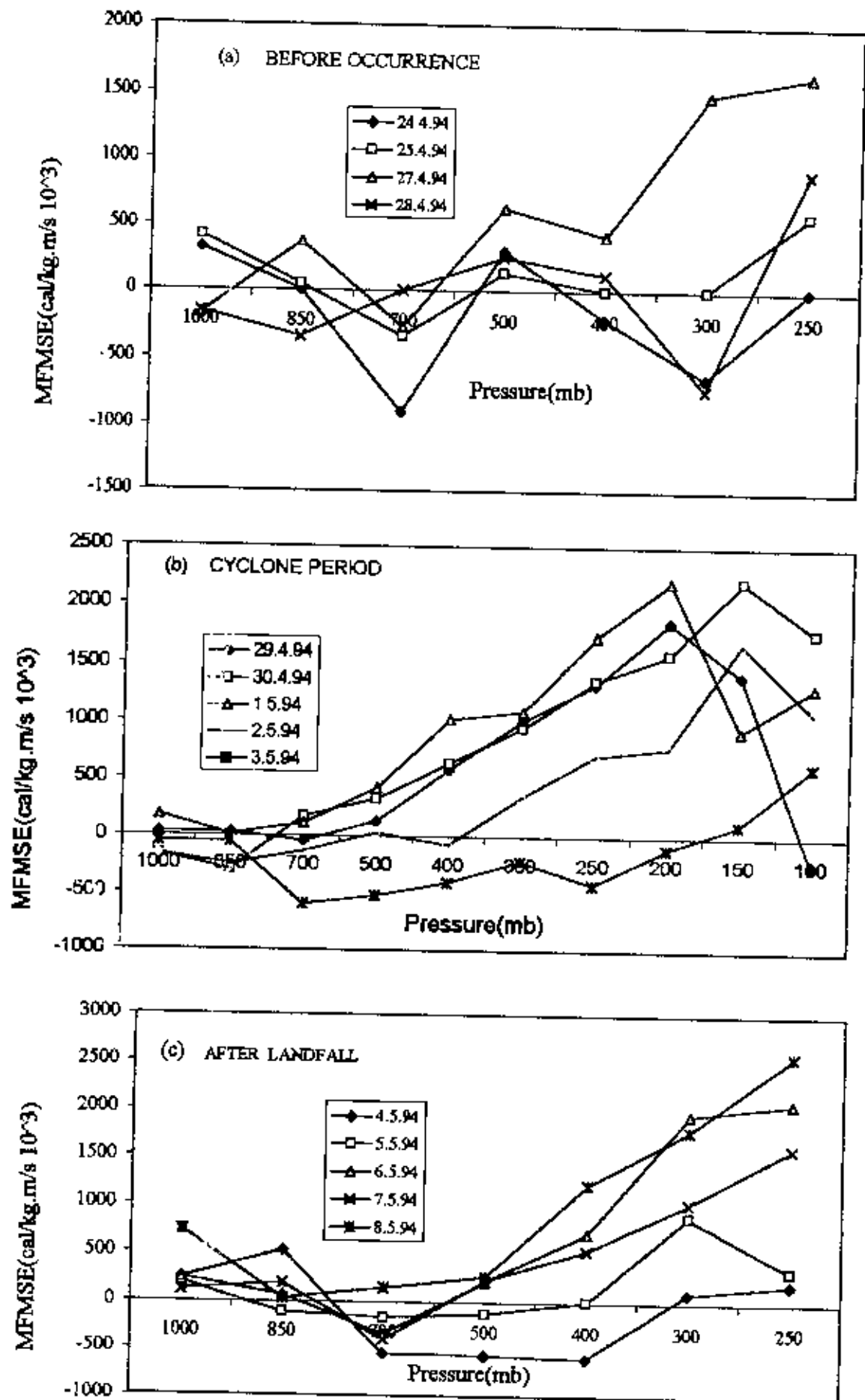


Fig. 5.4.8 (a-c). Variation of meridional fluxes of moist static energy at different isobaric level

(southward) and remain constant from 700-400 mb. Beyond 400 mb it turned into positive (northward) and increased linearly with the same sign up to 150 mb on 4<sup>th</sup> May and then decreased and again turned into negative (southward) at 100 mb. But on 5<sup>th</sup> May, it turned into positive (northward) beyond 400 mb and then fluctuated due to the change of wind velocity during landfall.

From the above figure [Fig. 5.4.7(a-c)], it is observed that, at 1000 mb flux direction was opposite to each other between cyclone period and after landfall. It is also observed that for before occurrence and after landfall flux is fluctuated due to the change of wind velocity but at cyclone period there was no such fluctuation. It increased linearly from layer to layer up to the upper level of the troposphere (i.e., up to 200 mb). At cyclone period it is seen that at the initiation of cyclone period and at the end of cyclone period flux direction was opposite to each other i.e., when one positive (northward) the other is negative (southward) and vice-versa.

#### **Meridional flux of moist static energy (MFMSE):**

Fig. 5.4.8(a-c) shows the variation of meridional flux of moist static energy at different isobaric levels from 1000-250 mb. At layer to layer it gave the same variation as that of meridional fluxes of dry static energy which is discussed earlier [Fig. 5.4.7(a-c)]. Here only the difference in magnitude. Because moist static energy is simply an addition of latent heat content with the dry static energy.

#### 4.2.5 Cyclone 5

Cyclone 5 occurred during the period 21 November 1995 to 25 November 1995. To observe its “before occurrence” and “after landfall” conditions, data were analyzed from 16 November 1995 to 30 November 1995. The track of the observed cyclone is shown in Fig. 3.

##### 4.2.5 (a): Energy components

###### Sensible heat (SH):

Fig. 5.5.1(a-c) shows the variation of sensible heat (SH) at different isobaric levels at different phases of cyclone 5. It is seen that at day to day there was no significant change observed for SH. But at layer to layer SH decreased linearly and was minimum at the top of the troposphere i.e., at 100 mb. This was due to the lower temperature at the upper troposphere.

###### Potential energy (PE):

The variation of potential energy (PE) at different isobaric levels at different phases of cyclone is shown in Fig. 5.5.2(a-c). It is seen that PE was minimum (near about zero) at the surface level i.e., at 1000 mb and increased gradually as pressure decreased. It is also observed that P.E attained maximum value at the top of the troposphere (i.e., at 100 mb) because of higher geopotential height at this level.

###### Latent heat content (LHC):

Latent heat content (LHC) variation at different isobaric levels at different phases of cyclone 5 is shown in Fig. 5.5.3(a-c). Before occurrence [Fig. 5.5.3(a)] it is seen that, from 1000-700 mb, there was no change of LHC for all the days (i.e., 16.11.95-20.11.95). At 500 mb LHC decreased slightly (except 18.11.95) and then remained constant up to 300 mb. At 250 mb LHC slightly increased for all the days. It is also seen that at 250 mb LHC increased abruptly at the initiation of cyclone i.e., on 20.11.95

During cyclone period [Fig. 5.5.3(b)] it is seen that for all the days (except 21.11.95) there was no observed change of LHC from 1000-300 mb. At the starting of cyclone i.e., on 21.11.95 it is observed that LHC fluctuated due to cloud formation. It is also observed that at middle troposphere i.e. at 250 mb LHC was maximum at the starting of cyclone (i.e., at 21.11.95) and at the end of cyclone (i.e., on 25.11.95).

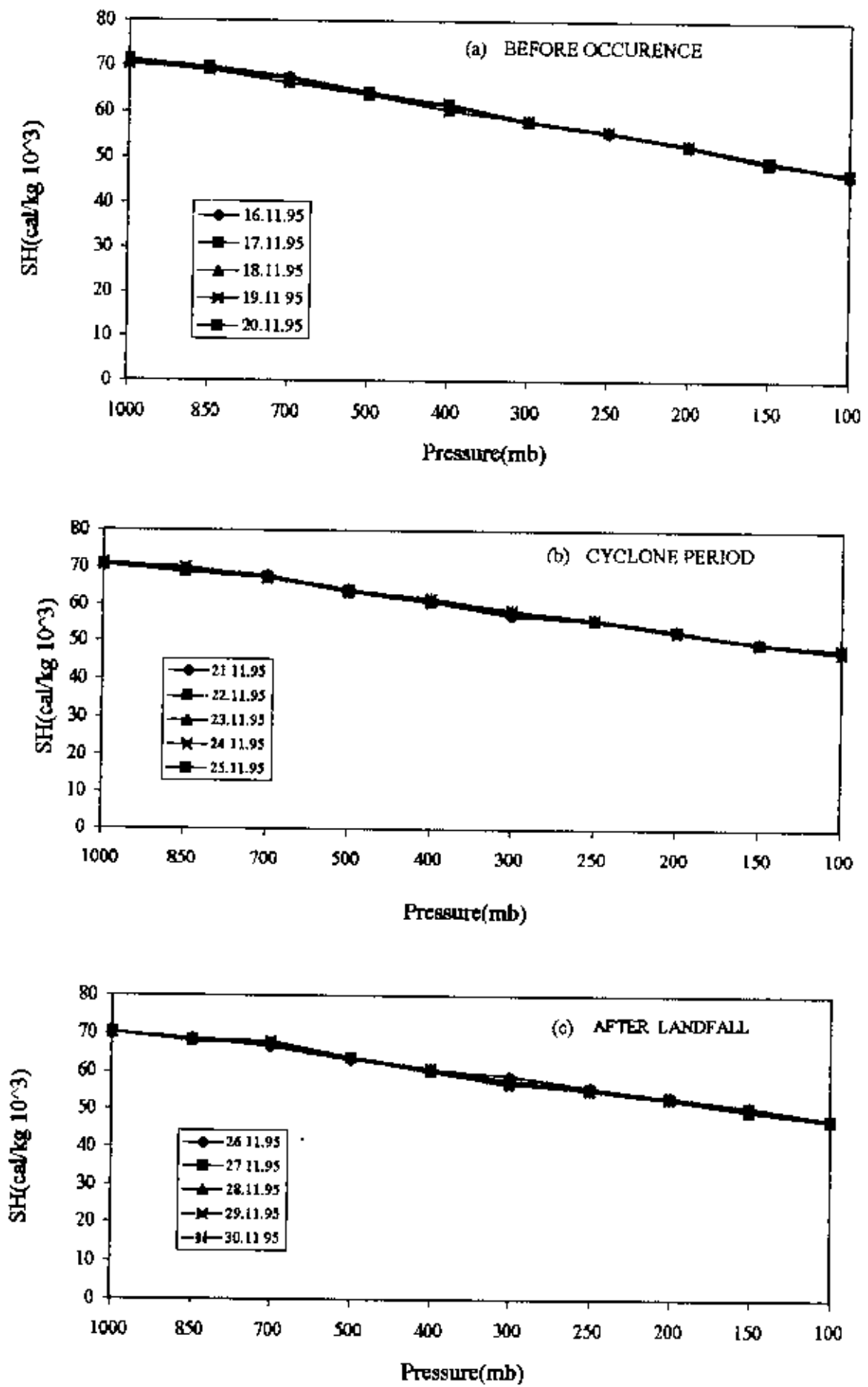


Fig. 5.5.1. (a-c). Sensible heat variation at different isobaric levels.

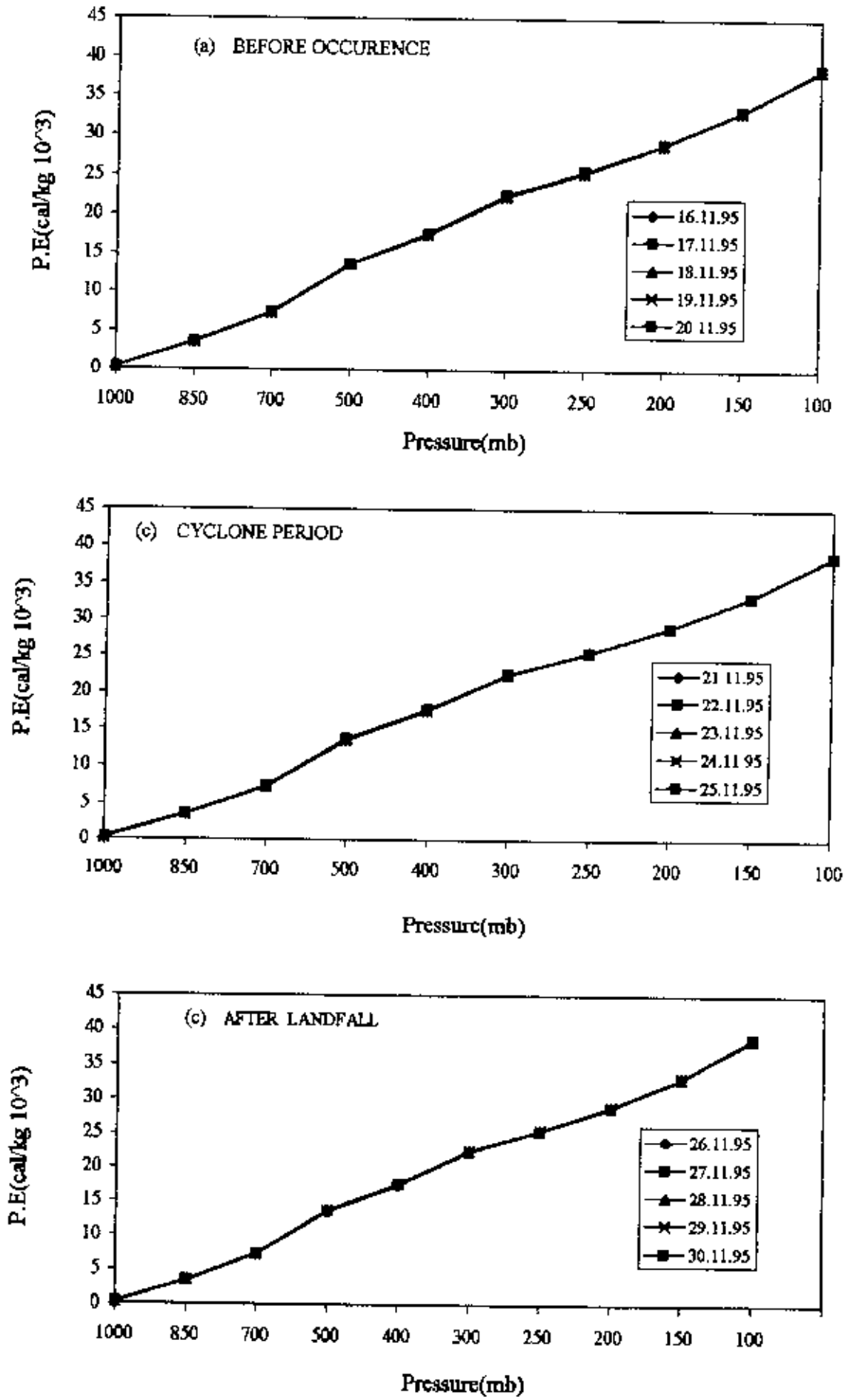


Fig. 5.5.2 (a-c). Potential energy variation at different isobaric levels.

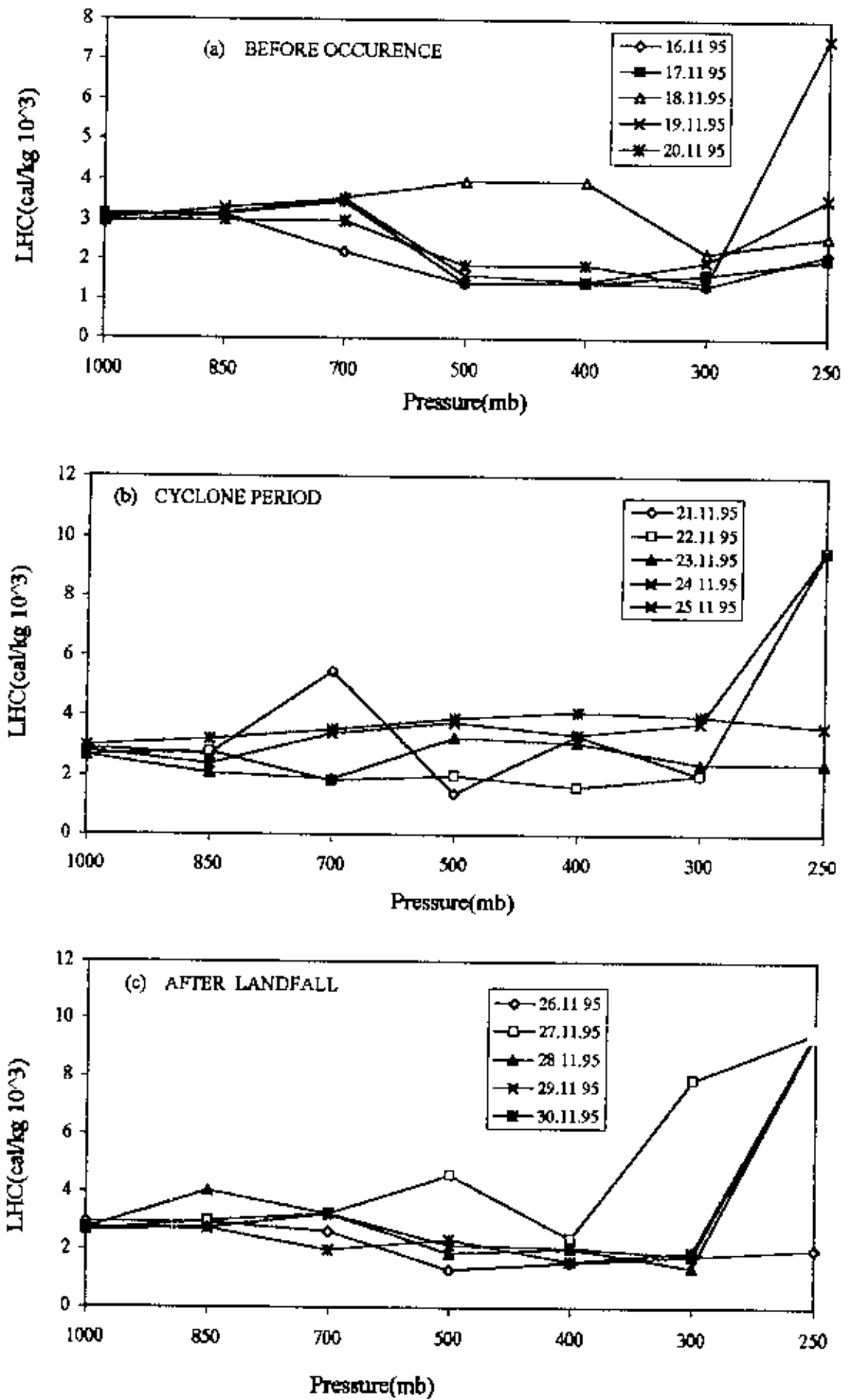


Fig. 5.5.3. (a-c). Latent heat content variation at different isobaric levels.

After landfall [Fig. 5.5.3(c)] it is seen that from 1000-300 mb levels there was no change of LHC for all the days (except 27.11.95). On 27.11.95 from layer to layer LHC fluctuated. At 250 mb LHC increased abruptly for all the days (except 26.11.95) and the value was also same for all the days. From this figure [Fig. 5.5.3(a-c)], it is observed that there was a common feature that at 250 mb for all the days (except 23, 24 and 26 November) LHC increased and attained maximum value. This was because middle troposphere is the cloud forming zone.

#### **Kinetic energy (KE):**

Fig. 5.5.4(a-c) shows kinetic energy (KE) variation at different isobaric levels at different phases of cyclone 5. From these figures it is observed that at before occurrence [Fig. 5.5.4(a)] KE was nearly zero from 1000-700 mb. Beyond 700 mb KE increased gradually for all the days and attained maximum value at 200 mb i.e., at the upper level of the troposphere. Beyond 200 mb KE decreased again.

At cyclone period [Fig. 5.5.4(b)] KE was near about zero from 1000-850 mb. Beyond 850 mb KE increased gradually for all the days and attained maximum value at 200 mb and then decreased. But at the starting of cyclone i.e., on 21.11.95 there was different feature. It is observed that after 850 mb, KE increased linearly from layer to layer and attained maximum value at 250 mb. Beyond 250 mb KE was nearly same.

Fig. 5.5.4(c) shows the variation of KE at different isobaric levels after landfall. It is seen that KE was nearly zero from 1000-850 mb. Beyond 850 mb KE increased gradually from layer to layer (except 26 and 28 Nov.) up to 200 mb and then decreased. On 26 and 28 Nov, it is observed that from layer to layer KE fluctuated due to the randomness of wind speed. It is also observed that at the starting of landfall i.e., on 26.11.95 KE was maximum at 250 mb due to higher wind speed during landfall. From Fig. 5.5.4(a-c) it is seen that KE was nearly zero at the lower level of the troposphere (i.e., 1000-700 mb), it increased gradually from middle to upper level of the troposphere (700-200 mb) and then decreased and was minimum at the top of the troposphere i.e., at 100 mb.

#### **4.2.5 (b): Energy fluxes**

##### **Zonal flux of dry static energy (ZFDSE):**

The variation of zonal flux of dry static energy (ZFDSE) at different isobaric levels is shown in Fig. 5.5.5(a-c). Here it is observed that at before occurrence [Fig.

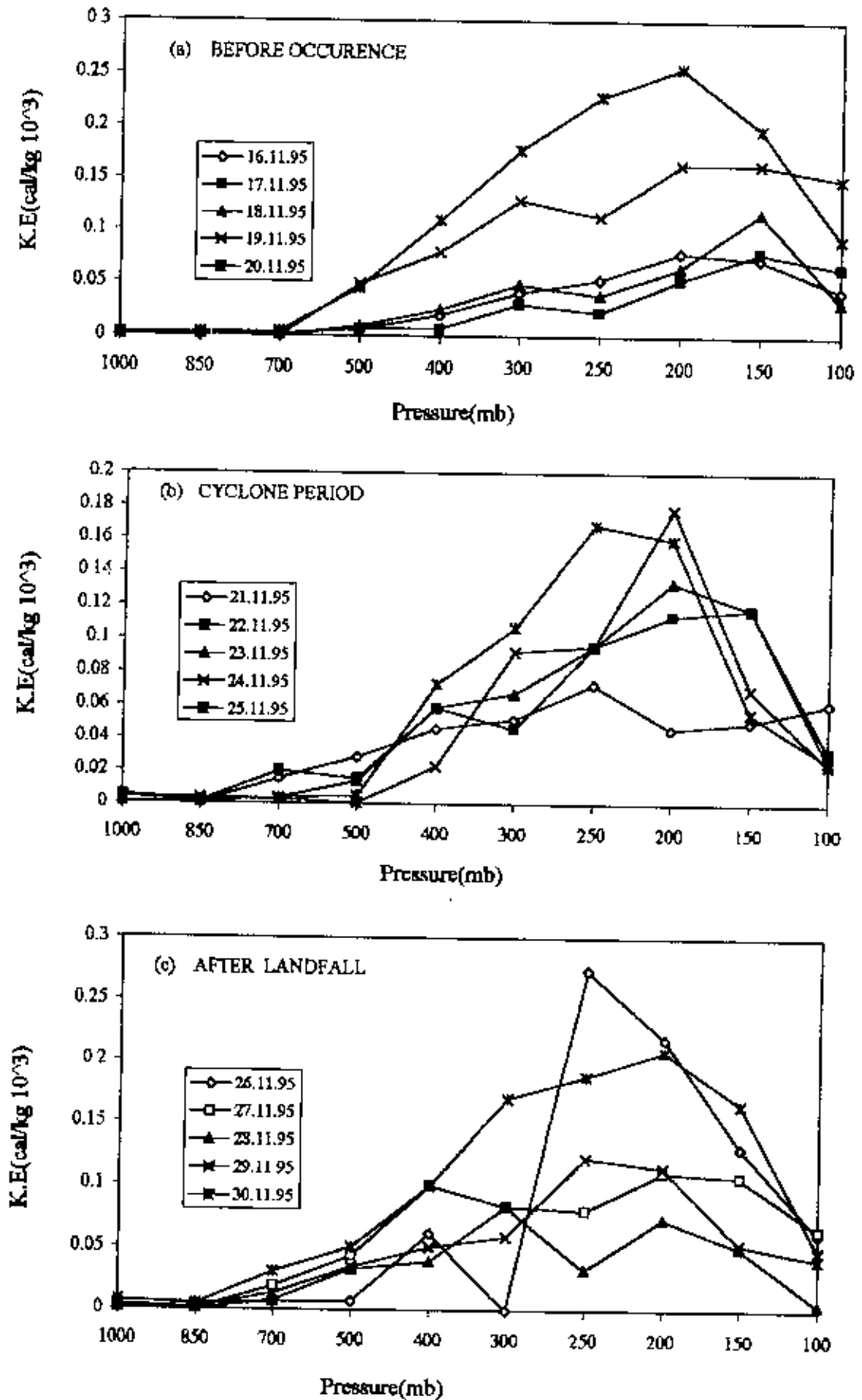


Fig. 5.5.4. (a-c) Kinetic energy variation at different isobaric levels



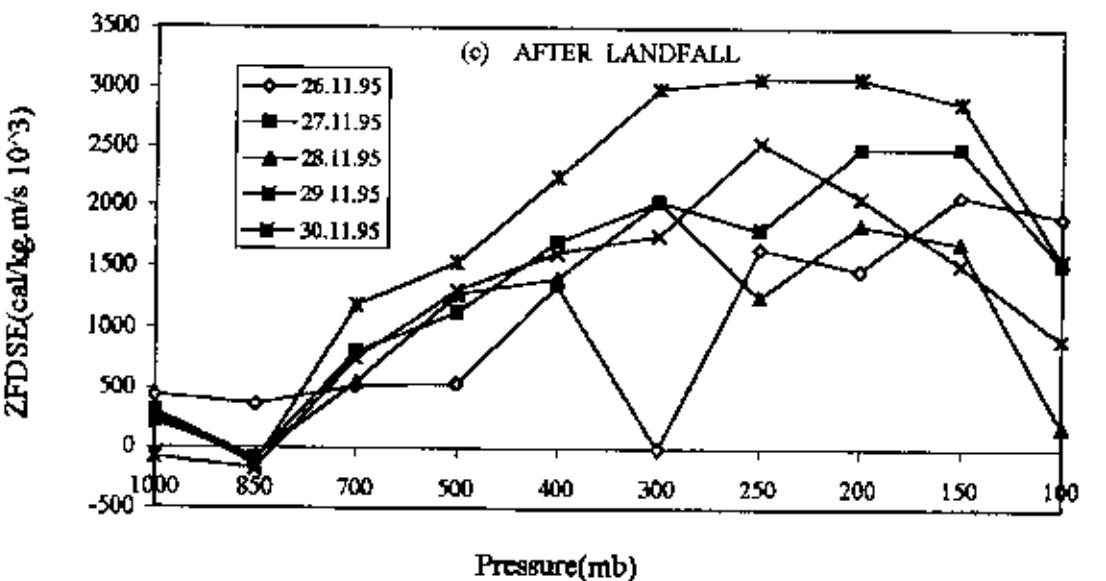
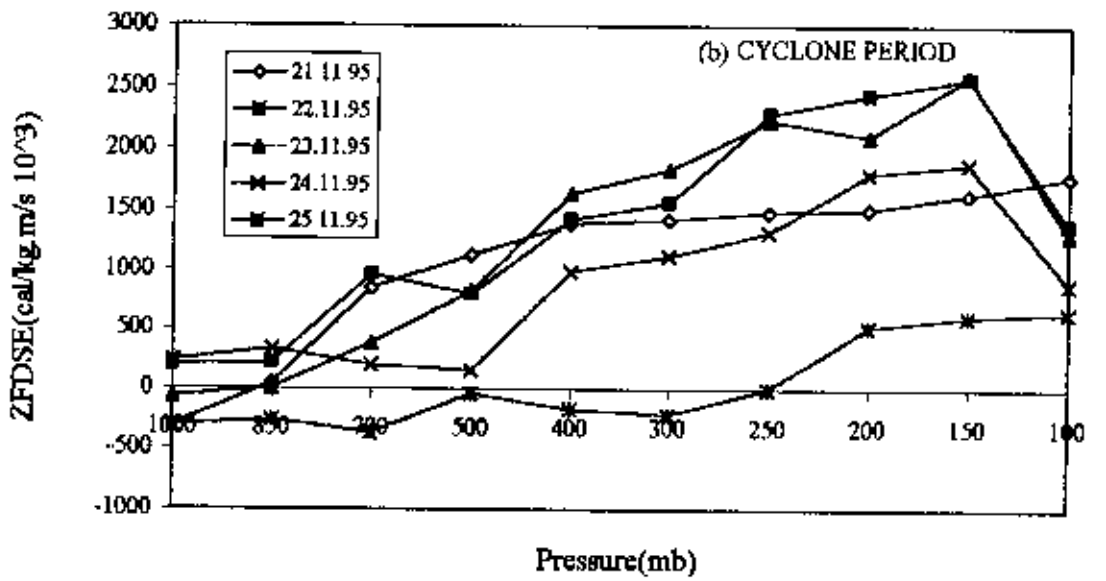
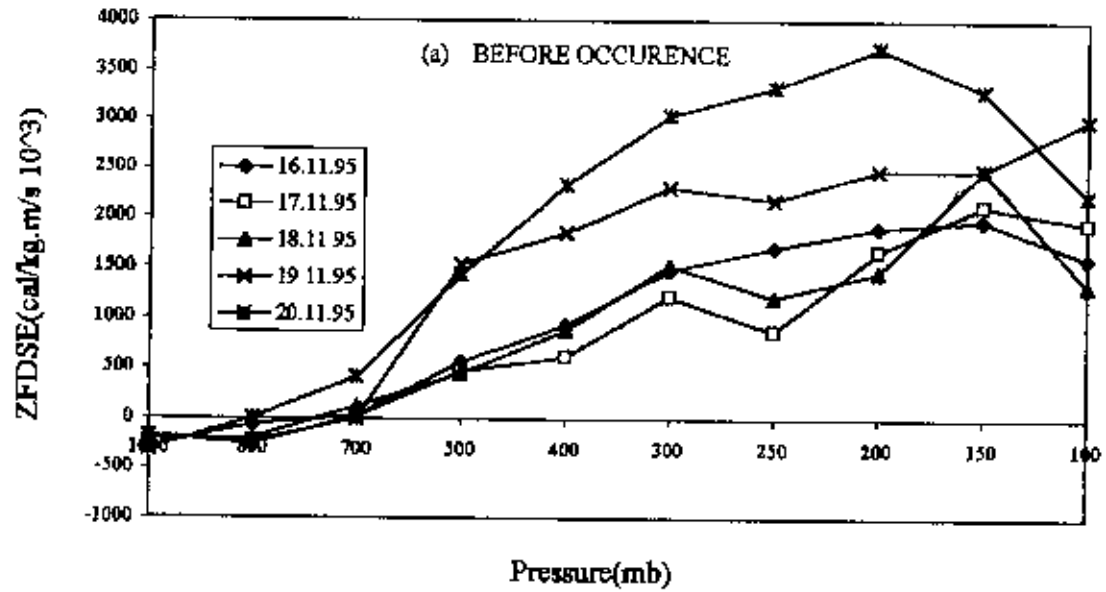


Fig. 5.5.5 (a-c) Variation of zonal fluxes of dry static energy at different isobaric levels.

5.5.5(a)] ZFDSE was negative (westward) for all the days from 1000-850 mb. Beyond 850 mb ZFDSE turned into positive (eastward) direction and increased gradually from layer to layer and was maximum at 200 mb. Beyond 200 mb it decreased again.

At cyclone period [Fig. 5.5.5(b)] it is seen that at 1000 mb ZFDSE was positive (eastward) on 22 and 24 Nov. 1995 and it was negative (westward) on 21, 23 and 25 Nov. 1995. At 850 mb it was positive (eastward) for all the days except at the end of cyclone (i.e., 25 Nov.) Beyond 850 mb, it increased gradually and attained maximum value at 150 mb and then decreased at 100 mb. At the end of cyclone (25<sup>th</sup> Nov.) it is seen that ZFDSE was negative (westward) from 1000-300 mb. Beyond 300 mb it turned into positive (eastward) and was zero at 250 mb. After 250 mb it increased gradually in the positive direction and was maximum at 100 mb.

After landfall [Fig. 5.5.5(c)], it is seen that ZFDSE was positive (eastward) for all the days (except 29 Nov.) at 1000 mb. At 850 mb ZFDSE was negative (westward) for all the days (except 26 Nov.). Beyond 850 mb it turned into positive and increased gradually from layer to layer up to 150 mb. At 100 mb ZFDSE decreased for all the days. At the initiation of landfall i.e., on 26 Nov. it is observed that ZFDSE was always positive (eastward) from 1000-100 mb and was fluctuated due to change of wind speed. At the end of landfall (i.e., on 30 Nov.) ZFDSE was constant from 300-150 mb due to no change of wind speed. From Fig. 5.5.5(a-c) it is observed that ZFDSE was negative (westward) at 1000 mb for before occurrence, ZFDSE was positive (eastward) at 1000 mb for after landfall. It is seen that wind direction was opposite at 1000 mb for before occurrence and after landfall. But at cyclone period ZFDSE was both positive (eastward) and negative (westward) at 1000 mb. It is also observed that at 100 mb ZFDSE decreased for all the days (except on 21<sup>st</sup> Nov.) due to decrease of wind speed. But at the starting of cyclone i.e., on 21<sup>st</sup> Nov. ZFDSE increased up to 100 mb due to increase of wind speed.

#### **Zonal flux of moist static energy (ZFMSE):**

The variation of zonal flux of moist static energy (ZFMSE) at different isobaric levels is shown in Fig. 5.5.6(a-c). Here it is seen that the graph pattern was same as that of ZFDSE which was discussed earlier in Fig. 5.5.5(a-c). Here only the difference was in magnitude. This was because ZFMSE is simply an addition of latent heat content with ZFDSE. Here it is seen that the pressure level was only up to 250 mb. This was because beyond 250 mb due point temperature was not found. So it was

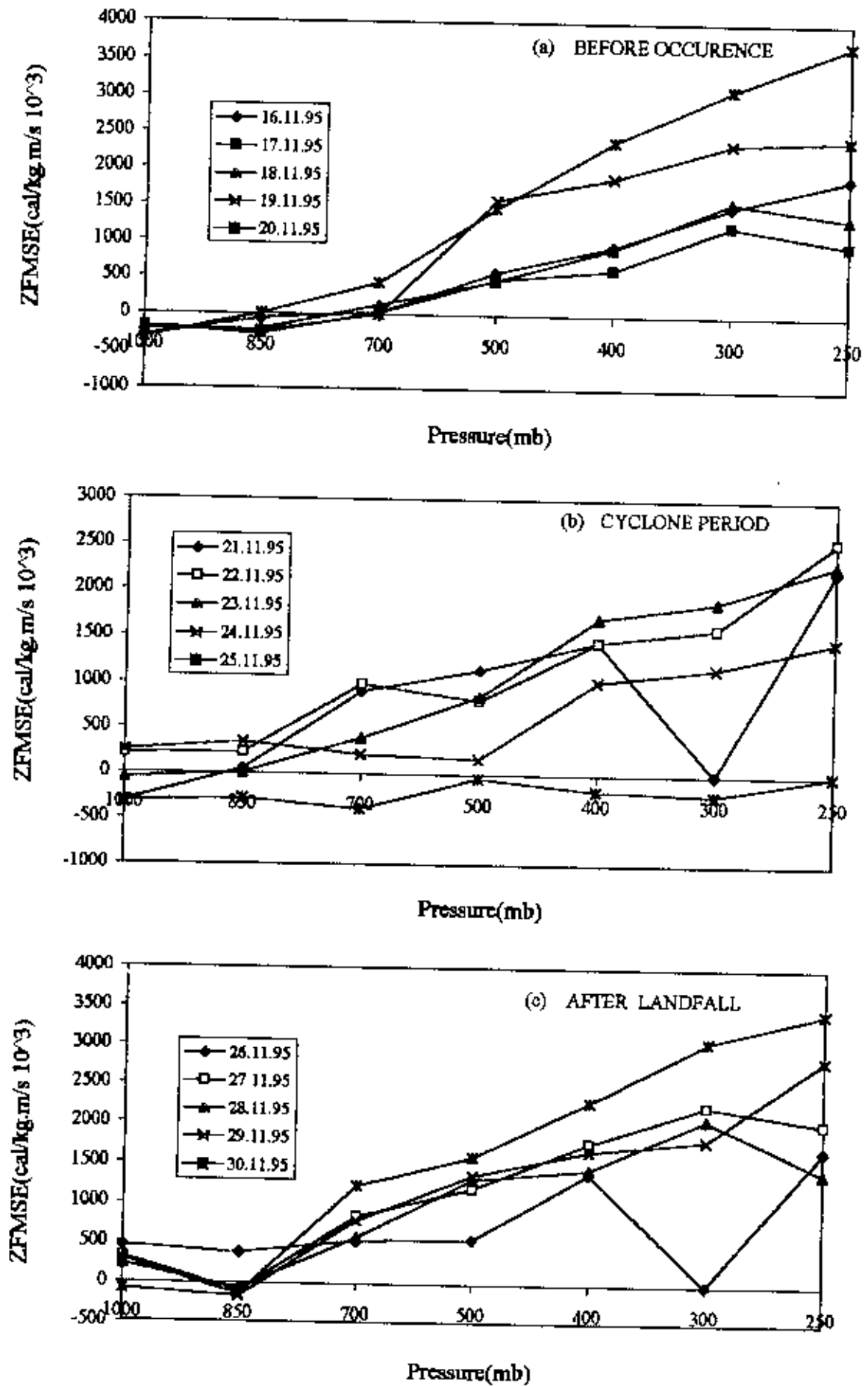


Fig 5.5.6 (a-c). Variation of zonal fluxes of moist static energy at different isobaric level

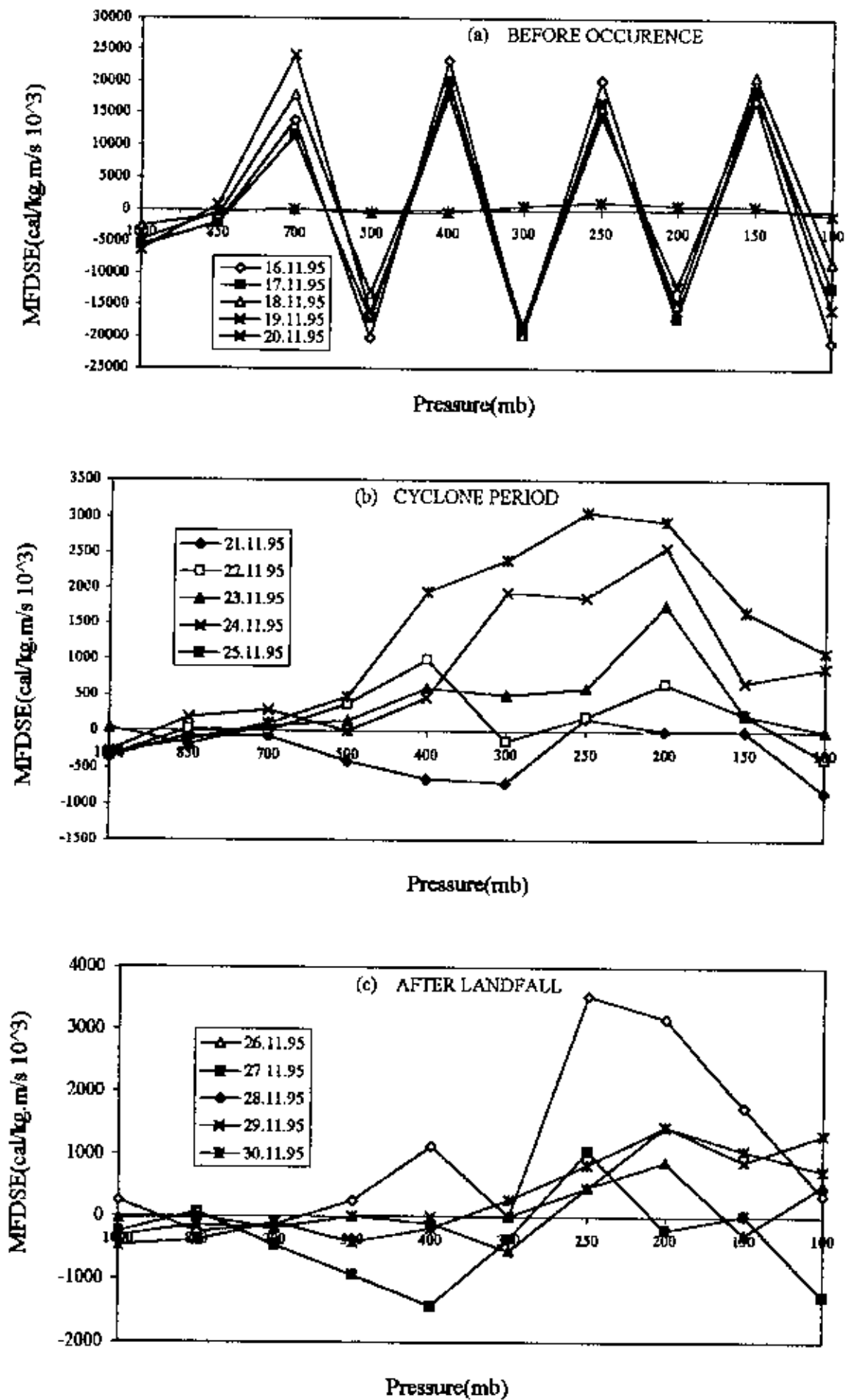


Fig. 5.5.7 (a-c). Variation of meridional fluxes of dry static energy at different isobaric levels.

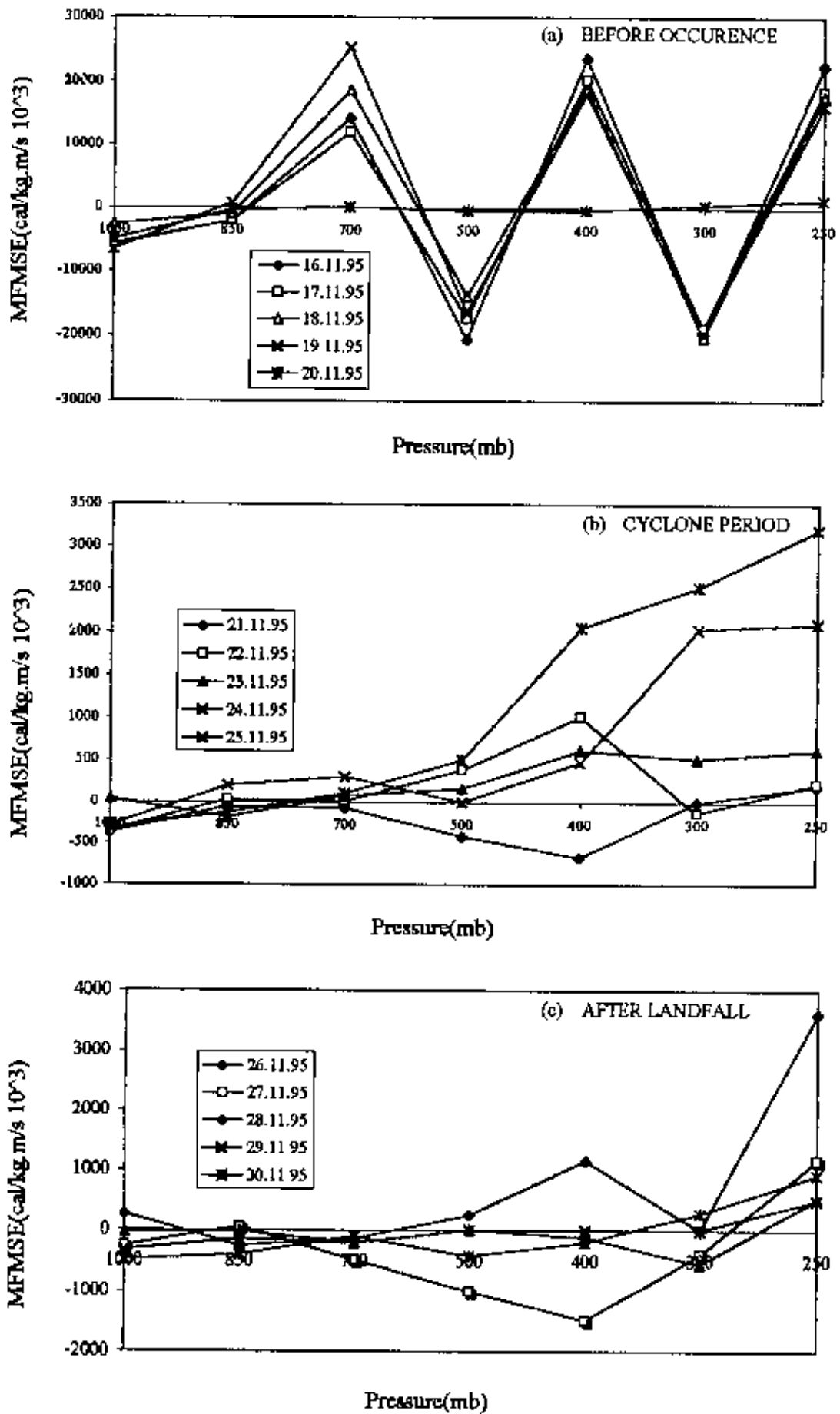


Fig. 5.5.8 (a-c). Variation of Meridional fluxes of moist static energy at different isobaric levels

not possible to calculate latent heat content beyond 250 mb. Therefore ZFMSE is observed only up to 250 mb level.

#### **Meridional flux of dry static energy (MFDSE):**

The variation of meridional flux of dry static energy (MFDSE) is shown in Fig. 5.5.7(a-c). Here before occurrence [Fig. 5.5.7(a)] it is seen that at day to day the variation of graph pattern was same. But at every layer MFDSE was changed and maintained a zig-zug path due to change of wind speed and direction. It is also observed that at the initiation of cyclone i.e., on 20<sup>th</sup> Nov., at layer to layer there was no change of MFDSE due to no change of wind speed.

At cyclone period [Fig. 5.5.7(b)] it is seen that MFDSE was negative (southward) for all the days (except 24 Nov.) from 1000-700 mb. Beyond 700 mb it turned into positive (northward) for all the days (except 21<sup>st</sup> Nov.) and then increased gradually up to 200 mb. Beyond 200 mb MFDSE decreased for all the days.

After landfall [Fig. 5.5.7(c)] it is seen that from 1000-300 mb MFDSE was negative (southward) for all the days (except 26 Nov.) Beyond 300 mb it turned into positive (northward) for all the days and increased up to 200 mb. Beyond 200 mb MFDSE decreased. It is also observed that at the starting of landfall i.e., on 26 Nov. MFDSE was always positive (northward) and fluctuated due to change of meridional wind component. During landfall (26 Nov.) MFDSE was maximum at 250 mb due to higher wind speed at this level. From Fig. 5.5.7(a-c), it is observed that flux direction was opposite for before occurrence and after landfall at 100 mb. But at cyclone period flux direction was both northward and southward at 100 mb.

#### **Meridional flux of moist static energy (MFMSE):**

Fig. 5.5.8(a-c) shows the variation of meridional flux of moist static energy (MFMSE) at different isobaric levels. Here it is seen that the graph pattern was same as that of variation of meridional fluxes of dry static energy (MFDSE) which is discussed earlier in Fig. 5.5.7(a-c). Here only the difference was in magnitude. It is also observed that the pressure level was only up to 250 mb. This was because beyond 250 mb due point temperature is not found.

#### 4.2.6. Cyclone 6

In this section a cyclone is described from November 1, 1996 to November 12, 1996. Among these days, actual "cyclone period" was November 5-7, 1996. To observe its pre-condition, energy is calculated from 1 November to 4 November 1996, and this period is called "before occurrence". To observe the post-condition of the observed cyclone, energy is also calculated from 8 November 1996 to 12 November 1996. This period is called "after landfall". The track of this cyclone is shown in Fig. 3.

##### 4.2.6.(a): Energy components

###### Sensible Heat (SH):

Fig. 5.6.1(a-c) shows the variation of sensible heat (SH) at different isobaric levels. From these figures it is seen that sensible heat decreased linearly as height increased (i.e., pressure decreased). It is observed that for all the levels there was no day to day variation and the graph pattern was same as before occurrence and after landfall. It is seen that sensible heat was maximum at 1000 mb i.e., near to the earth surface. This was due to the maximum temperature at the earth surface.

###### Potential energy (PE):

Variation Potential energy at different isobaric levels is shown in Fig. 5.6.2(a-c). Here it is seen that potential energy increased linearly with increasing height (i.e., pressure decreased) for before occurrence, cyclone period and after landfall. It is also seen that all graph patterns were almost same. This was because potential energy is the product of acceleration due to gravity and geopotential height. At a certain level for all the days geopotential height was more or less same. For this reason for all the levels day to day variation was symmetric and the graph pattern was same. After landfall [Fig. 5.6.2(c)], at 500 mb on 12 November it is observed that there is an abrupt increase of potential energy. This increase was due to the sudden increase of geopotential height on that day compared to the other day.

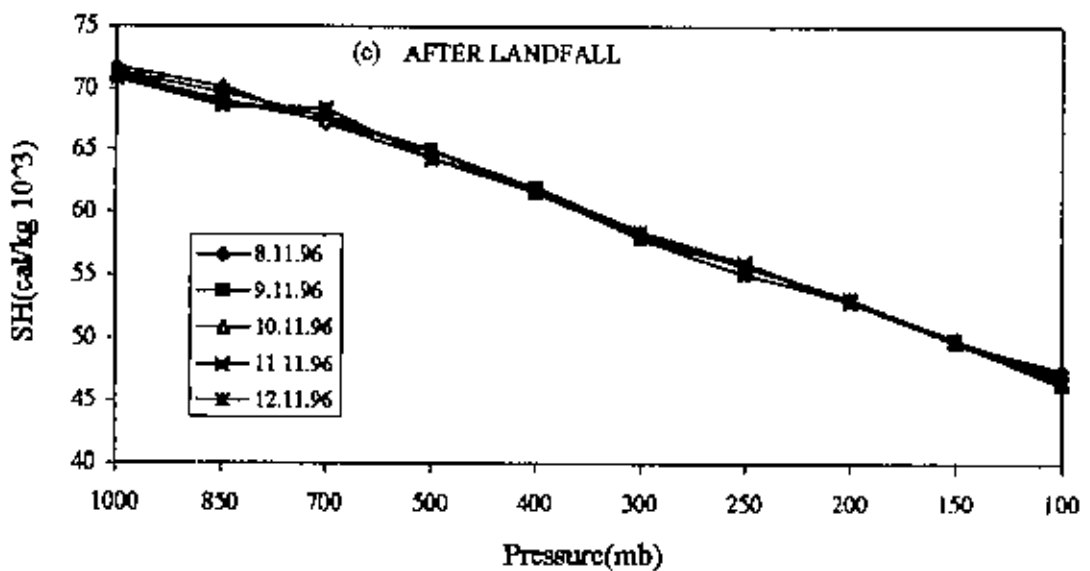
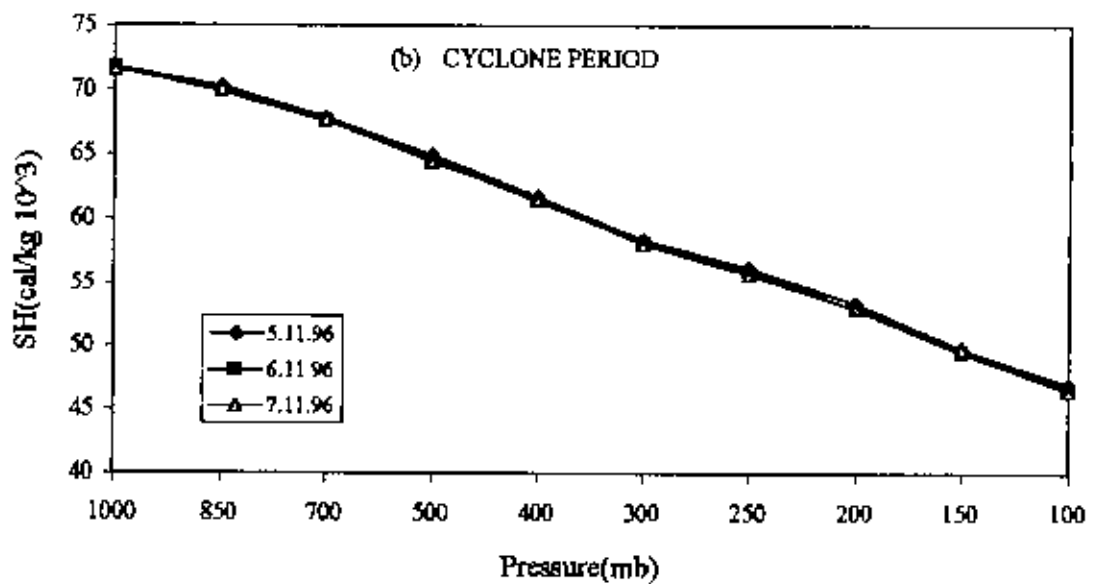
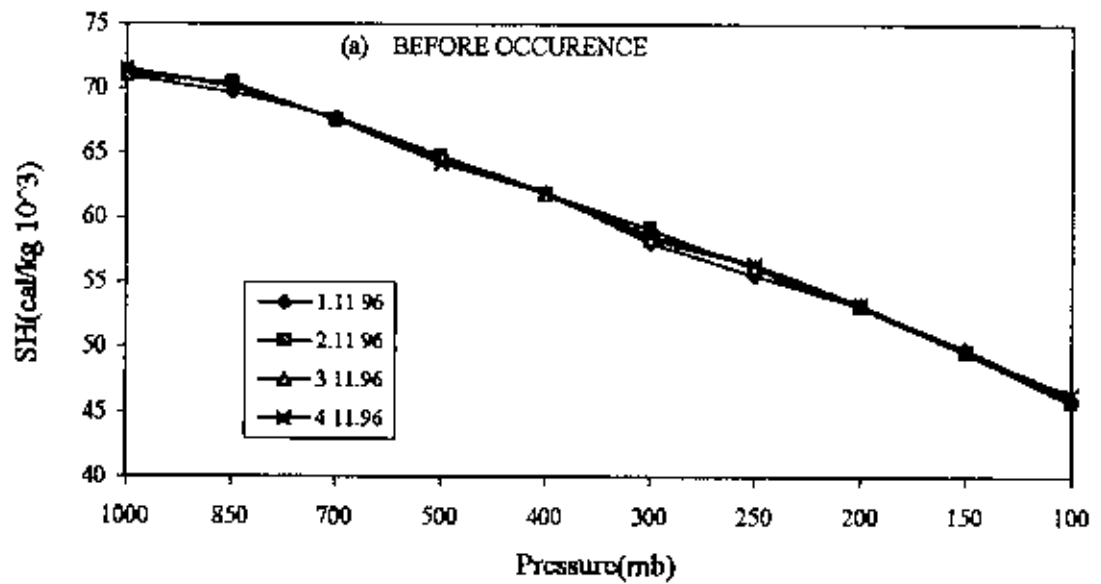


Fig. 5.6.1 (a-c) Sensible heat variation at different isobaric levels.





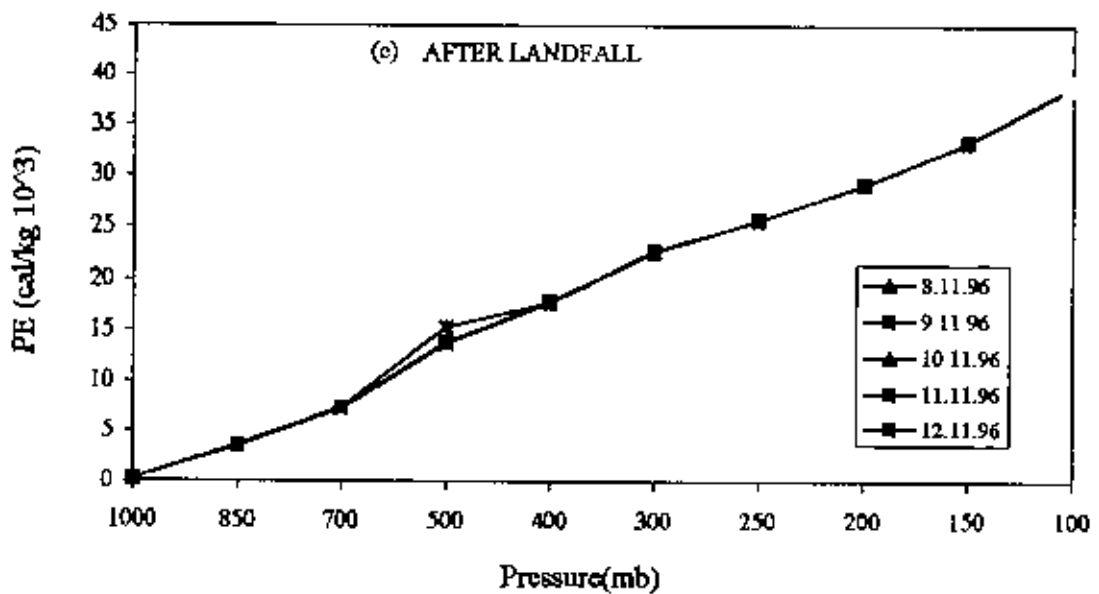
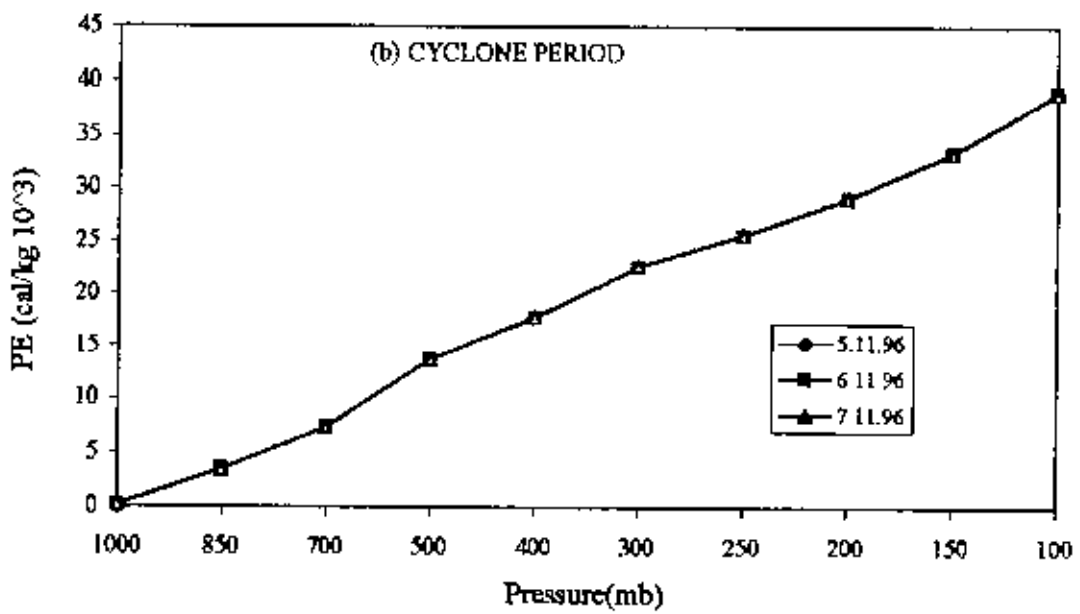
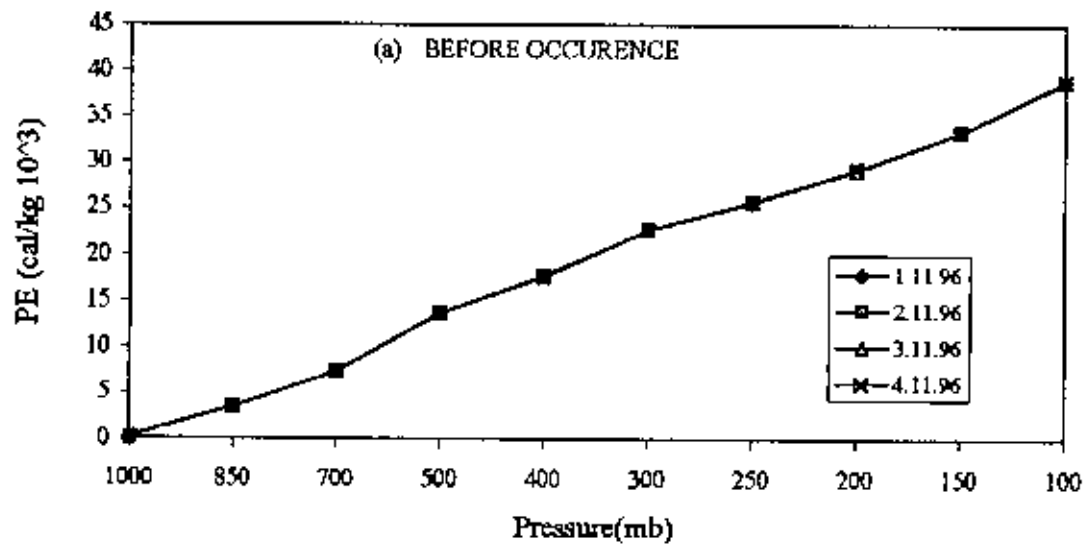


Fig. 5.6.2 (a-c) Potential energy variation at different isobarc levels.

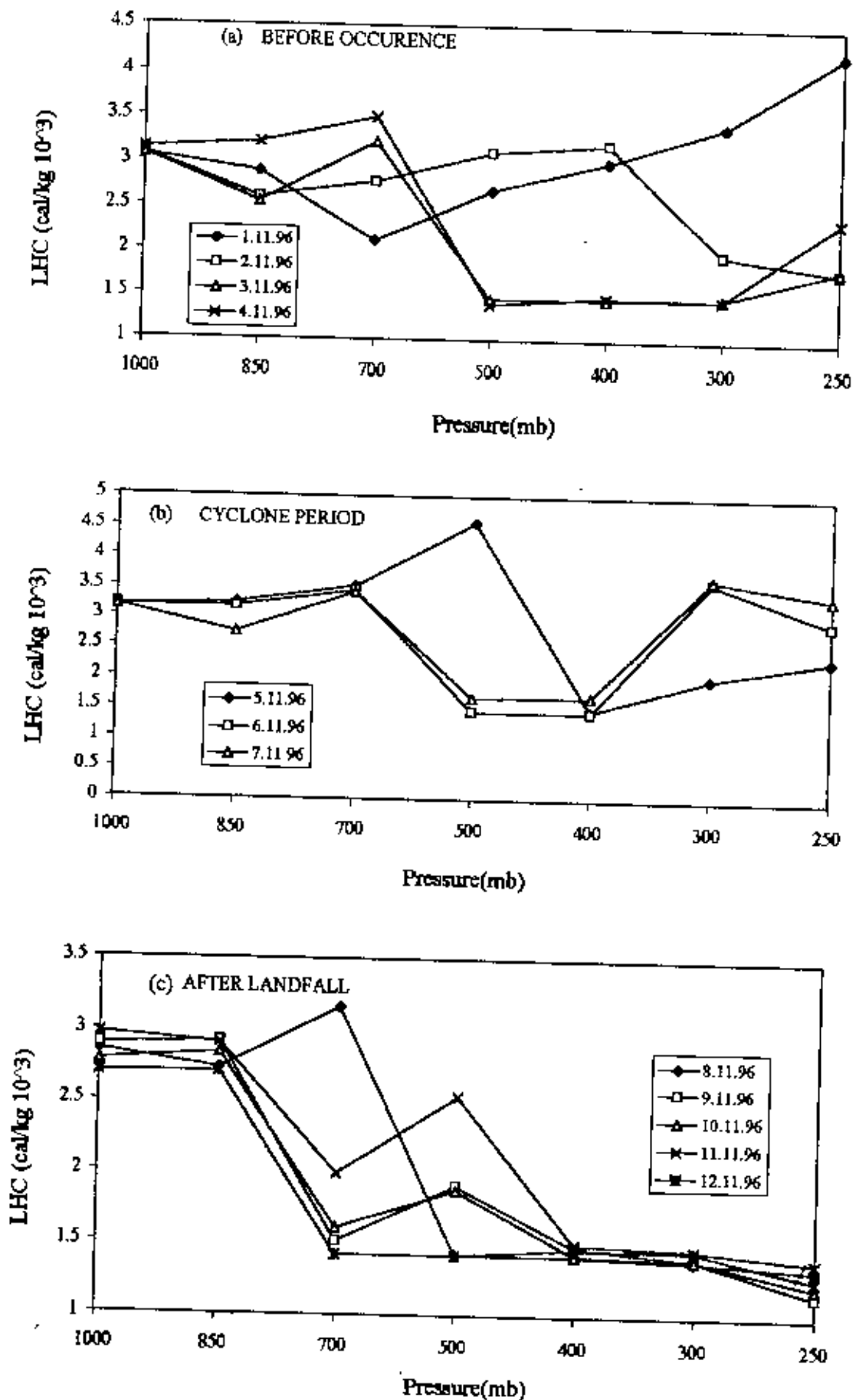


Fig. 5.6.3 (a-c). Latent heat content variation at different isobaric levels.



**Latent Heat Content (LHC):**

Fig. 5.6.3(a-c) shows the variation of latent heat content (LHC) at different isobaric levels. Before occurrence [Fig. 5.6.3(a)] it is seen that on first November from 1000 mb-700 mb, LHC decreased. Beyond 700 mb it increased linearly. On 2nd November, LHC decreased at 1000 mb-850 mb. Beyond 850 mb it increased linearly up to 400 mb and then decreased. On 3rd and 4th November, it increased up to 700 mb. After 700 mb it decreased abruptly at 500 mb and then remained constant up to 300 mb. After 300 mb it slightly increased at 250 mb.

At cyclone period [Fig. 5.6.3(b)] latent heat content (LHC) increased slightly from 1000 mb-700 mb for all the days. At the beginning of cyclone day (5.11.96) it increased from 1000 mb and attained maximum value at 500 mb. Beyond 500 mb it decreased abruptly at 400 mb and then increased slightly up to 250 mb. At 6.11.96-7.11.96 the graph pattern was same for all the levels. At these two days there was a very unstable condition. At first it increased up to 700 mb, then decreased at 500 mb and remained constant up to 400 mb. Beyond 400 mb it increased at 300 mb and then decreased at 250 mb.

After landfall [Fig. 5.6.3(c)] it is seen that at first latent heat content was unchanged at 1000 mb-850 mb for all the days. Then it decreased at 700 mb with the exception of 8.11.96. At that day (8.11.96) it increased at 700 mb and then decreased at 500 mb. It decreased for all the days at 400mb. Beyond 400 mb it remain unchanged up to 250 mb.

From the above figures [Figs. 5.6.3(a-c)] it is seen that at cyclone period, at the beginning of cyclone (5.11.96) it was maximum at 500 mb due to more latent heat released. At cyclone period it is also seen that at 6.11.96-7.11.96 there was a very unstable condition. At first it increased, then decreased then remain unchanged again increased, at last it decreased. Latent heat content increased when cloud is formed and decreased due to the incursion for more water vapor. After landfall it is also observed that for all the days there was no change of latent heat content beyond 400mb. This was due to the lack of cloud formation or there was no incursion of water vapor at these regions.

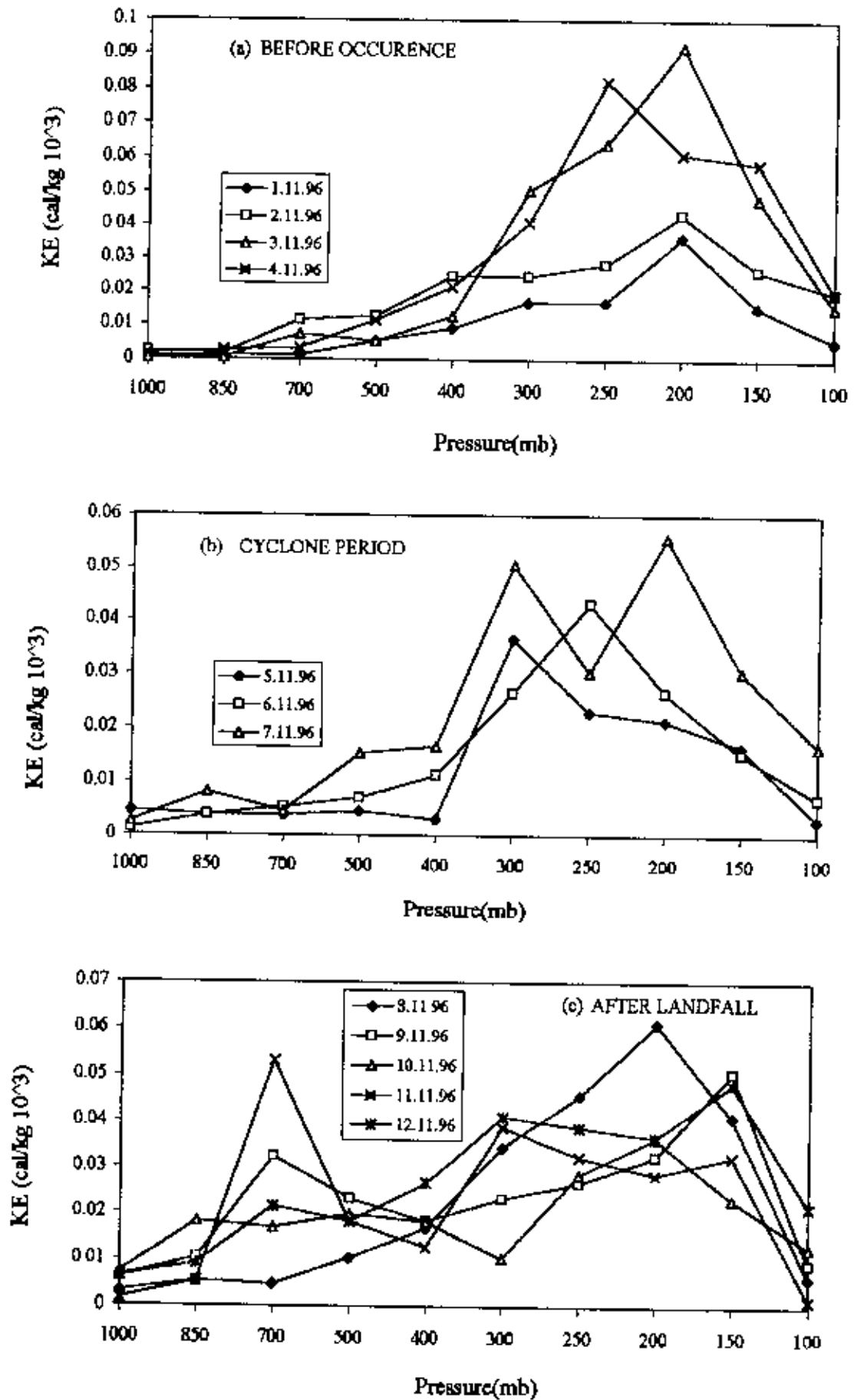


Fig. 5.6.4 (a-c). Kinetic energy variation at different isobaric levels.

### Kinetic Energy (KE):

Fig. 5.6.4(a-c) shows the variation of kinetic energy (KE) at different isobaric levels at before occurrence, cyclone period and after landfall. It is seen that before occurrence kinetic energy was near about zero for all the days at 1000 mb-850 mb. Beyond 850 mb KE increased up to 200 mb and then decreased.

At cyclone period, KE was near about same for all the days up to 400 mb. Beyond 400 mb, at the beginning of cyclone day (5.11.96) K.E. increased abruptly at 300 mb and then decreased. Beyond 400 mb, at the 2nd day of cyclone it increased up to 250 mb and then decreased. Beyond 400mb at the end of cyclone day (7.11.96) wind is changing at layer to layer. It increased abruptly at 300 mb, then decreased at 250 mb. It again increased at 200 mb and attained maximum value. Beyond 200 mb it decreased at higher levels.

After landfall [Fig. 5.6.4(c)] it is seen that at first, KE was nearly zero at 1000 mb and then increased up to 150 mb for all the days and then decreased at 100 mb. It is also observed that after landfall KE was maximum at 200 mb just after landfall (8.11.96) due to the maximum wind speed.

From the above figures [Figs. 5.6.4(a-c)] it is observed that KE was higher in the region 300 mb-150 mb than the other level. It is also seen that at cyclone period [Fig. 5.6.4(b)] there were two peaks i.e., maximum KE at 300 mb and 200 mb due to the maximum wind at the end of cyclone day (7.11.96) compared to the other day.

### 4.2.6.(b): Energy Fluxes

#### Zonal Flux of Dry Static Energy (ZFDSE):

Zonal flux of dry static energy (ZFDSE) at different isobaric levels is shown in Fig. 5.6.5(a-c). Before occurrence [Fig. 5.6.4(a)] it is seen that for all the days (except 2nd November), at first ZFDSE was negative (westward) up to 700 mb. But at 2nd November it was negative (westward) only at 850 mb. Beyond 700 mb for all the days ZFDSE was positive (eastward) and then increased with the same sign up to 200 mb due to the increase of zonal wind component. For all the days except 4 11.96, beyond 200 mb it decreased at 100 mb.

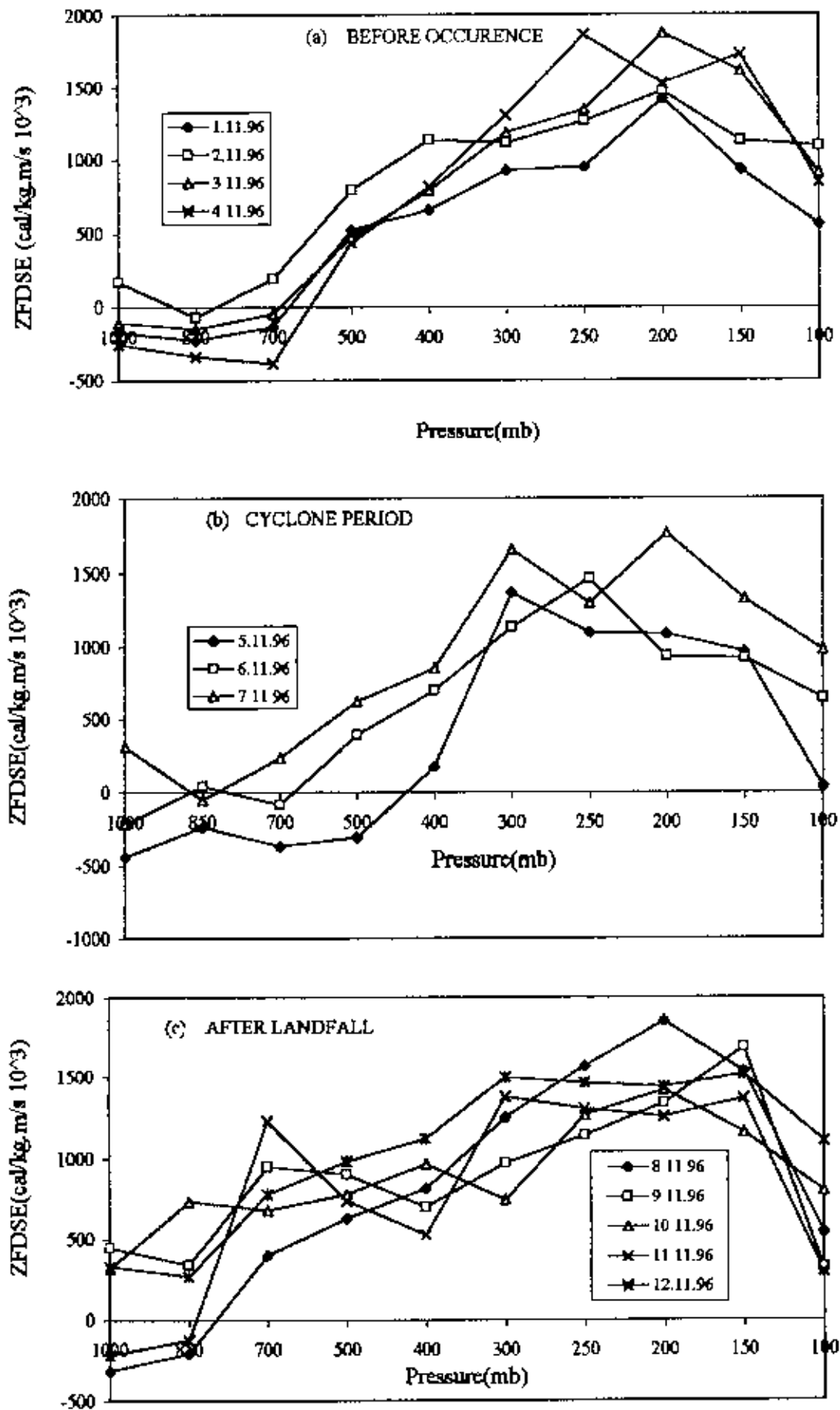


Fig. 5.6.5 (a-c). Variation of zonal fluxes of dry static energy at different isobaric levels.

At cyclone period [Fig. 5.6.4(b)] it is observed that for first day of cyclone (5.11.96) ZFDSE was negative (westward) at 1000 mb and maintained the same sign up to 500 mb. For 2nd day of cyclone (6.11.96) it attained near about zero at 850 mb and then negative (westward) at 700 mb. At the end of cyclone day (7.11.96), ZFDSE was positive (eastward) for 1000 mb and then decreased at 850 mb and attained the negative value (westward). Beyond 500 mb for the first day of cyclone (5.11.96) it increased up to 300 mb and then decreased at 250 mb. After 250 mb it remain unchanged up to 150 mb due to no change of zonal wind component. Beyond 150 mb it decreased and attained zero at 100 mb. Beyond 700 mb, for the 2nd day of cyclone (6.11.96) it increased linearly up to 250 mb and then decreased. At the end of cyclone day (7.11.96), beyond 850 mb it increased linearly up to 300 mb and then decreased at 250 mb due to the decrease of zonal wind component. After 250 mb it again increased and attained the maximum value at 200 mb and then decreased.

Fig. 5.6.5(c) shows the zonal flux of dry static energy (ZFDSE) at different isobaric levels for after landfall. Here it is observed that at 1000 mb-850 mb on 8.11.96 and 11.11.96 ZFDSE was negative (westward). Beyond 850 mb for all the days, it increased up to 150 mb and then decreased.

From the above figures [Figs. 5.6.5(a-c)] it is seen that at 1000 mb, before occurrence and cyclone period, ZFDSE was negative (westward) except at 2.11.96 (for before occurrence) and at 7.11.96 (at cyclone period). But after landfall, at 1000 mb it was positive (eastward) for most of the days. At cyclone period it is seen that ZFDSE was maximum at 300 mb and 200 mb at the end of cyclone (7.11.96) due to the maximum wind speed. It is also observed that for all the phases [before occurrence, cyclone period and after landfall] beyond 150 mb ZFDSE decreased for all the days.

#### Zonal Flux of Moist Static Energy (ZFMSE):

Zonal flux of moist static energy (ZFMSE) at different isobaric levels is shown in figure 5.6.6(a-c). Before occurrence [Fig. 5.6.6(a)] for all the days with the exception of 2nd November, ZFMSE was negative (westward) at 1000 mb and remain unchanged up to 700 mb with the same sign. Beyond 700 mb it increased linearly up to 250 mb.



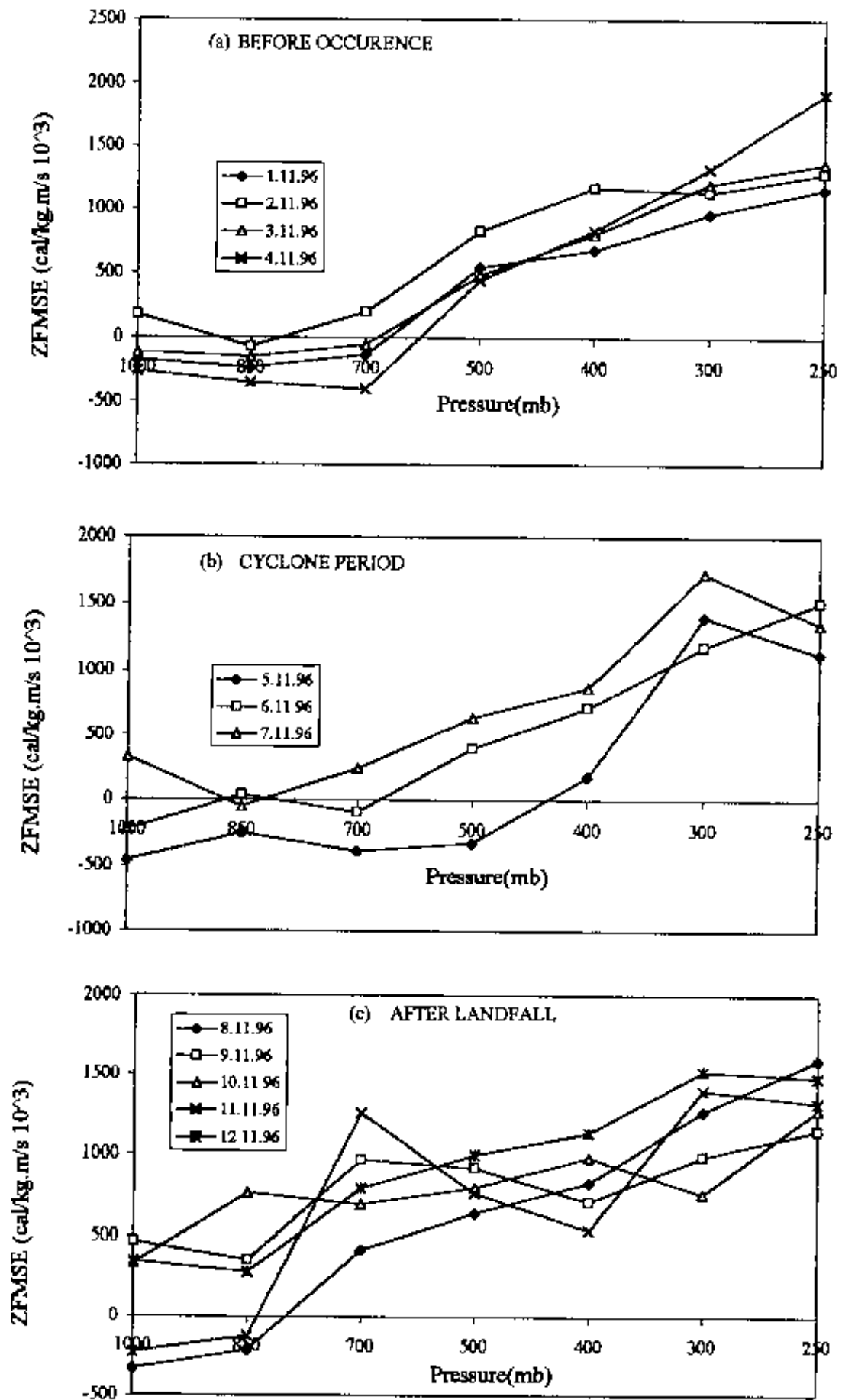


Fig. 5.6.6 (a-c). Variation of zonal fluxes of moist static energy at different isobare levels.



At cyclone period [Fig. 5.6.6(b)] it is seen that at the beginning of cyclone (5.11.95), ZFMSE was negative (westward) at 1000 mb-500 mb. Beyond 500 mb it turned into positive (eastward) and increased up to 300 mb and then decreased a little at 250 mb. At the 2nd day of cyclone (6.11.96), at 1000 mb and 700 mb it was negative (westward) and at 850 mb it was positive (eastward) and near about zero. Beyond 700 mb it turned into positive and increased linearly as pressure decreased. At the end of cyclone day (7.11.96), at 1000 mb it was positive (eastward), then turned into negative (westward) at 850 mb. Beyond 850 mb it again turned to positive and increased linearly up to 300 mb, then decreased a little at 250 mb.

After landfall [Fig. 5.6.6(c)] it is seen that at 1000 mb, ZFMSE was negative (westward) at 1000 mb-850 mb on 8.11.96 and 11.11.96. Beyond 850 mb for all the days (except 11.11.96) it increased linearly up to 250 mb. At 11.11.96 it was fluctuated due to change of wind velocity.

#### **Meridional Flux of Dry Static Energy (MFDSE):**

Fig. 5.6.7(a-c) shows the variation of meridional flux of dry static energy (MFDSE) at different isobaric levels. Before occurrence [Fig. 5.6.7(a)] it is seen that MFDSE was negative (westward) at 1000 mb-700 mb. Beyond 700 mb it turned into positive (eastward) and increased more or less linearly. Beyond 150 mb it decreased.

At cyclone period [Fig. 5.6.7(b)], MFDSE was negative (southward) at 1000 mb-500 mb at the beginning of cyclone day (5.11.96). Beyond 500 mb it turned into positive (northward) and increased up to 300 mb and then decreased. On 6.11.96 MFDSE was negative (southward) at 1000 mb, then turned into positive and attained zero at 850mb. At 700 mb it again turned into negative (southward) and then turned into positive (northward) and increased linearly up to 250 mb, then decreased. At the end of cyclone day (7.11.96) it was positive (northward) at 1000 mb and then turned into negative (southward) at 850 mb. Beyond 850 mb it again became positive (northward) and increased with the same sign up to 300 mb, then fluctuated due to change of meridional wind component.

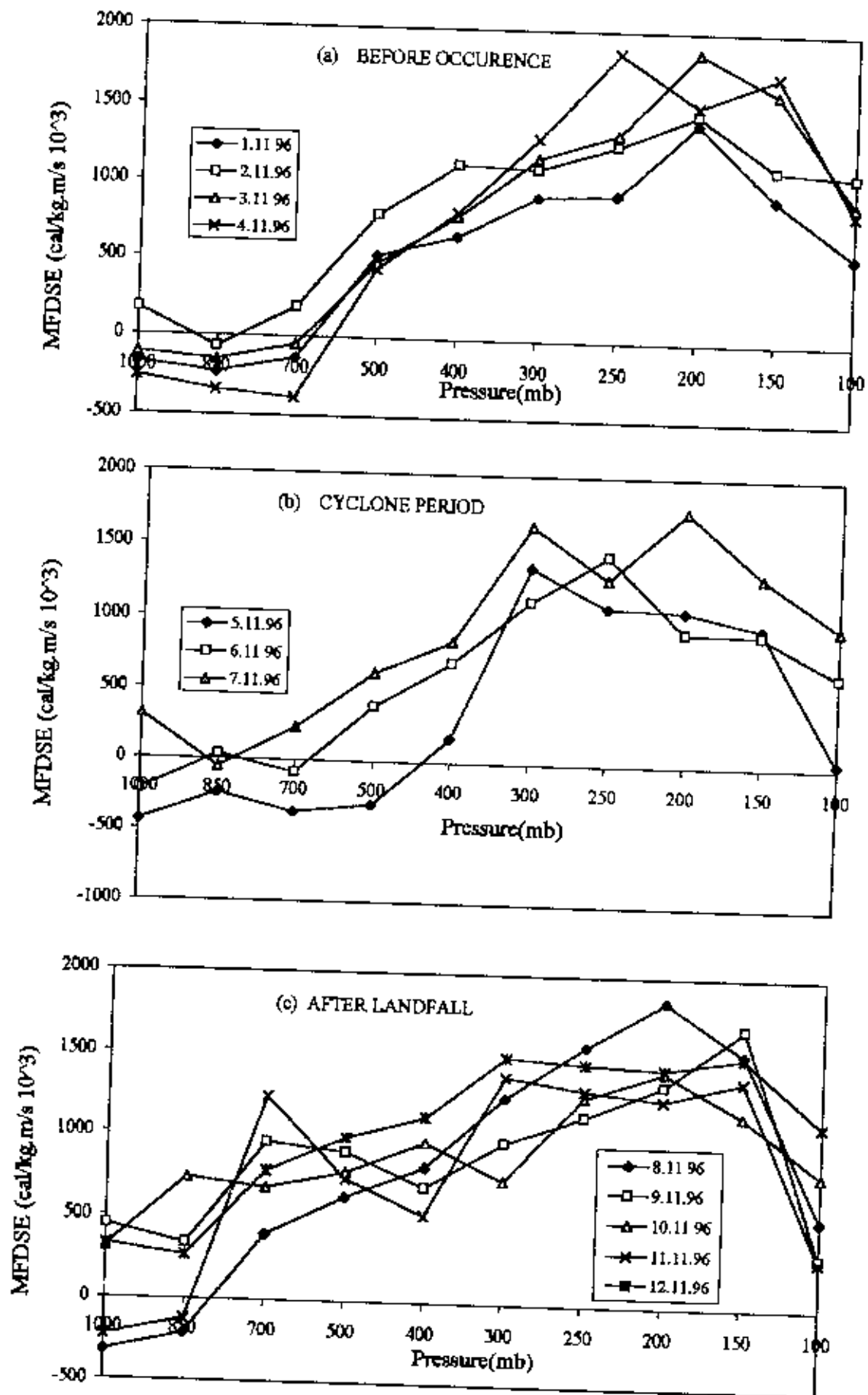


Fig. 5.6.7 (a-c). Variation of meridional fluxes of dry static energy at different isobaric levels.

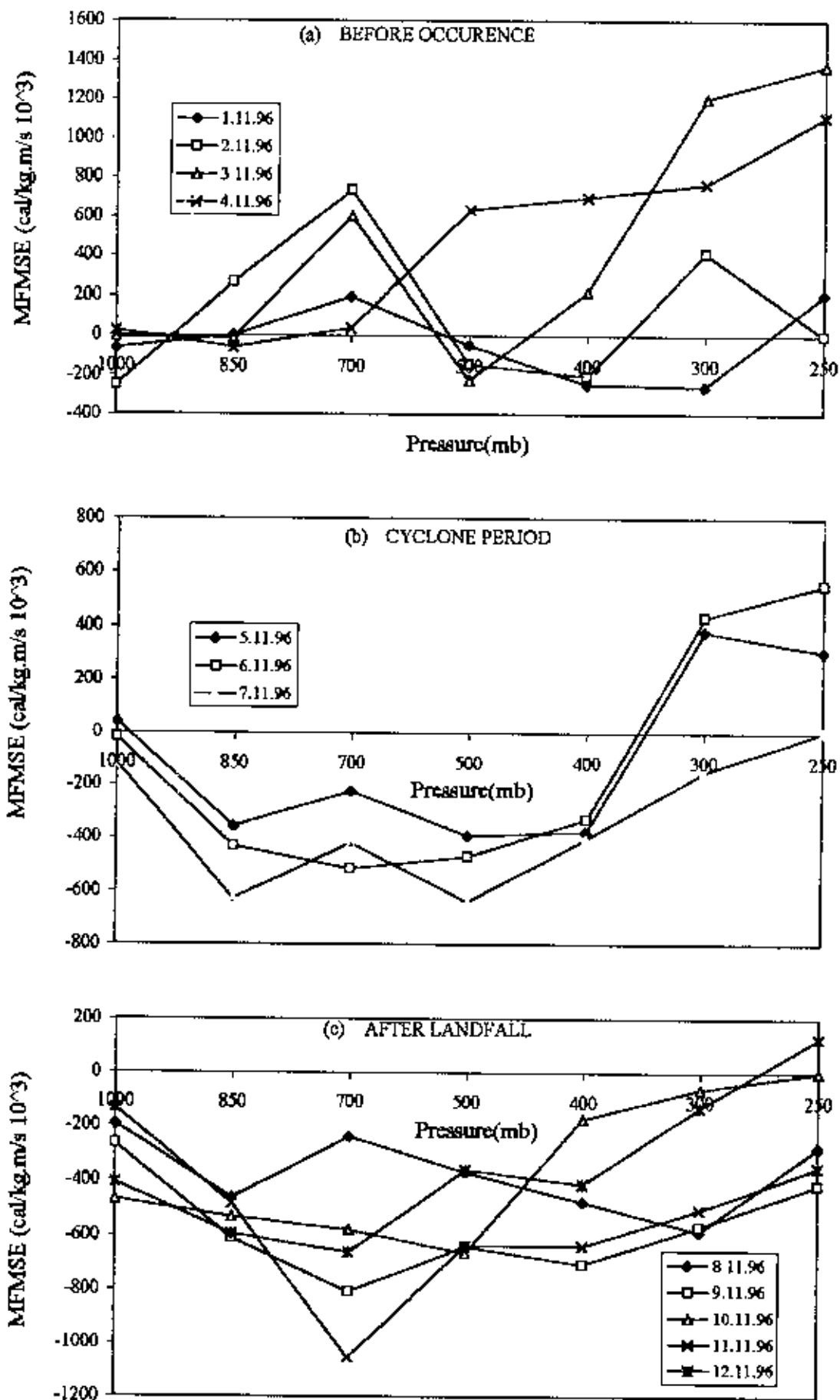


Fig. 5.6.8 (a-c). Variation of Meridional fluxes of moist static energy at different isobaric levels

After landfall [Fig. 5.6.7(c)] it is seen that MFDSE was negative (southward) at 1000 mb-850 mb on 8.11.96 and 11.11.96. Beyond 850 mb it turned into positive (northward) and increased for all the days up to 150 mb and then decreased. It is also seen that at 11.11.96 it was fluctuated due to change of meridional wind component.

#### **Meridional Flux of Moist Static Energy (MFMSE):**

Meridional flux of moist static energy (MFMSE) at different isobaric levels is shown in Fig. 5.6.8(a-c). Before occurrence [Fig. 5.6.8(a)] it is seen that on 1.11.96 at 1000 mb-850 mb, MFMSE was zero, then it slightly increased at 700 mb. Beyond 700 mb it turned to negative (southward) and increased with the same sign up to 300mb. Then turned into positive at 250 mb. On 2nd November it was fluctuated both in positive (northward) and negative (southward) direction due to change of meridional wind component and at last it tends to zero at 250 mb. On 3.11.96 it is seen that MFMSE was zero at 1000 mb-850 mb, then increased abruptly at 700 mb and turned into negative (southward) at 500 mb. Beyond 500 mb it again turned into positive (northward) and increased with the same sign, attained the maximum value at 250 mb. On 4.11.96 MFMSE was zero at 1000 mb-700 mb and then increased linearly up to 250 mb.

At cyclone period [Fig. 5.6.8(b)] MFMSE was zero and negative (southward) for all the days at 1000 mb. Beyond 1000 mb it increased in the negative direction at 850 mb, then remain near about unchanged with the same sign in the region 850mb-400mb. Beyond 400 mb it turned into positive (northward) and increased. But at the end of cyclone (7.11.96) it tends to zero at 250 mb.

After landfall [Fig. 5.6.8(c)] it is seen that for all the days MFMSE was negative at 1000 mb and then increased in the negative (southward) direction up to 700 mb. Beyond 700 mb it remain unchanged up to 400 mb and then decreased with the same sign up to 250 mb except 11.11.96. On 11.11.96 it turned into positive (northward) at 250 mb.

From the above discussion it is observed that before occurrence meridional fluxes of moist static energy was positive (northward) for all the days (except some region) and it was completely negative (southward) for after landfall. But at cyclone period [Fig.

5.6.8(b)] MFMSE was negative up to 400 mb for all the days and then turned into positive direction.

#### 4.2.7. Cyclone 7

A cyclone formed in the Bay of Bengal from 28 Nov. 1996 to 3 Dec. 1996 is explained in this section. This period is called "cyclone period". To observe its pre-condition, energy is calculated from 23 Nov. 1996 to 27 Nov. 1996, and this period is called "before occurrence". To observe the post condition of the observed cyclone, energy is also calculated from 4 Dec. 1996 to 8 Dec. 1996. This period is called "after landfall". The movement of this cyclone is shown in Fig. 3.

##### 4.2.7.(a): Energy components

###### Sensible Heat (SH):

Fig. 5.7.1(a-c) shows the variation of sensible heat (SH) at different isobaric levels for three phases of the analyzed cyclone. From these figures it is seen that sensible heat decreased as pressure decreased. It is also observed that SH was maximum at 1000 mb (near to the surface) due to maximum temperature at the earth surface compared to the other level.

###### Potential Energy (PE):

The variation of Potential energy (PE) at different isobaric levels at different phases of cyclone occurring 28.11.96-03.12.96 is shown in Fig. 5.7.2(a-c). From these figures it is seen that PE increased linearly as height increased (i.e. pressure decreased). There is a linear relationship between potential energy and geopotential height (Z). It is seen that the amount of PE at all phases was same and there was no day to day variation in each phase. It is also observed that for all the phases (before occurrence, cyclone period and after landfall) it was maximum at the upper level of the troposphere. There is no effect of PE on the cyclone.

###### Latent Heat Content (LHC):

Fig. 5.7.3(a-c) shows the latent heat content (LHC) variation of cyclone at different phases (Before occurrence, cyclone period and after landfall) of a cyclone. Before occurrence [Fig. 5.7.3(a)], at 1000 mb LHC was same for all the days, then it decreased

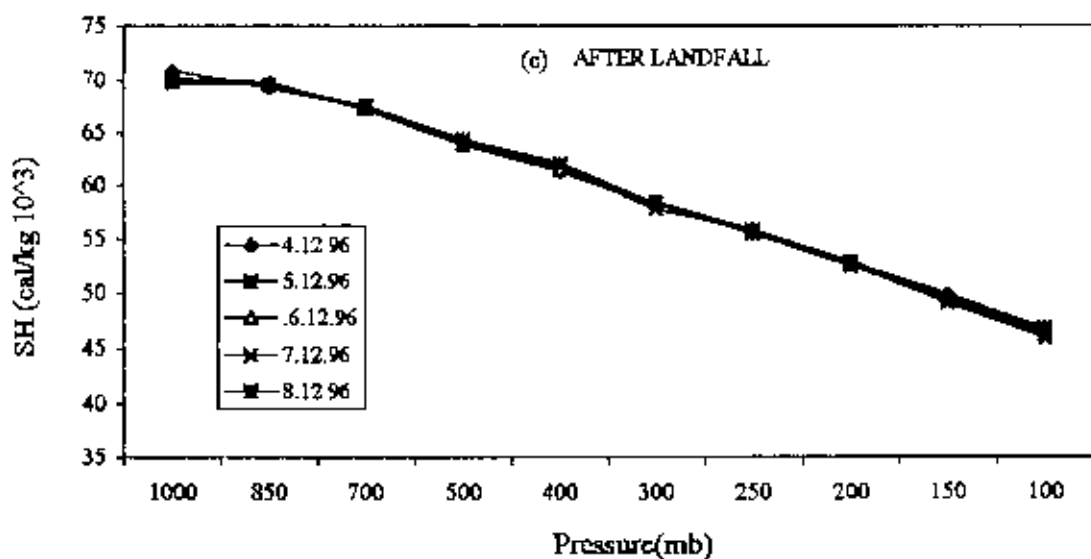
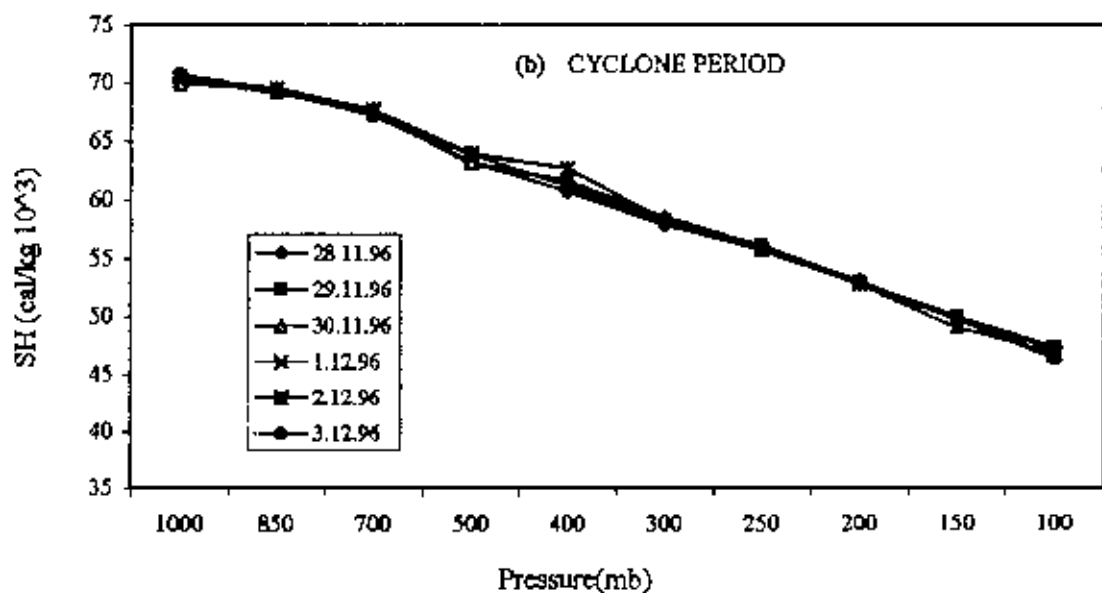
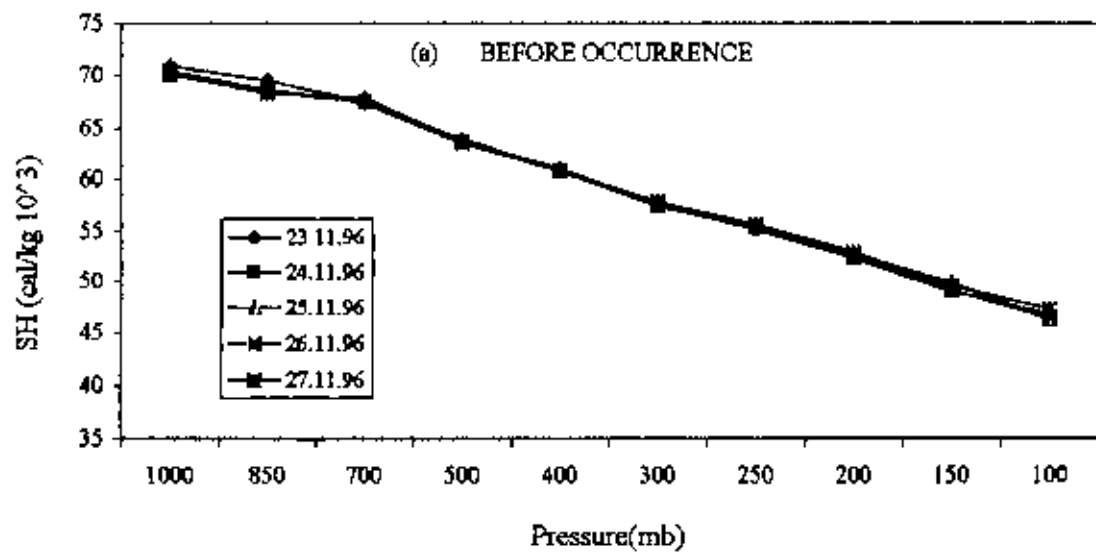


Fig. 5.7.1 (a-c). Sensible heat variatin at different isobaric levels.

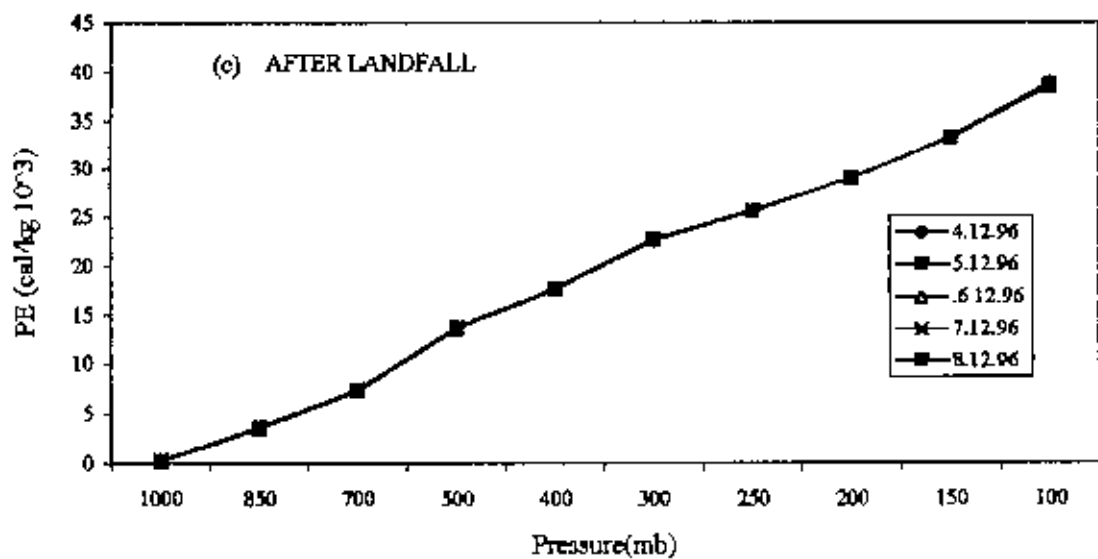
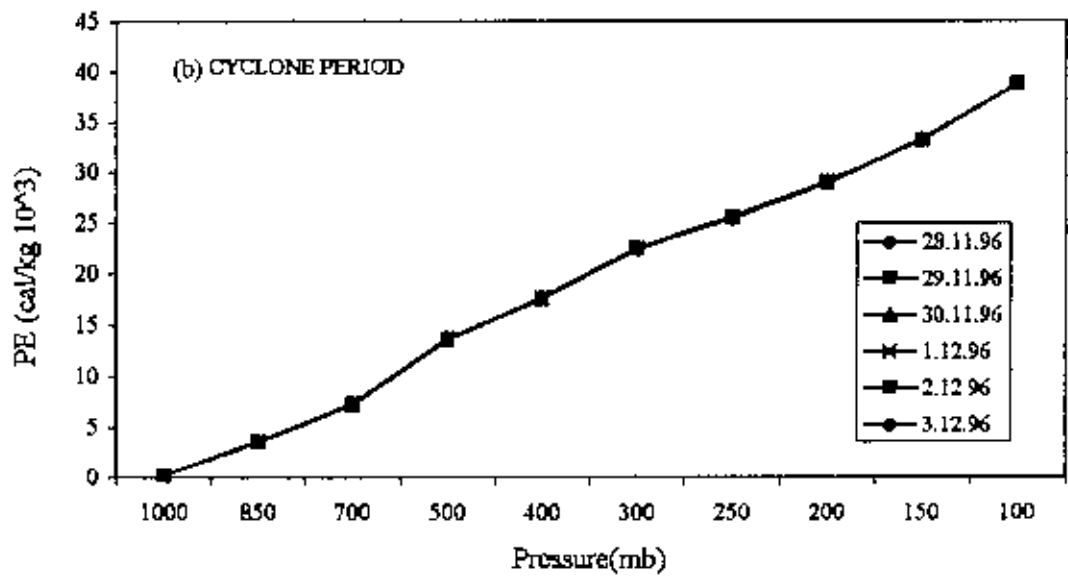
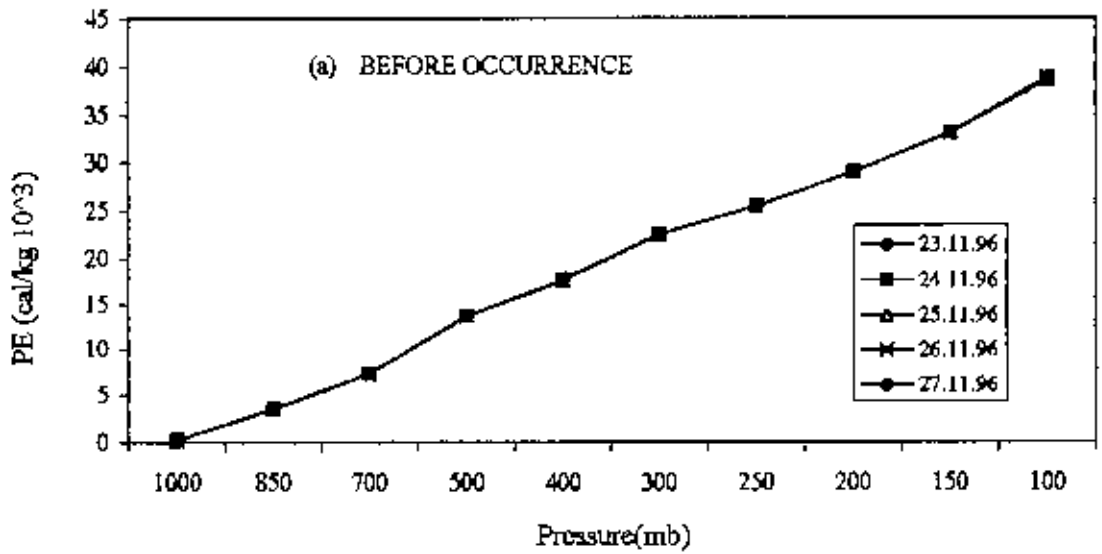


Fig. 5.7.2 (a-c). Potential energy variation at different isobaric levels.



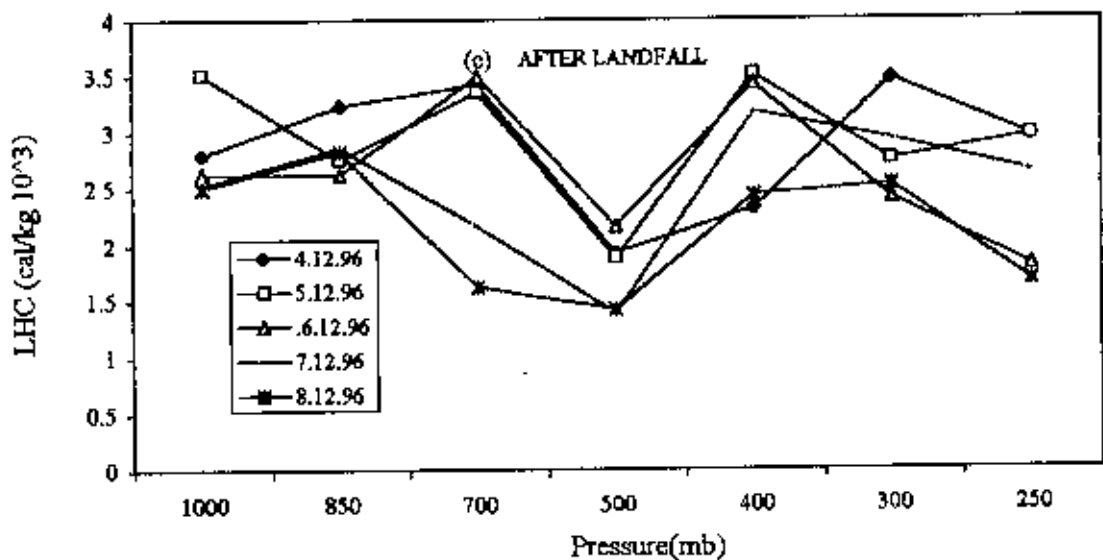
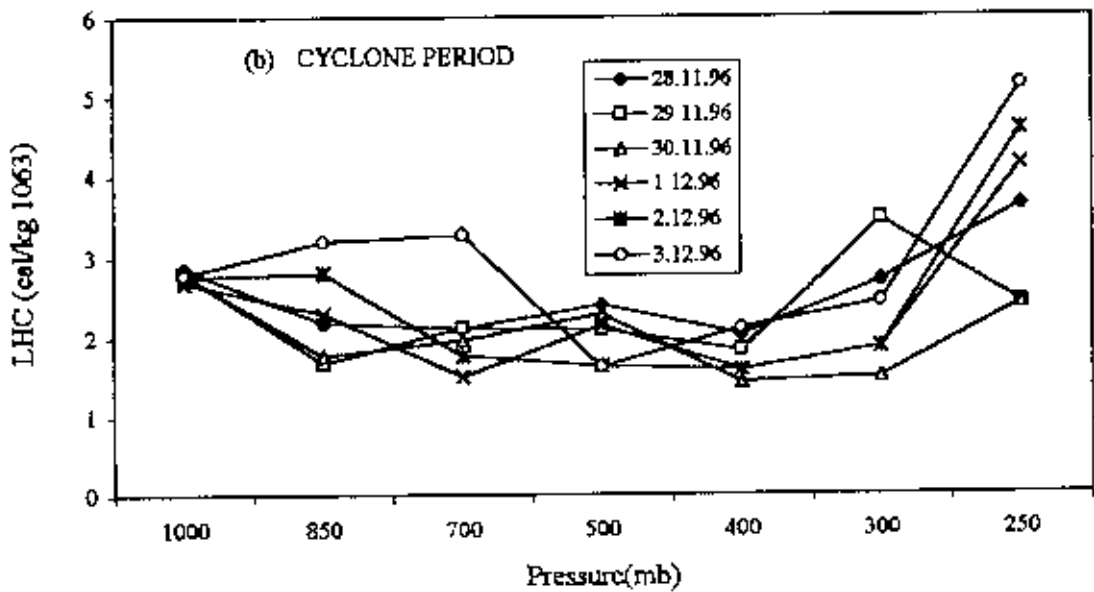
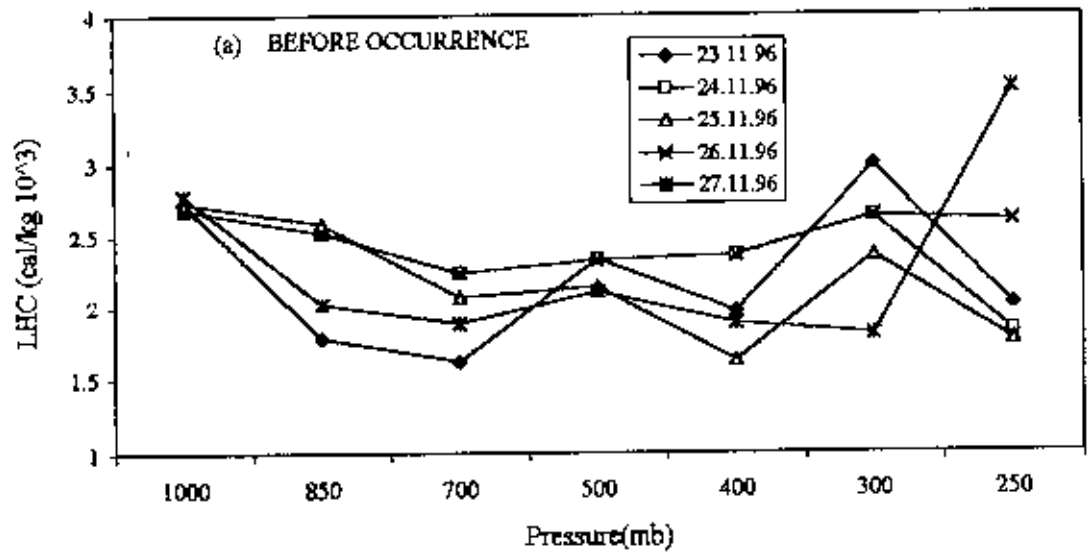


Fig 5.7.3 (a-c). Latent heat content variation at different isobaric levels.

up to 700 mb. Beyond 700 mb at 23.11.96 and 25.11.96 it increased with a fluctuation and finally decreased at 250mb. For 24.11.96 and 26.11.96 after 700 mb it increased gradually up to 250 mb. Beyond 700 mb for just before cyclone (27.11.96) it was approximately constant up to 300 mb, then there was sudden increase at 250 mb and attained maximum value.

At cyclone period [Fig. 5.7.3(b)] LHC was same for all the days at 1000 mb then slightly decreased (without 3.12.96) at 850 mb. In the region 850 mb-400 mb LHC was almost constant. Beyond 400 mb it increased for all the days except 3rd day of cyclone. On 29.11.96 it decreased at 250 mb. At the end of cyclone (3.12.96) LHC increased gradually up to 700 mb and then decreased at 500 mb. Beyond 500 mb it again increased linearly and attained the highest value at 250 mb (middle of the troposphere).

After landfall [Fig. 5.7.3(c)] it is seen that LHC was increased and decreased nature with a fluctuation. At 500 mb we observed that it decreased for all the days. This was due to the no cloud formation. Latent heat content is the indication of the cloud formation.

From the above figures [Fig. 5.7.3(a-c)] it is observed that just before cyclone (27.11.96) LHC was maximum at 250 mb because then more cloud is formed at that level. At the end of cyclone (3.12.96) it is also seen that LIHC gradually increased (without 500mb) and attained maximum value at the middle of the troposphere (250 mb). This is the cloud trimming zone and released latent heat at the level.

#### Kinetic Energy (KE):

Fig. 5.7.4(a-c) shows the variation of kinetic energy (KE) at different isobaric levels. From Fig. 5.7.4(a) it is seen that for all the days KE was almost zero from 1000 mb-850 mb and then increased linearly up to 200 mb. Beyond 200 mb it decreased and attained minimum value at 100 mb.

At cyclone period [Fig. 5.7.4(b)] KE was almost zero at 1000 mb-850 mb for all the days and then increased up to 200 mb. It decreased for all the days beyond 200 mb. It is also seen that at the middle of the troposphere (400 mb-150 mb) KE was large compared to the other level.

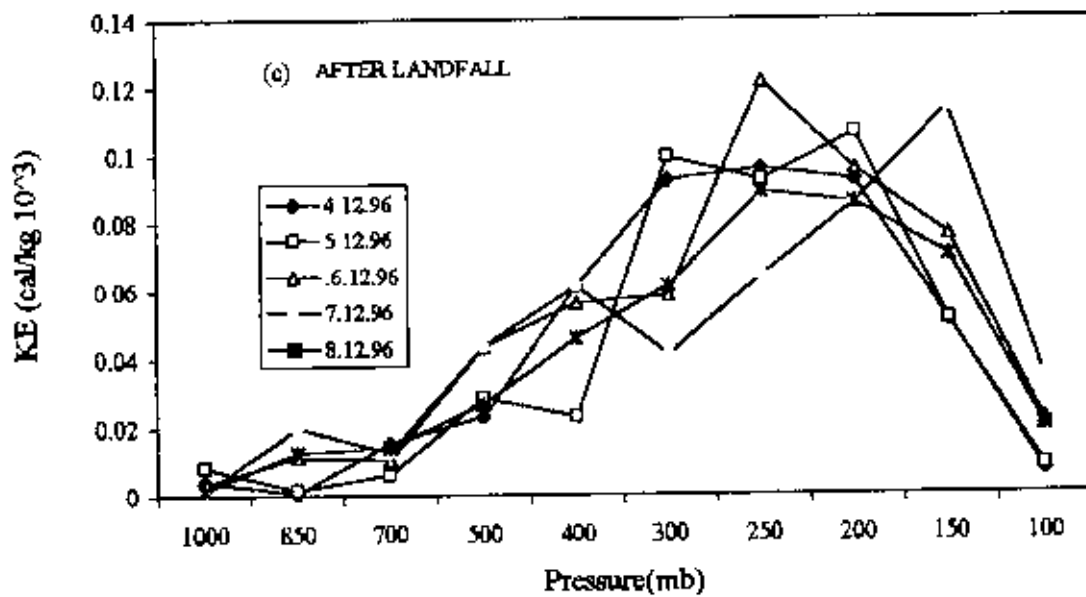
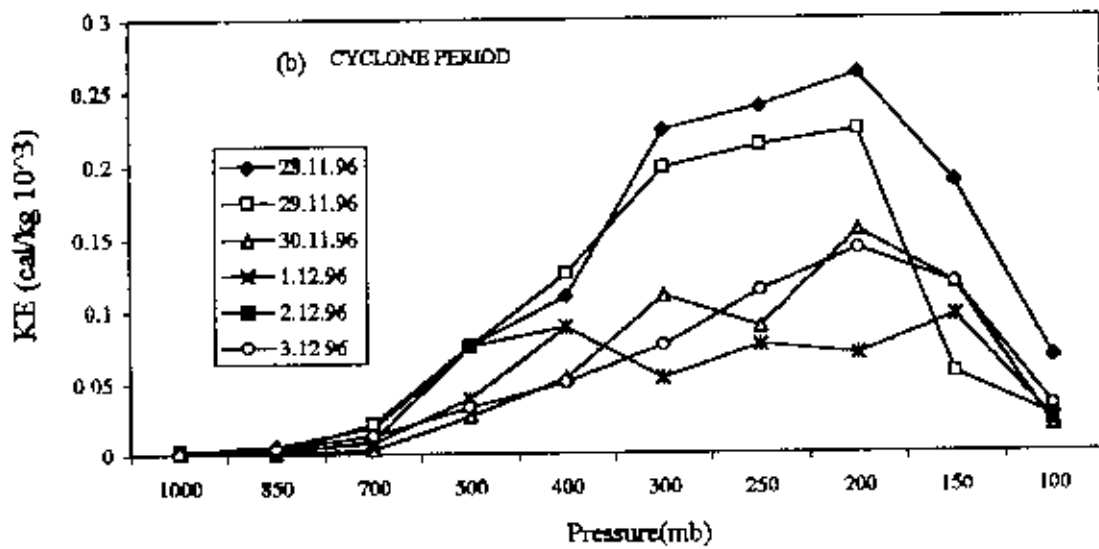
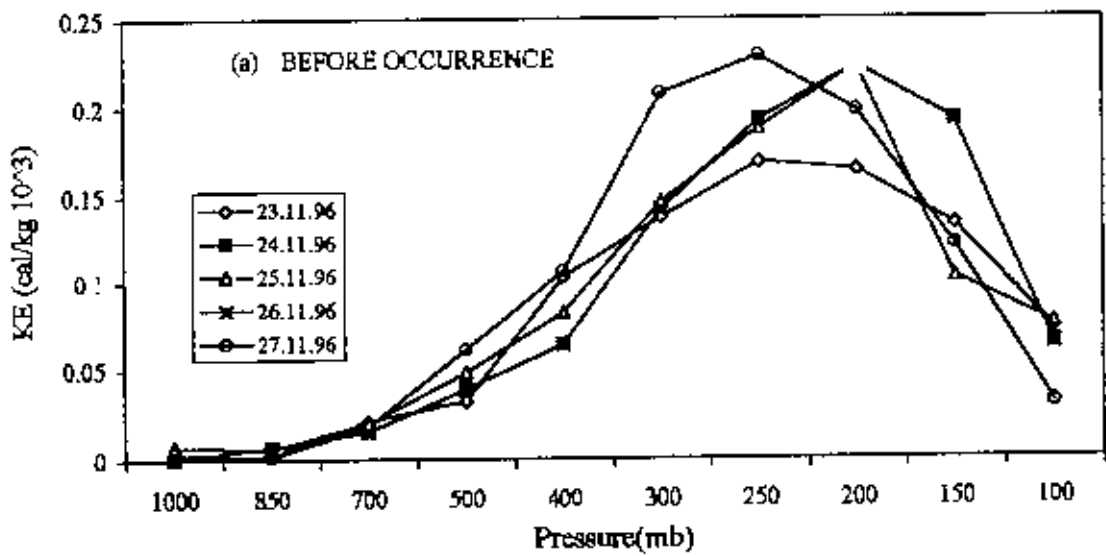


Fig 5.7.4 (a-c) Kinetic energy variation at different isobaric levels.

After landfall [Fig. 5.7.4(c)] it is seen that KE increased with a fluctuation from 1000 mb up to 200 mb for all days (without 7.12.96) and then decreased. But for 7.12.96 it increased up to 150 mb and then decreased.

From the above figures [Figs. 5.7.4(a-c)] it is seen that KE. was large in the region 400 mb-150 mb for all the phases compared to the other level. Kinetic energy increased linearly at 1000 mb-200 mb for before occurrence and cyclone period. It is also seen that at cyclone period KE was maximum at 200 mb because of higher wind speed at the beginning of cyclone (28.11.96). It is also observed that for all the phases (before occurrence, cyclone period, and after landfall) there was a common feature that beyond 200 mb KE decreased (except 7.12.96).

#### 4.2.7.(b): Energy fluxes

##### Zonal Flux of Dry Static Energy (ZFDSE):

Fig. 7.5 (a-c) shows the variation of zonal fluxes of dry static energy (ZFDSE) at different isobaric levels at different phases (before occurrence, cyclone period and after landfall) of a cyclone occurred on 28.11.96-3.12.96. For all the phases [Fig. 5.7.5(a-c)] graph pattern was nearly same (with some exception) i.e., from 1000 mb-200 mb it increased as pressure decreased i.e., height increased. Beyond 200 mb for all the phases it decreased due to decrease of zonal wind component at the upper level of the troposphere. Before occurrence and after landfall, at 1000 mb ZEDSE was positive (eastward) for all the days. But at cyclone period it was positive and negative at 1000 mb. It is seen that on 30.11.96-2.12.96 it fluctuated and maintained with a zig-zug path. This revealed that at the midtime of cyclone (30.11.96-2.12.96) the weather was very unstable i.e., layer to layer wind velocity was changing. It is also observed that at 200 mb ZFDSE was maximum at the starting of the cyclone (28.11.96) compared to the other day. This means that at that day zonal wind component was highest at 200 mb.

##### Zonal Flux of Moist static energy (ZFMSE):

Zonal flux of moist static energy (ZFMSE) at different isobaric levels at different phases i.e. before occurrence, cyclone period and after landfall is shown in Figs. 5.7.6(a-c).

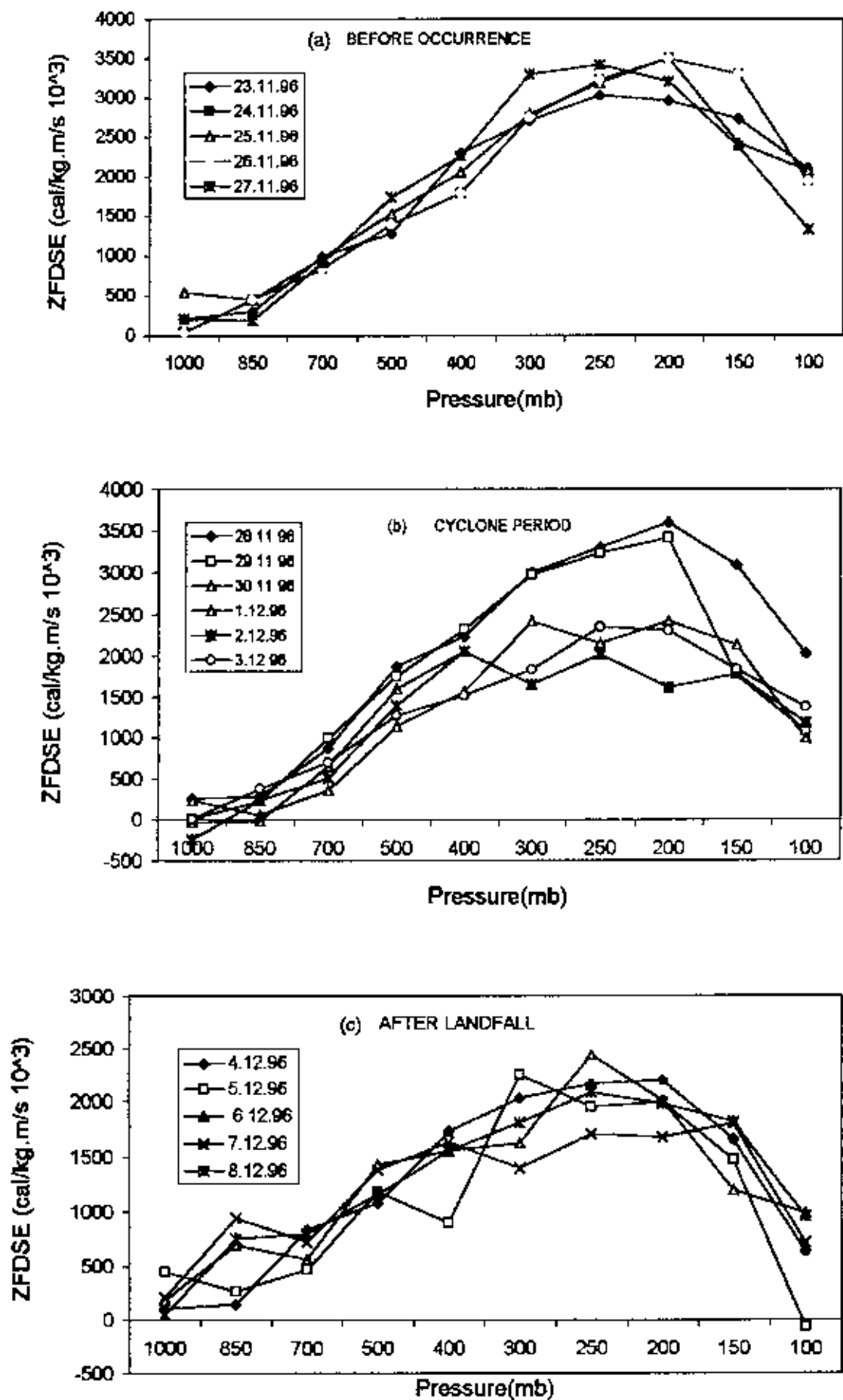


Fig. 5.7.5 (a-c). Variation of zonal fluxes of dry static energy at different isobaric levels.

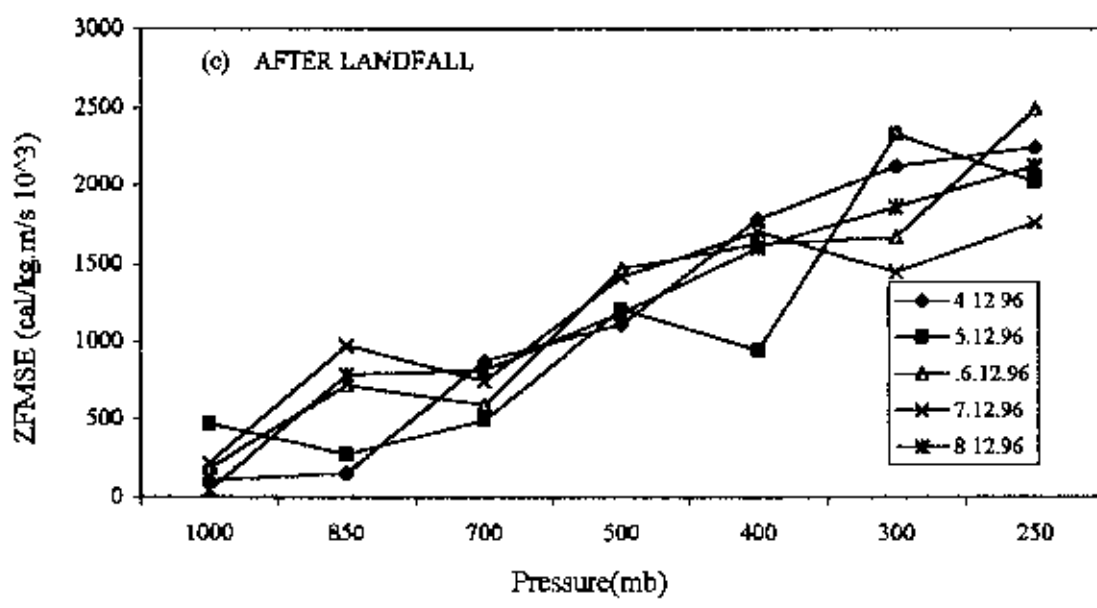
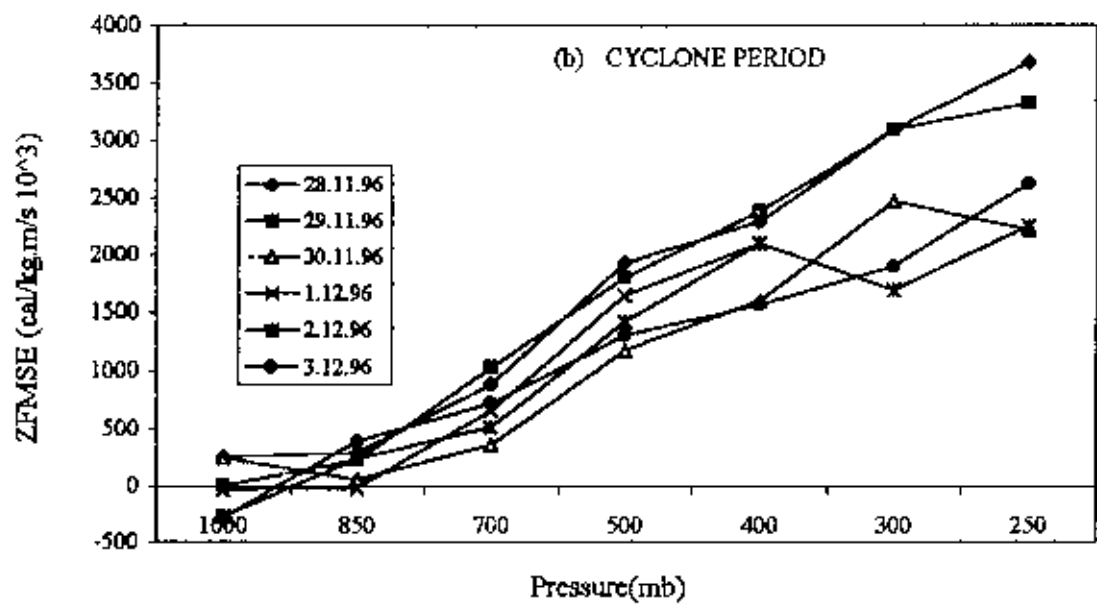
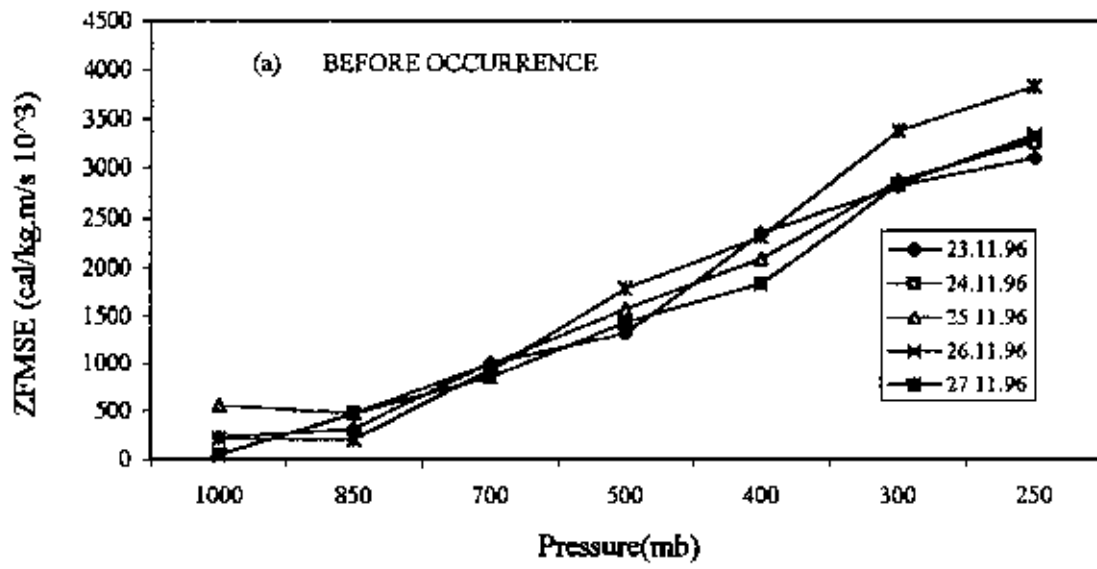


Fig. 5.7.6 (a-c). Variation of zonal fluxes of moist static energy at different isobaric levels.

For all the phases [Fig. 5.7.6(a-c)] it is seen that ZFMSE increased linearly from 1000 mb-250 mb. But after landfall [Fig. 5.7.6(c)] it is also seen that on 5.12.96-7.12.96 it increased with a fluctuation and maintained a zig-zug path. This was due to the change of zonal wind component at layer to layer.

Before occurrence and at cyclone period [Fig. 5.7.6(a-b)] the graph pattern was symmetric. The only difference was that before occurrence day to day variation at every layer was nearly same or close to each other. But at cyclone period day to day variation at every layer was large. Before occurrence and after landfall, at 1000 mb it was positive (eastward). But at cyclone period for two days (28.11.96 and 30.11.96) it was positive (eastward) and for two days (29.11.96 and 1.12.96) it was zero and at the end of cyclone (2.12.96-3.12.96) it was negative (westward) at 1000 mb. This revealed that at the end of cyclone (2.12.96-3.12.96) zonal wind component changes its direction at the surface level (i.e. at 1000 mb).

#### **Meridional Flux of Dry Static Energy (MFDSE):**

Fig. 5.7.7(a-c) shows the variation of meridional fluxes of dry static energy (MFDSE) at different isobaric levels. Before occurrence [Fig. 5.7.7(a)] it is seen that for all the days (23.11.96-27.11.96) MFDSE fluctuated at each level both in positive (northward) and negative (southward) direction. This was due to the change of wind velocity at each level for all the days. It is also seen that at 25.11.96 it was nearly constant for 400 mb-200 mb. This revealed that in this region there was a steady wind at that day.

At cyclone period [Fig. 5.7.7(a)] it is seen that at 1000 mb, from the beginning of cyclone (28.11.96-30.11.96) it was negative (southward), then On 1.12.96 it was positive (northward). At the end of cyclone (3.12.96) it was zero. From 1000 mb-700 mb, MFDSE increased gradually for all the days. Beyond 700 mb at 28.11.96 it increased linearly up to 300 mb and then decreased gradually up to 150 mb. At 100 mb it turned into negative (southward). Beyond 700 mb, on 29.11.96 it increased up to 300 mb and then decreased. On 3.12.96 it increased up to 150 mb. There is an interesting matter on 29.11.96 and 3.12.96 in cyclone period in the region 300 mb-100 mb. In this region when one increased

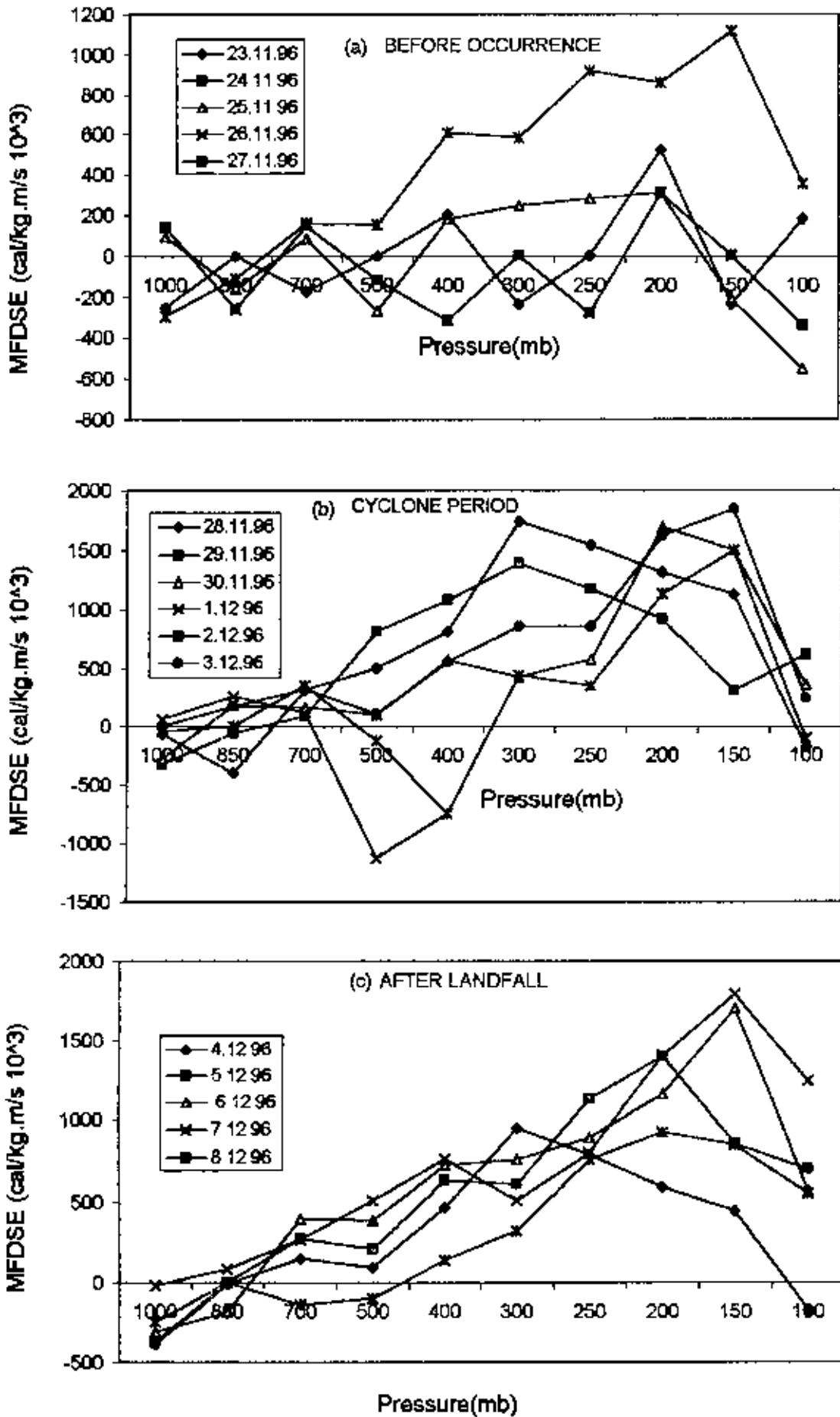


Fig. 5.7.7i (a-c). Variation of meridional fluxes of dry static energy at different isobaric levels.



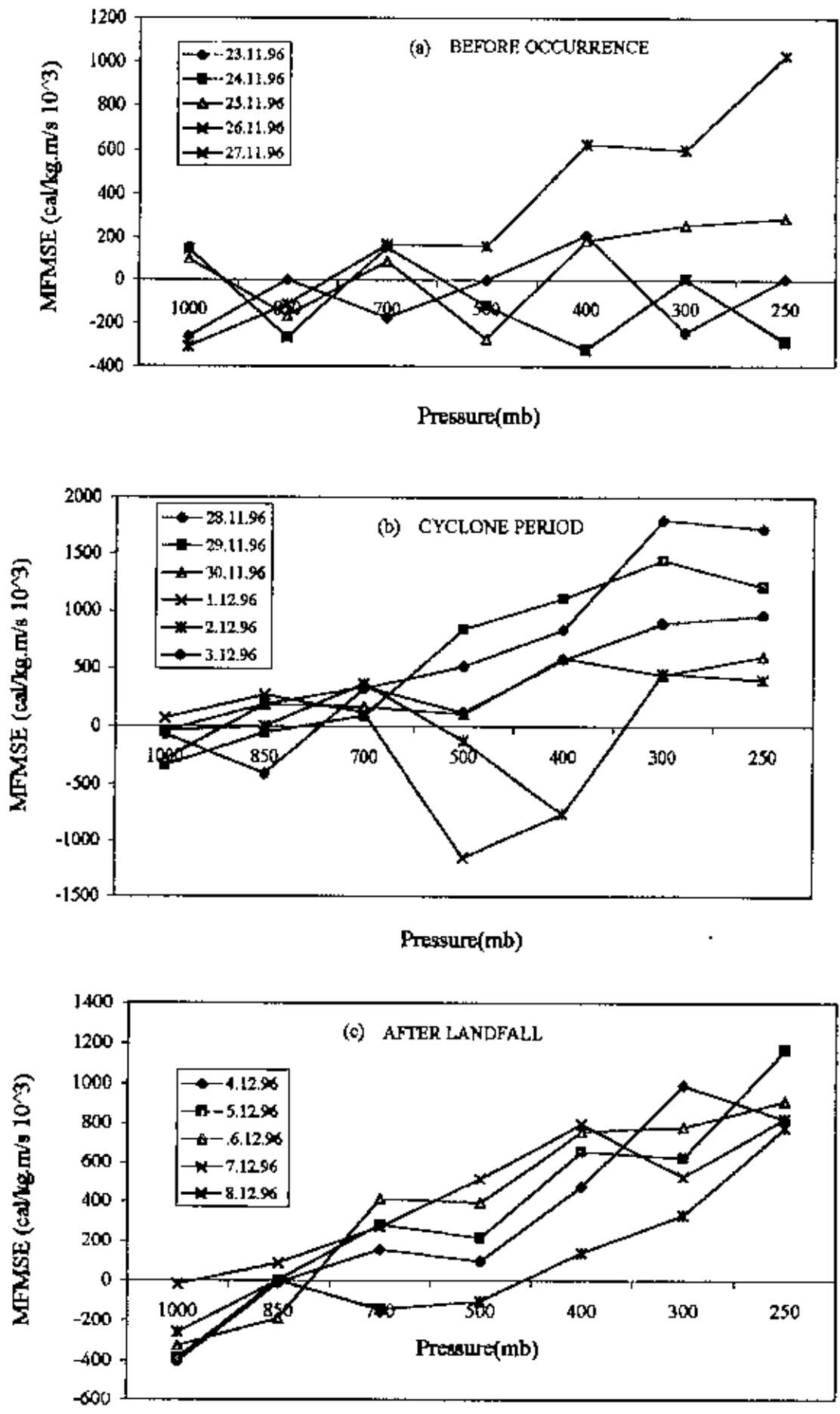


Fig. 5.7.8, (a-c). Variation of meridional fluxes of moist static energy at different isobaric levels

then the other decreased. At the middle period of the cyclone (30.11.96-2.12.96) it increased with a fluctuation both in direction (northward and southward) up to 150 mb and then decreased both in direction (northward and southward) at 100 mb.

After landfall [Fig. 5.7.7(c)] it is seen that at 1000 mb for all the days MFDSE was negative (southward). It increased to the positive (northward) direction for all the days except at the end of landfall (8.12.96). On 8.12.96 it was negative (southward) up to 500 mb, then it increased linearly up to 200 mb and then decreased. At the starting of landfall (4.12.96) MFDSE increased linearly up to 300 mb and then decreased up to 150 mb. At 100 mb it changed its direction from positive to negative.

#### **Meridional Flux of Moist Static Energy (MFMSE):**

Fig. 5.7.8(a-c) shows the variation of meridional flux of moist static energy (MFMSE) at different isobaric levels for before occurrence, cyclone period and after landfall. Before occurrence [Fig. 5.7.8(a)] the graph pattern was same as Fig. 5.7.7(a) which is discussed earlier. This was because MFMSE is simply an addition of latent heat content with MFDSE.

At cyclone period [Fig. 5.7.8(b)], MFMSE at 1000 mb was negative (southward) for all the days except 1.12.96. Then it increased linearly to the positive direction as pressure decreased (height increased) up to 300 mb. But at 500 mb and 400 mb for 1.12.8.96 and 2.12.96 it was negative (southward) due to the change of wind direction and then tend to positive (northward) direction. It is also seen that at 250 mb for all the days MFMSE decreased slightly.

After landfall it is seen that at 1000 mb for all the days MFMSE was negative (southward) and then turned into positive and increased linearly up to 250 mb.

From the above figures [Figs. 5.7.8(a-c)] it is observed that at cyclone period MFMSE was maximum at starting of cyclone (28.11.96) at 300 mb compared to the other days. This was due to the high wind speed at that day. It is also observed that at 250 mb MFMSE decreased slightly at cyclone period but after landfall it increased.

### 4.3 Energy and variables at different cyclonic phases

The energy and variables of the studied cyclones are analyzed at their different phases named Phase 1(Before occurrence), Phase 2(Cyclone period) and Phase 3(After landfall).

#### 4.3.1 Cyclone 1

Cyclone 1 is occurred from 5 May to 9 May 1990 over the Bay of Bengal. Its energy and variables are discussed here.

##### 4.3.1 (a): Energy components at different phases

###### Sensible heat (SH):

Fig. 6.1(a) shows the variation of sensible heat (SH) at different phases of a studied cyclone 1. It is seen that at phase 1 (before occurrence) SH was low but at phase 2 (cyclone period) SH was high. This was due to the increase of temperature at cyclone period. But at phase 3 (after landfall) SH was again low and near about the same as phase 1.

###### Potential energy (PE):

Fig. 6.1(b) shows the variation of Potential energy (PE) at different phases of cyclone 1. It is seen that PE was maximum at cyclone period (phase 2). This was because at cyclone period there existed very low pressure and for this reason geopotential height increased.

###### Latent heat content (LHC):

The variation of Latent heat content (LHC) at different phases of cyclone 1 is shown in Fig. 6.1(c). It is observed that LHC was same at phase 1 and phase 2. But at phase 3 (after landfall) LHC increased. This was because at this phase more cloud is formed and released latent heat that increased the magnitude of latent heat content.

###### Kinetic energy (KE):

The variation of kinetic energy (KE) at different phases of cyclone 1 is shown in Fig. 6.1(d). At phase 1 (before occurrence) KE is higher than at phase 3. This was because at phase 1 low pressure is just formed and wind speed increased a little bit. But at

phase 2 (cyclone period) KE was maximum compared to phase 1 and phase 3. This signifies the maximum wind speed at cyclone period.

#### **Total energy (TE):**

Fig. 6.1(e) shows the variation of total energy (TE) at different phases of cyclone 1. It is seen that the total energy was maximum at cyclone period (phase 2). Because at cyclone period sensible heat, potential energy and kinetic energy was maximum compared to before occurrence and after landfall.

#### **4.3.1 (b): Variables at different phases**

##### **Temperature:**

Time-temperature graph is shown in Fig. 6.1(f). It is observed that at phase 1 the temperature was very unstable i.e., at time to time temperature fluctuated. But at phase 2 (cyclone period), at first it increased abruptly and then maintained near about a constant value. Sensible heat was maximum at this phase because of increase in temperature. At phase 3 it is slightly increased on 12, May 1990 and then decreased.

##### **Wind speed:**

The variation of wind speed with time is shown in Fig. 6.1(g) It is seen that at phase 1 wind speed decreased on 2<sup>nd</sup> May 1990 and then it increased up to 4<sup>th</sup> May 1990 and again decreased on 5<sup>th</sup> May 1990. But at phase 2 (cyclone period) wind speed increased and attained maximum value on 6<sup>th</sup> May and then decreased gradually. At phase 3 it increased at the time of landfall and then decreased at the end of landfall. From this figure [Fig. 6.1(g)], it is seen that at these three phases there were three peaks. But at cyclone period (phase 2) the peak was maximum. For this reason we observed that KE was maximum at this stage.

##### **Wind direction:**

Time-wind direction graph at different phases of the studied cyclone 1 is shown in Fig. 6.1(h). At phase 1 (1-4 May, 1990) i.e., before occurrence, on 2<sup>nd</sup> May wind direction was norwesterly (180-90), on 3<sup>rd</sup> May it was nor-easterly (180-270) and on 4<sup>th</sup>

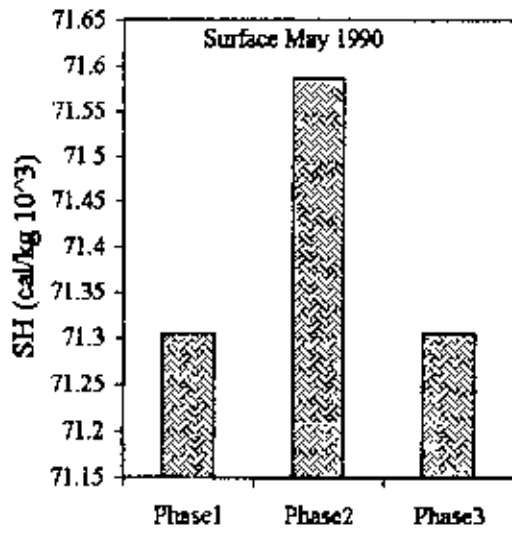


Fig. 6.1. (a): Sensible heat

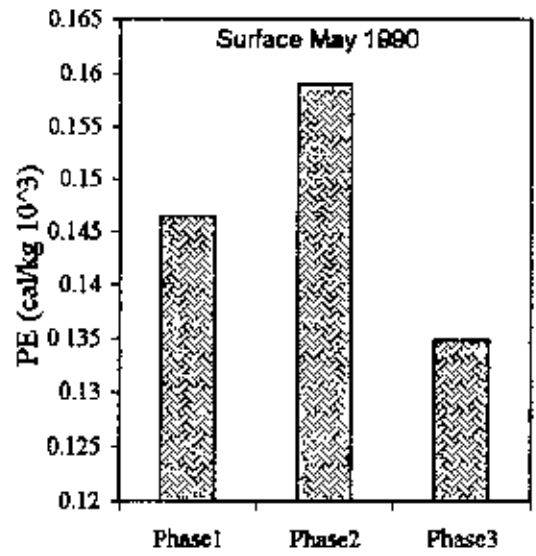


Fig. 6.1. (b): Potential energy

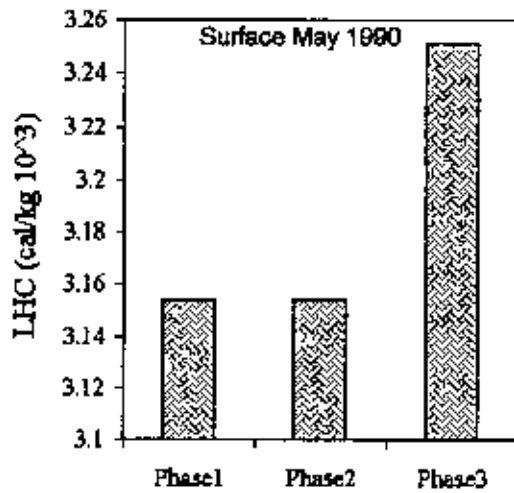


Fig. 6.1. (c): Latent heat content

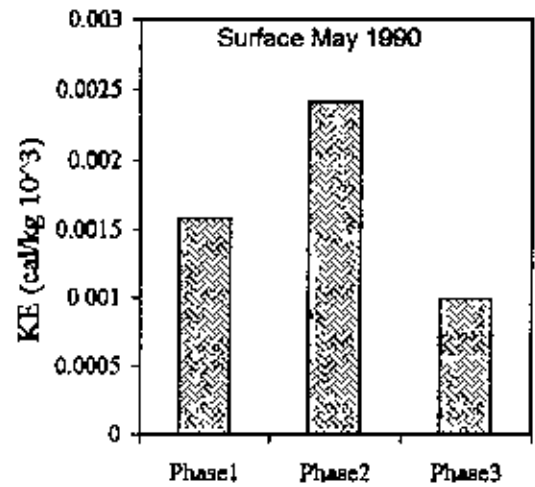


Fig. 6.1. (d): Kinetic energy

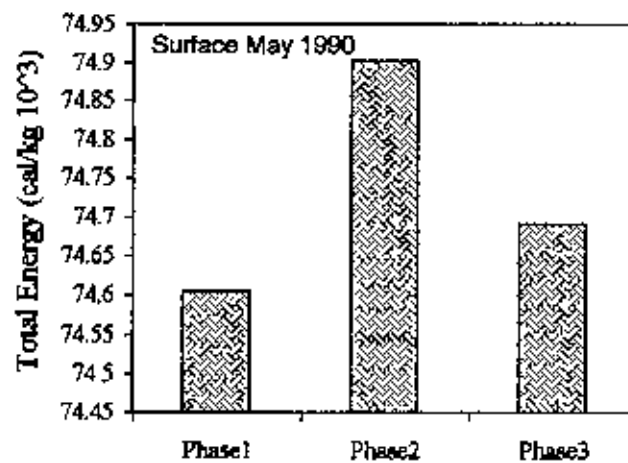


Fig. 6.1 (e): Total energy

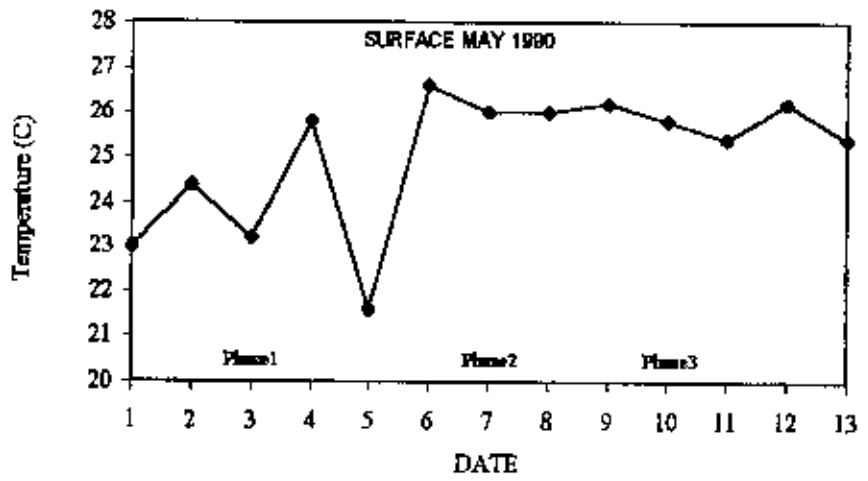


Fig. 6.1. (f): Time-temperature graph

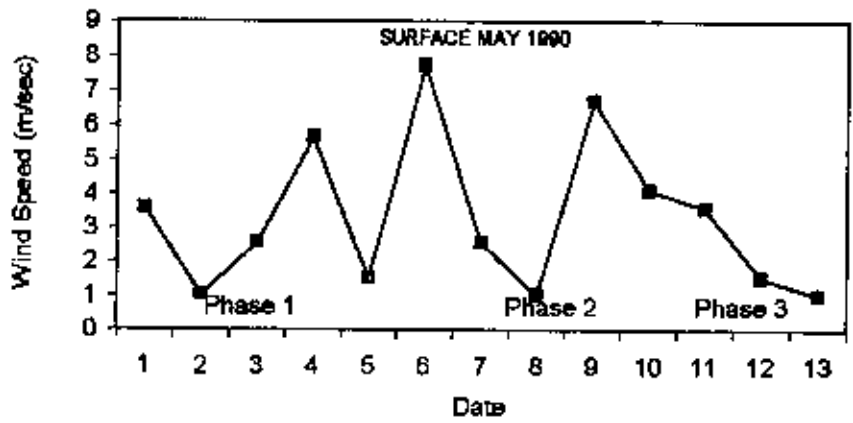


Fig. 6.1. (g): Time-wind speed graph

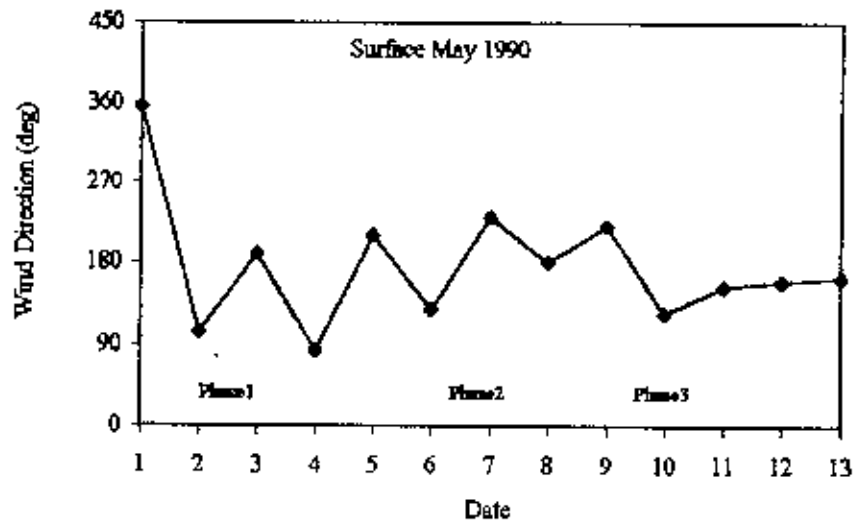


Fig. 6.1. (h): Time-Wind direction graph

May it was norwesterly (180-90). At phase 2 (5-9 May 1990) i.e., cyclone period, on 5<sup>th</sup> May wind direction was norwesterly (180-270), on 6<sup>th</sup> May it was norwesterly (180-90), on 7<sup>th</sup> May it was norwesterly (180-270), on 8<sup>th</sup> May it was norwesterly (180-90) and at the end of cyclone i.e., on 9<sup>th</sup> May it was again norwesterly (180-270). At phase 3 (10-13 Nov) i.e., during landfall wind direction was southward (northerly).

### 4.3.2 Cyclone 2

Cyclone 2 is occurred from 16 December to 18 December 1990 over the Bay of Bengal. Its energy and variables are discussed here.

#### 4.3.2 (a): Energy components at different phases

##### Sensible heat (SH):

Figure 6.2(a) shows the variation of sensible heat (SH) at different phases of a studied cyclone 2. It is seen that at phase 2 (cyclone period) SH was maximum compared to phase 1 and phase 2. This was because at cyclone period temperature increased and so sensible heat increased. But at phase 3 SH was minimum. This was because after landfall heavy rainfall occurred and temperature decreased so sensible heat decreased.

##### Potential energy (PE):

The variation of potential energy (PE) at different phases of cyclone 2 is shown in Fig. 6.2(b). From this figure it is seen that PE was very high at phase 1 (before occurrence). This was because just before cyclone low pressure is formed and geopotential height ( $z$ ) increased so increased potential energy.

##### Kinetic energy (KE):

Fig. 6.2(c) shows the variation of kinetic energy (KE) at different phases of cyclone 2. It is observed that KE was low at the very beginning of cyclone i.e., at phase 1. Then it increased and attained maximum value at cyclone period (phase 2). At cyclone period wind speed was maximum and for this KE attained maximum value. Then it decreased at phase 3 but it was higher than phase 1. This was because up to that time (during landfall) there exists some wind speed.

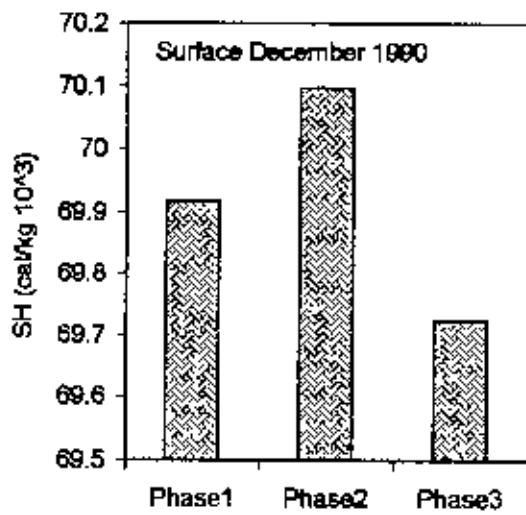


Fig. 6.2 (a): Sensible heat

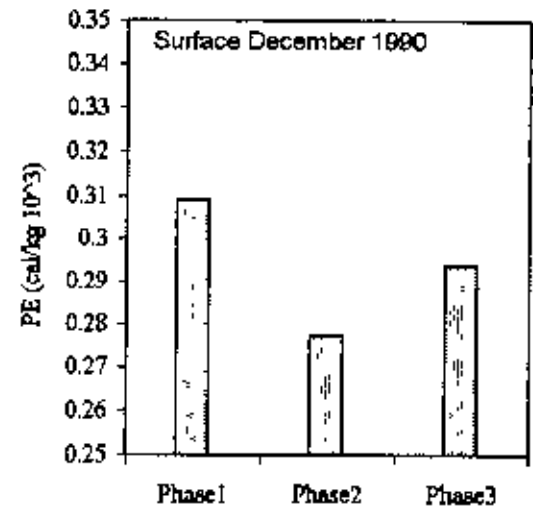


Fig. 6.2 (b): Potential energy

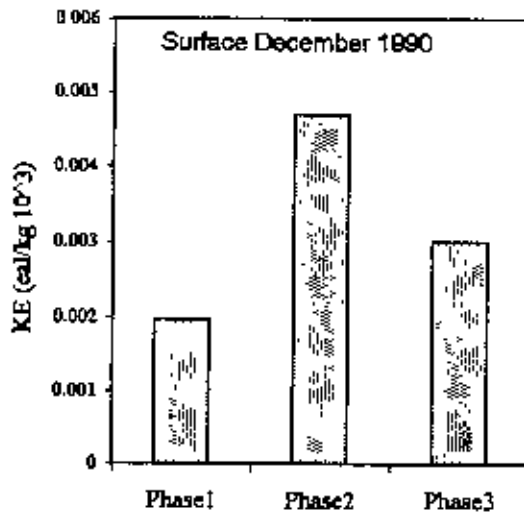


Fig. 6.2 (c): Kinetic energy

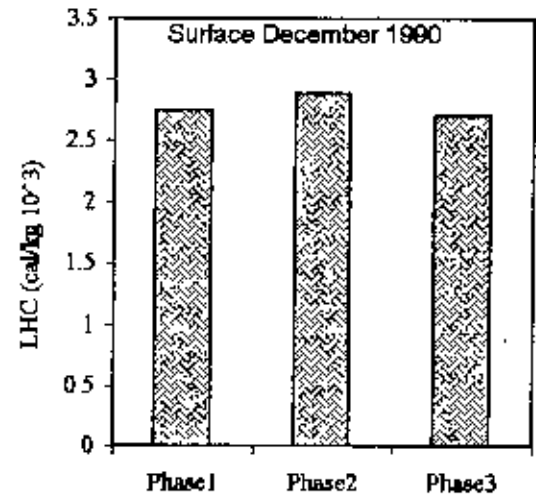


Fig. 6.2 (d): Latent heat content

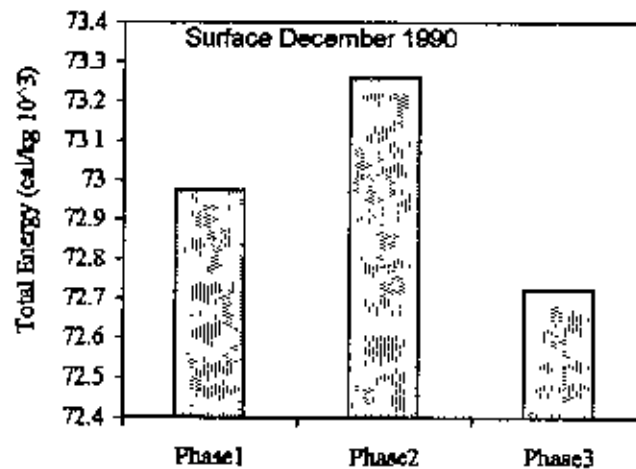


Fig. 6.2 (e): Total energy



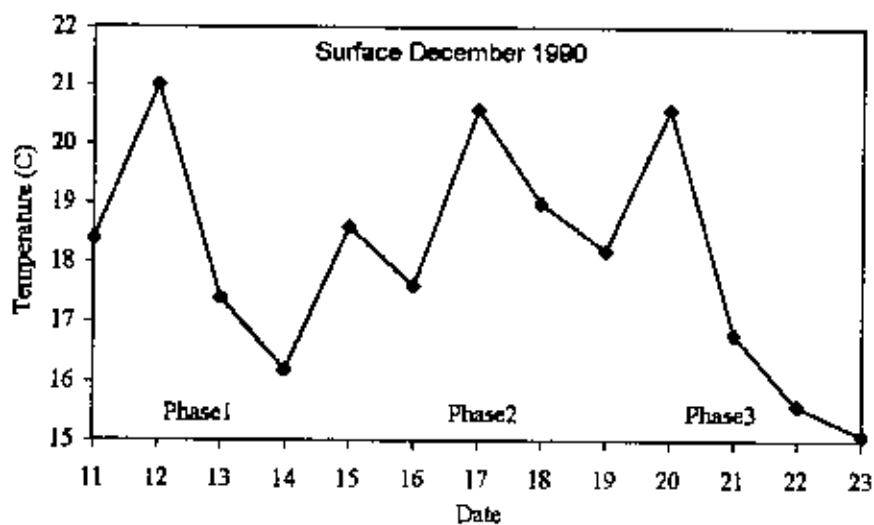


Fig. 6.2 (f) Time-Temperature graph

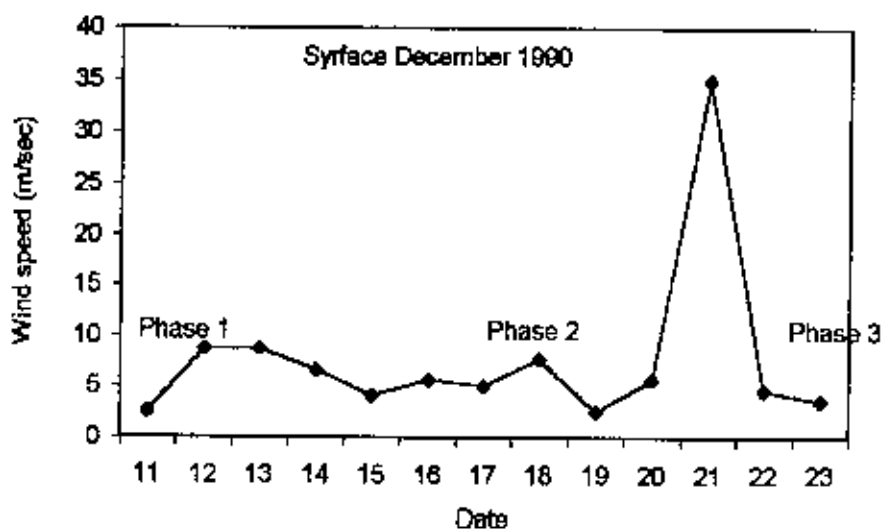


Fig. 6.2 (g) Time-Wind speed graph

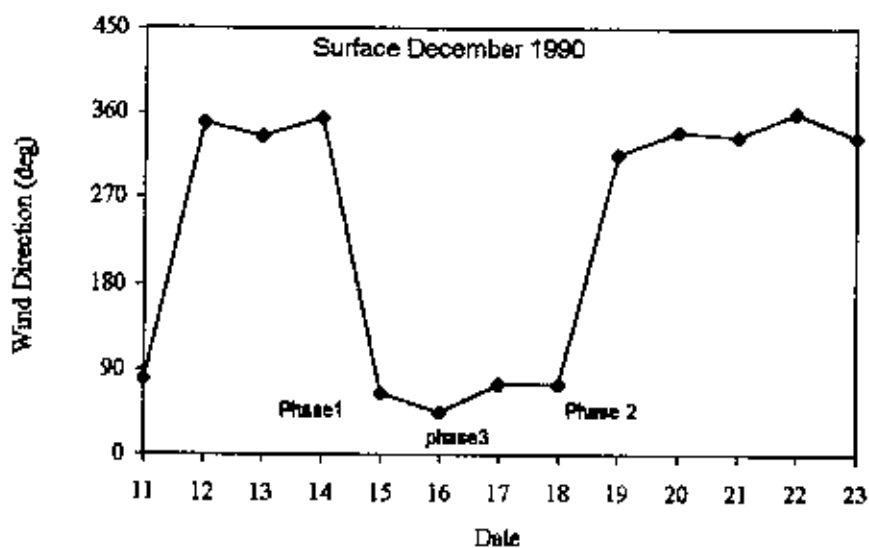


Fig. 6.2 (h) Time-Wind direction graph

**Latent heat content (LHC):**

The variation of latent heat content (LHC) at different phases of cyclone 2 is shown in Fig. 6.2(d). At phase 2 (cyclone period) LHC was higher than at phase 1 (before occurrence) and at phase 3 (during landfall). It is seen that at phase 2 temperature increased due to release of latent heat and as a result LHC increased.

**Total energy (TE):**

The variation of total energy (TE) at different phases of cyclone 2 is shown in Fig. 6.2(e). From this figure it is observed that total energy was minimum after landfall (phase 3) and maximum at cyclone period (phase 2). After landfall total energy was minimum because of minimum sensible heat and minimum latent heat content at this stage. At cyclone period total energy was maximum because at this stage all the energy components were maximum except potential energy

**4.3.2 (b): Variables at different phases****Temperature:**

The variation of temperature with time at different phases of cyclone 2 is shown in Fig. 6.2(f). At phase 1, temperature increased on 12 Dec. 1990 and then decreased. At phase 2 (cyclone period), at first temperature increased, then decreased and again increased. At this stage more or less temperature increased. During landfall temperature increased on 20 Dec., then decreased and attained minimum value at the end of landfall (23 Dec. 1990).

**Wind speed:**

Fig. 6.2(g) shows the variation of wind speed with time at different phases of cyclone 2. It is seen that at phase 1 and phase 2 wind speed was near about same and the variation was not so differ. After landfall (phase 3), it is observed that on 11 Dec. 1990 wind speed increased abruptly and reached to the maximum value and then reduced to the same value as before (phase 2).

**Wind direction:**

Fig. 6.2(h) shows Time-wind direction graph at different phases of cyclone 2. From this graph it is seen that at phase 1, (11-15 Dec 1990) on 12<sup>th</sup> Dec, wind direction was southeasterly (270-360), then from 12-14 Dec, wind direction was northward i.e., southerly (360) and on 15<sup>th</sup> Dec, i.e., at the initiation of cyclone wind direction was eastward i.e., westerly (90). At phase 2 (16-18 Dec, 1990) i.e., cyclone period, for all the time wind direction was eastward i.e., westerly (90). At phase 3 (19-23 Dec 1990) i.e., after landfall wind direction was northward [southerly (360)].

**4.3.4 Cyclone 3**

Cyclone 3 is occurred from 25 April to 30 April 1991 over the Bay of Bengal. Its energy and variables are discussed here.

**4.3.3 (a): Energy components at different phases****Sensible heat (SH):**

Fig. 6.3(a) shows the variation of sensible heat (SH) at different phases of cyclone 3. It is observed that SH was low at phase 1 and phase 2 and it was near about the same. But at phase 3 (after landfall) it was maximum compared to phase 1 and phase 2. This was because after landfall latent heat released and for this temperature increased so SH increased.

**Potential energy (PE):**

The variation of potential energy (PE) at different phases of cyclone 3 is shown in Fig. 6.3(b). From this figure it is seen that before cyclone (phase 1) PE is slightly higher than at phase 3 (after landfall). This is because just before cyclone (phase 1) a low pressure is formed and geopotential height increased and so PE increased. But at cyclone period (phase 2) PE was maximum due to the maximum increase of geopotential height.

**Latent heat content (LHC):**

Fig. 6.3(c) shows the variation of latent heat content (LHC) at different phases of cyclone 3. At phase 1 LHC was very low due to no formation of cloud. But at phase 2

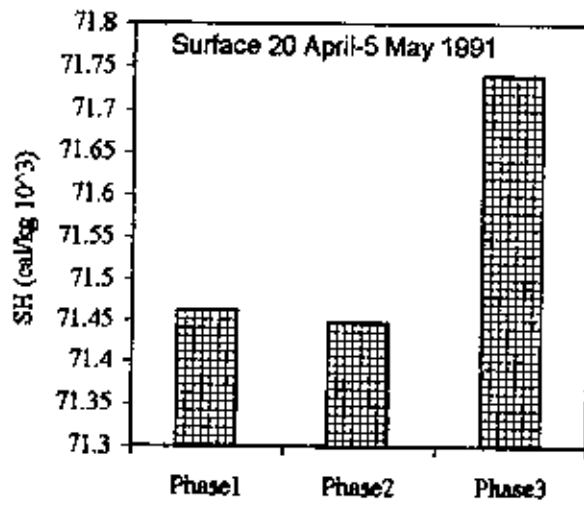


Fig. 6.3 (a): Sensible heat.

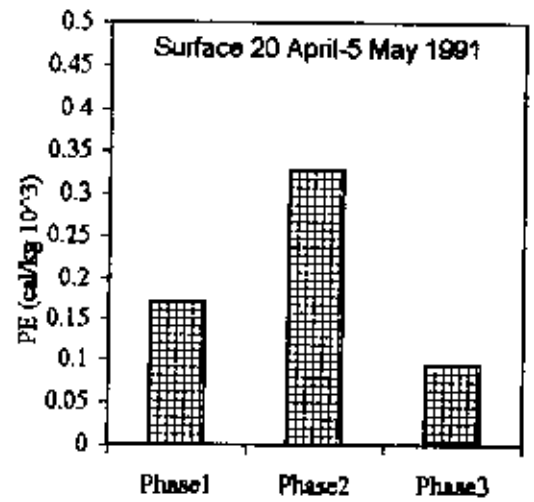


Fig. 6.3 (b): Potential energy.

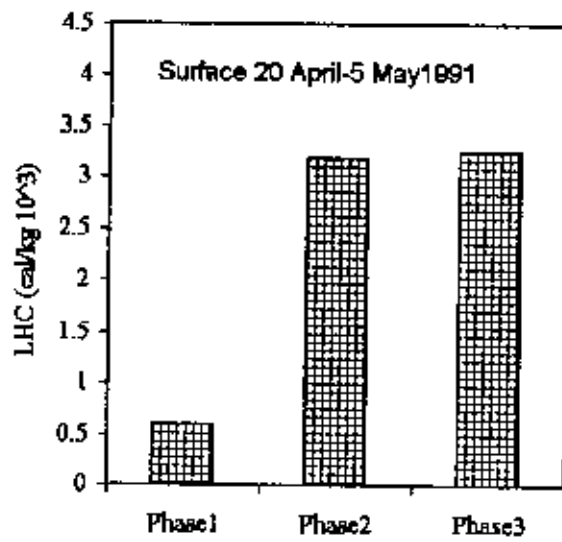


Fig. 6.3 (c): Latent heat content

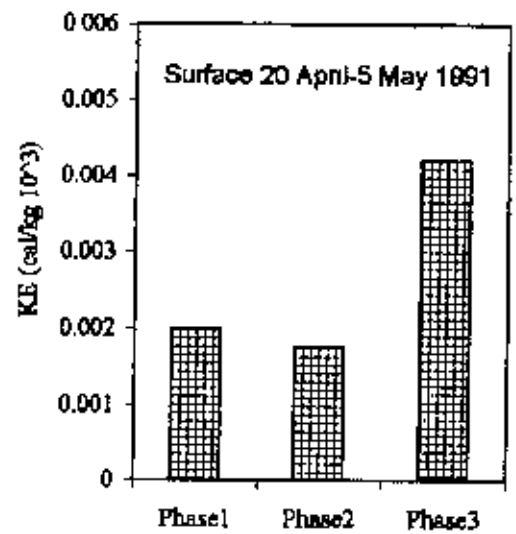


Fig. 6.3 (d): Kinetic energy

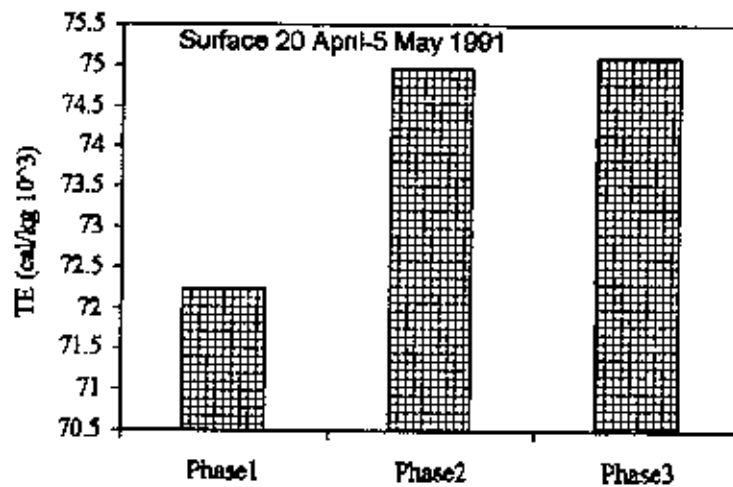


Fig. 6.3 (e): Total energy.

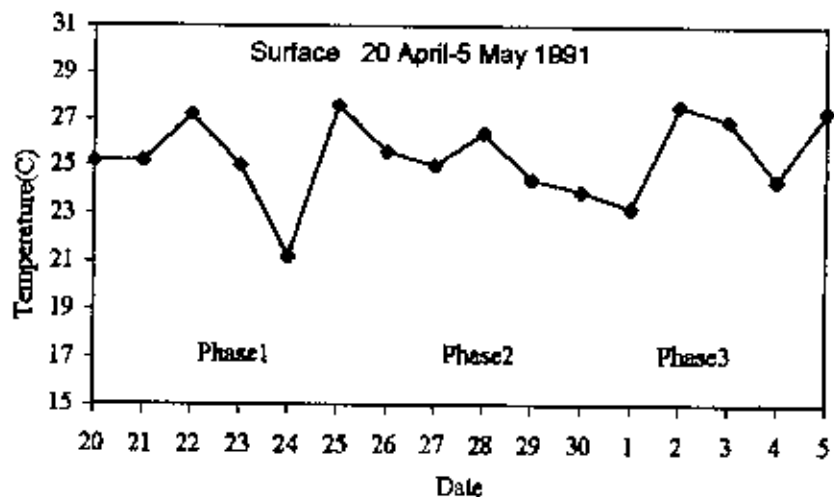


Fig. 6.3 (f). Time-temperature graph.

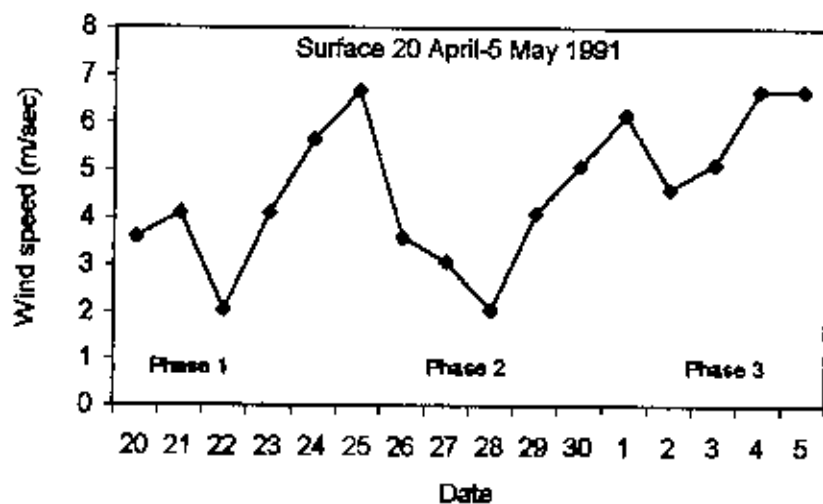


Fig. 6.3 (g). Time-Wind speed graph.

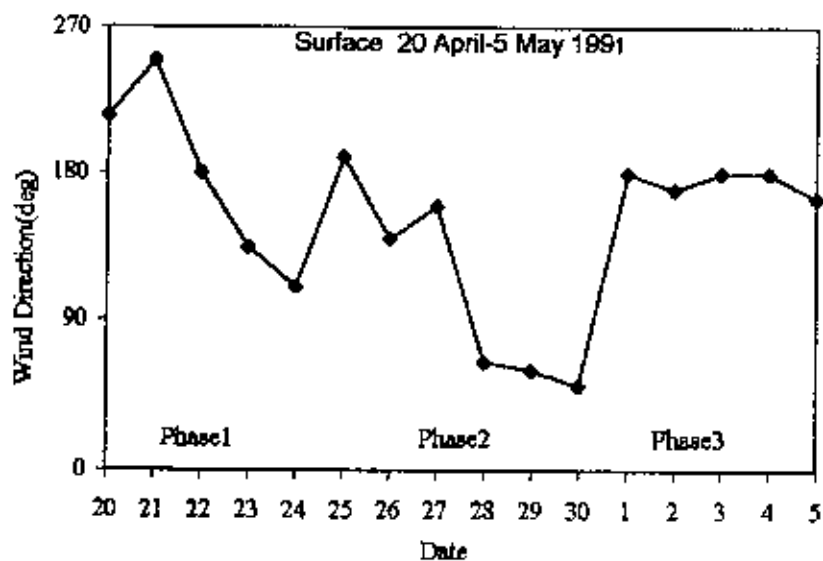


Fig. 6.3 (h). Time-Wind direction graph.

(cyclone period) and phase 3 (after landfall) LHC was very high and near about the same (at phase 3 it was slightly high). This high value of LHC was an indication of more cloud formation at cyclone period and after landfall.

#### **Kinetic energy (KE):**

The variation of kinetic energy (KE) at different phases of cyclone 3 is shown in Fig. 6.3(d). From this figure it is observed that KE was low at phase 1 and phase 2. But at phase 3 KE was maximum due to high wind speed.

#### **Total energy (TE):**

The variation of total energy at different phases of cyclone 3 is shown in Fig. 6.3(e). At phase 1 (before occurrence) total energy was very low due to the lower energy components at this phase. At phase 2 and phase 3 total energy was high and was maximum at phase 3. This was because different energy components were maximum (except PE) at phase 3.

### **4.3.3 (b): Variables at different phases**

#### **Temperature:**

The variation of temperature with time at different phases of cyclone 3 is shown in Fig. 6.3(f). From this figure it is observed that at phase 1, phase 2 and phase 3 the variation of temperature with time was near about the same. But on 24 April 1991 the temperature was slightly low and on 5<sup>th</sup> May 1991 the temperature was slightly high. At phase 3 this slightly high temperature was the result of high sensible heat at this phase.

#### **Wind speed:**

Fig. 6.3(g) shows the variation of wind speed with time at different phases of cyclone 3. It is observed that wind speed at different phases changed with time and maintained a zig-zug path. Here at time to time wind speed increased and decreased so that the weather was very unstable. It is also observed that after landfall (phase 3) wind speed increased and attained maximum value on 4-5 May 1991. This was why KE was maximum after landfall.

**Wind direction:**

Fig. 6.3(h) shows time-wind direction graph at different phases of cyclone 3 occurred from 25-30 April 1991. At phase 1 (20-24 April 1991) i.e., before occurrence, on 21 April wind direction was northeasterly (180-270), on 22 April it was remain the same i.e., northeasterly (270-180), at the initiation of cyclone i.e., on 23-24 April wind direction was norwesterly (180-90). At phase 2 (25-30 April) i.e., at cyclone period, on 25-27 April wind direction was remain same as that of the initiation of cyclone (23-24 April) i.e., norwesterly (180-90) and on 28-30 wind direction was southwesterly (90-0). At phase 3 (1-5 May) i.e., after landfall wind direction was southward i.e., northerly (180).

**4.3.4 Cyclone 4**

Cyclone 4 is occurred from 29 April to 3 May 1994 over the Bay of Bengal. Its energy and variables are discussed here.

**4.3.4 (a): Energy components at different phases****Sensible heat (SH):**

Fig. 6.4(a) shows the variation of sensible heat (SH) at different at different phases of cyclone 4. From this figure it is observed that from phase 1 to phase 3 sensible heat increased gradually and it was maximum at phase 3 i.e., after landfall. At phase 3 SH was maximum because at this phase temperature was maximum.

**Potential energy (PE):**

The variation of potential energy (PE) variation at different phases of cyclone 4 is shown in Fig. 6.4(b). From phase 1 to phase 3, PE is gradually decreased. It is observed that at phase 1 PE was maximum. This was because just before cyclone (phase 1) a low pressure is formed, so geopotential height ( $z$ ) increased. This increase of geopotential height increased PE at this phase.

**Latent heat content (LHC):**

Fig. 6.4(c) shows the variation of latent heat content (LHC) at different phases of cyclone 4. Here it is seen that LHC increased gradually and attained maximum value at

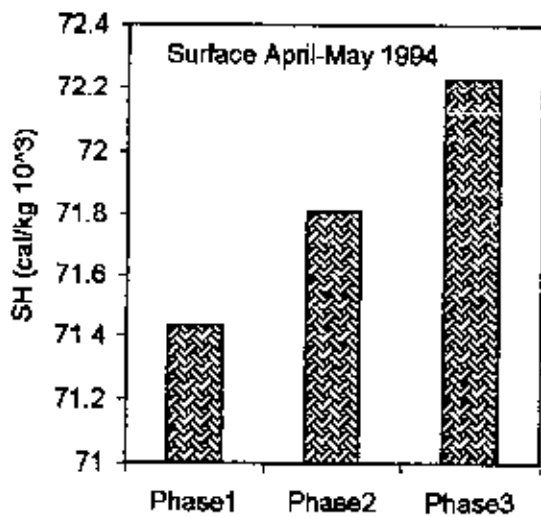


Fig. 6.4 (a) Sensible heat

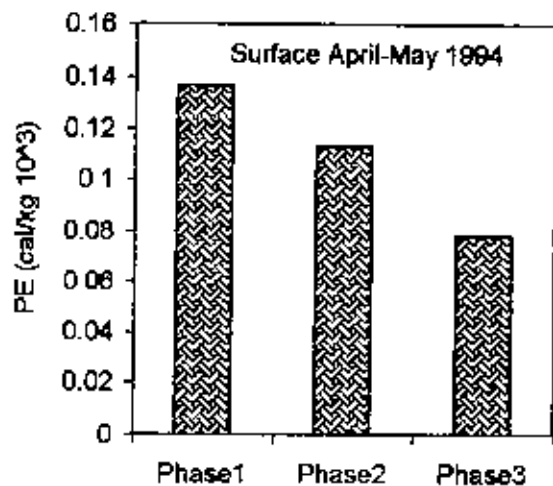


Fig. 6.4 (b) Potential energy

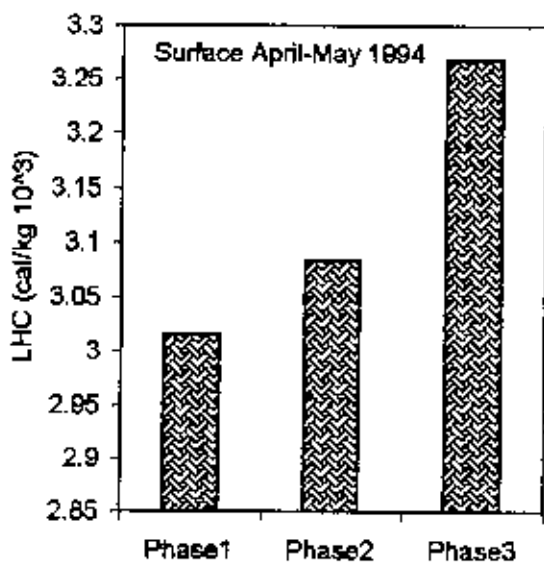


Fig. 6.4 (c) Latent heat content

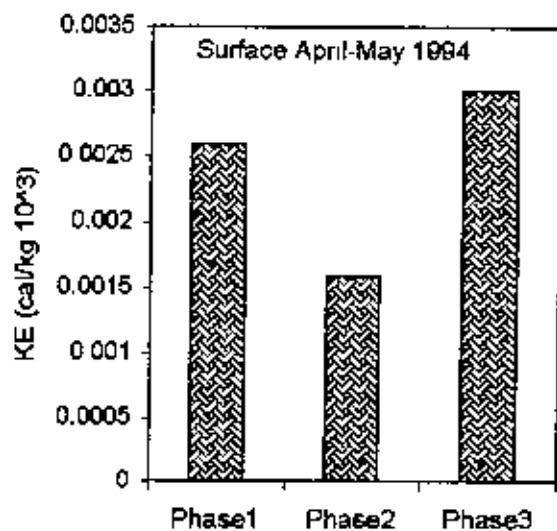


Fig. 6.4 (d) Kinetic energy

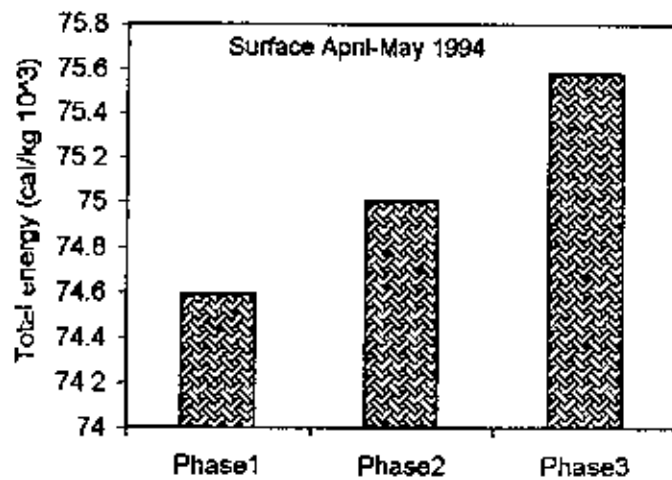


Fig. 6.4 (e) Total energy



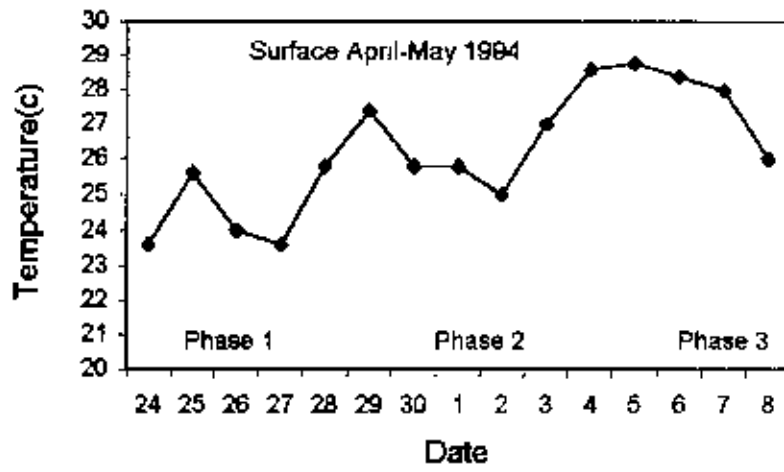


Fig. 6.4 (f) Time-Temperature graph

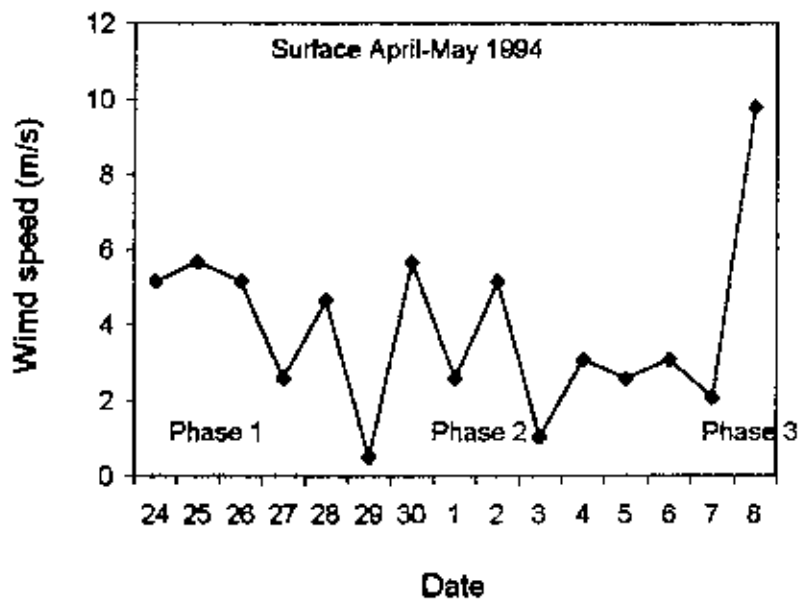


Fig. 6.4i (g) Time-Wind speed graph

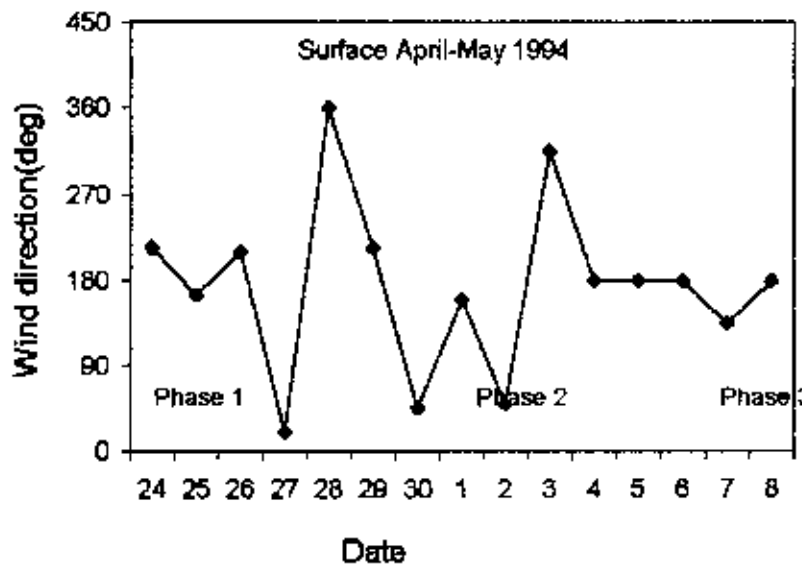


Fig. 6.4i (h) Time-Wind direction graph

phase 3. At this phase more cloud formed and released more latent heat so that LHC increased. As a result heavy rainfall occur during landfall.

#### **Kinetic energy (KE):**

Variation of kinetic energy (KE) at different phases of cyclone 4 is shown in Fig. 6.4(d). Here KE was high at phase 1 compared to phase 2. This was because at phase 1 (just before occurrence) a low pressure is formed and strong wind was blowing. But it is observed that at phase 3 (after landfall) KE was maximum again due to high wind speed.

#### **Total energy (TE):**

The variation of total energy at different phases of cyclone 4 is shown in Fig. 6.4(e). Here it is seen that total energy was low at phase 1. At phase 2, it increased and attained maximum value at phase 3. This maximum total energy at phase 3 was due to the maximum energy components (except PE) at this phase.

### **4.3.4 (b): Variables at different phases**

#### **Temperature:**

Fig. 6.4(f) shows time-temperature graph. At phase 1 it is seen that, at first temperature increased and then decreased. Similarly at phase 2, at first temperature increased and then decreased. But at phase 3, temperature increased and became maximum and then maintained a constant value. Due to this increase in temperature sensible heat was maximum at this phase (phase 3).

#### **Wind speed:**

The variation of wind speed at different phases of cyclone 4 is shown in Fig. 6.4(g). At phase 1 for first three days (24-26 April) wind speed was near about the same. Beyond that (i.e., after 26 April) every day wind speed changed i.e., increased or decreased. At the end of phase 3 (8 May 1994) it is observed that wind speed increased abruptly and was maximum. For that KE was maximum at phase 3.

**Wind direction:**

Time-wind direction graph at different phases of cyclone 4 occurred from 29 April-3 May is shown in Fig. 6.4(h). It is observed that at phase 1 (24-28 April), on 24-26 April wind direction was northeasterly (270-180), on 27 April it was southwesterly (90-0), on 28 April wind direction was southeasterly (270-360). At phase 2 (29 April-3 May) i.e., cyclone period, on 29 April wind direction was northeasterly (270-180), on 30 April it was southwesterly (90-0), on 1<sup>st</sup> May wind direction was norwesterly (90-180), on 2<sup>nd</sup> May it was southwesterly (90-0), and at the end of cyclone i.e., on 3<sup>rd</sup> May wind direction was southeasterly (270-360). At phase 3 (4-8 May) i.e., during landfall it is observed that wind direction was southward i.e., northerly (180).

**4.3.5 Cyclone 5**

Cyclone 5 is occurred from 21 November to 25 November 1995 over the Bay of Bengal. Its energy and variables are discussed here.

**4.3.5 (a): Energy components at different phases****Sensible heat (SH):**

Fig. 6.5(a) shows the variation of sensible heat (SH) at different phases of cyclone 5. It is observed that at phase 1 (before occurrence) SH was high compared to the other two phases i.e., phase 2 (cyclone period) and phase 3 (during landfall). This was because just before cyclone atmospheric temperature increased that increased SH at before cyclone.

**Potential energy:**

The variation of potential energy at different phases of cyclone 5 is shown in Fig. 6.5(b). Here it is seen that at phase 2 (cyclone period) and phase 3 (during landfall) PE was high compared to phase 1 (before occurrence). This high PE was due to higher geopotential height at these two phases (i.e., phase 2 and phase 3).

**Latent heat content (LHC):**

The variation of latent heat content (LHC) at different phases of cyclone 5 is shown in Figure 6.5(c). Here it is seen that at phase 1 (before occurrence) LHC was maximum compared to phase 2 and phase 3. Here at phase 1 temperature was high, so more water evaporate and then condensed and released more latent heat. This is why at phase 1 LHC was high.

**Kinetic energy (KE):**

Fig. 6.5(d) shows the variation of kinetic energy (KE) at different phase of cyclone 5. It is seen that at phase 1 (before occurrence) KE was minimum due to lower wind speed. But at phase 2 i.e., at cyclone period K.E increased and attained maximum value at phase 3 i.e., during landfall. Here we observed that during landfall KE was maximum due to higher wind speed.

**Total energy (TE):**

The variation of total energy at different phases of cyclone 5 is shown in Fig. 6.5(e). Here we observed that at phase 1 (before occurrence) total energy was high compared to phase 2 and phase 3. The effect of sensible heat is much more on total energy. Here we observed that at phase 1 SH was higher. We also observed that LHC was also higher at phase 1. So total energy was maximum at phase 1. It is also observed that during landfall (phase 3) total energy minimum due to lower SH and LHC.

**4.3.5 (b): Variables at different phases****Temperature:**

The variation of temperature with time at different phases of cyclone 5 is shown in Fig. 6.5(f). From this figure it is observed that at phase 1 (16-20 Nov.) on 16-18 Nov. 1995 temperature was near about the same. On 18-19 Nov. temperature decreased abruptly. At phase 2 (21-25 Nov.) i.e., at cyclone period, it is seen that at the initiation of cyclone (20<sup>th</sup> Nov.) temperature increased abruptly and then increased gradually up to 24<sup>th</sup> Nov. At the end of cyclone i.e., at 25<sup>th</sup> Nov. temperature decreased abruptly. At phase 3 (26-30 Nov.) i.e., during landfall temperature decreased.

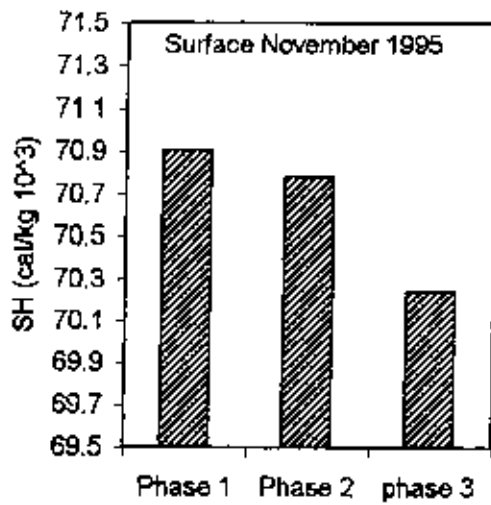


Fig. 6.5 (a): Sensible heat

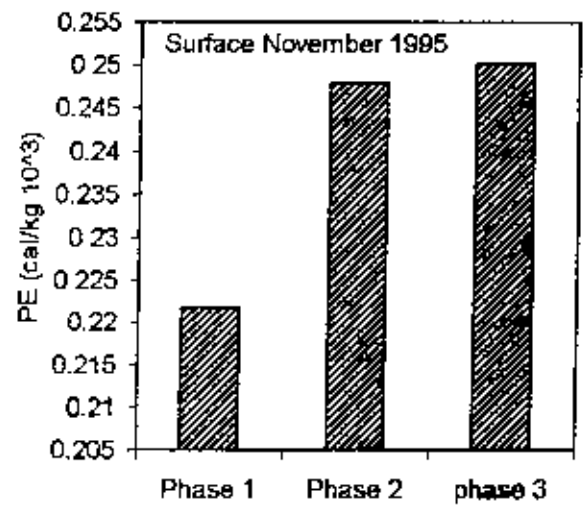


Fig. 6.5 (b): Potential energy

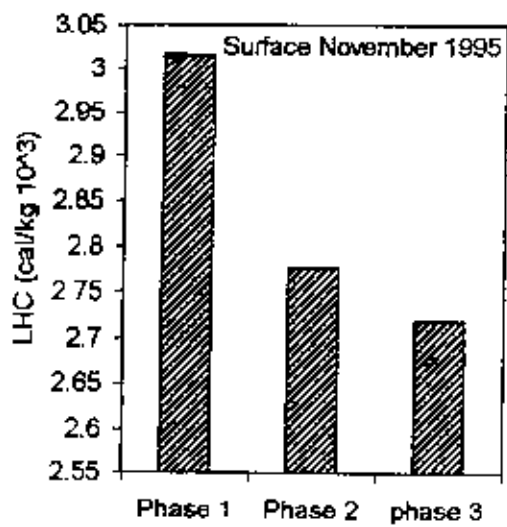


Fig. 6.5 (c): Latent heat content

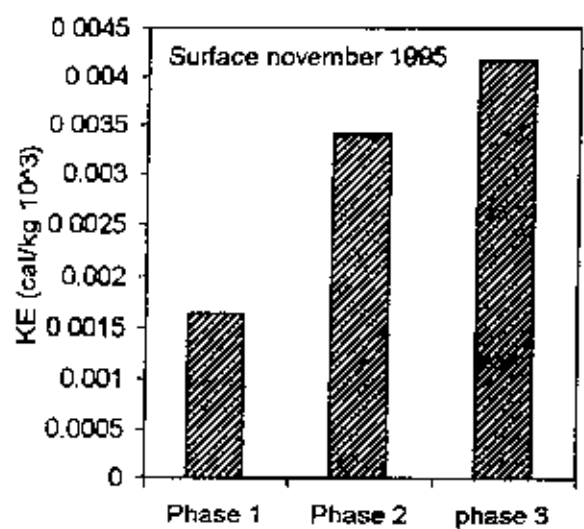


Fig. 6.5 (d): Kinetic energy

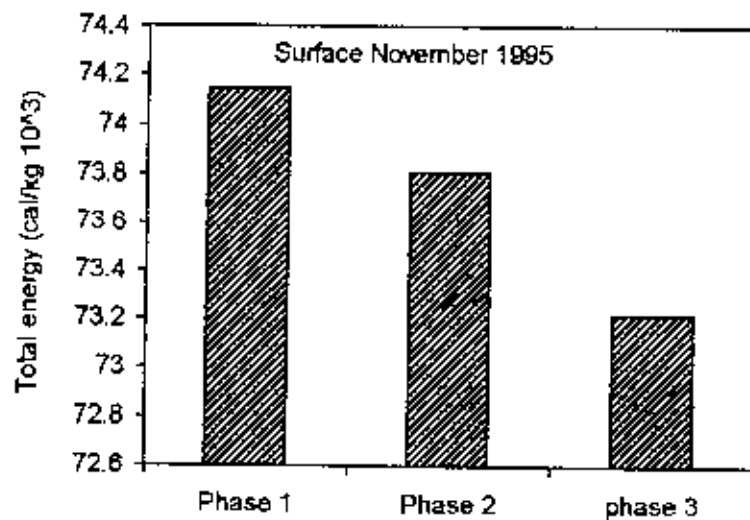


Fig. 6.5 (e): Total energy

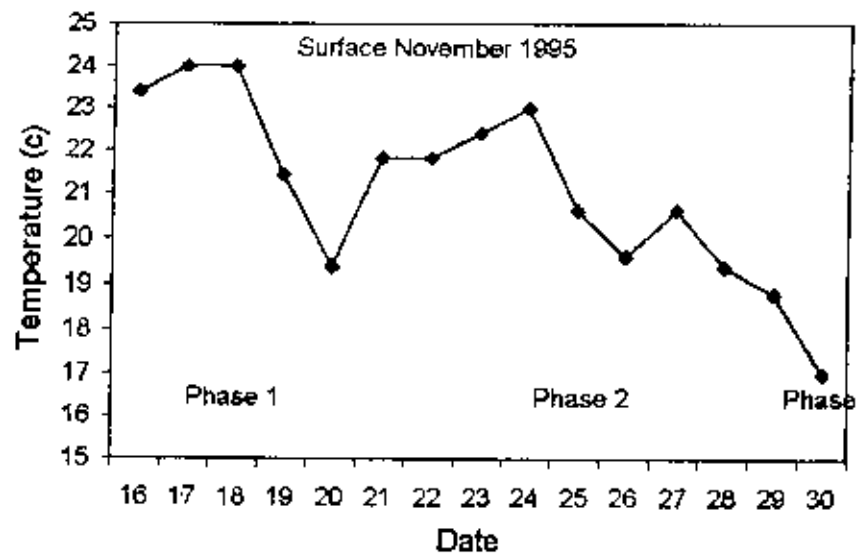


Fig. 6.5i (f): Time-temperature graph

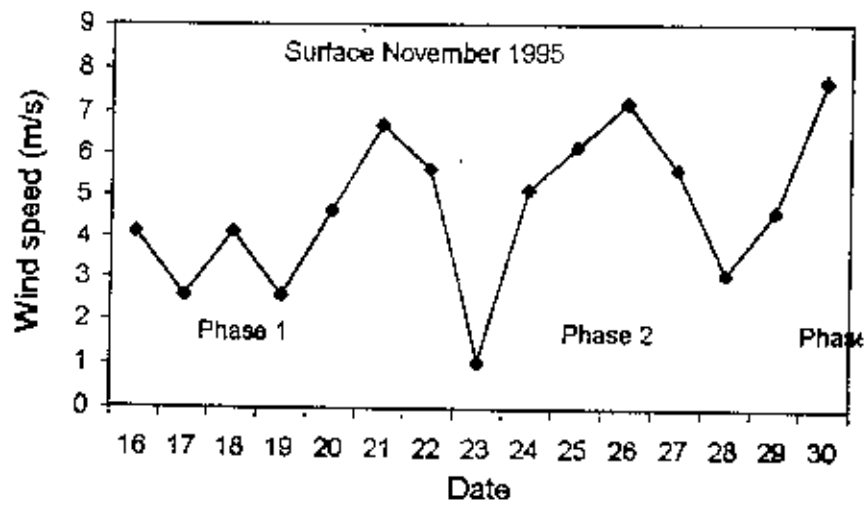


Fig. 6.5j (g): Time-wind speed graph

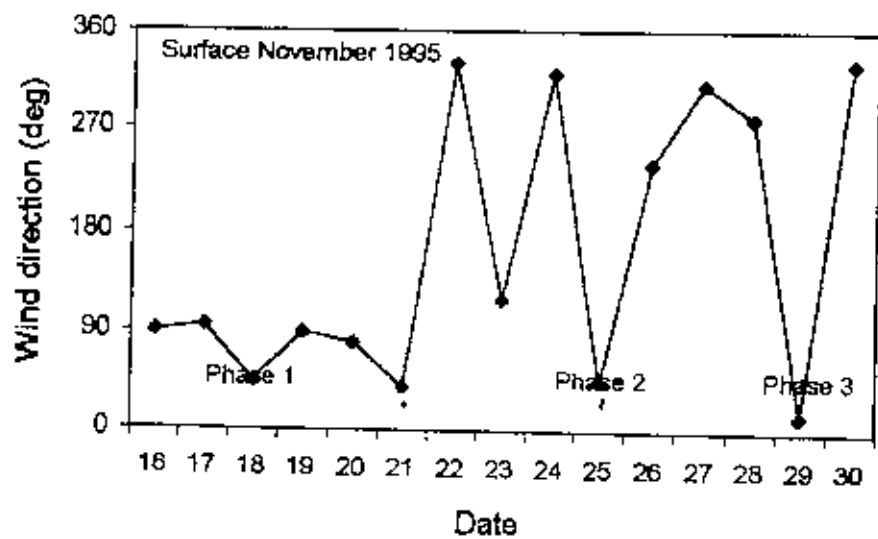


Fig. 6.5k (h): Time-wind direction graph

**Wind speed:**

Fig. 6.5(g) shows the variation of wind speed with time at different phases of cyclone 5. At phase 1 (16-20 Nov. 1995) i.e., before occurrence wind speed fluctuated from 16-19 Nov. At the initiation of cyclone (20-21 Nov.) wind speed increased abruptly. At phase 2 (21-25 Nov.) i.e., during cyclone wind speed decreased on 2<sup>nd</sup> and 3<sup>rd</sup> day (i.e., 22-23 Nov.) and then increased gradually up to 26<sup>th</sup> November (i.e., during landfall). At phase 3 (26-30 Nov.) i.e., after landfall wind speed decreased on 27-28 Nov. and then increased and attained maximum value at the end of landfall.

**Wind direction:**

Fig. 6.5(h) shows time-wind direction graph at different phases of cyclone 5 occurring on 21-25 November 1995. It is observed that at phase 1 (16-20 Nov.), on 16-17 Nov. wind direction was eastward i.e., westerly (90), on 18-20 Nov. it was southwesterly (90-0). At phase 2 (21-25 Nov.) i.e., at cyclone period, on 21<sup>st</sup> Nov. wind direction was same as before i.e., southwesterly (90-0). On the 2<sup>nd</sup> day of cyclone i.e., on 22<sup>nd</sup> Nov. wind direction increased abruptly and the direction was southeasterly (270-360). On 23<sup>rd</sup> Nov. wind direction was norwesterly (180-90) and on 24<sup>th</sup> Nov. wind direction again increased abruptly and the direction was again as before (21 Nov.) i.e., southeasterly (270-360). At the end of cyclone i.e., on 25 Nov. wind direction decreased abruptly and the direction was southwesterly (90-0). At phase 3 (26-30 Nov.) i.e., during landfall, on 26<sup>th</sup> Nov. wind direction was northeasterly (180-270), on 27-28 Nov. the direction was southeasterly (270-360), on 29<sup>th</sup> Nov. wind direction was southwesterly (90-0) and at the end of landfall i.e., on 30<sup>th</sup> Nov. wind direction was southeasterly (270-360). From the above figure [Fig. 6.5(h)], it is observed that at phase 2 i.e., at cyclone period, at day to day the wind direction changed i.e., during cyclone the weather was very unstable.

**4.3.6 Cyclone 6**

Cyclone 6 is occurred from 5 November to 7 November 1996 over the Bay of Bengal. Its energy and variables are discussed here.

#### 4.3.6 (a): Energy components at different phases

##### Sensible heat (SH):

Fig. 6.6(a) shows the variation of sensible heat (SH) at different phases of cyclone 6. It is observed that at phase 1 (before occurrence) and phase 3 (after landfall) sensible heat was near about same. But at phase 2 (cyclone period) sensible heat was maximum than the other two phases. This was due to the higher atmospheric temperature at cyclone period

##### Potential energy (PE):

The variation of potential energy (PE) variation at different phases of cyclone 6 is shown in Fig. 6.6(b). From this figure, it is observed that PE was higher at phase 3 (after landfall) than at phase 1 (before occurrence) and at phase 2 (cyclone period). Here during landfall, low pressure slightly increased at the surface level that increased geo-potential height. So PE increased at the time of landfall.

##### Latent heat content (LHC):

Fig. 6.6(c) shows the variation of latent heat content (LHC) at different phases of cyclone 6. Here it is seen that LHC was higher at phase 2 (cyclone period) than at phase 1 (before occurrence). This was because at cyclone period temperature was high, water evaporate. So water vapor go lifted upward and then condensed and released latent heat. At cyclone period more cloud formed that released latent heat. So LHC was higher at cyclone period than the other two phases.

##### Kinetic energy (KE):

The variation of kinetic energy (KE) at different phases of cyclone 6 is shown in Fig. 6.6(d). It is found that KE was nearly zero at phase 1 (before occurrence). This was because, before occurrence the weather was calm i.e. there was no flow of wind. At phase 2 (cyclone period) KE slightly increased. This was because wind speed increased slightly at cyclone period. But at phase 3 (during landfall) KE was maximum due to the high wind speed during landfall.



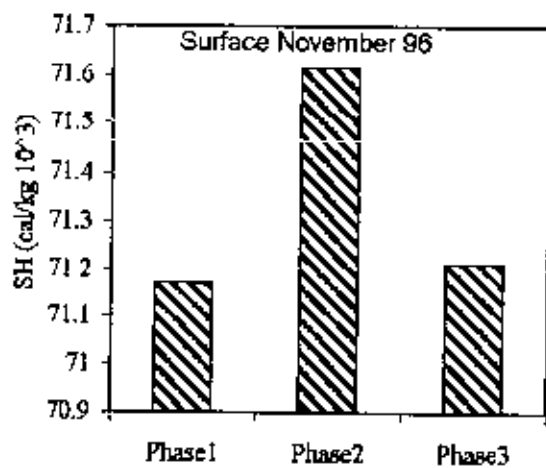


Fig. 6.6 (a): Sensible heat

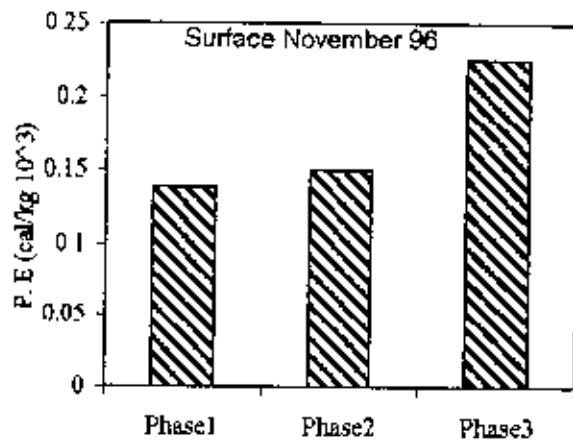


Fig. 6.6 (b): Potential energy

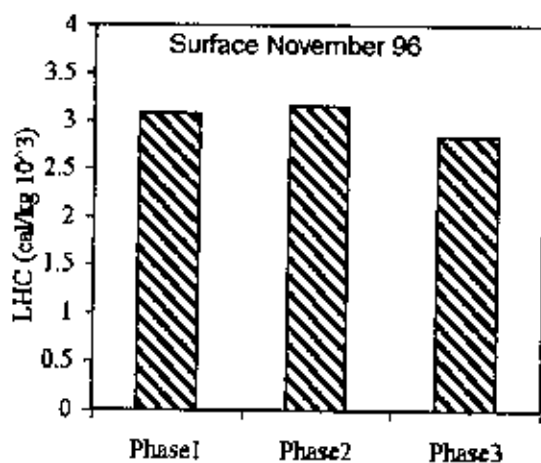


Fig. 6.6 (c): Latent heat content

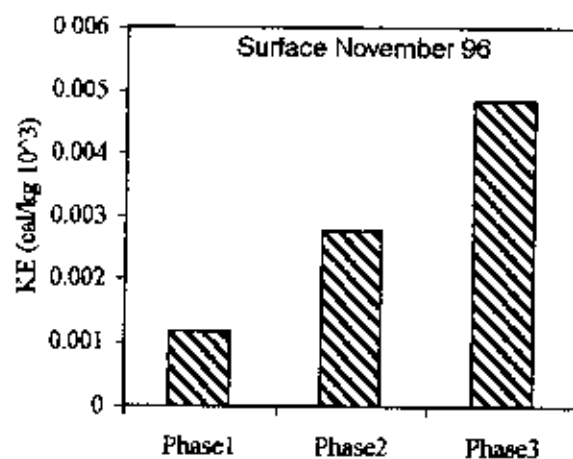


Fig. 6.6 (d): Kinetic energy

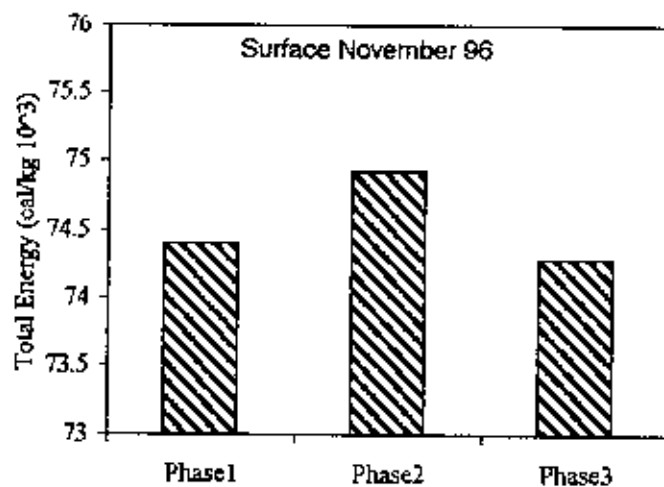


Fig. 6.6 (e): Total energy

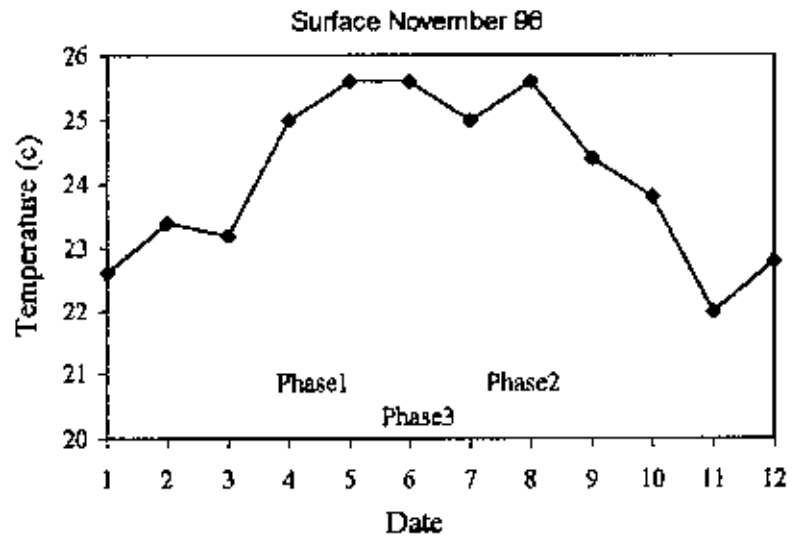


Fig. 6.6 (f): Time-Temperature graph

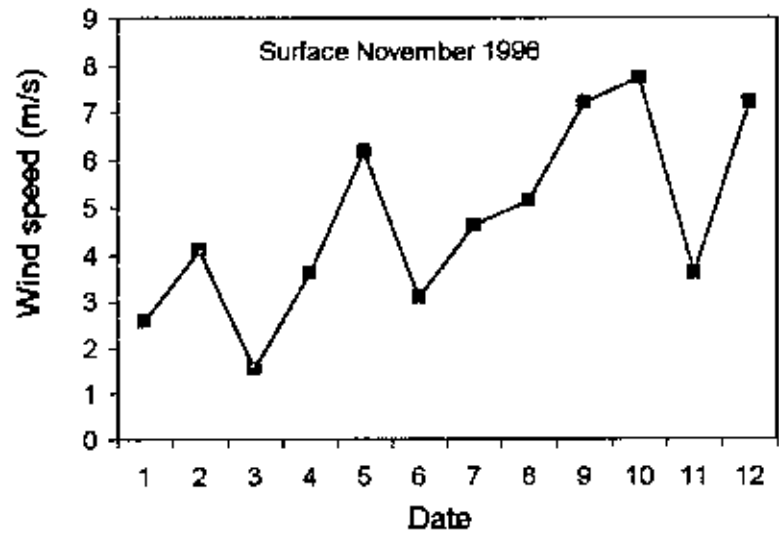


Fig. 6.6 (g): Time-Wind speed graph

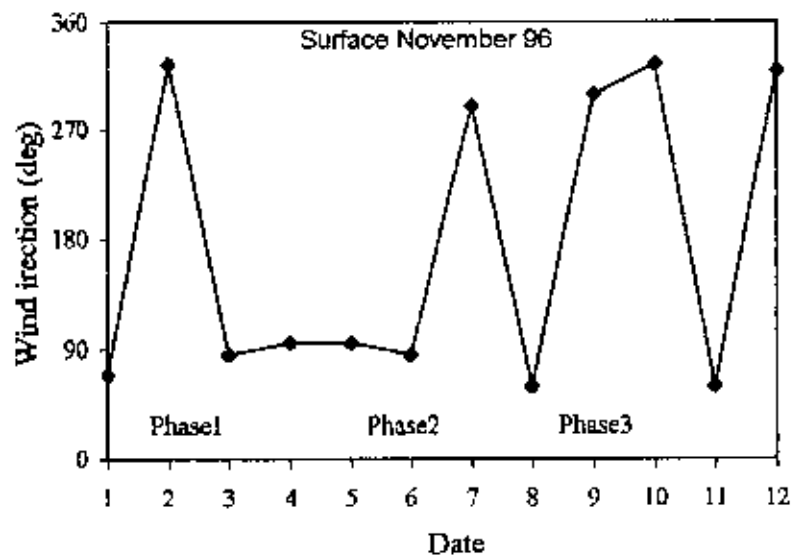


Fig. 6.6 (h): Time-Wind direction graph

**Total energy (TE):**

Fig. 6.6(c) shows the variation of total energy (TE) at different phases of cyclone 6. It is seen that total energy was slightly greater at phase 1 (before occurrence) than at phase 3 (after landfall). But during cyclone period (phase 2) total energy was maximum. This was due to the maximum sensible heat and latent heat content at cyclone period.

**4.3.6 (b): Variables at different phases****Temperature:**

Time-temperature graph at different phases of cyclone 6 is shown in Fig. 6.6(f). At phase 1 (1-4 Nov.) i.e., before occurrence temperature was near about same at first three days (1-3 Nov.) but at the initiation of cyclone i.e., 4<sup>th</sup> Nov. temperature increased abruptly. At phase 2 (5-7 Nov.) i.e., at cyclone period temperature was maximum and remained constant. This was because at cyclone period sensible heat was maximum. At phase 3 (8-12 Nov.) i.e., during landfall, it is observed that from day to day temperature decreased gradually.

**Wind speed:**

Fig. 6.6(g) shows time-wind speed graph at different phases of cyclone 6. At phase 1 (1-4 Nov.) it is observed that wind speed fluctuated. At phase 2 (5-7 Nov.) i.e., at cyclone period wind speed was higher for first day of cyclone (5<sup>th</sup> Nov.) compared to the other two days (6-7 Nov.) At phase 3 (8-12 Nov.) it is observed that wind speed increased gradually up to 10<sup>th</sup> Nov. It is also observed that wind speed was maximum at phase 3 for 9<sup>th</sup>, 10<sup>th</sup> and 12<sup>th</sup> Nov. For this reason KE was maximum at this phase i.e., during landfall.

**Wind direction:**

Time-wind direction graph at different phases of cyclone 6 occurring on 5-7 November is shown in Fig. 6.6(h). It is seen that at phase 1 (1-4 Nov.) on 2<sup>nd</sup> November wind direction was southeasterly (270-360) and at the initiation of cyclone i.e., on 3-4 Nov. wind direction was eastward i.e., westerly (90). At phase 2 (5-7 Nov.) i.e., cyclone period, on 5-6 Nov. wind direction remained same i.e., westerly (90) as that of the initiation of cyclone (3-4 Nov.) and at the end of cyclone i.e., on 7<sup>th</sup> Nov. it is seen that

wind direction was southeasterly (270-360). At phase 3 (8-12 Nov.), on 8<sup>th</sup> Nov. wind direction was southwesterly (90-0), on 9-10 Nov. it was southeasterly (270-360). On 11 Nov. wind direction was southwesterly (90-0) and on 12 Nov. wind direction was again southeasterly (270-360).

#### 4.3.7 Cyclone 7

Cyclone 7 is occurred from 28 November to 3 December 1996 over the Bay of Bengal. Its energy and variables are discussed here.

##### 4.3.7 (a): Energy components at different phases

###### Sensible heat (SH):

Fig. 6.7(a) shows the variation of sensible heat (SH) at different phases of cyclone 7. It is observed that at phase 1 (before occurrence) SH was slightly higher than at phase 2 (cyclone period). This is because temperature was slightly higher at the initiation of cyclone.

###### Potential energy (PE):

The variation of potential energy (PE) at different phases of cyclone 7 is shown in Fig. 6.7(b). Here PE was maximum at phase 1 (before occurrence). This was because geopotential height was maximum at this phase due to the higher temperature at the initiation of cyclone.

###### Latent heat content (LHC):

The variation of latent heat content (LHC) at different phases of cyclone 7 is shown in Fig. 6.7(c). Here it is seen that at phase 3 (after landfall) LHC was greater than phase 1 and phase 2. Because during landfall more cloud formed that released latent heat and rainfall occurs.

###### Kinetic energy (KE):

The variation of kinetic energy (KE) at different phases of cyclone 7 is shown in Fig. 6.7(d). It is showed that at phase 1 (before occurrence) KE was higher than at phase 2

(cyclone period). But it is observed that at phase 3 (during landfall) KE was maximum. This was because during landfall wind speed was high that increased KE.

#### **Total energy (TE):**

The variation of total energy (TE) at different phases of cyclone 7 is shown in Fig. 6.7(e). Here it is seen that at phase 1 (before occurrence) total energy was a little bit greater than at phase 2 (cyclone period). This was because at the initiation of cyclone temperature was higher that increased SH and PE and so increased total energy at phase 1.

#### **4.3.7 (b): variables at different phases**

##### **Temperature:**

Time-temperature graph at different phases of cyclone 7 is shown in Fig. 6.7(f). Here it is observed that at phase 1 (23-27 Nov.) i.e., before occurrence, at first temperature decreased from 23-25 Nov. But at the initiation of cyclone i.e., on 26-27 Nov. temperature increased slightly. At phase 2 (28 Nov-3 Dec.) i.e., at cyclone period temperature remained constant for first two days of cyclone (28-29 Nov.) then decreased on 30 Nov. Beyond 30 November temperature increased gradually up to 4<sup>th</sup> Dec. i.e., at the end of cyclone. At phase 3 (4-8 Dec ) i.e., during landfall temperature decreased gradually.

##### **Wind speed:**

Fig. 6.7(g) shows time-wind speed graph at different phases of cyclone 7. At phase 1 (23-27 Nov.) i.e., before occurrence it is observed that wind speed fluctuated i.e., at day to day wind speed changed. At phase 2 (28 Nov.-3 Dec.) wind speed was nearly same for all the days except 2<sup>nd</sup> Dec. But at phase 3 (4-9 Dec.) i.e., during landfall wind speed increased gradually and attained the highest value on 6<sup>th</sup> Dec. For this reason, during landfall KE increased.

##### **Wind direction:**

Fig. 6.7(h) shows time-wind direction graph at different phases of cyclone 7 occurring on 28<sup>th</sup> November-3<sup>rd</sup> December 1996. From this figure it is observed that, at

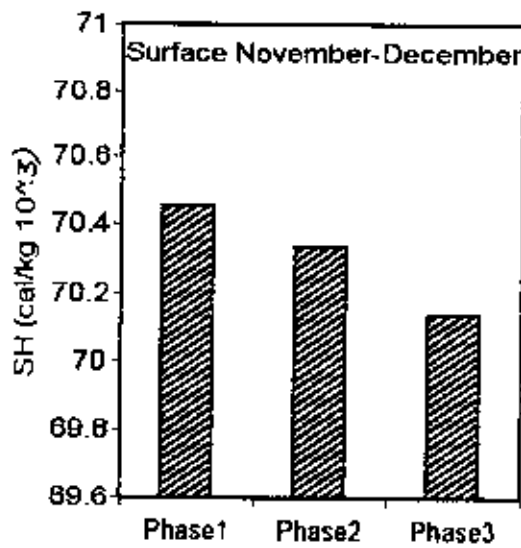


Fig. 6.7 (a): sensible heat

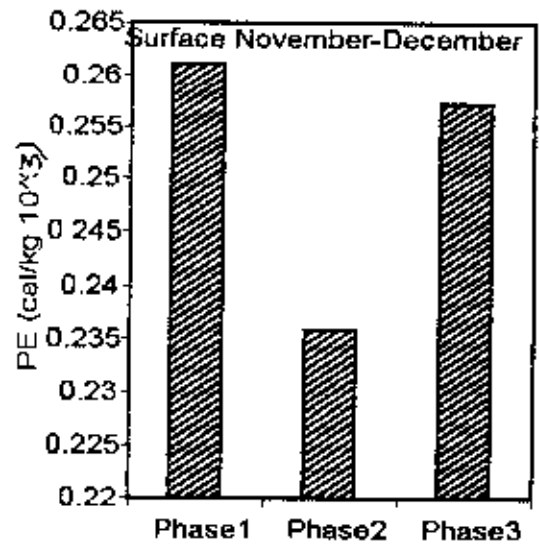


Fig. 6.7 (b): Potential energy

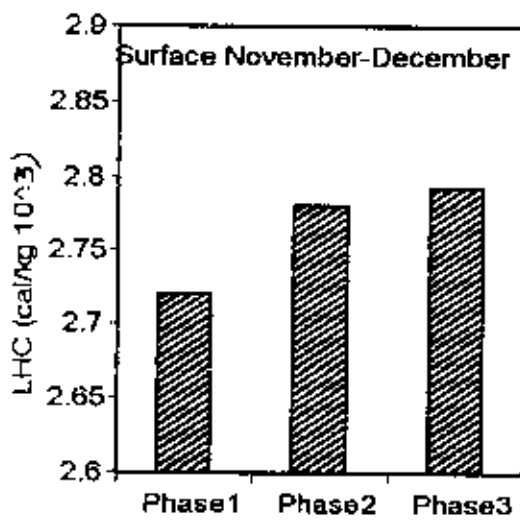


Fig. 6.7 (c): Latent heat content

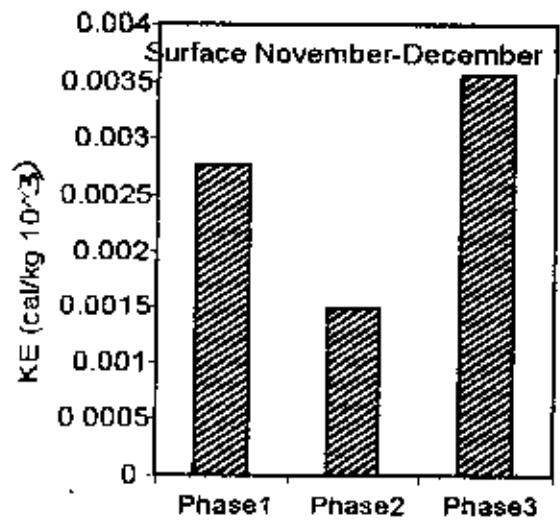


Fig. 6.7 (d): Kinetic energy

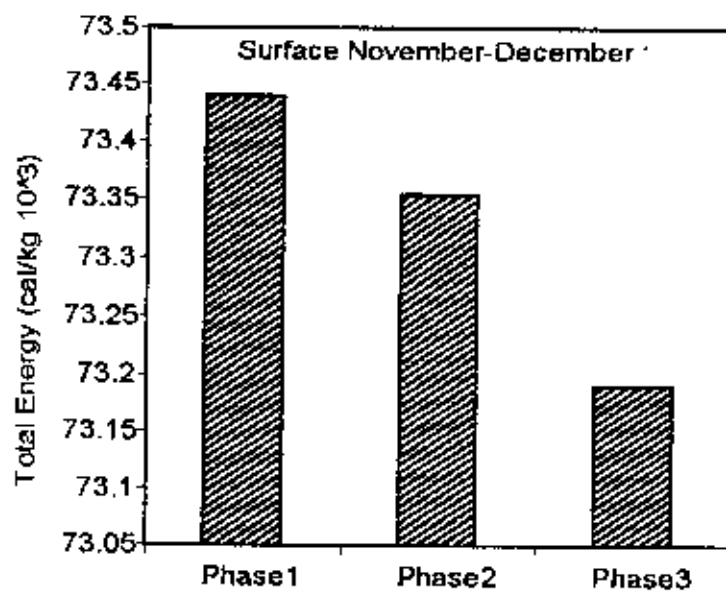


Fig. 6.7 (e): Total energy

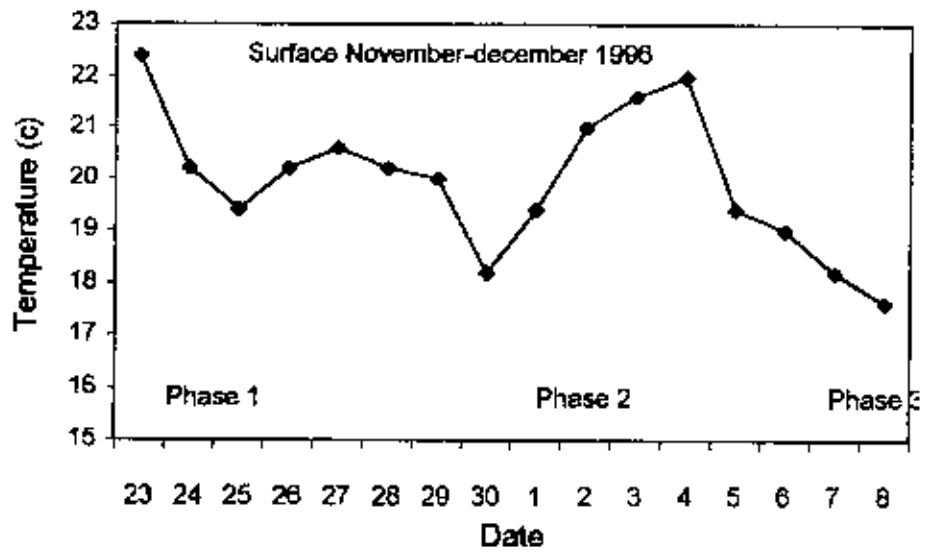


Fig. 6.7 (f). Time-temperature graph

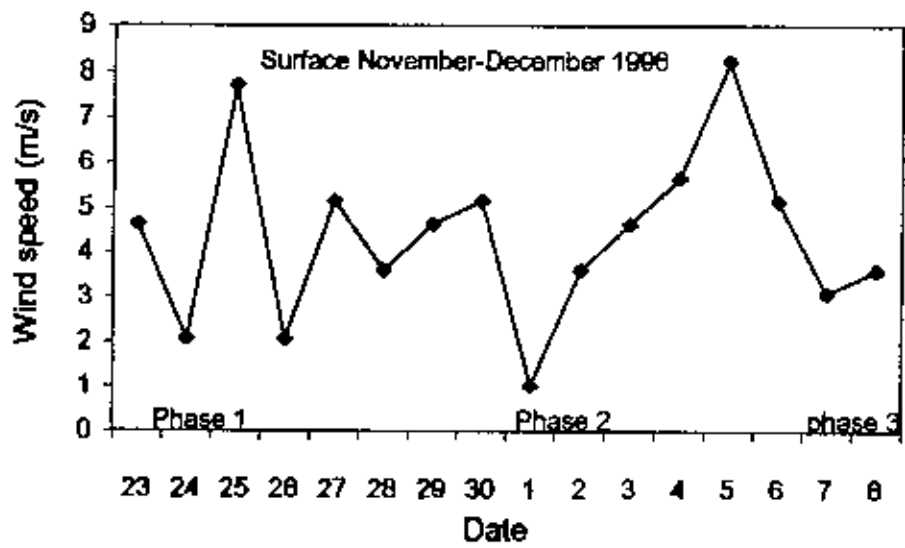


Fig 6.7i (g) Time-wind speed graph

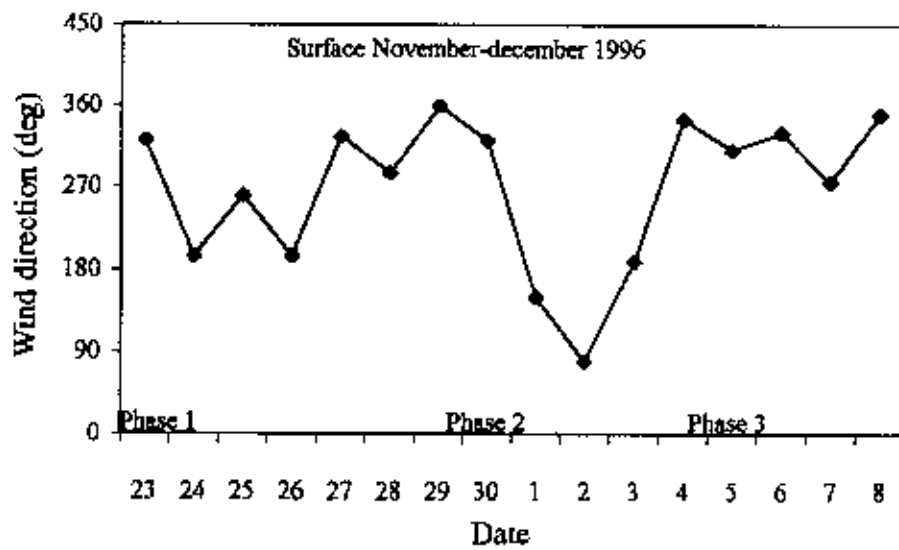


Fig. 6.7i (h). Time-wind direction graph

phase 1 (23-27 Nov.) i.e., before occurrence, on 23<sup>rd</sup> Nov. wind direction was southeasterly (270-360), on 24-26 November wind direction was northeasterly (270-180) and at the initiation of cyclone, wind direction was southeasterly (270-360). At phase 2 (28 Nov.-3Dec.) i.e., at cyclone period, on 28-30 Nov. wind direction remained same i.e., southeasterly (270-360) as that of the initiation of cyclone. On 1-2 Dec. wind direction was norwesterly (180-90) and at the end of cyclone period wind direction was northeasterly (180-270). At phase 3 (4-8 Dec.) wind direction was southeasterly (270-360).



# CHAPTER-5

## ENERGY BUDGET

## CHAPTER-5

### Energy Budget

In this chapter energy budget for all the analyzed 7 cyclones is discussed. The energy calculated at the station Dhaka is compared with that at the station Chittagong.

Fig. 7.1 shows energy budget of sensible heat (SH) for seven cyclones. From this figure it is seen that out of this seven cyclones maximum value of SH was occurred during cyclone 4 which occurred on 29.4.94-3.5.94. This maximum SH signifies that atmospheric temperature was maximum during cyclone 4 compared to the other cyclone. The minimum value of SH was occurred during cyclone 2 (on 16.12.90-18.12.90). This minimum SH means that at that time atmospheric temperature was low during cyclone 2 compared to the other cyclone. The average SH was little bit high during cyclone 4 while it was low during cyclone 2.

Fig. 7.2 shows energy budget of potential energy (PE) for seven cyclone. From this seven cyclone it is observed that PE was maximum during cyclone 1 which occurred on 5.5.90-9.5.90. This maximum PE signifies the highest geopotential height during cyclone 1. PE was minimum during cyclone 2 which occurred on 16.12.90-18.12.90. The average potential energy was also high in cyclone 1. From Fig. 6.2, it is also observed that PE was nearly same from cyclone 2 – cyclone 7. This was because geopotential height was nearly same for cyclone 2 – cyclone 7.

Energy budget of latent heat content (LHC) for seven cyclones is shown in Fig. 7.3. It is seen that LHC was maximum during cyclone 2 which occurred on 16.12.90-18.12.90. This was because during cyclone 2, there were more incursion of water vapor and then condensed that increased LHC. It was minimum during cyclone 7 which occurred on 28.11.96-3.12.96. So, during cyclone 7 there was less cloud formation and rainfall was low. Average LHC was also high during cyclone 2. So, more rainfall occurred during cyclone 2.

Energy budget of kinetic energy (KE) is shown in Fig. 7.4. From this figure it is seen that KE was maximum during cyclone 1 which occurred on 5.5.90-9.5.90. The average KE was also high during cyclone 1 compared to the other cyclone. This maximum KE signifies the high wind speed during cyclone 1. Kinetic energy was

minimum during cyclone 4 which occurred on 29.4.94-3.5.94. It is seen that wind speed was very low during cyclone 4 compared to the other cyclone.

Energy budget of total energy is shown in Fig. 7.5. It is observed that total energy was maximum during cyclone 1 which occurred on 5.5.90-9.5.90. This maximum total energy was due to the maximum sensible heat, maximum potential energy and maximum kinetic energy. Total energy was minimum during cyclone 2 (which occurred on 16.12.90-18.12.90) and during cyclone 5 (which occurred on 21.11.95-25.11.95). Here it is clear that total energy was large for pre-monsoon cyclones (cyclone 1, cyclone 3 and cyclone 4) than that of post-monsoon cyclones (cyclone 2, cyclone 5, cyclone 6 and cyclone 7).

Energy budget of zonal flux of dry static energy (ZFDSE) for seven cyclones is shown in Fig. 7.6. It is seen that ZFDSE was maximum during cyclone 1 which occurred on 5.5.90-9.5.90. This was because during cyclone 1 sensible heat and potential energy was large during cyclone 1. This maximum ZFDSE was also due to the maximum zonal wind component during cyclone 1 compared to the other cyclone. ZFDSE was minimum in cyclone 5 which occurred on 21.11.95-25.11.95. This was because during cyclone 5 wind speed was very low that reduced ZFDSE. It is also observed that in cyclone 5 sensible heat and potential energy was low. So ZFDSE during cyclone 5 was minimum. The average ZFDSE was also high during cyclone 1 compared to the other cyclone. From Fig. 6.6 it is also observed that for every cyclone (cyclone 1-cyclone 7) ZFDSE was positive (eastward) i.e., for every cyclone zonal wind component was westerly.

Fig. 7.7 shows energy budget of zonal flux of moist static energy (ZFMSE) for seven cyclones. It is seen that ZFMSE was maximum during cyclone 4 which occurred on 29.4.94-3.5.94. Because during cyclone 4 sensible heat was maximum and the zonal wind component was also high. ZFMSE was minimum (negative and westward) during cyclone 5 which occurred on 21.11.95-25.11.95. This was because during cyclone 5 sensible heat and potential energy was lower and zonal wind component was also lower and negative (westward).

Energy budget of meridional flux of dry static energy (MFDSE) for seven cyclones is shown in Fig. 7.8. From this figure it is seen that MFDSE was maximum in cyclone 5 which occurred on 21.11.95-25.11.95. This maximum MFDSE was due to the maximum meridional wind component in the positive direction during cyclone 5.

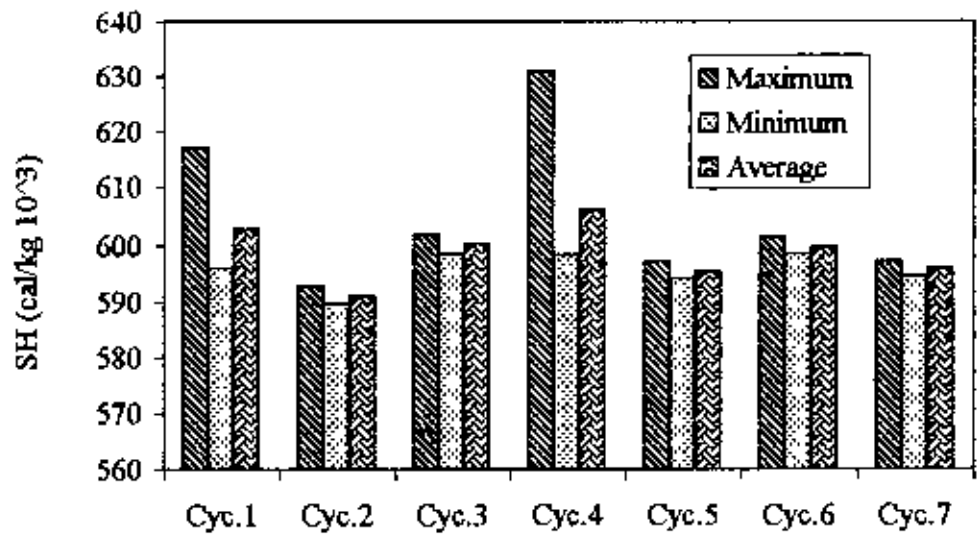


Fig. 7.1 Sensible heat

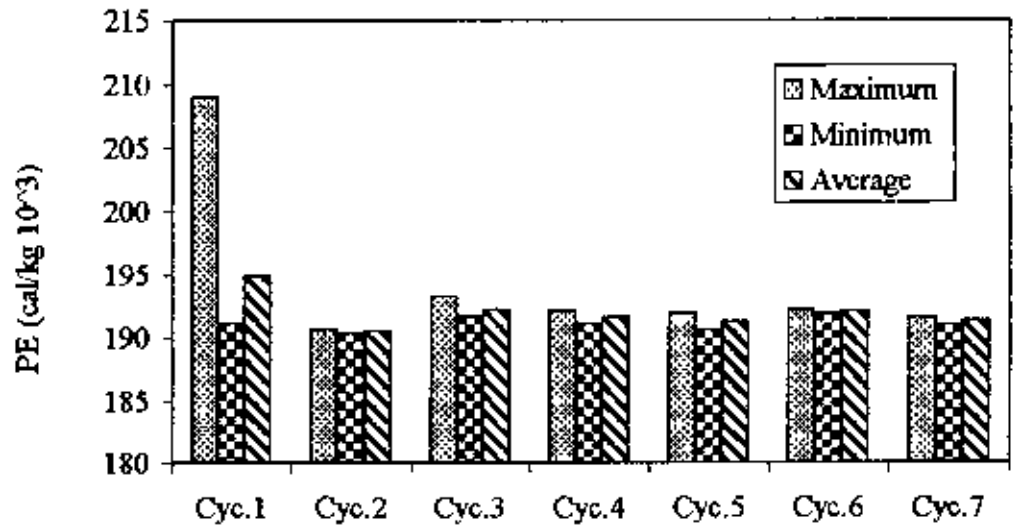


Fig. 7.2 Potential energy

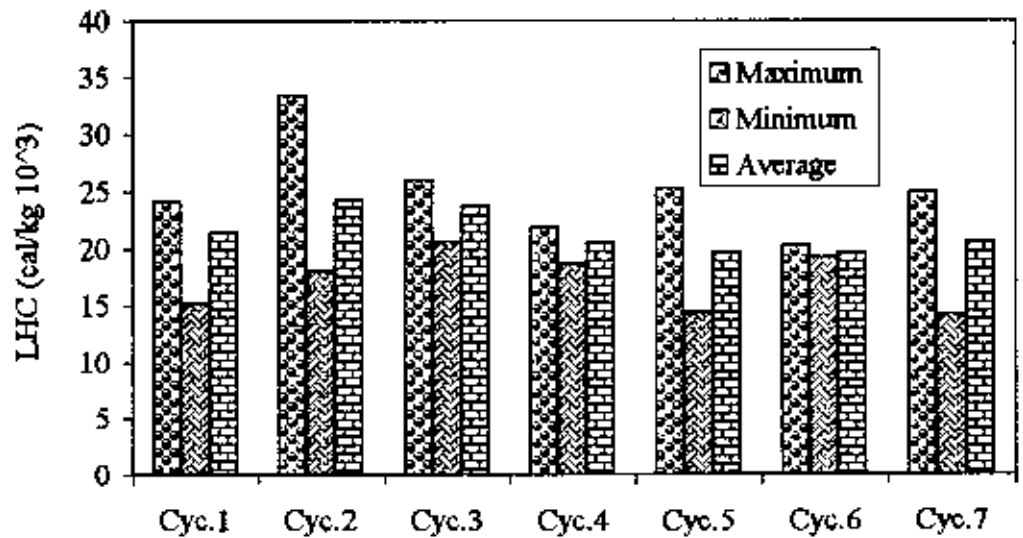


Fig. 7.3 Latent heat content

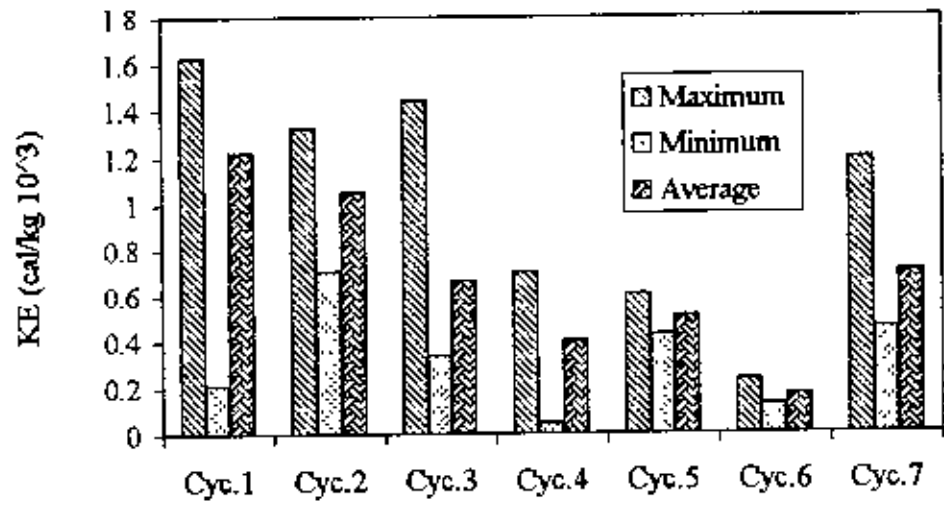


Fig. 7.4 Kinetic energy

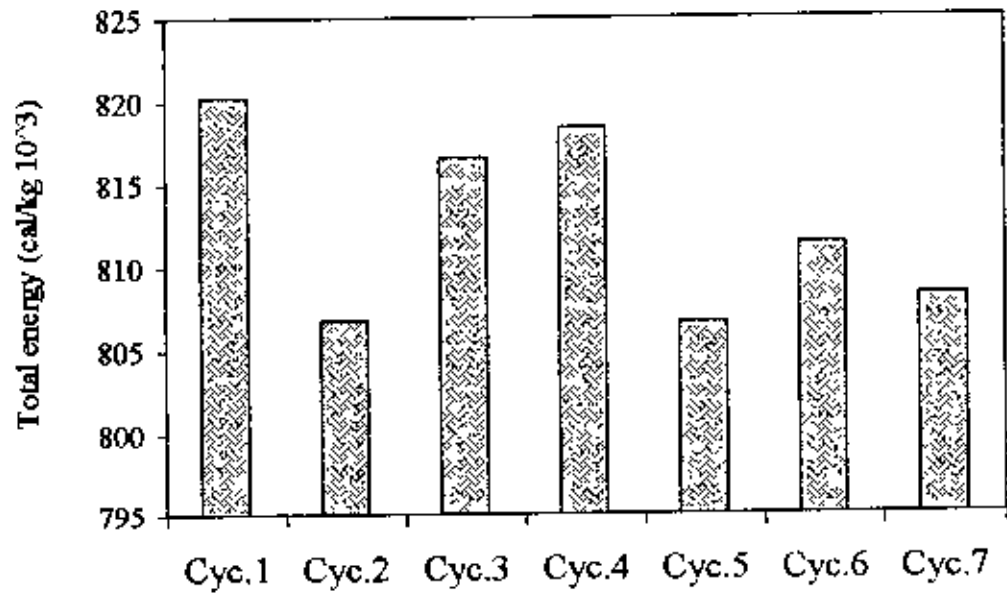


Fig. 7.5 Total energy

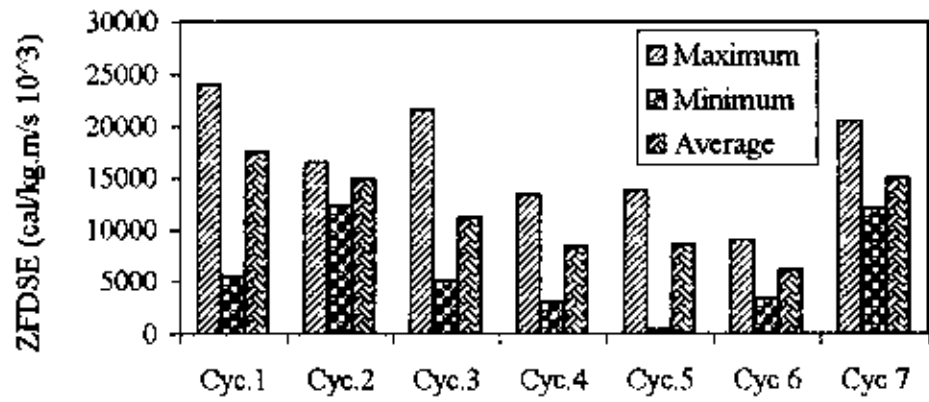


Fig. 7.6 Zonal fluxes of dry static energy

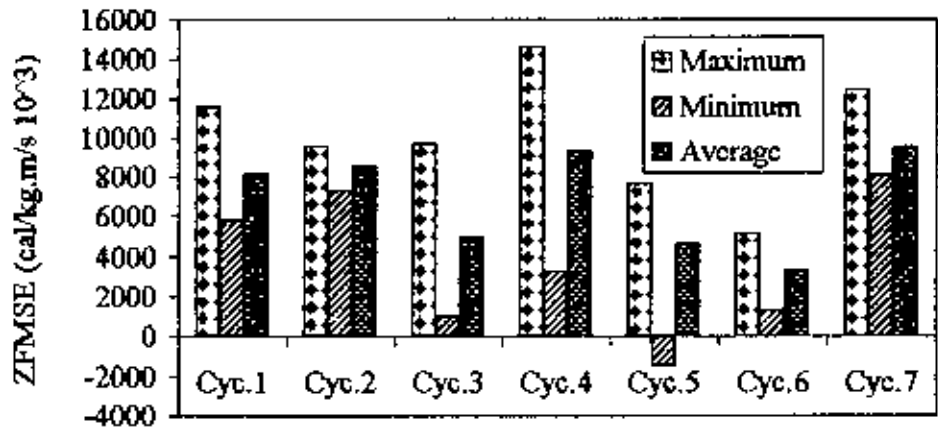


Fig. 7.7 Zonal fluxes of moist static energy

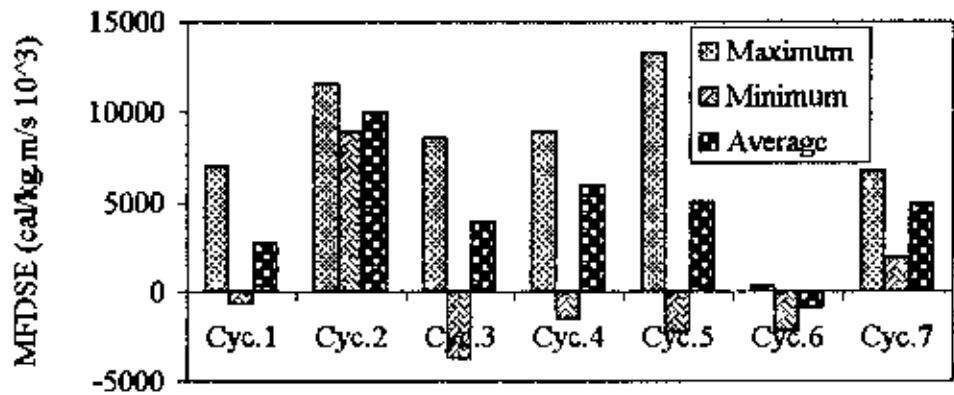


Fig. 7.8 Meridional fluxes of dry static energy

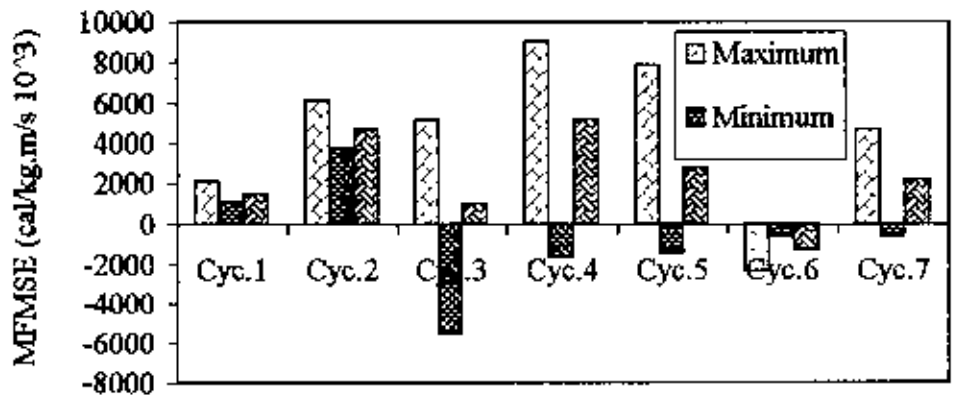


Fig. 7.9 Meridional fluxes of moist static energy

MFDSE was minimum (negative and southward) during cyclone 3 which occurred on 25.4.91-30.4.91 because of higher meridional wind component in the negative (southward) direction.

Fig. 7.9 shows meridional flux of moist static energy (MFMSE) for seven cyclones. It is seen that during cyclone 4 (which occurred on 29.4.94-3.5.94) MFMSE was maximum. This was because, it is seen that during cyclone 4 sensible heat was maximum and meridional wind component was also higher in the positive (northward) direction. MFMSE was minimum (negative and southward) in cyclone 3 which occurred on 25.4.91-30.4.91. This was because during cyclone 3 meridional wind component was higher in the negative (southward) direction. Average MFMSE was also higher during cyclone 4 due to higher (average) sensible heat and meridional wind component.

Fig. 7.10(a-e) shows comparison of energy budget of sensible heat (SH) between Dhaka and Chittagong stations for five cyclones. From Fig. 7.10(a) it is seen that during cyclone 1 (which occurred on 5.5.90-9.5.90) SH was maximum at Chittagong (cyc.1c). This was because at cyclone period atmospheric temperature was high at Chittagong. Sensible heat was minimum at Dhaka (cyc.1) due to low temperature at Dhaka compared to Chittagong. This indicates that cyclone 1 moved more northward than northeastward.

Fig. 7.10(b) shows comparison of SH between Chittagong and Dhaka for cyclone 3. From this figure it is seen that SH was maximum at Chittagong (cyc.3c) for cyclone 3 which occurred on 25.4.91-30.4.91. This maximum SH was due to the highest temperature at Chittagong. Minimum SH was observed at Dhaka (cyc.3) because of low temperature compared to Chittagong. This indicates that the movement of cyclone 3 was similar to that of cyclone 1.

Comparison of sensible heat (SH) between Chittagong and Dhaka for cyclone 4 (which occurred on 29.4.94-3.5.94) is shown in Fig.7.10(c). Here SH was maximum at Dhaka (cyc.4) compared to Chittagong (cyc.4c). Here it is seen that during cyclone 4 atmospheric temperature was high at Dhaka. And it is also seen that SH was minimum at Chittagong (cyc.4c). This indicates that cyclone 4 moved northeastward than northward.

Fig. 7.10(d) shows comparison of SH between Chittagong and Dhaka for cyclone 6 which occurred on 5.11.96-7.11.96. From this figure it is seen that SH was maximum at

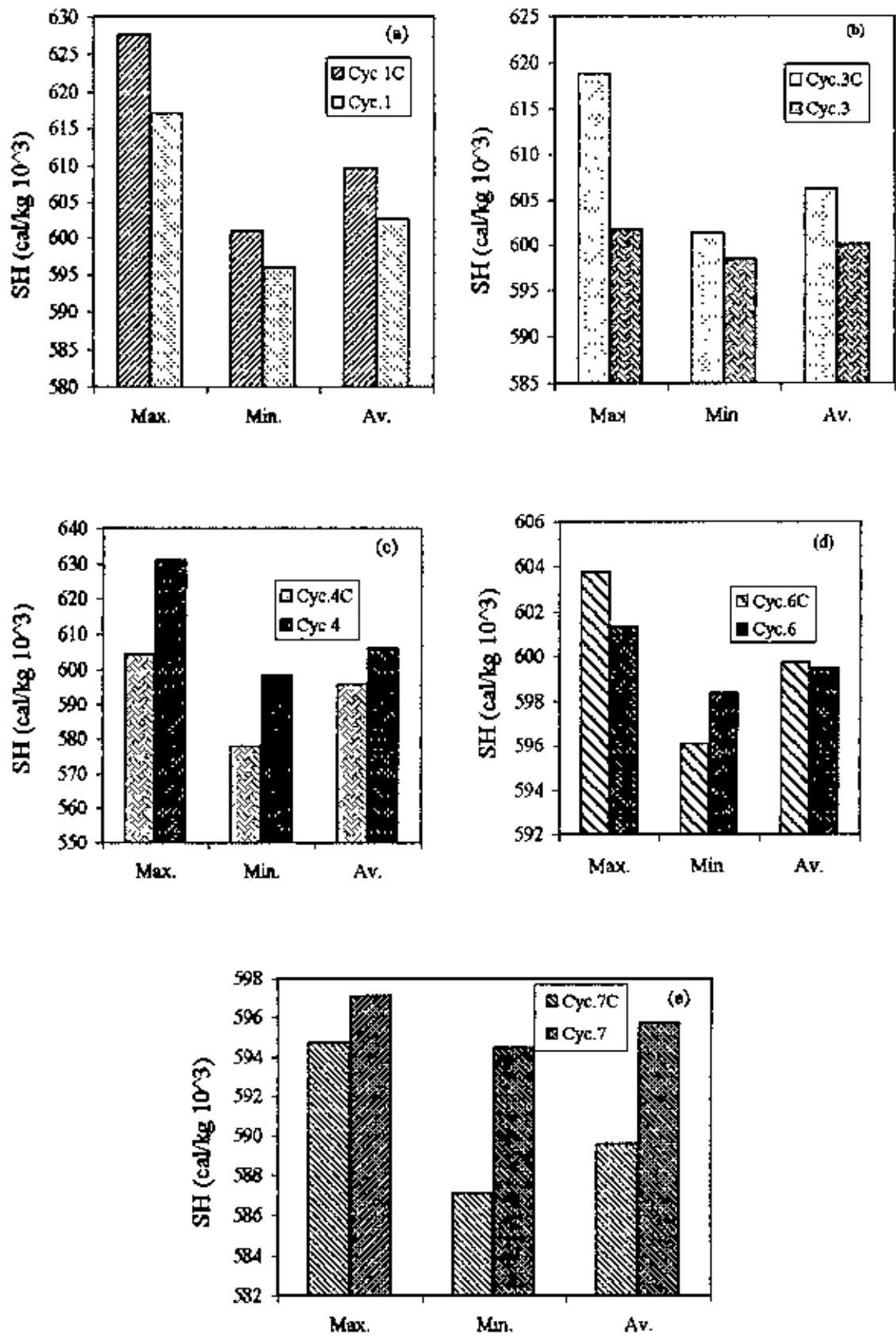


Fig 7.10 (a-e) Sensible heat



Chittagong (cyc.6c) compared to Dhaka (cyc.6). This maximum SH was for highest atmospheric temperature at Chittagong. Sensible heat was also minimum at Chittagong (cyc.6c). This was because for the other day of cyclone temperature was also low at Chittagong.

Comparison of sensible heat between Chittagong and Dhaka for cyclone 7 which occurred on 28.11.96-3.12.96 is shown in Fig. 7.10(e). Here SH was maximum at Dhaka (cyc.7) compared to Chittagong (cyc.7c). Here it is seen that for cyclone 7 temperature was high at Dhaka. Minimum SH observed at Chittagong (cyc.7c) due to low temperature compared to Dhaka. The movement of cyclone 7 was similar to that of cyclone 4.

Comparison of energy budget on potential energy (PE) between Chittagong and Dhaka is shown in Fig. 7.11(a-e). From Fig. 7.11(a) it is seen that for cyclone 1 PE was maximum at Dhaka (cyc.1) compared to Chittagong (cyc.1c). This was due to the highest geopotential height at Dhaka. It is observed that PE was minimum at Chittagong (cyc.1c) because of lower geopotential height. Average PE was also high in Dhaka (cyc.1).

Fig. 7.11(b) shows comparison of PE between Chittagong and Dhaka for cyclone 3. It is seen that PE was maximum both at Chittagong (cyc.3c) and Dhaka (cyc.3) and was almost same. Minimum PE was at Chittagong (cyc.3c) because of lower geopotential height. It is also observed that at Dhaka maximum, minimum and average PE was same due to no change of geopotential height.

Fig. 7.11(c) shows comparison of PE between Chittagong and Dhaka for cyclone 4. It is seen that at Chittagong (cyc.4c) PE was maximum. Here in Chittagong geopotential height was higher. Minimum PE was also at Chittagong (cyc.4c). This was because for another day of cyclone geopotential height was lower at Chittagong. But average PE was higher at Dhaka (cyc.4)

Comparison of PE between Chittagong and Dhaka for cyclone 6 is shown in Fig. 7.11(d). Here maximum PE was at Chittagong (cyc.6c) compared to Dhaka (cyc.6). Minimum PE was also at Chittagong (cyc.6c). Average PE was higher at Dhaka (cyc.6).

Fig. 7.11(e) shows comparison of PE between Chittagong and Dhaka for cyclone 7. Here it is seen that PE was maximum at Dhaka (cyc.7) compared to Chittagong. But PE was minimum at Chittagong (cyc.7c). Average PE was higher at Dhaka (cyc.7) due to higher geopotential height.

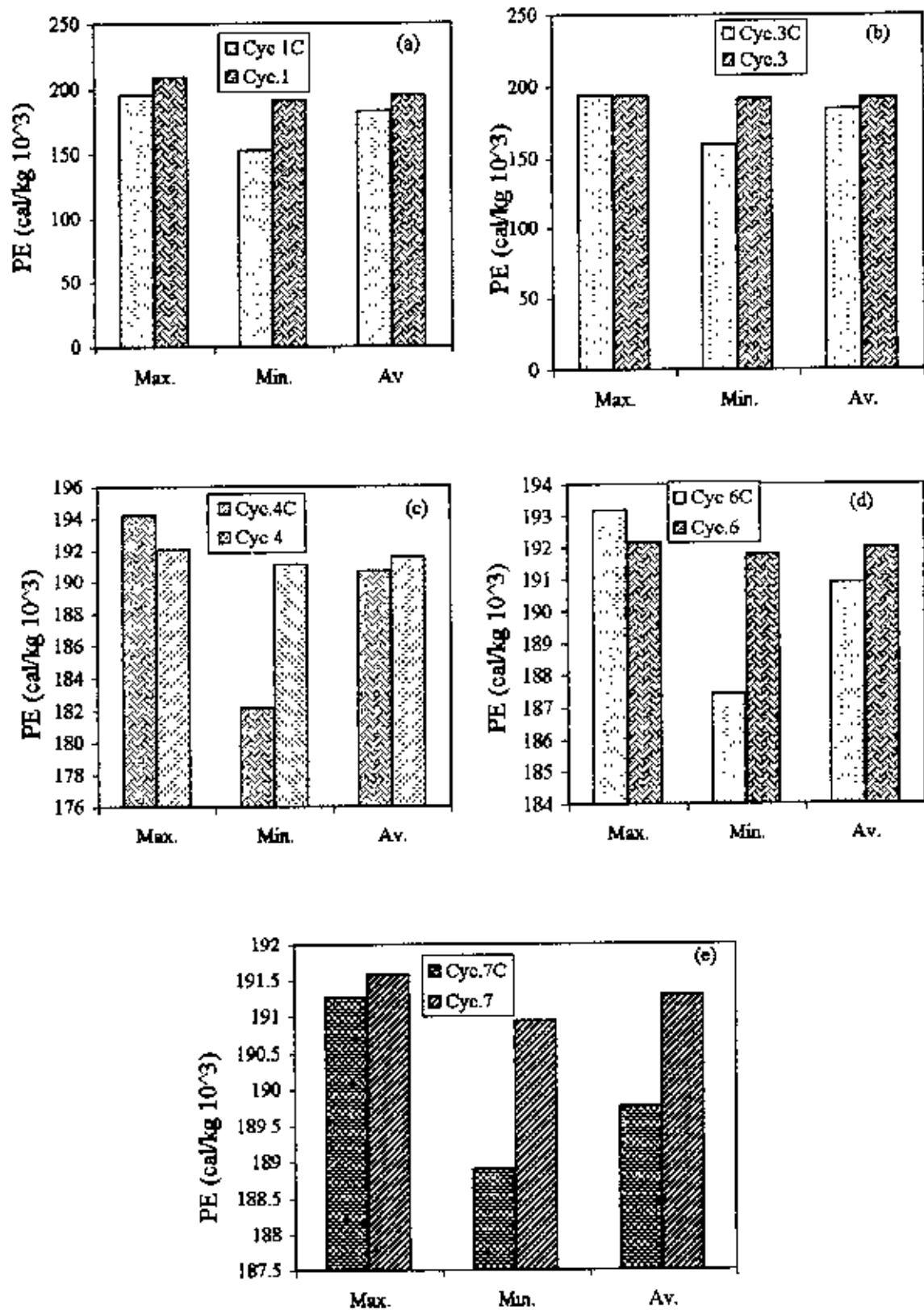


Fig. 7.11(a-e): Potential energy

From the Fig. 7.11(a-c), it is seen that for five cyclones PE was maximum for cyclone 1 and cyclone 7 at Dhaka. Potential energy was maximum for cyclone 4 and cyclone 6 at Chittagong. And maximum PE was same for cyclone 3 both at Chittagong (cyc.3c) and Dhaka (cyc.3) due to the same geopotential height. It is also seen that for all of five cyclones there was a common feature that PE was minimum at Chittagong compared to Dhaka and PE was higher at Dhaka compared to Chittagong.

Fig. 7.12(a-e) shows comparison of latent heat content (LHC) between Chittagong and Dhaka for five cyclones. From Fig. 6.12(a-d) it is observed that LHC was maximum at Chittagong compared to Dhaka. This was because at the initiation of cyclone ocean surface temperature increases that evaporate water. And at Chittagong there was more incursion of water vapor then condensed and released latent heat. So out of five cyclones LHC at Chittagong was maximum for four cyclone [Fig. 7.12(a-d)]. But for cyclone 7 [Fig. 7.12(e)] maximum LHC was almost the same for both Chittagong (cyc.7c) and Dhaka (cyc.7). For all five cyclones LHC was minimum at Dhaka due to less cloud formation. And average LHC was also higher at Chittagong for all five cyclones. From Fig. 7.12(a-e) it is seen that at Chittagong LHC was highest. So at Chittagong more cloud formed and heavy rainfall occurred compared to Dhaka.

Comparison of kinetic energy (KE) between Chittagong and Dhaka is shown in Fig. 7.13(a-e). Here it is seen that out of these five cyclones Kinetic energy was maximum at Dhaka for three cyclones i.e., for cyclone 1 (cyc.1), cyclone 3 (cyc.3) and cyclone 7 (cyc.7). For cyclone 4 (cyc.4c) and cyclone 6 (cyc.6c) KE was maximum at Chittagong. It is also observed that at Dhaka average KE was also higher for all five cyclones except cyclone 6 compared to Chittagong. For all five cyclones KE was minimum at Dhaka due to lower wind speed. The wind speed at the right side was strong compared to forward.

Comparison of total energy (TE) between Chittagong and Dhaka is shown in Fig. 7.14(a-e). It is seen that out of five cyclones total energy was high for three cyclones i.e., for cyclone 1 (cyc.1c), cyclone 3 (cyc.3c) and cyclone 6 (cyc.6c) at Chittagong compared to Dhaka. For the other two cyclones i.e., for cyclone 4 (cyc.4) and cyclone 7 (cyc.7) total energy was high at Dhaka compared to Chittagong. The effect of sensible heat is much more on total energy. We observed that total energy was maximum whose sensible heat

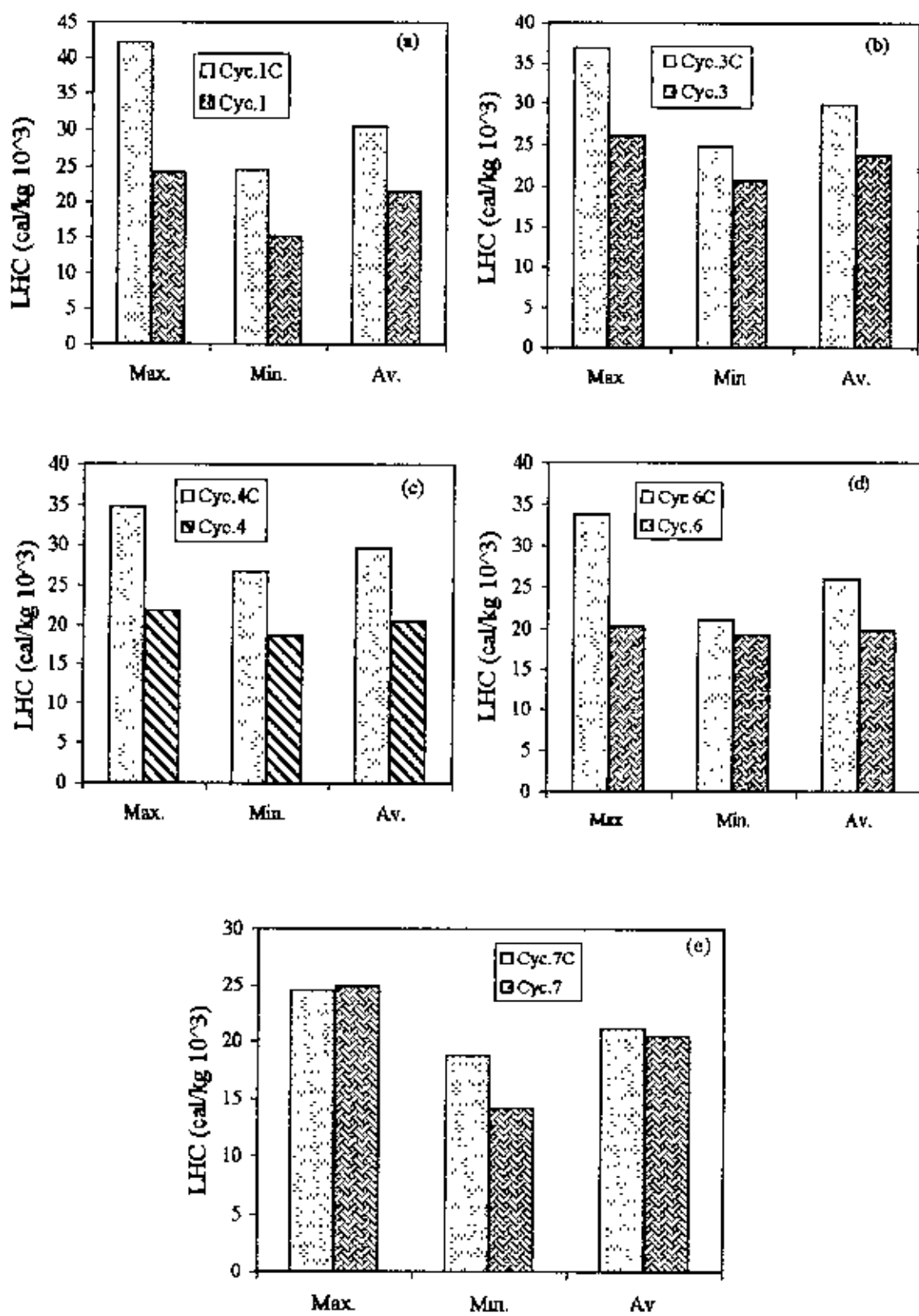


Fig. 7.12 (a-e): Latent heat content

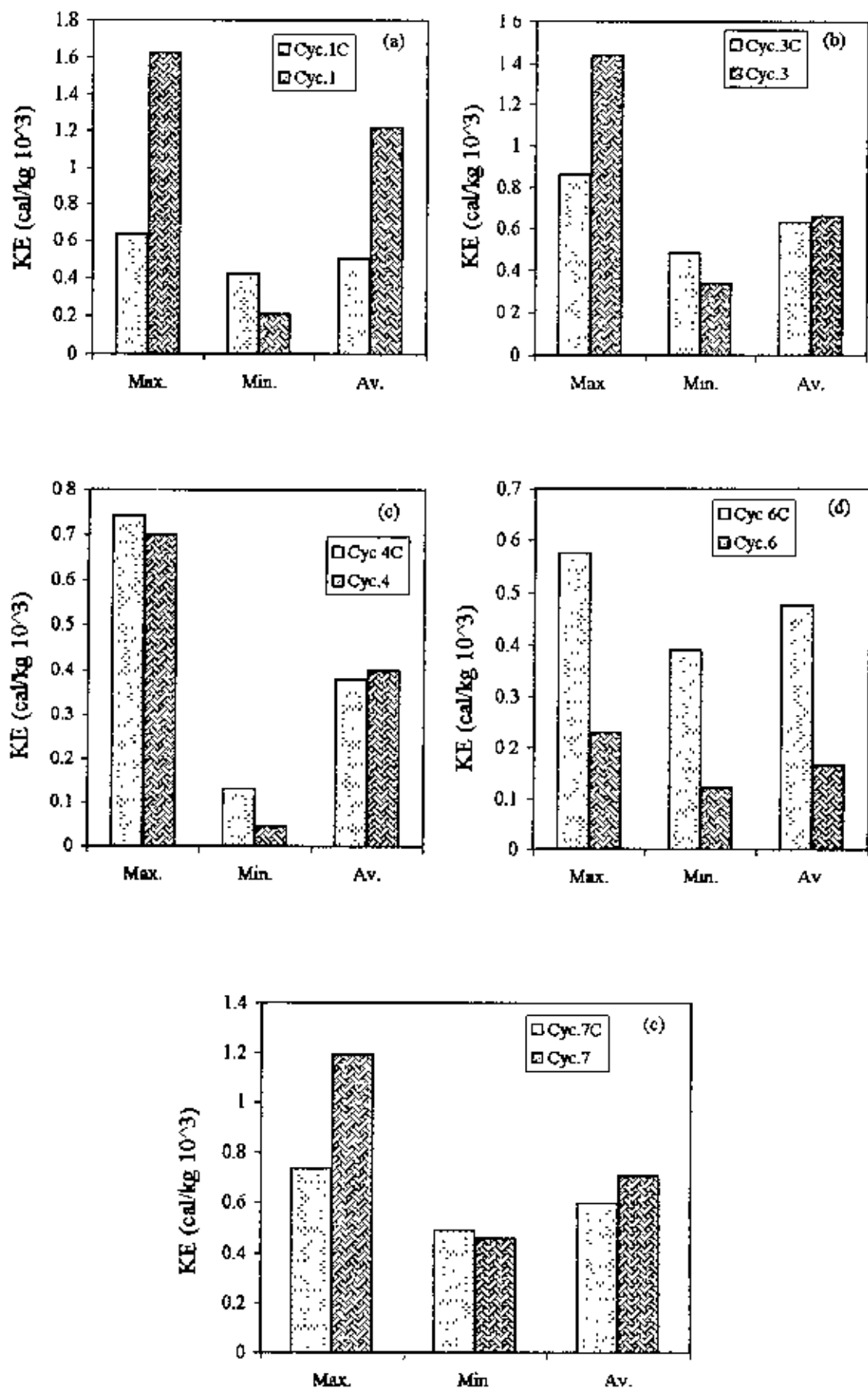


Fig. 7.13 (a-e): Kinetic energy

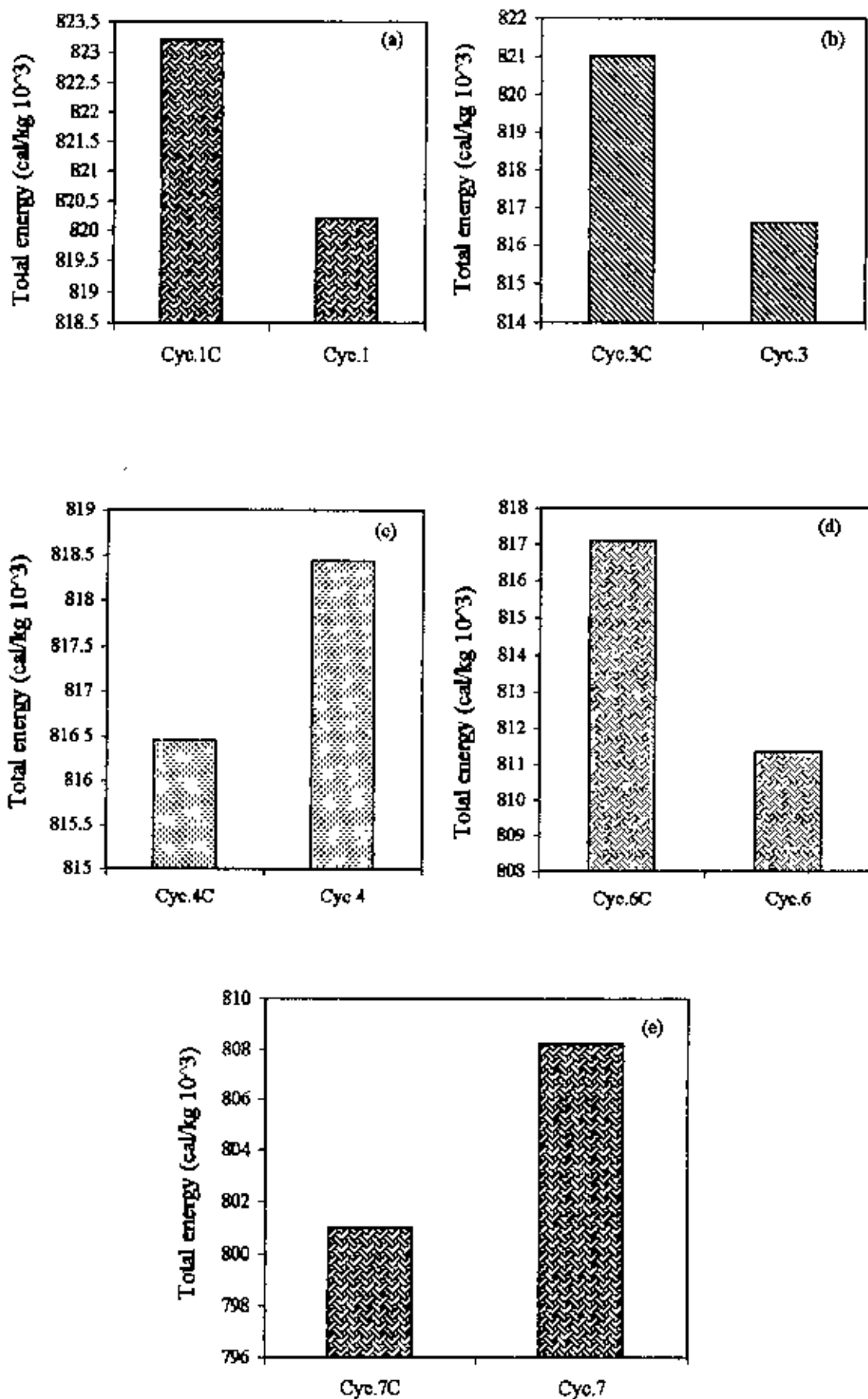


Fig. 7.14 (a-e): Total energy

was higher. From Fig. 7.14(a-e) we observed that for most of the cyclone total energy was higher at Chittagong. This is because Chittagong is situated near the ocean and when cyclone formed temperature increased that increased sensible heat and water evaporate that also increased latent heat content. So total energy was higher at Chittagong for most of the cyclone.

# CHAPTER-6

## CONCLUSIONS

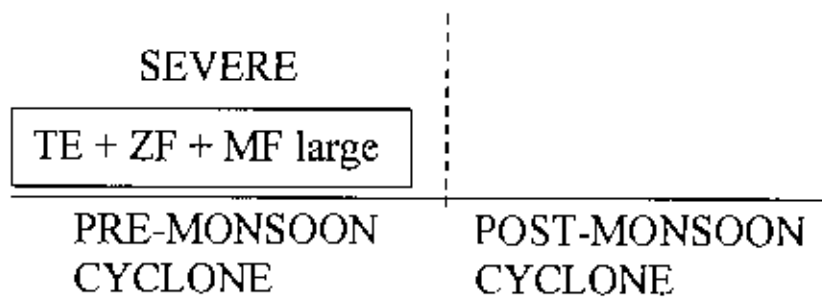
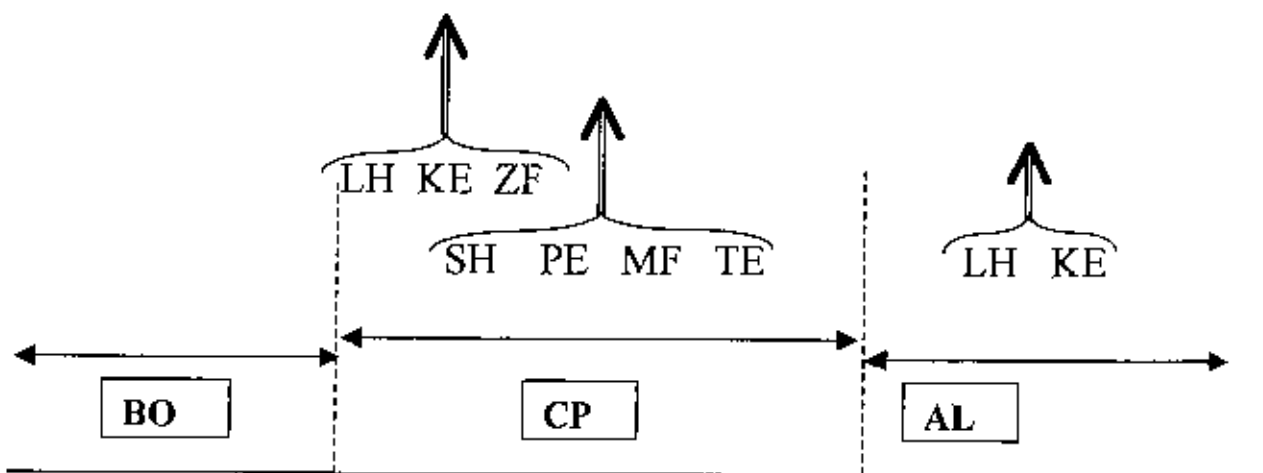
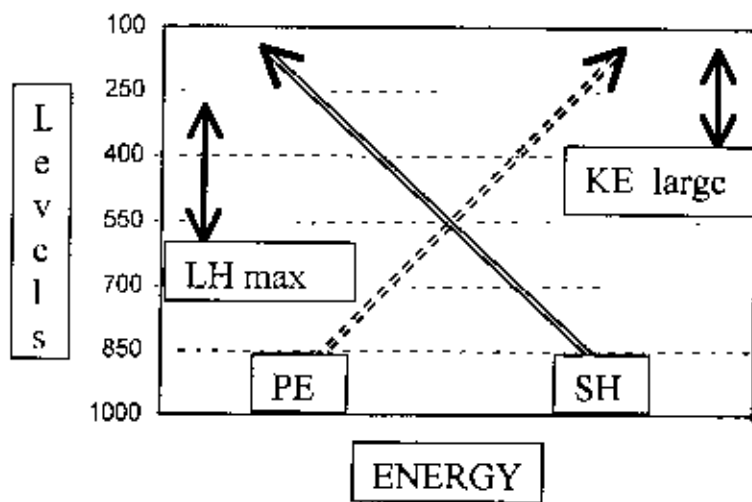


## CONCLUSIONS

From the above study the following conclusions can be drawn:

- i) The sensible heat decreased with the increase of height. For most of the cyclones it was large during the cyclone period compared to the other phases.
- ii) The potential energy increased with the increase of height. For most of the cyclones it was maximum during cyclone period.
- iii) There was almost no variation observed for latent heat at different phases at the lower level. For most of the cyclones latent heat content increased at the starting of cyclone and after landfall. It was maximum at the middle troposphere (500-250 mb).
- iv) For all of three phases kinetic energy increased from middle to upper level and was nearly zero from lower to middle troposphere. For most of the cyclones kinetic energy was maximum at the initiation of cyclone period and after landfall. It was large at 300-150 mb level.
- v) Westward zonal flux was observed up to ~ 700 mb level. Beyond this level it was eastward. For most of the cyclones the magnitude of zonal flux was found large just before starting cyclone period and was maximum at 250-150 mb level.
- vi) Meridional flux varied between northward and southward for both before occurrence and during cyclone period. Its magnitude was large during cyclone period. However, after landfall for most of the cyclones it was southward.
- vii) The zonal and meridional fluxes were high for pre-monsoon cyclones than that of post-monsoon cyclones.
- viii) The total energy was large for pre-monsoon cyclones compared to that of post-monsoon cyclones.

From this analysis we may conclude that pre-monsoon cyclone is more severe than post-monsoon cyclone. However, to understand the real environmental condition at different cyclone phases we need more study on the tropospheric energy of cyclone using dense data network and also using remote sensing data.



## References

1. Fahima K., 1989. "*Track prediction tropical cyclones formed in the Bay of Bengal using numerical method*", M. Phil Thesis, submitted to the Dept. of Physics, BUET.
2. Palmen, E., 1956. "*Formation and development of tropical cyclones*". In Proc. tropical cyclone symp. Bur. Meteorol., Melbourne, Australia Brisbane, P 213-231
3. Richi, H., 1954. "*Tropical meteorology*". Mc Graw-Hill, New York.
4. Anthes, R.A., and Johnson, D.R., 1996. "*Generation of available potential energy in Hurricane Hilda (1964)*". Mon. Wea. Rev., P 291-302.
5. Godske, C.L., Bergeron, T., Bjerkhes, J., and Bundgaard, R.C., 1957. "*Dynamic Meteorology and weather forecasting*". Amer. Meteorol. Soc., Boston, Massachusetts, P 555.
6. Miller, R.G., 1958. "*Statistics and predictability of weather*". In. studies in statistical weather prediction. Travelers weather Res. center, Hartford, Connecticut. P 137-153
7. Bergeron, T., 1954. "*The problem of tropical hurricanes*". Quart. J. Roy. meteorol. Soc. **80**, P 131-164.
8. Miller, B. I., 1964. "*A study of the filling of hurricane Donna (1960) over land*". Mon. Wea Rev. **92**, P 389-406.
9. Mostofa, G., 1986. M.Sc Thesis, Dhaka university, 1986.
10. Donn. W. L., 1975. Meteorology, Mc Graw-Hill, P 318-328.
11. Raghavan, S., 1990. "*Structure of tropical cyclones in the Bay of Bengal*", Mausam, **41**, 2, P 325-328.
12. Raghavan. S., 1993. "*Some recent results on tropical cyclone core structure from modern observational techniques*", in '*Advances in tropical meteorology*'. Ed. R. N. Keshavamurty and P. C. Joshi, Tata Mc Graw-Hill, New Delhi, P 277-288.
13. NOAA technical report 1984. NESDIS, 11. September.
14. Weatherford, C. L., 1987. "*Typhoon structural evolution*", Ph. D. Thesis, Colarado state university, Colarado.
15. Raghavan S., Rengarajan S., Ramaswni V., and Premkumar S. W., 1989. "*Some structural features of a Bay of Bengal tropical cyclone*", Mausam (1989) **40**, 1, P 65-72.

16. Sikka D.R., 1975. "Forecasting the movement of tropical cyclones in the India seas by non-divergent barotropic model", India J. Met. Hydrol, Geophys. **26**, 3, P 323-325.
17. Natarajan R. and Ramamurthy K. M. 1995. "Estimation of central pressure of cyclonic storms in the Indian seas". Indian J. Met. Hydrol, Geophys. **26**, 1, P65-66.
18. Fletcher's formula, 1994. Bull, Am. Met. Soc., **4**, P 457.
19. Ghosh S. K. and Roy T. K., 1990. "A cyclonic storm wave model for the Bay of Bengal and the Arabian Sea". Mausam **41**, 3, P 371-374.
20. Basu B. K., Ghosh S. K. 1987. "A model of surface wind field in a tropical cyclone over Indian seas", Mausam **38**, 2, P 183-192.
21. Tripathi S. N. and Saxena V. P., 1995. "Vertical structure of a Bay of Bengal cyclonic storm". Indian J. Met. Hydrol. Geophys., **26**, 4, P 479-486.
22. Mandal J. C., Kalsi S. R., Veeraraghavan K., and Halder S. R. 1990. "Some aspects of Bay of Bengal cyclone of 29 January to 4 February 1987", Mausam., **41**, 3, P 385-395.
23. Nootan Das, Desai D. C., and Biswas N.C., 1989. "Cyclone and depression over the Indian seas and the Indian sub-continent during 1987." Mausam, **40**, 1, P 1-12.
24. Gupta G. R., Desai D. S. and Biswas N. C., 1991 "Cyclones and depressions over the Indian seas during 1989". Mausam, **42**, 1, P 1-16.
25. Bhaskar Rao D.V. 1997. "Tropical cyclone simulation with Emanuel's convection scheme", Mausam. **48**, 2 P 113-122.
26. Kelkar R. R. 1997. "Satellite-based monitoring and prediction of tropical cyclone intensity and movement". Mausam **48**, 2 P 157-168.
27. Prasad K. 1997. "Prediction of tropical cyclones by numerical models – A review", Mausam **48**, 2 P 225-238.
28. Mohanty U. C. and Akhilesh Gupta 1997. "Deterministic methods for prediction of tropical cyclone tracks", Mausam **48**, 2 P 257-272.
29. Akhilesh Gupta and Mohanty U. C. 1997. "Secondary convective rings in an intense asymmetric cyclone of the Bay of Bengal", Mausam **48**, 2 P 273-282.

